Order Number 9304691

Neuroethology of saccadic eye movements in chickens

Letelier Parga, Juan-Carlos, Ph.D.

City University of New York, 1992

U·M·I
300 N. Zeeb Rd.
Ann Arbor, MI 48106

NEUROETHOLOGY OF SACCADIC EYE MOVEMENTS IN CHICKENS

by

Juan-Carlos Letelier Parga

A dissertation submitted to the Graduate Faculty in Biology in partial fulfillment of the requirements for the degree of Doctor of Philosophy, the City University of New York.

1992

This manuscript has been read and accepted for the Graduate Faculty in Biology in satisfaction of the dissertation requirement for the degree of Doctor of Philosophy.

17 September 1992
date

Chairman of Examining Committee
Prof. Josh Wallman, City College

9/18/92
date

Executive Officer
Dr. Peter C. Chabora
Dr. Richard L. Chappell (Acting)

Prof. Olivia McKenna, City College

Prof. Lee Mitchell, City College

Prof. Craig Evinger, SUNY

Prof. Fred Miles, National Eye Institute

Supervisory Committee

The City University of New York

Abstract

Neuroethology of saccadic eye movements in chickens

by

Juan-Carlos Letelier Parga

Adviser: Professor Josh Wallman

The peculiar saccadic oscillations of birds have received scant attention compared with mammalian saccadic eye movements. This dissertation studies two main aspects concernings these eye oscillations in chickens: a) their kinematical description and b) the activity patterns, in awake subjects, of motoneurons innervating the superior oblique muscle.

A complete spatial description of eye position in the orbit was obtained by recording eye position around three axes of rotation. During fixations it was found that the range of the horizontal, vertical and torsional components of eye position were similar, each having a value of 15°. Futhermore, in contrast to the case in primates, the amount of torsion was found to be independent of the horizontal and vertical components. The mean amplitude in change of gaze direction was less than 3°.

Saccadic oscillations in chickens occur at the rate of 1/sec. They are very stereotyped cyclotorsional movements of the eyeball, having a frequency of 28Hz, an amplitude of 10-12° that does not decay exponentially and a mean speed of 600°/sec. The three position components are strictly linked during oscillations: the eye moves intorsionally, upward and temporally or extorsionally, downward and nasally. While the net eye displacements in both eyes are not always yoked, oscillations are strictly yoked: when one eye is in the intorsional phase of an oscillation the other is in the extorsional phase and *viceversa*. The pattern of oscillations appears independent of the net saccadic displacement. Saccades that barely move the eye exhibit the same pattern of oscillations as large saccades. Oscillations are actively produced by a sequence of contractions and relaxations of the two

obliques. The contribution to the oscillations of the other four extraocular muscles is less than 5%. Although avian saccades are highly invariant, auditory and visual stimuli given during saccades can shorten saccades.

The motor pool innervating the chick's superior oblique contains two functionally distinct classes of motoneurons. One subpopulation (Tonic) fires during fixations with a rate than increases with intorsion and pauses for at least 35 msec at the beginning of each saccade. The second subtype (Phasic) is totally silent for all fixations and fires a sequence of bursts time-locked to the intorsional phase of each oscillation. A similar division is found among the input fibers coming from the medial longitudinal fasciculus into the trochlear nucleus. Mammalian-like extraocular motoneurons with a tonic-phasic pattern of activity were not observed in the trochlear nucleus. This functional segregation among chicken extraocular motoneurons constitutes an exception to the rule of uniform activation found in the majority of vertebrate motor pools. The firing of Phasic motoneurons appears to be optimized for generating the fastest and most energetically efficient eyeball oscillations. The data collected was used to build a model of the avian saccadic machinery in which the neural command controlling oscillations is not used in producing the net saccadic displacement. Also a theory explaining how saccadic oscillations can be used to increase visual sensitivity to moving objects, using known properties of avian tectal cells and the optical flow produced by oscillations, is advanced.

ACKNOWLEDGMENTS

This thesis was made possible by the support and help of many people who will remain unnamed. The only exception is Diane Greenstein who deserves my eternal gratitude. She supported me with her patience, sense of humor, unbounded optimism and editorial skills. Without her this long and crazy adventure of obtaining a Ph.D. at CUNY would have ended very differently.

TABLE OF CONTENTS

List of Tables and Figures

Tables

Figures

Chapter 1

Chapter 2

Chapter 3

CHAPTER ONE

Introduction and Overview

The problem of motor control.

A critical issue in neurobiology is how the nervous system generates and controls coherent movements. This problem is particularly important because it touches two significant theoretical issues. First, any movement engages many muscles, each of which must be precisely controlled in its force output and temporal relations with respect to other participating muscles. Thus, movement confronts us with the more general problem of how the nervous system produces the coordinated action of neural assemblies. Second, as any behaviour could be simply interpreted as a correct sequence of muscular actions, one could argue that crucial aspects of our understanding of how "purposive behaviour" is created would naturally flow from a precise knowledge of the organization of motor systems.

Since Sherrington's studies at the beginning of the century, the segmental muscle system of vertebrates has been studied extensively to understand how coherent movement is generated. Limb muscles, where afference and efference are clearly separable, and their associated spinal motoneurons make an experimentally accessible system to study the problem of coordination. Nevertheless, the experimental task is a complex one: the geometry of the limb system changes during execution of a movement and the values of its mechanical parameters such as torques and moments of inertia vary as well. Furthermore, as motoneurons of neck or limb muscles are located in the spinal cord it is difficult to record their activity in awake animals.

The oculomotor system, a model system.

The motor system defined by the 12 oculorotary ("extraocular") muscles, (each eye is moved inside the orbit by 6 muscles, their associated motor pools and much of the premotor circuitry, make up the "oculomotor system." It is a system without some of the difficulties found in the study of spinal motor systems. The "output" of the oculomotor system is particularly

simple. The eye moves inside the orbit by the contraction and relaxation of the oculorotary muscles in a way analogous to the pure rotation of a sphere around its center of symmetry. The movement of the eye involves only the contraction/relaxation of extraocular muscles without the participation of joints that make the biomechanical analysis of movement difficult. Thus, as a good approximation, the angular displacement of the eyeball, when measured with respect to some arbitrary "resting" position, is a good indicator of the contraction state of extraocular muscles. The motoneurons innervating the extraocular muscles are located inside the skull in well defined nuclei, permitting the recording of their electrical activity in awake animals.

The behaviors of the oculomotor system are many and varied. They range from maintaining eye position with respect to the eye orbit (periods of fixations), moving the eye at speeds from 0.1-50 °/sec (optokinetic and vestibular movements) and very fast high speed *saccadic* movements (400 °/sec). This spectrum of behaviors can easily be triggered and manipulated in many vertebrate groups ranging from teleosts to primates. Thus, a complete set of activation states of these muscles and motor pools are accessible for experimental work. As some of these behaviors can be triggered by visual stimuli, the oculomotor system is an excellent model for studying problems of sensory motor coordination.

However, in spite of the desirable features of the oculomotor system, it is not clear that results obtained studying it are fully applicable to other muscle systems. For example, proprioception, a fundamental aspect of segmental motor systems, seems to play only a minor role in the oculomotor system as extraocular muscles do not normally experience unexpected loads (Keller and Robinson, 1971).

Types of eye movements

This thesis revolves around the neuroethology of avian rapid eye movements. Because avian fast eye movements have been neglected as a research subject, the importance of the results obtained in this thesis can only be assessed by comparing them with equivalent results obtained in mammals, in which fast eye movements have been extensively studied.

In primates, fixations (periods where the eye is still) are interrupted 1-2 times per second by stereotyped rapid eye movements called **saccades.** Saccadic eye movements always have a sigmoidal like time course and move the eyeball at high velocities. In humans, a 40° saccade lasts about 100 msec (figure 1.1) and achieves maximal velocities of approximately 500°/sec. Saccadic duration and maximal velocity correlate positively with saccade amplitude. Saccades serve to bring new parts of the image of the visual world to the retinal zone of highest acuity (the fovea, in primates), thus saccades are interpreted as "foveating" movements that serve the purpose of shifting gaze direction. While most of the time no conscious record exists of the continuous saccadic scanning of the visual world, the fact that saccade can be directed towards predetermined visual targets proves that saccades cab be voluntary eye movements in some circumstances.

Contrasting with the high speed and acceleration of saccadic eye movements, the eye also moves at much lower speeds (0.1-50 °/sec). These slow movements appear under three different circumstances. Angular acceleration of the head that stimulates the semicircular canals causes both eyes to rotate in the opposite sense of the head (Vestibulo Ocular reflex, VOR). Rotation of the complete visual field (or a big portion of it) induces both eyes to move in the same direction at approximately the same angular speed as the visual field movement (Optokinetic reflex). Both of these reflexes are interrupted before the eye reaches an extreme position in the orbit by fast movements called "quick phases" which share many properties with saccades. Quick phases recenter the eye in the orbit. These alternating slow and fast phases are called vestibular and optokinetic nystagmus (OKN) respectively. The third circumstance triggering slow eye movements consists of the movement of a slow speed object against a background. In primates, this visual stimulation induces the eye to follow the moving object at approximately the same speed, this reflexive eye movement is called smooth pursuit.

Types of muscle fibers in extraocular muscles

Extraocular muscles are special in that they are made of a mixture of "twitch" and "slow-no-twitch" muscle fibers (Hess and Pilar, 1963; Spencer

and Porter, 1988). While mammalian skeletal striated muscles are also a mixture, they are made of different subtypes of "twitch" fibers. All subtypes show "all-or-none" responses to electrical stimulation but differ in contraction speed and resistance to fatigue (Burke, 1981). However in the mammalian extraocular system, in addition to "twitch" fiber types, "slow-no-twitch" fibers that lack "twitch" responses and have a graded contraction have been found. These "no-twitch" muscle fibers resemble "slow" fibers found in amphibians and birds. In mammals, very few striated muscles have such "no-twitch" muscle fibers. Other muscles that shown such mixture of muscle fibers in mammals are the tensor tympani and some larynx muscles (Fernand and Hess, 1969).

Extraocular muscles fibers are spatially segregated, the orbital aspect of each muscle is rich in "twitch" fibers while the global surface contains "slow-no-twitch" fibers as well as twitch fibers (Hess and Pilar, 1963; Pachter, 1983; Spencer and Porter, 1988). The anatomical and spatial segregation of fiber types, coupled with the clear separation between fast (saccades) and slow (nystagmus, slow pursuit) eye movements had great theoretical importance with regard early concepts of oculomotor control.

The concept of uniform recruitment in motor pools

An important problem of motor control is how the amplitude of a muscle contraction is controlled. Because every motoneuron controls a single muscle unit composed of many identical muscle fibers, it is possible that the nervous system could independently control each motor unit by independently activating each motoneuron. In every muscle a wide range of muscle units exists with respect to force generation. Thus, in principle, every muscle contraction could be generated in a different number of ways by activating different subsets of muscle units. Furthermore, as the tension generated by a muscle unit depends on the discharge frequency of its motoneuron, the force output of a muscle unit could be controlled by modulating the firing rate of its motoneuron. In summary, the force output of a muscle can be controlled by two factors: a) *the number* and *identity* of active motoneurons and b) the *rates* at which active motoneurons fire. These two factors act in concert to control muscle output (Kernell and Sjoholm, 1975; DeLuca, 1985). While rate modulation plays a role in

modulating the force output, its contribution is variable and always subordinated to a general mechanism that controls and specifies the number of active motoneurons.

Old empirical evidence (Denny-Brown and Pennybacker, 1938; Henneman, Somjen and Carpenter, 1965) indicates that muscle units, hence motoneurons, are not activated independently of each other, but a clear order (an "orderly recruitment") exists in their activation. A rank can be established among motoneurons based only on their activation threshold. The nervous system activates motoneurons always in the same sequence and deactivates them in the inverse order. The recruitment order is such that low force motor units are activated before high force motor units. This order of activation appears to be largely independent of the type of movement in which the muscle participates, and is the same for reflexes as for voluntary contractions.

To explain the pervasive fact that all motor pools for segmental muscles show an orderly recruitment, a theory about motor control was advanced by Henneman. Henneman's idea supposes that the all motoneurons in a given pool receive exactly the same presynaptic input. Thus, at any instant each motoneuron is traversed by the same amount of current but the depolarization induced by such input current depends on the "input resistance". Motoneurons with high resistance would reach the threshold for spike initiation earlier than cells with a low resistance. As it appears that input resistance is inversely correlated with soma size, small cells have larger resistances and thus fire first (Mendell, Collins and Koerber, 1990). This correlation, known as "the size principle", is the central idea of Henneman's theory. The following three articles give a detailed review of these concepts; Henneman et al, (1974); Henneman and Mendell, (1981) and Henneman, (1990).

The contribution of the size principle is to link a biophysical fact (input resistance is strongly correlated with surface area, thus with total size) with an anatomical hypothesis (the total input arriving at a motor pool is diffuse, unspecific and it is homogeneously distributed among motoneurons) to explain a physiological phenomena (motoneurons are activated in an unique and invariant sequence). Thus, a logical conclusion that follows

from the size principle is that no functional segregation could exist among motoneurons. All the members of a given pool must have the same qualitative responses for all types of movements.

Exceptions to the rule of uniform recruitment of motor units have been known for at least 40 years (Denny-Brown, 1949; Henneman, 1990). These exceptions permitted, in the 1950's, the development of the idea of *parallel* motor systems. This notion supposed that different rules of activation would apply in "normal" and "unexpected" movements or for slow and fast movements. Thus "tonic" and "phasic" motoneurons would be used for different types of movements (Granit and Phillips, 1957). These ideas about multiple motor systems acting upon a given muscle, plus the known dichotomy about fast and slow eye movements in the mammalian oculomotor system, led to the hypothesis that the two populations of muscle fibers in the extraocular muscles would have different functional roles (Jampel, 1967). Slow-no-twitch fibers would be involved in producing slow movements and maintaining fixations, while fast ("twitch") fibers would only produce saccades. This functional segregation would imply that the motor pools of extraocular muscles would be equally divided. One fraction of motoneurons would be only activated during saccades, while the other group would be involved in fixations and slow speed eye movements. Although this notion of functional segregation among extraocular motoneurons is not currently supported by data in the case of mammals, it triggered an intense period of research on the oculomotor system.

Response of mammalian extraocular motoneurons.

In 1970 three different reports described the firing pattern of extraocular motoneurons in awake monkeys (Fuchs and Luschei, 1970; Robinson, 1970; Schiller, 1970), these three reports upheld the notion that all extraocular motoneurons had essentially identical firing patterns. Instead of finding motoneurons which were specifically active during saccades and silent during fixations, and *vice-versa*, it was found that all motoneurons have the same discharge pattern (figure 1.2). As expected, the discharge of extraocular motoneurons correlate positively with eye position. During saccades into the pulling direction of the muscle they innervate ("on" direction), motoneurons reach a higher discharge level than expected from

frequency versus position curves. During these short periods, comparable to the duration of the saccade, extraocular motoneurons show an additional burst of activity that produces the high acceleration reached by the eye. This pattern of activation, that was predicted by Robinson (Robinson, 1964), is called "pulse and step". The "step" change in discharge frequency produces the net change in eye position between successive fixations, while the high acceleration of the eyeball during saccades is created by the "pulse" (mammalian extraocular motoneurons are also referred as "burst-tonic") (see figure 1.2). The discharge rate ($f(t)$), during fixations, slow speed movements and saccades is roughly related to eye position ($E(t)$), speed ($E'(t)$) and acceleration ($E''(t)$) (Keller, 1973) by:

$$f(t) = k(E(t) - \Theta) + rE'(t) + mE''(t) \qquad (1)$$

Θ = **eye position threshold**

Equation (1) summarizes results obtained during fixation, pursuit, vergence, nystagmus and saccades in cats and primates. No functional segregation appears to exist inside the motor pools controlling extraocular muscles, all extraocular motoneurons participate in all types of eye movements. Thus, as in spinal motor nuclei, a single response type is found among extraocular motoneurons. But mammalian extraocular motoneurons, while still showing a uniform recruitment order, are peculiar, but not unique, in their extended dynamical range. Once recruited, an abducens motoneurons can change its discharge rate from 50 sp/sec to 300 sp/sec if the eye moves temporalward. As extraocular motoneurons must cope with an unusually large range of muscle lengths, rate modulation could be a strategy to maintain muscle tension under shortening. Rate modulation seems to be more prominent in extraocular muscles than in segmental muscles where the changes in the length muscle are not as large. For example, in cat's deltoid, a doubling in the output force is associated with a 12% increase (from 26 sp/sec to 29 sp/sec) in the discharge rate of motoneurons (DeLuca, 1985), while a similar change in force would double the discharge rate of extraocular motoneurons.

The presence of uniform recruitment in the specialized motor system that moves the eye, in which a) proprioception seems to play a different role than the servo type mechanism found in segmental muscles, b) muscles

contain two types of muscles fibers (twitch and non-twitch) and c) the "behaviors" produced by these muscles appear to be segregated in two classes (slow and fast) was, to certain extent, a surprise (see the paper of Jampel (1967) and the discussion section of Fuchs and Luschei (1970) and Robinson, (1970)). This finding appears to support the notion that uniform recruitment must be an universal feature of the organization of motor pools, and that independent activation of motoneurons is neither possible or desirable.

Generation of the saccadic motor commands and models.

The problem of producing a contraction of a given amplitude is only one of the two main tasks that each motor system must perform. The other task is producing a coherent movement that involves the correct timing of many muscles. The nervous system generates these patterns of movement by the participation of various neuronal populations. For reflexes, the pattern is generated by the participation of proprioception and the intersegmental network that links various motor pools at the level of the spinal cord. In general some level of coordination is achieved by segmental circuits that can even produce the temporal pattern by themselves without the intervention of supraspinal centers. These circuits, called Pattern Generators (PGs), produce the correct time course for the contraction of a single muscle as well as the coordination between all the muscles involved in repetitive actions (i.e. walking, breathing). But another level of coordination also exists, movements, like walking, involve so many muscles that a higher level of control must be imposed upon spinal PGs. In effect, descending signals are necessary for equilibrium and adapting gait to uneven terrain. Recent studies in cats show that PGs are located in supraspinal centers as well (Koshland and Smith, 1989). Many aspects of PGs like their anatomical and physiological organizations, the interrelation between spinal and central oscillators and the generation of non-stereotyped movements, are still unresolved questions.

The mammalian oculomotor system has provided a good model to study the problem of muscle coordination. Saccades, in monkeys and humans, are not random events due to neuronal "noise" in the premotor circuits. In effect, some saccades are obviously triggered by images of

visual objects in the periphery of the retina. Some unknown "attentional" mechanism decides that one of these peripheral objects must be seen with greater acuity and initiates a saccade that will bring the image of such an object to the fovea. These "visually evoked" saccades serve to study the transformation of visual evoked activity into motor commands. But saccades are not only driven as a response to increase visual acuity of visual targets, without any doubts other processes continuously manipulate premotor circuits for producing saccades. The existence of such processes is easily demonstrated by the continuous performance of saccadic eye movements in the dark.

How visual stimulation in a non-foveal area is translated into a motor command is an interesting problem of motor coordination. Current models of the mammalian saccadic machinery suggest that the optic tectum produces a desired eye position neural signal that arrives at a neural group the purpose of which is to produce a neural signal similar to the "pulse" component found in motoneuronal discharges (Robinson, 1975; Deubel, Wolf and Hauske, 1984; Scudder, 1988). This transient component is fed to the motoneurons jointly with its integral over time. The integral provides a position signal to hold the eye steady during the post-saccadic period. The combination of both neural signals is the motor command to the extraocular motoneurons (figure 1.3). Because the tonic component of the motor signal is the integral of the phasic component, the eye usually does not drift after saccade completion. The overall saccadic mechanism is not "ballistic" in the sense that the motor command is totally generated before saccade onset. On the contrary, the motor command is generated just prior and during each saccade, a feedback mechanism stops the motor command when the eye is at, or near, the target. The feedback signal is not proprioceptive, instead it is an efference copy signal of the position command arriving at motoneurons.

As mentioned earlier, activation modes for motoneurons other than uniform recruitment are known, and some of these exceptions have been described in detail (Henn and Cohen, 1975; Hoffer et al., 1987; McCue and Guinan, 1988). Some of these exceptions imply that a motor pool is functionally divided into classes of motoneurons and the division is fixed

and static (Granit and Phillips, 1957; McCue and Guinan, 1988). Such functional segregation could be due to a heterogeneous input arriving to the motor pool. Other exceptions are more remarkable in that it seems that a motor pool can be used in different "modes" according to the type of movement in which a muscle is engaged (Desmedt and Godaux, 1981). Another of such examples happens in the cat's sartorius where the recruitment rule valid during waking is different from the one during running (Hoffer et al., 1987).

Avian oculomotor system

The present thesis investigates a case where a clear exception to orderly recruitment seems to exist in the avian oculomotor system. The case concerns a puzzling type of fast eye movement found thus far only in birds. While similar in the gross anatomy of extraocular muscles, and in the existence and organization of reflex eye movements like VOR and OKN, the avian oculomotor system possesses a clear difference in the time course of saccadic eye movements.

Instead of the monotonic trajectories depicted in figure 1.1, avian saccades have prominent oscillations of the eyeball (figure 1.4A and 1.4B). In chickens, these oscillations are mostly cyclotorsional, consisting of 2-6 cycles with an almost invariant frequency of 28Hz, an amplitude of 10-12 degrees and a mean duration of 180 msec. Since these oscillations were first partially described, in pigeons (Nye, 1969), they have been found in all species of birds in which precise eye position recordings have been made: Owls (Steinbach and Money, 1973; Steinbach, Angus and Money, 1974), Chickens (Turkel and Wallman, 1977), Tawny frogmouth {*Podargus strigoides*}, Boobook owl {*Ninox novaeseelandiae*}, Bush thick-knee {*Burhinus grallarius*}, Laughing kookabura {*Dacelo gigas*} (Pettigrew, Wallman and Wildsoet, 1990). Nevertheless these oscillatory eye movements have not been described in any group outside birds. Furthermore, mammalian-like saccades do not appear to occur in chickens and pigeons; rather, in these two species all fast eye movements involve eyeball oscillations. These peculiar eye movements raise two questions:

a) What are the physiological functions of these oscillations?

b) How are the oscillations generated?

The first question cannot be resolved by utilizing concepts developed in mammals. Mammalian saccades are movements directing the fovea to areas of interest. The retina of chickens and pigeons is so different from mammalian retinae that it should not be assumed, without supporting evidence, that avian oscillations are part of a gaze directing mechanism.

Chickens, and pigeons, have a panoramic field of view of moderate acuity of vision not like the "tunnel-like" vision of foveated animals which has a great acuity near the fovea but decays two orders of magnitude towards the periphery. In chickens the density distribution of photoreceptors and ganglion cells is more homogeneous than the one found in primates. The central retina has only 7 times more ganglion cells than the periphery (Ehrlich, 1981). In primates the ratio is 150 to 1 (Perry and Cowey, 1985) and 35 to 1 in cats (Wässle, Levick and Cleland, 1975) (figure 1.5). Thus, chickens do not have to produce eye movements to look at objects with great acuity. The distributions of photoreceptors and ganglion cells are such that, contrary to the situation in foveated animals, constant high levels of acuity (equivalent to the visual acuity found at 10° of eccentricity in primates) can be achieved over a wide retinal area.

Since avian saccadic oscillations were first described in 1969 four theories have been presented concerning their possible functions. These include a) polishing the cornea (Nye, 1969), b) participating in a saccadic suppression mechanism (Brooks and Holden, 1973), c) promoting aspects of visual perception (Turkel and Wallman, 1977) and d) shaking the vitreous humor facilitating the flow of nutrients out of the pecten (Pettigrew, Wallman and Wildsoet, 1990). These theories have not been adequately tested, all of them suffer from lack of descriptive data, and the three dimensional trajectory of avian saccadic oscillations has not been described.

How saccadic oscillations are generated is a multidimensional problem that involves many levels of analysis. The most important levels include: a) the relative activation of extraocular muscles during saccades, b)

the firing pattern of motoneurons, and c) the activity of premotor centers involved in producing the overall movement. Of these three levels the one concerning the discharge pattern of motoneurons during saccades is particularly important.

Current models of the saccade generator (Robinson, 1975; Scudder, 1988) are based on the existence of a single type ("burst-tonic") of extraocular motoneuron. It is not easy to see how these models can explain the generation of saccadic oscillations without introducing major modifications. The main problem is that the error signal (signal ME in figure 1.3) can not drive motoneurons with a 30Hz oscillation. However, realistic models of the avian saccadic machinery can not be built until some knowledge of the real discharge pattern of avian extraocular motoneurons is obtained. The most interesting possibility would be that a special subset of avian extraocular motoneurons are uniquely devoted to the production of oscillations. Such a possibility would imply a strict functional segregation in some extraocular motorpools and consequently a different organization of the inputs from premotor centers to these (segregated) motorpools.

This thesis explores avian saccades and tries to illuminate their physiological functions and the organization of extraocular motor pools. Two main types of experiments were carried out: a) a full kinematic description of saccades (Chapter 2) and b) recordings from motoneurons innervating the superior oblique (Chapter 3). With the data collected a model of the avian saccadic machinery will be presented and compared with the mammalian case.

CHAPTER TWO

KINEMATICS OF SACCADIC EYE MOVEMENTS IN THE CHICK.

Introduction

Description of a behavior is an essential first step for understanding its functions or the physiology of the motor system involved in its production. This has been particularly true for the mammalian oculomotor system. In primates, knowledge about eye movements immediately suggested anatomical and physiological aspects of their oculomotor system. Some examples vividly illustrate the importance of the behavioral analysis of eye movements in revealing the underlying physiology.

a) The simultaneous, and conjugate, movement of both eyes *(Hering's law)* indicates the existence of specific anatomical pathways between motor nuclei controlling the two eyes.

b) The clear dichotomy between fast and slow eye movements implies that independent and parallel, neural centers specify eye movements (Robinson, 1968).

c) Measurements of human fast eye movements under artificial conditions, such as increasing the eye's moment of inertia for example, were used to predict the correct force pattern generated by extraocular muscles during normal fast eye movements (Robinson, 1964).

Birds, which apparently have a unique oculomotor behavior in their eye oscillations, have received scant attention compared with mammals. Since 1969, when saccadic oscillations where first described in the pigeon, less than 2 dozen papers have addressed the topic of avian eye movements, while in the same period thousands of papers on the behavior and physiology of the mammalian oculomotor system have been published. Thus, most of the basic operating parameters of the avian oculomotor system, beginning with a description of the eye trajectory during saccades,

are yet unknown. For example, little has been published on the normal range of eye positions in any bird or if, as in primates, the degree of cyclotorsion depends on the eye attitude (Donder's law). Even the "purpose" of the pervasive avian saccadic oscillations is an open and unsettled question. The only avian oculomotor behaviors quantitatively studied are the "reactive" visual reflexes involved in gaze stabilization (Wallman et al., 1982; Gioanni et al., 1983).

This chapter provides an initial kinematic description of saccadic eye movements in chickens (*Gallus gallus domesticus*) that takes into consideration the intrinsic 3-dimensional nature of saccadic oscillations. The data collected will be used to infer some properties of the avian oculomotor system. Given the paucity of data on avian fast eye movements, most of the results obtained in this chapter can only be compared with similar results obtained in mammals, especially in primates. To introduce the main elements of the behavioral analysis of eye movements a summary of the principal results of the anatomy and physiology of primate oculomotor system follows.

Overview of primate eye movements.

In primates, the eyeglobe is located inside the orbital cavity, in which it fits easily. In addition to the eye, other tissues, referred as the *ocular adnexa*, are found inside the orbit. Seven muscles, called *ocular muscles,* belong to the ocular adnexa. Two very different functions are subserved by ocular muscles. The *levator palpebrae* originates next to the orbital apex and inserts into the upper lid; its function is to raise the eyelid. The other six ocular muscles, known as *extraocular muscles* or (less frequently) *oculorotary muscles,* are inserted in different positions on the eye and rotate the eye.

As a first approximation, the six extraocular muscles act like three non-interacting antagonist/agonist pairs: the *medial* and *lateral rectus* (the latter also known as the *abducens muscle*), the *inferior* and *superior rectus,* and the *superior* and *inferior obliques*. Five extraocular muscles, the four recti and the superior oblique, originate in a tendon surrounding the optic nerve next to the apex of the orbit: the *ring of Zinn.* The inferior oblique

originates from the anterior part of the orbit near the opening of the lacrimal duct. All recti and the inferior oblique are directly attached to the eyeball by means of wide and fragile tendinous insertions.

The course of the superior oblique is atypical, it passes through a cartilage loop (*the trochlea*) located in a naso-dorsal position of the orbital margin. The net effect of the geometrical disposition of the superior oblique is to produce an intorsion, instead of an elevation, of the eyeball when it contracts. In some mammals, another ocular muscle, the *retractor bulbi,* is inserted at the back of the eye and has the function of retracting the eye into the orbit. The six extraocular muscles move the eye in such a way as to produce mostly rotations of the eyeball around a fixed point close to the geometrical center of the eye. Translations of the eyeball are considered negligible, as the center of the eye moves less than 0.5 mm for a 40° saccade (Fry and Hill, 1962) when the *retractor bulbi* is not activated.

Reference frame used to describe eye positions.

Any kinematical analysis of the position of an object must be described with respect to some defined reference frame. In the case of the eye, the reference frames and the vocabulary used to describe eyeball rotations are varied and sometimes intimidating in their apparent complexity. Description of eye movements is simplified by treating them as simple rotations about a fixed point (center of rotation) and ignoring any translational component. A brief description of one reference frame used in oculomotor research will be given here; a more detailed description can be found in the Methods section of this chapter and in Appendix-A.

Three anatomical entities on the eye implicitly create a meaningful reference frame to describe eye rotations (figure 2.1). The *visual axis* (sometimes called incorrectly *the optic axis*) is defined by the line connecting the external point of fixation and the center of the eye. The *equatorial plane* passes vertically through the equator of the eye. Finally, the *horizontal plane* is a plane perpendicular to the equatorial plane and also contains the optic axis. In frontal-eyed animals when the eye is in the primary ("resting") position the *horizontal plane* is approximately horizontal. In other positions, the horizontal plane is no longer horizontal.

A cartesian reference frame can be defined by taking the center of rotation of the eye as the origin **O**, the fixation axis as the axis **OX'** and the axis **OY'** as the intersection between the equatorial and horizontal planes. The **OZ'** axis is defined by demanding that it must lie in the eye equatorial plane and form, in conjunction with **OX'** and **OY'** a "right hand" reference frame (in technical terms; $\vec{OZ'} = \vec{OX'} \times \vec{OY'}$). The reference frame used in this thesis is defined for the left eye as it is important to realize that both eyes are not superimposable but rather mirror images of each other. A "zero" eye position is defined by the *primary eye position*. In this position, attained with the body and head in a normal erect position, the fixation axis is horizontal and looks straight ahead.

Eye movements can be decomposed along rotations around three axes. The *sign* (or sense) of rotations must be defined according to a coherent rule. In this thesis rotations were defined as positive if they followed the right hand rule. A horizontal rotation is defined as a rotation about the **OZ'** axis which, in the primary eye position is vertical. Positive horizontal rotations, called abductions, move the visual axis towards the temporal side. A vertical rotation is defined as a rotation around the **OY'** axis, which in the primary eye position, is horizontal. A positive vertical rotation depresses the eye (i.e. optic axis moves downward) while a negative vertical rotation elevates the optic axis. A torsional rotation is achieved by rotating the eye about the **OX'** axis. Positive torsional rotations are called "intorsions", if it is negative it is an "extorsion". Although the convention for rotations just explained is mathematically coherent (i.e. all three fundamental axis are treated in a similar way) it is counterintuitive in its treatment of vertical rotations. In effect, upward movements are treated as "negative" rotations, this clashes with the normal tradition of the oculomotor field in which upward movement are usually considered positive. In this thesis the mathematical treatment of eye position data followed the sign conventions just defined, but graphs were done with elevations represented as positive going curves.

While the six extraocular muscles act synergistically to produce each movement of the eye, as a first approximation the lateral and medial recti

produce horizontal rotations, the inferior and superior recti produce the vertical rotations and the obliques produce torsional movements.

Properties of fixations and eye movements.

Humans, and non-human primates like *Rhesus*, have a wide oculomotor range. In humans the maximal range is about 120° horizontal x 90° vertical x 20° torsion. The human "periprimary" range, a qualitative concept describing the sub-range where the eye spends "most" of the time, is smaller, 15° horizontal x 15° vertical x 4° torsion (Collewijn, Ferman and Van Den Berg, 1988; Henn, 1988). Furthermore, in all this space of theoretically possible eye positions most positions are actually forbidden by a neural restriction upon the amount of torsion. Since the last century it has been known that torsion is not a free parameter. It covaries with the horizontal and vertical components of eye position. In other words, the amount of torsion for any eye position is a direct mathematical function of the horizontal and vertical eye position (Donder's law). While Donder's law states only the existence of a relation between the three components of eye position, Listing's law explicitly gives the functional dependence between these three variables. This restriction on which eye positions are permitted does not arise from some mechanical or geometrical factors concerning extraocular muscles. In some situations, such as sleep (Nakayama, 1975), Donder's law does not hold, and thus reflects a dynamic coordination between the motor commands arriving at the six extraocular muscles.

Types of eye movements

Eye movements, in human and non-human primates, can be classified into two types according to the maximal speed reached by the eyeglobe: *fast* (above 100°/sec) and *slow* (below 100°/sec). Slow eye movements appear under the following four conditions, three of them reflexes: 1) Vestibulo Ocular Reflex, (VOR) as a result of vestibular stimulation, when the subject is rotated, even in the dark, the eyes move in a direction opposite to that of the imposed rotation, 2) Optokinetic Nystagmus, (OKN) as a result of a slow movement of the whole visual field the eyes follow the direction of movement at almost the same speed, 3) Smooth Pursuit when a small object moves, at speeds below 100°/sec, the eye follows the object with approximately the same speed and 4) Vergence when the angle between the

left and right optic axis change to put in register both retinal images. Vergence eye movements, which are triggered by the defocus of the retinal image (accomodative vergence) or by non-zero disparity between both retinal images (fusional vergence), are the only exceptions to Hering's law, as they produce disconjugate movements and are the only type of voluntary slow eye movements.

Properties of human saccades and quick phases.

In normal viewing each period of fixation is interrupted, 2-3 times a second, by a quick eye movement that redirects the direction of gaze. Humans perform thousands of such movements every day without apparent conscious effort. But the fact that humans can direct their gaze at will to any portion of the visual field shows that these very fast movements can be under voluntary control. *Saccades*, as these fast eye movements are called, move the eye with a sigmoidal time course (figure 1.1) at speeds of 100-400°/sec with an acceleration in excess of 10000°/sec^2. Saccades always occur in both eyes simultaneously and move both eyes in the same direction. Saccades appear functionally specialized to foveate visual objects.

The duration of saccades (**D**) is approximately an affine function of its amplitude (**A**) (Bahill, Brockenbrough and Troost, 1981) $\mathbf{D} = \mathbf{d}_0 + \alpha\mathbf{A}$ (figure 2.2A), with α equal to 2.2 msec/° For example, a 40° saccade lasts almost 100 msec. The mean velocity, defined by $\overline{\mathbf{V}} = \mathbf{A} / \mathbf{D}$, is not constant for saccades of different sizes. The dependence of **D** on **A** implies that: $\overline{\mathbf{V}} = \mathbf{A} / (\mathbf{d}_0 + \alpha\mathbf{A})$, thus $\overline{\mathbf{V}}$ is also a function of saccade amplitude, with an asymptotic value of $\overline{\mathbf{V}} \rightarrow 1/\alpha$ (figure 2.2B). The peak velocity ($\mathbf{V}_{max}$) also increases with saccade amplitude but levels off at around 500-600°/sec (figure 2.2C). The ratio between $\mathbf{V}_{max}$ and $\overline{\mathbf{V}}$ is approximately constant for saccades of different amplitudes ($(\mathbf{V}_{max} / \overline{\mathbf{V}}) \cong 1.6$) (figure 2.2D).

In the artificial situation of most experiments, saccades are usually restricted to one dimensional rotation, usually around the vertical axis, but normal saccades have in general horizontal, vertical and torsional components. The relations between amplitude, duration, and speed of saccades varies with their direction. Saccades towards the primary eye position (*centripetal saccades*) are faster than saccades moving the eye away

from the primary position (*centrifugal saccades*). The difference in speed is slight and only noticeable for saccades greater than 15° (Jurgens et al., 1981). Another type of difference relates to the specific extraocular muscle producing the saccade: *abducting saccades* (i.e where the abducens muscle contracts) are slower than *adducting saccades* (i.e. where the medial rectus provides the pull) (Boghen et al., 1974). While saccades appear to be "machine-like" movements with a stereotyped time course, they can be modified by systemic factors such as fatigue (Schmidt et al., 1979) or drugs (Aschoff, Becker and Weinert, 1975). These factors make the relations between saccade amplitude and speed more variable and the saccades sluggish. Although saccades can in principle move the eye in excess of 90°, 85% of them move the eye less than 15° (Bahill, Adler and Stark, 1975). In general, large changes of gaze direction are produced by a combination of saccades and quick head movements (Barnes, 1979).

In laboratory situations, the target of a saccade can be defined and manipulated precisely. In more complex situations, when the target is not a simple "point" but a figure like a line or a triangle, the saccades usually end in the middle of the target figure. It seems that the visual process which defines saccade amplitude and direction is a cooperative process that takes into account the entire array of visual inputs to define the saccadic endpoint (Findlay, 1982; Ottes, Van Gisbergen and Eggermont, 1984).

During saccades, visual perception is momentarily disrupted (Volkmann, 1986). The fast movement of the retinal image produced by saccades usually does not generate a perception of motion, and during saccades there is a small reduction in the overall sensitivity of the visual system equivalent to 0.5 log units. Saccadic suppression, as this reduction in sensitivity is known, is due in part to central factors that actively alter perception and not only to the blurring of the retinal image (Volkmann, 1986). While saccadic suppression is well documented, it has also been reported (rather paradoxically) that saccades can enhance the detection of some classes of moving objects (Deubel and Elsner, 1986). This last fact should be kept in mind when considering the unsolved problem of the physiological function of avian saccadic oscillations.

Saccades, once initiated, are not easily modifiable by external stimuli. Classical studies (Westheimer, 1954) showed that saccades, directed to simple point-like targets, have a latency of 150-200 msec and, once initiated, continue to move the eye towards the target even if it disappears or changes position. In some experiments, in which the target is briefly flashed for a period of less than 200 msec, a saccade begins even after the visual stimulus has been extinguished. The continuation of saccades after target disappearance suggested that the saccadic machinery does not use visual feedback during saccades to reach the target. It was hypothesized (Young and Stark, 1963) that the saccadic system received visual inputs only in discrete moments separate from each other by refractory periods in which visual inputs do not modify the ongoing (or imminent) saccade. Once a saccade is initiated, visual stimuli have no discernible effect upon eye trajectory. It seems that the saccadic motor command is prepared in advance of the movement and once initiated it cannot be modified at midcourse. Turning off or moving the target does not change the eye trajectory of the initial saccade. The programming of saccadic events suggests that the saccadic subsystem (comprising the visual and motor subparts) cycles through three different states (Young and Stark, 1963) including Targeting: the visual scene is scanned and a target defined; Synthesis: the motor command for extraocular muscles is created; and Execution: the saccade is performed. After saccade completion a new targeting period begins and the cycle repeats itself 2-3 times per second.

The "sampled data" schema of the saccadic machinery just briefly described proved to be a first approximation that had to be modified. Systematic experiments in which the target was briefly moved once or twice ("double-step" experiments) revealed a more complex organization of the saccadic system (Becker and Jürgens, 1979). The major change was that visual information had a continuous influence upon the generation of saccades. Instead of a simple targeting state in which visual information was relevant, double step experiments revealed that visual information acts in a continuous manner to abort or change the amplitude of the saccadic commands *before saccade initiation.* Thus if a target moves 100-80 ms

before a saccade the resulting saccade will point to a position in between the old and new target positions.

Saccades are sometimes called *ballistic* movements, a misnomer as ballistic movements are characterized by the absence of internally produced active forces. Saccades are better described as *preprogrammed* movements since internal forces (the output of extraocular muscles) are continuously applied in saccadic midflight. The time course of such forces once initiated cannot be modified or canceled until the eye reaches its destination. The 100-200 msec reaction time associated with voluntary triggered saccades explains why visual stimulation during saccades does not have an effect upon saccadic trajectory.

Properties of human "quick phases".

The reactive reflexes OKN and VOR are periodically interrupted by centripetally (i.e., toward the primary eye position) oriented fast eye movements called quick phases, which are very similar to saccades. Quick phases and saccades share the same sigmoidal time course and relation between amplitude and duration, although some reports have described small but statistically significant differences between saccades and quick phases (Jurgens et al., 1981). The kinematic differences between saccades and quick phases are minimal when compared with the biological factors that trigger both behaviors. Saccades are voluntary while quick phases are an automatic and unsuppressable consequence of OKN and VOR. As VOR is universal among vertebrates a current speculation about the origin of saccades is that the neural circuitry involved in the production of quick phases was "captured" by foveated animals to produce voluntary saccades towards visual targets appearing in the periphery of the visual field (Robinson, 1981).

Tension applied by extraocular muscles.

The high speed reached by the eyeglobe during saccades is due to a particular pattern of force generated by extraocular muscles. It was predicted (Westheimer, 1954) that during saccades, extraocular muscles simply generated a step change in tension (figure 2.3A). Measurements of the eye moment of inertia (Robinson, 1964) revealed that the force pattern

suggested by Westheimer would produce much slower saccades. Instead, at the beginning of saccades extraocular muscles must generate some extra amount of tension to produce the high acceleration profile of primate saccades (figure 2.3B).

Review of avian saccadic eye movements.

Birds, as *bona fide* vertebrates, share many aspects of the anatomy of the eye, ocular adnexa, and orbital cavity with mammals. The avian eye, while reflecting the basic vertebrate plan, possesses anatomical features not found in the species (cats, primates, rabbits) generally used in oculomotor research. For example, birds have a ring of scleral osicles exists around the limbus and a highly vascularized pyramidal structure protruding into the vitreous chamber, the *pecten oculi,* whose physiological role is still unclear. A large and irregular *Harderian gland* covers a large portion of the posterior and ventral orbit. Secretions from Harder's gland are emptied into a pouch formed by the nictitating membrane and the front of the eye. In addition to the normal complement of six extraocular muscles, two other muscles, the *Pyramidalis* and the *Quadratus,* involved with the control of the nictitating membrane, are attached to the back of the eye.

The geometrical arrangement of the six oculorotary muscles is as in mammals, with the exception of the superior oblique. The superior oblique originates in the nasal part of the orbit near the origin of the inferior oblique and runs directly, without passing through any trochlea-like structure, into the dorsal aspect of the eyeglobe where it is inserted. Despite the difference in the location of the insertion of superior oblique its primary action is, as in mammals, the intorsion of the eyeball. The insertions of avian extraocular muscles are not tendinous but rather like a "delta" of very fine and delicate fibers. In chickens, the insertion of the superior oblique is approximately 3-6 mm wide.

The encasing of the chicken eye in the orbit socket is tight. The orbital space is slightly bigger than the eyeball so that all 8 ocular muscles and the two glands must share the small orbital space. In 4 week old chickens, the anterior part of the eyeglobe protudes outside the orbit. In owls, the eyeglobe is cylindrical and fits into a tubular orbit that constrains

horizontal and vertical movements even more. These anatomical considerations have led some to suggest that avian eye movement should be negligible.

> *"The eye has little chance to move in its socket. All accessory apparatus and muscles are modified to fit into very narrow quarters. Such movements as do occur are supplemented by head movements to bring the object to be fixated into full view."* (Chard and Gundlach, 1938)

While Chard and Gundlach's argument about the tight anatomical encasing of bird eyes reflects an anatomical fact, it has not been followed by physiological measurements. Thus, in general the degree of eye immobility in birds is unknown. More importantly, no data exists about the different oculomotor strategies of different avian species (an exception is found in Wallman and Pettigrew (1985). Thus a first reason to study avian eye movements is to refute or substantiate Chard and Gundlach's idea. A second reason concerns the rich variety of anatomies and life styles of birds. A third reason is to understand the peculiar oscillations of the eyeball that accompany every fast eye movement. Current evidence shows that saccadic oscillations are found in all birds. Even owls with their minuscule saccades show 4° saccadic oscillations. The functions of saccadic oscillations, as well as the mechanisms producing them have not yet been clarified. Perceptual and vegetative functions have been ascribed to them, but a careful description of these movements has been lacking. Finally the most important reason to study avian eye movements, particularly their fast eye movements, is to explore the generality of our current models of oculomotor function and organization based on mammalian data.

The first report describing avian fast eye movements (Nye, 1969) focused only on two components (horizontal, vertical) of eye position. Furthermore, the optical method used to record eye position has a strong cross coupling between torsion and the other two components of eye position. Later reports (Steinbach, Angus and Money, 1974; Turkel and Wallman, 1977; Wallman and Pettigrew, 1985) focused on a single component of eye position. The torsional component of eye position was left unmeasured in all published reports on avian fast eye movement (with

the exception of (Steinbach, Angus and Money, 1974)). Beside ignoring torsion, these studies could not clarify the types of oculomotor strategies and circumstances where they were used. For example, the implicit principle that saccadic eye movements serve to fixate objects has not been proven true in pigeons or chickens. The retina of these granivoruous birds is rather peculiar in having an uniformly high density of cellular elements, suggesting that "foveation" could be a less important task given their panoramic field of view. Thus it is necessary to understand the precise role of changes in gaze direction in animals with more homogeneous retinas.

This chapter will address the following three topics:

a) Basic properties of fixations like the range of eye positions, the validity of Donder's law and the mean duration of fixations.

b) A 3-dimensional analysis of chicken saccades. A thorough description of oscillations will be presented. The analysis will concentrate on the duration, amplitude, time course and modifiability of saccadic oscillations.

c) The mechanical nature of oscillations. Are these movements passive oscillations of the eyeball or are they produced by a sequence of contractions and relaxations?

Methods.

All the experiments reported in this chapter were done on 3-4 week old normal White Leghorn chicks (*Gallus gallus domesticus*) hatched in the laboratory of Dr. Josh Wallman at City College of New York. Chicks were maintained in temperature controlled brooders under a 14L/10D day cycle. The main experimental procedures were:

a) recording of eye movements

b) surgical implantation of a headpiece to assure complete head immobility during recording sessions

c) data analysis

d) recording of eye muscle tension in deeply anesthetized chickens.

Eye position recording.

Eye position was measured using a three dimensional magnetic search coil method (Robinson, 1963) based on measuring the electro motive force (emf) induced by a surrounding magnetic field in a small conducting coil, or sets of coils, called "eye coils" or "scleral coils," solidly attached to the eye. Under the special circumstances of a fast time varying and homogeneous magnetic field, the induced emf on the eye coil is only a function of its orientation with respect to the magnetic field. The fundamental physical principle behind this recording method is simple:

Let S be a region of space where a homogeneous sinusoidal magnetic field $\vec{H}(t)$ exists (figure 2.4A). $\vec{H}(t)$ can be described by:

$$\vec{H}(t) = \vec{V}.g(t) = \vec{V}.(a\sin(2\pi ft)) \quad \vec{V} = \text{static vector}$$

Let C be a circular coil of radius r made of p coplanar turns of conducting wire. According to Faraday's law an emf will be induced in the coil C:

$$emf(t) = -\Phi'(t) \qquad \Phi(t) = \text{magnetic flux}$$

The magnetic flux crossing the coil C is equal to:

$$\Phi(t) = \int_C (\vec{H}(t) \bullet \vec{n}(t)) d\tau \qquad d\tau = \text{surface element}$$

where $\vec{n}(t)$ is a normal vector to C describing the orientation of C, at time t, with respect to the same reference frame used to described $\vec{H}(t)$.

The search coil method demands an uniform field $\vec{H}(t)$, in that case the last integral is equal to:

$$\Phi(t) = aA_c \sin(2\pi ft)\cos(\vec{V},\vec{n}(t)) \qquad A_c = p\pi r^2 = \text{total coil area}$$

Thus the emf is then:

$$emf(t) = \beta \cos(\vec{V},\vec{n}(t))\cos(2\pi ft) \qquad \beta = aA_c 2\pi f$$

In the case where $\vec{n}(t)$ varies slowly compared with the driving frequency f of the magnetic field, $\cos(\vec{V},\vec{n}(t))$ is constant over many cycles, the value of emf(t) can be used to measure $\cos(\vec{V},\vec{n}(t))$, the relative orientation of C with respect $\vec{H}(t)$. A simple scheme would be to measure the mean value of emf(t) over a given period of time. But the mean value of emf over many cycles has two disadvantages. The first is that it does not distinguish between $\vec{n}(t)$ and $-\vec{n}(t)$. The second reason is that in the case that another magnetic field $\vec{H}_2(t) = \vec{V}_2 \cdot g_2(t)$ with a different orientation were to be present, the mean value of emf(t) would not discriminate between the contributions of both fields. A procedure to solve this problem is to perform a "weighted average" of emf(t) with a suitable reference function, a method known as Phase Lock Amplification.

Suppose then that the region S contains two mutually perpendicular magnetic fields that are in temporal quadrature; i.e. $\vec{H}_1(t) = \vec{V}_1 \cdot (a\sin(2\pi ft))$ and $\vec{H}_2(t) = \vec{V}_2 \cdot (a\cos(2\pi ft))$ (figure 2.4B). The eye coil would have an emf that can be separated into two components:

$$emf(t) = emf_1(t) + emf_2(t)$$

$$= \beta_1 \cos(\vec{V}_1, \vec{n}(t)) \cos(2\pi ft) + \beta_2 \cos(\vec{V}_2, \vec{n}(t)) \sin(2\pi ft)$$

Next, this electrical signal is multiplied with a suitable reference function. Let $r1(t) = \sin(2\pi ft))$ a reference function:

$$MV = \int_{\text{many cycles}} emf(t) r1(t) dt = \int_{\text{many cycles}} (emf_1(t) + emf_2(t)) r1(t) dt$$

$$= \beta_1 \cos(\vec{V}_1, \vec{n}(t)) x \int_{\text{many cycles}} \cos(2\pi ft) r1(t) dt +$$

$$\beta_2 \cos(\vec{V}_2, \vec{n}(t)) x \int_{\text{many cycles}} \sin(2\pi ft) r1(t) dt$$

$$= \beta_1 \cos(\vec{V}_1, \vec{n}(t)) x \int_{\text{many cycles}} \cos(2\pi ft) \sin(2\pi ft) dt +$$

$$\beta_2 \cos(\vec{V}_2, \vec{n}(t)) x \int_{\text{many cycles}} \sin(2\pi ft) \sin(2\pi ft) dt$$

Because of the quadrature of the two trigonometrical functions driving both magnetic fields the first integral vanishes. The second integral is equal to a constant term plus a time function of double the frequency of the magnetic field. Thus:

$$MV = \lambda \cos(\vec{V}_2, \vec{n}(t)) + \varepsilon(2f) \qquad (*)$$

The first term reflects the orientation of the coil with respect to the field $\vec{H}_2(t)$. Electronically this term is obtained by filtering (smoothing) signal (*). If the reference function is chosen to be $r2(t) = \cos(2\pi ft))$ then $\cos(\vec{V}_1, \vec{n}(t))$ would have been obtained instead, that is the relative orientation of the eye coil with respect to $\vec{H}_1(t)$.

The circular symmetry of coil C shows that a rotation around its principal axis NN' (figure 2.4B) will leave all the magnetic fluxes unchanged. Thus a recording system based on <u>two</u> magnetic fields and <u>one</u> eye coil C would be "blind" to rotations around the principal axis of symmetry of C. If a second coplanar eye coil C2 is attached to C as to be perpendicular, the problem is solved. Rotations around NN' while leaving unchanged the fluxes traversing C would change the fluxes through coil C2.

Thus by simultaneously monitoring the emf induced in coils C and C2 it is possible to know the orientation of the reference frame induced by the two eye coils.

In practice all the mathematical analysis outlined here is embodied in electronic circuits that automatically perform analog approximations to the procedure of integration and selection. Currently commercially available circuits boards, known as "phase detectors", perform all the functions required for Phase Lock Amplification. These circuits accept two inputs, one is the emf(t) signal and the other the reference signal, and give an output proportional to $\cos(\vec{V}_2, \vec{n}(t))$. One important restriction is that $\vec{n}(t)$ must change slowly when compared with the magnetic field. The step (*) is done by an electronic "low-pass" filters that clips out all the high frequencies found in the signal MV attenuating the term $\varepsilon(2f)$ 70-90 dB with respect the first term of (*).

Thus, in order to ensure that the method outlined gives a correct eye position two conditions must be fulfilled: $\vec{H}_1(t)$ and $\vec{H}_2(t)$ must be perpendicular and continually in temporal quadrature. Another condition is that the intensity of both fields must be high enough to assure a good signal/noise ratio. It must be noticed that the method outlined gives the relative orientation of coils C and C2 with respect to fields $\vec{H}_1(t)$ and $\vec{H}_2(t)$ a further step, explained in Appendix A, is necessary to obtain the coils' orientation with respect to an external reference frame like the orbit or the head.

In this set up, two eye coils were attached in the chicken's left eye. Ideally one eye coil, C1, was in plane **Y'Z'**, the other, C2, in plane **X'Y'** (see figure 2.1 for conventions). The emf of coil C1 was "phase compared" (or "phase detected") against a magnetic field in the direction **OY'** and against a field in direction **OZ'**. The emf of coil C2 was compared against a field in direction **OY'**. Thus the phase detectors provided three outputs:

$O_1 = f_1(\cos(\vec{n}_1, \vec{V}_{ox}))$ "vertical" output

$O_2 = f_2(\cos(\vec{n}_1, \vec{V}_{ox}), \cos(\vec{n}_1, \vec{V}_{oy}))$ "horizontal" output

$O_3 = f_3(\cos(\vec{n}_1, \vec{V}_{ox}), \cos(\vec{n}_1, \vec{V}_{oy}), \cos(\vec{n}_2, \vec{V}_{oy}))$ "torsional" output

The outputs O_1, O_2 and O_3 represent eye position in an approximate form. The mathematical transformations upon these 3 outputs in order to obtain the real eye position in Ficks coordinates are explained in Appendix A.

Implementation of the driving magnetic field

Two pairs of square coils, 0.8 m by side and made of 40 turns of multistranded 18 gauge wire, were placed on four faces of a 0.8x 0.8x 0.8 m cube. One pair was placed on the "top" and "bottom" faces, while the other in the "east" and "west" faces (figure 2.5). The two members of each pair were connected in parallel between themselves and with a high voltage capacitor (C=0.022MF, V=600 volts) to form a LCR circuit. Both pairs of coils were handmade and optimized to have the same resonant frequency, f=29.4 KHz. Each pair of coils was then driven by a high power, wideband amplifier (Hafler-500) at a power of 200 Watts. The controlling signals to the amplifier were time varying sinusoids produced by a handmade sine/cosine wave generator (Optican et al., 1982) designed to continually maintain, using a feedback mechanism, a 90° phase separation between its two outputs (i.e. the outputs were in "quadrature"). Thus the electrical current in both pairs of coils were:

$$I_1 = A_1 \sin(2\pi ft))$$
$$I_2 = A_2 \cos(2\pi ft))$$

These electrical currents generated time-varying magnetic fields with the same frequency and in temporal quadrature. The spatial description of these two magnetic fields, one for each pair of coils, is complex for a generic point in space, but very simple for the center of symmetry of the cube holding the square coils. Each pair of coils produces, in the center of the cube, a uniform magnetic field parallel to the symmetry axis passing through the centers of the coils. By the principle of superposition these two

magnetic fields are added to create, in the very center of the cube, a field equal to:

$$\vec{H}(t) = a_1 \sin(2\pi ft)\vec{j} + a_1 \cos(2\pi ft)\vec{k}$$

It can be shown (Robinson, 1963) that the field $\vec{H}(t)$ is fairly homogeneous near the center of symmetry. A displacement of 5 cms perpendicular to the axis of symmetry changes $\vec{H}(t)$ by about 3%. Thus the final result of this setup is to create, in the 5 cm cubic region located in the center of symmetry of both pairs of coils, two sinusoidally varying, uniform and perpendicular magnetic fields that are always in temporal quadrature. The feedback technique used to assure a constant phase shift between the two magnetic fields was extremely sensitive to flux changes across the small feedback coils. Thus meticulous care was taken to minimize such changes. All the connecting cables belonging to the feedback portion of the sine/cosine wave generator were shielded with mu-metal magnetic shield and firmly attached. Failure to do so renders the feedback mechanism of the Optican's circuit unstable.

Description of eye coils.

The first application of the scleral coil technique to record the 3 dimensional eye position used a suction (non flexible) contact lens. One eye coil was wound concentric to the pupil. The second eye coil was, in the same contact lens, in the plane **X'Z'** (figure 2.5) (Robinson, 1963). Recently the hard contact lens has been replaced by a more comfortable deformable silicon contact lens (Ferman, Collewjin and Van Den Berg, 1987).

In chickens, where it would be very difficult to fit any type of contact lens, the particular anatomy of the avian eye can be used to attach two eye coils on top of its dorsal aspect. Because the young chicken's eye protudes outside the orbit, its dorsal aspect can be easily accessed by cutting a small flap of skin. Thus a small mechanical assembly can be positioned on top of the eye to support the eye coils. Our eye coils consisted of 10 turns (7 mm diameter) of fine varnished copper wire (AWG 43). Two of these coils were glued together at a right angle. One coil was used to detect vertical and horizontal components of eye position, the other served to detect the

torsional component of eye position. A small glass post glued to the eye served to hold the two eye coils (see surgical procedures).

Calibration of recording system.

Two different types of calibrations were carried out. The first was to calibrate the electronic components of the system. Ideally the system is built in such a way that an eye coil lying in the plane **YZ** (figure 2.5) and rotated around the axis **OY** would only signal a vertical deflection. In practice, this never happens, in effect the temporal quadrature of the two magnetic fields is not perfect. The capacitance and inductance of the "Top/Bottom" and "east/west" coils are not identical, thus they induced different shifts in the electrical currents controlled by the sine wave generator. The two sets of coils producing the driving magnetic fields were not perfectly perpendicular and the woodwork and winding regularity were not identical. These unavoidable deviations can be compensated almost completely by a precise fine tuning of the electronics used in controlling the magnetic fields and in phase detection. The second type of calibration involved the fact that the eye coils were not exactly colinear with the reference frame of the eye defined by the optic axis and the equatorial plane. In such a case an eye rotation around the axis **OY** would erroneously appear as a combination of vertical, horizontal and torsional rotations (see Appendix A).

Calibration of electronics.

The calibration of the electronic part of the recording system was carried out by a functional test of the system. The two eye coils were put in the point **0** (figure 2.5) in such a way that one coil was vertical, exactly lying in plane **ZX**, the other eye coil was horizontal (in plane **XY**). A small galvanometer rotated the eye coils around any of the axes **OX, OY** and **OZ.** Initially a 10° rotation around the axis **OY** was given. This rotation should only be detected by the phase detector giving O_1, the outputs O_2 and O_3 should not detect such movement. If this was not the case, the phase shift between the outputs of the sine/cosine wave generator was changed in order to minimize the amplitude in O_2 and O_3. At the same time the reference signal used to calculate O_3 was slightly shifted to diminish the variations in O_3. The next step was to rotate the eye coils around the **OZ** axis, again in

theory the variations on outputs O_1 and O_3 should be zero. This situation was achieved by shifting the reference signals arriving to both detectors. The final outcome of this procedure was to minimize the cross-talk to 5%, thus a pure 10° vertical movement showed as a 10° vertical movement with 30" horizontal and 30" torsional components. The electronic system (especially the driver circuit for the magnetic field) was sensitive to variations in temperature, thus it was kept turned on for at least two days before each recording session when it was calibrated twice, before and after each session.

Calibration of kinematic errors.

To compensate for the unavoidable offset between the implicit reference frames defined by the eyeball and by the two eye coils C1 and C2, a photographic method based on an idea of Hamada (1984) was used. This method measures the relative position of an object with respect to the pupil. The chicken was fixed in the recording system with its optic axis pointed approximately in the OX direction. A camera (fitted with a macro lens) was positioned with its optical axis pointing in the most probable orientation of the chicken optic axis (65° from the mid sagittal plane and 8° down). The camera had a circular flash concentric to its optic axis. In theory, if the chicken looked directly towards the camera (i.e., the optic axis of the camera and the chicken's optic axis coincide) the image of the circular flash should be concentric with the chicken's pupil, whereas if the eye looked into another direction the image of the flash would not be concentric with the pupil. A series of pictures were taken (72 in each session) so that it was possible to capture some pictures where the eye looked directly into the camera. The outputs O_1, O_2 and O_3 were recorded during each picture so that it was possible to solve the equations that give the horizontal and vertical offsets between the two reference frames. The torsional offset could not be obtained with this photographic method, thus the average of the torsional component of 1000 fixations was calculated. It was assumed that the expected average was 0°, and was corrected by the calculated torsional average. Because the eye coils were put in an orientation as similar as possible to the eye's natural orientation, the effect of this correction was small.

Surgical procedures

Two main surgical procedures were done on each chicken. The first was the installation of a headpiece firmly attached to the skull to permit total control of head orientation during recording sessions. The second procedure, performed two days after the first and two hours before the recording session, was to install the eye coils.

Installation of headpiece.

The mounting of the headpiece was done with the chicken under deep anesthesia (Equithesin: 0.35 ml/100 g supplemented by 0.2 ml/100 g every 2 hrs). The chicken was placed in a stereotaxic instrument with the beak horizontal to approximate a natural head position for an unrestrained chicken. This position was approximately 40 degrees rotated, beak upward, with respect to the position used in the stereotaxic atlas of the pigeon (Karten and Hodos, 1967). After removing a rectangle of skin on the top of the skull and scraping away the periosteum, two T-shaped keyholes (located 15-20 mm apart) were drilled on top of the head, one in each frontal bone, using a small dental drill. The relative positioning of these keyholes was not critical. Into each hole a stainless steel screw (00/90), with the head ground down to 0.1 mm in thickness, was introduced, head down, into the space between the dura and the bone and secured to the bone with a nut and washer using a miniature hex wrench (Small Parts, MT-HW28). The screws and nuts were sterile to begin with and were maintained clean of blood to permit tightening the nut. The headpiece was positioned in between the two anchoring screws and attached to them and the skull with dental acrylic (figure 2.6A), while being held by the manipulator arm of the stereotaxic apparatus. The headpiece stayed firmly in place for at least three weeks.

Construction of headpiece.

The headpiece must be rigid enough to withstand the tension generated by the contraction of the neck muscles during recording sessions without deforming. The headpiece consisted of a rectangular block (13mm x 5mm x 4mm thick) of dental acrylic molded around two stainless steel screws (00/90) 3/16" long which were inserted, 10 mm apart parallel to each other, head side down. The exposed thread of these two screws (3 mm)

was used to fix the chicken head to a stereotaxic device by means of an slender metal attachment plate that contained 2 holes that accommodate the two protruding screws of the headpiece (figure 2.6B). This attachment method provided good immobilization of the chicken's head without producing any discomfort. The headpiece was made by lowering a plate, identical to the attachment plate, with two 3/16" screws fastened to it into soft dental acrylic. After the acrylic set, the nuts were freed and the metal template was detached from the acrylic. The headpiece was carved to the desired rectangular shape using a small grinding tool.

Installation of eye coils.

Two days after the installation of the headpiece the chickens were anesthetized with an approximate gas mixture of: Nitrous oxide (80%), Oxygen (19.4%) and Halothane (0.6%). All local wounds were injected with local anesthetic during this procedure as well as during the recording session. The dorso-equatorial aspect of the eyeball was accessed by cutting a small skin flap and opening the orbit near the dorsal rim. A small patch of sclera was cleared. Gas anesthesia was discontinued and the chicken was left to recover for two hours. The chicken was restrained by putting it inside a sock and attached, via the headpiece, to a specially made head holder device. The left eye was positioned in the center of the magnetic fields and the optic axis was approximately in the **OX** direction. At this point a 4 mm long glass post (0.1 mm external diameter) was glued, with Histoacryl surgical adhesive (Braun Melsungen), to the eyeball approximately perpendicular to the chicken optic axis. The eye coils were attached to the glass post using dental wax of low melting point. To avoid large kinematic errors the eye coils were placed with an orientation as close to the orientation defined by the eyeball as possible.

Data analysis and definitions.

All three outputs from the phase detectors were sampled by a computer at 0.71 msec/sample. A specially made circuit, built by Dr. Chris Harris, detected on line the beginning of each saccade and produced a trigger signal that was used by the sampling program to store 512 points beginning 100 msec before saccade onset. Hundreds of saccades and OKN quick-phases were stored for each chicken. Saccades were obtained by simply

recording the spontaneous eye movements of the chicken. A specially made semi-interactive program permitted, "off line", to select in each saccade the beginning, the end and the peaks of the oscillatory cycles as well as to reject spurious events (the trigger circuit was not perfect) or abnormal saccades (very rare events) by manually moving a cursor on the display of digitized traces. At this stage, using the data obtained from the photographic calibration the data was transformed in order to express eye position in Fick's coordinates. The data transformation, which is essentially equivalent to a change of basis between two reference frames, was done using special programs that require as input the angular offset between the eye coil and the implicit reference frame defined by the eyeglobe. The timing data thus obtained was used to calculate saccade parameters such as net eye displacement, duration, segment amplitude etc.

After the raw data was processed eye position was represented by three numbers: TORSION, VERTICAL AND HORIZONTAL also known as cyclotorsion, elevation and azimuth which were the Fick coordinates of eye position. Any eye position was then unequivocally determined by a triplet of numbers (Torsion, Vertical, Horizontal). In analogy to a cartesian reference frame each one of these numbers is also called a "component" of eye position.

Saccade: Each chicken saccade was distinguished by the presence of oscillations. If a fast (over 100°/sec) eye movement did not show eyeball oscillations it was not classified as a "saccade", but these events were very rare (see Results). The start of oscillations defined the **saccade beginning** and the end of oscillations defined the **saccade end** (figure 2.7). The **saccade duration** was defined as the time between saccade beginning and saccade end. **Saccade amplitude** (sometimes referred to as saccadic displacement) is the amount of rotation expressed in degrees, in 3-D space, to change eye position between the beginning and the end of a saccade. Thus, the amplitude of a saccade was calculated using the Euler-D'Alembert theorem (see Appendix A). A **peak** is the eye position at the peak of each oscillation. A **segment** (or **subphase**) is the eye trajectory between two consecutive peaks. The **first segment** is the segment between the beginning of the saccade and the first peak. The **amplitude of a segment** is the

amplitude of the rotation, in 3-D space, to change the eye position between the peaks defining the segment. Segments are classifiable as **intorsional** if the eye moves toward a more intorsional peak and as **extorsional** otherwise. Saccades can be classified according to the type of the first segment, when the first segment is intorsional the saccade is said to have a **positive(+) sign**, when the first segment is extorsional the saccade has a **minus(-) sign.** It must be emphasized that the Euler-D'alembert's theorem served as basis to define the **instantaneous axis of rotation**. In theory a single rotation is necessary to go from any eye position to any other eye position. This rotation is described by a set of four real numbers: the equation of the axis of rotation (3 numbers) and the magnitude (1 number) (see Appendix A).

Muscle tension measurements

In some experiments the isometric tension generated by the superior oblique in anesthetized chickens was recorded using a purpose built amplifier. The tension transducer was a FT03 (Grass Co.) equipped with "yellow" and "black" springs. The resonant frequency of the transducer in this configuration was 330 Hz and had an output of 1.5 mv/K/Volt applied. The very low sensitivity, essentially 14 μvolts/g, was an unavoidable consequence of the high resonant frequency. A high resonant frequency was opted for in order to be sure that oscillatory records of muscle tension were genuine and not artifacts produced by self-oscillations of the tension transducer. The transducer was incorporated as a branch of an RC Wheastone bridge which was excited by a 4kHz sine wave. The bridge output was amplified by a hand made Phase-Lock amplifier using the same 4kHz driving signal as reference (figure 2.8).

In these experiments chickens were deeply anesthetized with Equithesin (0.35 ml/100 g and supplemented by 0.15 ml/100 g every 2 hrs). The orbit was opened dorsally, as was usually done for attaching the glass post that supported the eye coils, and with great care the insertion of the superior oblique was detached from the eyeball and attached to the force transducer by a silk thread. This manipulation was very difficult because the muscle fibers of the superior oblique at the level of the insertion are very delicate and easily damaged. The muscle was stretched until it reached a normal operating length. During all these manipulations great care was used

in order to free the superior oblique from all the other tissues as well as to not damage its innervation, origin or other extraocular muscles. The muscle tensions were recorded with a Grass polygraph and on FM magnetic tape.

Muscle geometry

To determine the muscle action of the superior oblique the following procedure was used. Heads of four recently killed chickens (3 week old) were placed in the usual orientation in the stereotaxic device. The top and posterior parts of the orbit were carefully removed. This procedure exposed the insertions and origins of the superior oblique, superior rectus, lateral rectus and quadratus. A needle attached to the micromanipulator was used as pointer to measure the coordinates of the insertion and origins of the three visible oculorotary muscles. Unfortunately the insertions of the inferior oblique, inferior rectus and the medial rectus were not visible. During the dissection eye shape was maintained with small injections of saline in the vitreous chamber. To calculate the muscle unit moments (i.e.,. the lines of action of the muscles) the geometrical data about the origin and insertion was used to calculate an unitary vector representing the force produced by each muscle in the eye primary position. The primary eye position was approximated by a) considering the mean angle between the equatorial plane and the midline estimated to be 19° and b) the inclination of the equatorial plane with respect to the horizontal plane estimated to be 8°. Thus the line of actions of these muscles were calculated in the reference frame of the eyeball. Next, a geometrical model of the eyeball was used to obtain an approximate location of the point of application of each force. Because the eye of 3 weeks old chickens is an ellipsoid rather than a sphere a geometrical model of the eye based on published data (Gottlieb, Fugate-Wentzek and Wallman, 1987) was used to approximate the vectors representing the point of application of the force produced by each of the three extraocular muscles. The unit moment vector for the three muscles was calculated as the vector product of the force unitary vector (a normal vector in the direction of the line of action) and the vector between the geometrical center of the eye and the point of application of the force. Thus, if n1 is the vector representing the line of action of the superior oblique and A1 is the vector representing the point of application of the force produced by the superior oblique (i.e., A1 can be interpreted as the average location of the insertion

expressed in the coordinates of the eye, not of the stereotaxic instrument) the unit moment vector is equal to A1xn1.

Visual and auditory stimulation during saccades.

Auditory and visual stimuli, locked to saccade onset, were used to study the "in flight" modifiability of saccades. For visual stimulation, chickens were placed in the center of a striped drum while eye movements were recorded. During randomly selected saccades the drum was briefly moved, 40 msec after saccade onset, for about 90 msec at 40°/sec. Auditory testing was similar but instead of moving the drum a loud sound (150 msec of a 1500Hz pure tone), was given 40 msec after saccade onset. In both types of experiments only the horizontal component of eye position was recorded. The duration of "normal" saccades (i.e. without sensory stimulation during saccade) was compared with "stimulated" saccades.

RESULTS

Properties of fixations

While this thesis is mostly concerned with saccadic eye movements some results were obtained concerning the periods of fixations. Three aspects of fixations were analyzed: a) **the range of eye positions,** b) **the applicability of Donder's law to chickens** and c) **the duration of fixations.** Conclusions were based on 999 consecutive fixations, of the left eye, obtained in each of 14 subjects. To maintain arousal, moving objects or loud sounds were presented to the chickens during the recording time.

Spontaneous oculomotor range

Table 2.1 presents the range of eye positions in the conditions described above. The eye moved approximately (14° Horizontal) x (18° Vertical) x (14° Torsional). Note that the range of torsional eye positions was equivalent to the range of the horizontal and vertical components. While table 2.1 reflects the upper limit of the range for each component, most of the time the eye was maintained in some central part of the spontaneous range. In general, gaze direction remained confined in a small subrange (figure 2.9) of approximately (5° horizontal) x (5° vertical). Qualitative, but extensive, observations indicated that the presentation of a novel static, or moving, object in the periphery of the visual field was not followed by a corresponding shift in the direction of gaze directed towards the object.

Torsion is not functionally related to gaze direction.

The fixation data suggest a lack of coupling between the 3 components of eye position, thus a given gaze direction can be achieved with different amounts of torsion. In other words, Donder's law does not hold for chickens. To demonstrate that torsion was unrelated to the other two components of eye position two methods were used. A qualitative method was to plot the fixation data in a 3-D plotting computer program. Invariably the set of fixations was visualized as a highly scattered 3-D ellipsoid "cloud" indicating the lack of a functional relation among all three components of eye position. A quantitative method, based on the variation

of the density of points at different spatial scales (see Appendix B), was also used to test the validity of Donder's law. The algorithm is an attempt to quantify the "dimensionality" of a set of points by analyzing the local variations in density. Ideally this method should give 1, 2 and 3 for a line, a surface and a volume respectively. For fixation data this analytical method gave 2.74 as its dimension. This value was close to the value 2.86 obtained for 999 randomly selected sets of 3 numbers (figure 2.10).

Duration of fixations.

Fixations lasted approximately 1.5 sec in chickens (figure 2.12 and table 2.2). Fixations of less that 400 msec, or more than 4 seconds, were very rare. For every subject the distribution of fixation durations was skewed towards small values (figure 2.11).

Properties of saccades

Periods of fixations were interrupted by saccades. Chicken saccades always contained between 2 and 6 oscillations of the eyeball and were the only type of fast eye movements seen (figure 1.3 and figure 2.13). During hundred of hours of observations, across many chickens and tens of thousands of saccades, fewer than 10 fast eye movement events which did not present eyeball oscillations were observed. *Flicks* and *impulses* (Nye, 1969), mammalian like saccades or periods of smooth pursuit were never observed in the head-fixed preparation used in this thesis.

Eyeball oscillations appeared during: a) spontaneous saccades b) quick phase of optokinetic nystagmus, c) quick phases of the vestibular ocular reflex. Eye oscillations were a true characteristic of chicken saccades and not an artifact introduced by the recording method or the mathematical transformations done on the data. The effects of such mathematical transformations upon the data are shown in figure 2.13. The top panel (figure 2.13A) is the "raw" data: i.e. the direct output of the phase detectors (O_1, O_2 and O_3 see methods section of this chapter). Two mathematical transformations were done on the data. The first, the goniometric transformation, obtained the position of the eye coils with respect to the reference frame of the laboratory (figure 2.13B). The second, the kinematic transformation, obtained the position of the eye with respect to the eye orbit

and expressed it in Fick's coordinates (figure 2.13C). Because the misalignment between the implicit reference frames defined by the eye and the two eye coils was never greater than 10° the traces in 2.13B and 2.13C are very similar. Thus saccadic oscillations were not an artifact of the recording/correcting procedures.

Chicken saccades were logically decomposed into two parts: a) the **net displacement of the eyeball**, that defined the saccade amplitude and b) **saccadic oscillations**. The strict correlation between *fast eye movements (saccades)* and *oscillations* suggested that oscillations were an integral part of chicken saccades at the same time that justified their name as: **saccadic oscillations.** Each of the two components will be described in term of its amplitude, duration, speed, symmetry and interrelationships.

Properties of the saccadic displacement

Spontaneous saccades, in the head-fixed preparation, produced on average small changes in eye position. Almost a fifth (17%) of saccades moved the eye less than 1° and 85% of saccades moved the eye less than 4° (figure 2.14). The mean saccadic displacement, measured as the 3-D amplitude, of 10 chickens was 2.3° and the median was 3.1°. All chickens presented a similar distribution of saccadic displacements. The mean duration for spontaneous saccades was approximately 170 msec (figure 2.15 and table 2.3). Saccades lasting more than 200 msec were not uncommon while only few saccades lasted less than 70 msec. Some variability of saccade duration existed among chickens, and even for the same chicken on different occasions. The average saccadic speed defined as the saccadic displacement divided by the saccade duration was on the order of 15-30°/sec (figure 2.16). No differences existed between saccades beginning with an intorsional ("Plus) or extorsional subphase ("Minus").

Moreover no relation seemed to exist between net eye displacement (saccade amplitude) and saccade duration, neither between some components of saccade amplitude (i.e. torsional) and duration. Saccades rotating the eye less than 2° lasted well in excess of 200 msec, while 10° saccades were sometimes executed in less than 120 msec (figure 2.17).

Properties of saccadic oscillations.

Saccadic oscillations were mostly cyclotorsional (figure 1.4B and figure 2.13) and always contained vertical and horizontal components when eye position was in Fick's coordinates. Saccadic oscillations with only one component were never seen. As soon as the eye began to oscillate all three components showed the movement and no significant time lags were distinguished. For the first cycles the amplitudes of the three components were, approximately in the proportion 4/2/1 (Torsion/vertical/horizontal) (figure 2.18). The *motion direction* of the three components were strictly linked: a) Intorsional-Upward-Temporalward or b)Extorsion-Downward-Nasalward (figure 2.19). These temporal relations between the three components were a constant property of chicken saccades and identical in all chickens. Saccadic oscillations produced a very definite spiral-like movement of gaze direction (figure 2.20).

Independence between saccadic oscillations and initial eye position

The eye trajectory during saccadic oscillations appeared independent of the initial or final eye positions. Saccades that moved the eye between the same initial and final points could show different number of oscillations and different signs. The saccadic sign (i.e. the direction of first subphase) was unrelated to initial eye position (figure 2.21), as it was homogeneously distributed with respect to the torsional component of eye position. Thus, saccades that began in an extorsional eye position had the same probability of beginning with an intorsional or extorsional subphase and *vice-versa*.

Saccadic oscillations are strictly coupled in both eyes

In contrast to net eye displacement, which could be uncoupled between the two eyes, saccadic oscillations started approximately simultaneously, lasted the same amount of time and were always conjugate. When one eye performed a saccade, the other eye also initiated a saccade beginning in a 6 msec window centered around the starting point and with the same duration. During saccadic oscillations when one eye moved extorsionally the other **always** moved intorsionally and *vice-versa* (figure 2.22). This last relationship was found in all saccades and in all chickens.

Duration of saccadic oscillations

Chicken saccadic oscillations are very stereotyped movements. The oscillatory part of the saccadic trajectory seemed invariant, not changing within or between chickens. The oscillations were approximately sinusoidal with a fundamental frequency of 28 Hz that appeared independent of oscillation amplitude. The inter-peak time changed at most 2 msec across saccades (figure 2.23A).

The subphase duration, excluding the first subphase, was 17-19 msec. In all chickens studied the duration of oscillatory cycles was approximately the same (table 2.4). A definite trend existed in that the duration of subphases changed from 17 msec, during the first oscillatory cycle, to 19 msec in later cycles (figure 2.23B). The average subphase duration was 18 msec which corresponds to a frequency of 28Hz approximately.

Amplitude of saccadic oscillations.

Oscillations reached their maximal amplitude by the second subphase, or half-cycle, and declined as each saccade progressed (figure 2.24 and table 2.5). In general the third subphase was the largest with an amplitude of 8-12°. Later subphases had smaller amplitudes. Subphase amplitude declined with each oscillatory cycle; the final subphases, just before saccade termination, had an amplitude of 2-3°. The decline did not fit an exponential curve, it was slower.

Eye speed during saccadic oscillations.

The eyeball reached very high speeds during oscillations. The speed profile of the *instantaneous speed* (computed at 0.71 msec interval as explained in Appendix A) also showed the oscillatory nature of chicken saccades. The peak speed attained during each oscillation, was approximately 550-700°/sec (figure 2.25) which was reached during the midcourse of each subphase. At the oscillation peaks the eyeball speed approached zero. The *average speed during oscillations* was somewhat lower, in the order of 450-500°/sec (figure 2.26 and table 2.6).

Eye acceleration during saccadic oscillations.

The profile of the instantaneous speed showed that the pattern of acceleration was not the same during all subphases. Two facts were noticed:

a) the highest velocity was not reached at the same moment, after a peak, in all subphases. For subphase #1 the peak velocity was reached 5 msec after its initiation, but peak velocity was only reached 8-10 msec after the peak for subphases #2,3,4 (figure 2.27). But, if the different duration of subphases is used to scale the results, it was found that the peak velocity always occurred at 50% of the duration of the oscillatory cycle. The peak speed was never reached in the first subphase.

b) for subphases 2, 3, and 4 a impulsive event accelerated the eye 6-8 msec after the initiation of the subphase.

Symmetry and homogeneity of saccadic oscillations.

The temporal course of the oscillatory cycles was very similar from cycle to cycle but some definite differences were distinguished. The differences concerned the **different speeds** of intorsional subphases and the different **temporal course** of the first saccadic subphase.

The first subphase was clearly asymmetric according to the direction of the subphase. Extorsional first subphases were faster, larger and shorter than their intorsional counterparts (table 2.7). The duration and amplitude of the first subphase were not free to take any value, as would be the case if the oscillations were analogous to randomly gating a sinewave where the duration and amplitude of the first phase would have an uniform distribution. Instead both parameters approached a normal distribution but with different means depending upon the direction of the subphase. As a general rule intorsional first subphases were longer, smaller and slightly slower that extorsional counterparts. Thus of all the possible values for amplitude and duration that the first subphase could have it appeared to be constrained into two "modes".

For subsequent oscillations intorsional subphases were slightly faster, by 5-10%, than extorsional subphases (figure 2.28 and table 2.8). Of the

first 8 subphases intorsional subphases were faster for subphases 2,3,4,5,6 and 7.

Saccadic oscillations during OKN quick phases.

Quick phases of OKN always contained oscillations with the same properties as saccadic oscillations during spontaneous saccades. The number of cycles, the frequency, the amplitude and speed were similar for saccades and quick phases. The mean amplitude of quick phases was bigger than for spontaneous saccades (figure 2.29). Quick phases of 10-15° amplitude were common during OKN. The duration of quick phases was similar to the duration of spontaneous saccades and it was not influenced by the quick phase direction. The duration of quick phases was not correlated with the net eye displacement (figure 2.30).

The duration of individual oscillatory cycles during OKN quick phases was also approximated by a 28Hz sine wave. The main difference between quick phases and spontaneous saccades was the presence of a systematic shift in eye position (figure 2.31, compare with figures 2.13 and 2.19). For example, during extorsional OKN, quick phases appeared to slowly move the eye towards more intorsional eye positions.

The amplitude and symmetry of oscillations did vary. The subphases that were "pulling" the eyeball in the same direction as the net displacement lasted longer and were larger. For example during extorsional OKN (the quick phases are intorsional) the intorsional subphases were larger than extorsional subphases. If the OKN direction was reversed (now quick phases are extorsional) the extorsional subphases became larger (figure 2.32).

The variations of the amplitude of oscillations during OKN quick phases showed how two movements were superimposed during saccades. One movement was the oscillatory component, the other was a slow change in net eye position. In figure 2.33 the average position of the saccadic peaks have been plotted for quick phases and spontaneous saccades beginning with an intorsional subphase ("+" saccades). The two polygonal lines are rough diagrams of the time course of an "average" spontaneous saccade or quick phase. It appeared that the net eye displacement during OKN quick phases

occurred gradually. This result could be an artifact of the averaging techniques used to generated the polygonal lines thus it must confirmed using other techniques.

Mechanical action of three extraocular muscles.

The pulling direction of three extraocular muscles were measured in four chickens (only left eyes were used). Table 2.9 shows the mean values of the following parameters: a) angle between equatorial plane and midline, b) length of muscle, c) position of origin, d) position of the anterior part of insertion, e) position of the posterior part of insertion, for the Superior Oblique, Lateral Rectus and Superior Rectus. A coordinate system was defined for these measurements by using the highest point of the equatorial plane as origin (i.e. as point (0,0,0)) and a Cartesian system aligned to the axis of the stereotaxic. The insertions in all these muscles were wide, in the order of 4-7 mm, and very fragile and the origins were found around the optic nerve.

The geometrical data served to calculate: a) the "line of action" (i.e., the pulling direction) of these muscles in the coordinates of the eye, b) the point of application of the force, in the coordinates of the eye, produced by those muscles and c) by combining a) and b) the unitary moments (i.e. the torques) produced by these muscles. While quantitative data was not obtained for the Inferior Oblique, Medial Rectus and Inferior Rectus it was possible to give a qualitative assessment of their mechanical action. As explained in the methods section the calculation of a muscle unit moment requires some model of the eye shape and of the relative position of the eye in the primary position with respect to the orbit.

Table 2.10 shows the mean values of the unit moments for the Superior Oblique, Lateral Rectus and Superior rectus. As a right hand coordinate system was used, elevations of the eyeball are negative numbers, intorsions and abductions are positive numbers with this convention. For every muscle the primary mechanical action is in accordance with the pattern generally found among vertebrates; the Superior Oblique produces an intorsion and the Superior Rectus an elevation. The secondary action of the Superior Oblique is an elevation, for the Superior Rectus it is an

extorsion. The mechanical action of the Medial Rectus, the Inferior Rectus and the Inferior Oblique were not quantified but qualitative actions were deduced. Based on the relative positioning of the origins and insertions, the main actions of the Inferior Oblique are extorsion and depression. In the case of the Inferior Rectus and Medial Rectus the main actions are depression and adduction respectively.

Instantaneous axis of rotation during oscillations.

To further quantify oscillations, the **instantaneous vector of angular speed** during oscillations was calculated in two chickens (see methods and Appendix A). Every uniform rotation, big or small, can be described in terms of the axis of rotation (Euler-D'Alembert theorem, Appendix B) and its magnitude. Thus the instantaneous vector of angular speed has the direction of the axis of rotation and a magnitude equal to the value (in radians) of the rotation. This interpretation of rotations has the advantage that it permits to compare two rotations even when the initial position of the eye differ. During each saccade, the eye position at two successive moments (0.71 msec apart) were used to calculate the instantaneous axis of rotation. The following procedure was used to calculate the mean of the instantaneous axis of rotation during saccades (50 saccades in two chickens).

During each saccade the instantaneous axis of rotation was calculated 0.71 msec apart. On average 250 vectors were obtained from each saccade, from this set of vectors were eliminated the vectors representing the peaks of oscillations as they are not representative of the oscillations, their magnitude is very small. This elimination was simply done by ignoring vectors with a small amplitude. Furthermore, the vectors representing extorsional cycles were mathematically inverted in order to appear as being produced during intorsions. After this manipulation the set of vectors was used to calculate an average instantaneous axis of rotation for this saccade. The procedure was repeated for the rest of the saccades and this family of "average instantaneous axis of rotation" was used to calculate a grand average and a dispersion. For both chickens it was found that the average instantaneous axis of rotation were totally circumscribed to spherical section of 4° x 9°. Thus, during oscillations the axis of rotation stayed in a small conical section. The population of vectors was described by an average across

oscillations and saccades for the two chickens. The average direction of the vector of angular speed was spanned by the vector :

$$\vec{L} = 0.9\vec{i} - 0.4\vec{j} + 0.15\vec{k}$$

$$\vec{L} = 0.88\vec{i} - 0.44\vec{j} + 0.14\vec{k}, \quad \textbf{Chicken\#1}$$

$$\vec{L} = 0.91\vec{i} - 0.36\vec{j} + 0.15\vec{k}, \quad \textbf{Chicken\#2}$$

This line, which is expressed in the coordinate system of the eye, implies that the rotation is mostly a rotation around the axis **OX' (i.e. close to the optic axis)** (see figure 2.1). The angular speed vectors were also calculated in the orbit reference frame. The relative dispersion between the eye and orbit descriptions of these vectors were compared. In both descriptions a similar degree of dispersion was observed.

The point in the retina which is located along the instantaneous axis of rotation experiences zero tangential velocity. Because of the natural dispersion found among angular speed vectors, this retinal point also changed moment by moment but always stayed in a spherical section of 4° x 9°. By using the average direction $\vec{L}$ it is possible to calculate, for each chicken, the retinal region Ω that on average senses the least amount of rotation during oscillations. All other retinal points experienced an angular speed proportional to their distance to the region Ω (figure 2.34).

The approximate location of regions Ω in the retina, with respect to the tip of the pecten, was evaluated. In two anesthetized chickens, different from the chickens were Ω and $\vec{L}$ were calculated, the relative position of the line joining the center of the pupil and the tip of the pecten ("pecten axis") with respect to the optic axis was measured. In these chickens the pecten axis was 8.5° nasally (N=2, 10° and 7° nasal) and 17.5° upward (N=2, 15° and 20° upward) from the optic axis. This angular data, plus the known dimensions of the chicken eyeball, were used to calculate the coordinates of the dorsal tip of the pecten on the retina (figure 2.34) (a small effect was not taken into account in this calculation. Because the "pecten axis" was measured using an external optical instrument it really does not intercept the tip of the pecten on the back of the retina. Instead it intercepts the image of the tip of the pecten. The spatial difference between the image and the real

object can be calculated using the properties of the nodal points of the schematic eye of the chicken. A quantitative argument indicates that an overestimation is done of the distance between the tip of the pecten and the posterior pole of the eye is done when the optical aspects just mentioned are ignored)

It was found that Ω is located at 1.5 mm from the pecten tip along a line following the ventro-dorsal plane of the pecten on the retina. In figure 2.34 the data concerning the Ω regions and the "pecten axis" are plotted together and with a line representing the average position and orientation of the pecten in the left eye of chickens.

Contraction pattern of superior oblique muscle.

The direction of the axis of rotation during oscillations suggested that, of the six extraocular muscles, the two obliques played a prominent role in producing oscillations. If the superior oblique was deafferented, by cutting its nerve supply, the trochlear nerve, (3 chickens) or detaching its insertion on the dorsal aspect of the eye globe (1 chicken), oscillations were clipped of their intorsional half but maintained the 28Hz fundamental frequency. If the inferior oblique was sectioned, the extorsional half of oscillations disappeared (2 chickens). When both obliques were simultaneously disabled (2 chickens) saccadic oscillations decreased to less than 5% of their normal amplitude (figure 2.35). In all these lesioning experiments the initial manipulation was done under anesthesia and eye movements recorded two days later.

The tension generated by the superior oblique in an acute experiment was recorded. In a deeply anesthetized chicken, which continued to perform 1-2 saccades per minute, the superior oblique was carefully detached from its insertion on the dorsal aspect of the eyeball. Care was taken not to damage its origin, nerve supply or the other extraocular muscles. The tendon was attached to a force transducer and the tension recorded on a polygraph. The pattern of force over time was itself oscillatory and had the same frequency as eyeball oscillations (figure 2.36).

Saccade shortening by sensory stimuli given during saccades.

Saccades in chickens were shortened by visual or auditory stimulation given at mid course. Saccades duration was measured in two conditions: a) the visual field was briefly rotated during saccades and b) a loud sound was given during saccades. These two stimuli were randomly given in some saccades ("stimulated saccades") during the rest of saccades no stimuli were given ("control saccades"). The duration of stimulated saccades was compared against the duration of control saccades. Stimulated saccades were shorter ($p < 0.001$, t test) than control saccades (figure 2.37, table 2.8A and table 2.8B). Saccades were shortened, on average, by 34 msec when the visual field was moved and by 52 msec when a sound was given. While "stimulated" saccades were shorter than "control" saccades no differences were detected in the magnitude of their horizontal displacements.

Discussion

The experimental results described in this chapter help to characterize behavioral aspects of the chicken's oculomotor system. While the principal aim of this study was to clarify important questions related to saccadic oscillations data was also gathered about the periods of fixations. Thus the discussion of the results will be divided in two sections: one devoted to fixations, the other to saccades. But the implications of the head fixed preparation must be explored. It can be argued that all the results obtained do not reflect the normal operation of the avian oculomotor system because the head fixed situation is a very unnatural one for chickens. Rabbits, for example, show very different oculomotor strategies between the natural and the head fixed situation (Collewijn, 1977). It must be noticed that saccadic oscillations are not an artifact due to restraint. Saccadic oscillations have been detected in awake unrestrained chickens (Pratt, 1982) and 28Hz contractions of the superior oblique were also detected in the anesthetized preparation.

Properties of fixations in chickens.

Observations of eye position during fixations indicate that the torsional component is independent of the horizontal and vertical components and has an equivalent range. The spontaneous range of eye

positions in the head-fixed chicken may be visualized as a "cube" of 15° on each side. Furthermore the amplitude of quick phases during OKN (figure 2.29) shows that 15° eye movements are possible in chickens. The spontaneous range of fixations, and the amplitude of quick phases, show Chard and Gundlach's notion (Chard and Gundlach, 1938) based on morphological considerations, about the non-existent avian eye movements to be incorrect. Although, 85% of saccades move the direction of gaze in a small conical region of 4°, this restricted range of movement reflects an oculomotor strategy rather than the existence of mechanical constraints. During OKN gaze performs regular and wide excursions of 15-20°. The chicken eyeball is thus capable of moving inside the orbit despite the mechanical constraints present inside the avian orbit.

The wide range of the torsional component of eye position could be related to the lateral placement of chicken's eyes. Torsional eye movements could be required to follow objects moving in the frontal visual field. However, in chickens the movement of objects in the binocular field does not trigger tracking movements in any consistent manner. Furthermore most of the time the eye remains within in a small subset of the spontaneous range such that gaze direction stays in a (5°horizontal) x (5°vertical region).

In primates Donder's law is valid, i.e. for every gaze direction a vertical line in the visual world is always mapped onto the same retinal position. In chickens, the independence of the torsion, from the horizontal and vertical components, imposes special problems for the visual system in the determination of the absolute orientation of borders found in visual scenes. For every gaze position a vertical line in the outside world can be mapped into many retinal images depending on the amount of torsion. Thus an extra step must be made by the visual system of the chicken to determine the real orientation of the image falling onto the retina.

Recent experiments show Donder's law to be approximately valid for humans (Ferman, Collewjin and Van Den Berg, 1987), although irregular deviations of approximately 5% exist in every human. These deviations are not totally random as they are minimal when the eye in the primary position and grow with more eccentric positions, but at any given eye position the deviations are not deterministic. Non-deterministic deviations in the degree

of torsion create an interesting problem from the standpoint of visual perception. In effect, how is it possible to the visual system to compute the real orientation of borders in the visual image if the retina can "wobble" in an uncontrolled way? It can be argued that the visual system of primates does not calculate the absolute orientation of borders, only their relative orientation. Thus a small uncertainty in the degree of torsion could be tolerated because the relative orientation of borders is independent from the degree of torsion. But recent psychophysical experiments in humans (Haustein and Mittelstaedt, 1990) show that the visual system can compute the absolute orientation of borders, true vertical lines are detected against uniform backgrounds. This ability depends on the strict correspondence between gaze direction and the degree of torsion. It seems that this ability of detecting the absolute orientation of borders uses some type of *efference copy signal,* from the oculomotor system, into the visual system to compensate for the deviation from Donder's law.

In chickens, deviations with respect to an ideal Donder's law are much greater than in humans. Deviations are of the same order of magnitude as the 15° torsional range, thus it is misleading of refering to "deviations"; it is more accurate to say that torsion is not a function of the direction of gaze. Two eye positions with the same horizontal and vertical components can differ by 10° in their torsional components. Again it can be argued that the uncertainty about the absolute orientation of borders is not a real "problem" for the chicken's visual system. But it can be assumed that for birds, flying animals, it must be important to asses the true orientation of borders with respect to gravity. Thus if chickens, like humans, are to detect the true orientation of borders their visual system must perform similar operations as in humans but with the added complexity that these operation must take into account the degree of torsion.

Eye movements and the binocular field.

Diverse studies (Martinoya, Rey and Bloch, 1981; Martin, 1986a; Martin, 1986b) have shown that birds with laterally placed eyes have a crescent shaped frontal binocular visual field. The binocular field projects upon an area called the "red area", because of the accumulation of "red" oil droplets, on the dorsal retina. It has been argued (Martinoya, Rey and

Bloch, 1981) that the binocular field mediates stereopsis in birds by a mechanism based, as in mammals, on retinal disparity. The small periprimary range, the non-validity of Donder's law and the fact that the two eyes do not always move in a conjugate way are factors that might reduce the contribution of the binocular field to a depth perception mechanism. The extent and shape of the binocular field are continuously changing. The amount of overlap between the right and left monocular visual fields changes from fixation to fixation. The binocular field, which is the intersection of both monocular fields, changes accordingly. Because both eyes do not move in a conjugate manner these changes can profoundly affect the size and shape of the binocular field. Unfortunately simultaneous 3-D recordings of both eyes were not done in this thesis, so a precise picture of the variations of the binocular field over time is not available. But a quick calculation gives a qualitative idea of the expected changes in the shapes of the binocular field. The binocular field covers 10° at its widest point. If this measurement was taken with the eye in the middle of its normal oculomotor range lower and upper bounds can be calculated for this dimension. If both eyes converge 7° (1/2 of their usual horizontal range) the amount of overlap would be about 24°. On the other hand if both eyes diverge by 5° from the average position the amount of overlap would be 0°. Similar arguments hold for the vertical extension of the binocular field. Thus the amount of overlap will depend on the eye positions of the two eyes but it will vary between 0° to 30°.

Beside the amount of overlap between the two monocular visual fields their relative orientation must be considered (figure 2.38). One hidden assumption behind the concept of the "binocular field" is that an object located in that field generates retinal images in *corresponding* retinal locations. The assumption of retinal correspondence between the left and right retinal images of a single object lies at the center of the mechanism for stereopsis found in mammals. In chickens the independence of the positions of both eyes and the fact that the amount of torsion is not specified by gaze direction introduce further complications in solving the correspondence problem. To produce such a correspondence, the visual system would have to take into account the degree of torsion of both eyes. Thus if the "binocular field" really mediates stereopsis in chicken the mechanisms must

be necessarily be more complex than in mammals. One possibility is that the visual system of chickens can be in different "modes" with respect to depth perception, thus during certain periods where stereopsis is desirable the eyes can adopt a concordant orientation for binocular vision.

Mean duration of fixations

The mean duration of fixations across chickens seems to be fairly similar (figure 2.12) approximately 1400 msec, compared with the 300-600 msec found in humans (Enoch, 1959). This long duration of fixations, when compared to humans, can be interpreted as a manifestation of the low "desire" of chickens to explore their visual surroundings by means of changing the direction of gaze. Unfortunately the consequences upon fixation duration of different visual environments were not explored. Thus it can not be asserted if fixation duration changes according to the type of visual scene as it has been reported for humans (Enoch, 1959; Harris, 1989). But undoubtedly some factors, which can be visual or intrinsic (like fatigue), do affect the mean duration of fixations.

Saccades are usually small in chickens.

Smooth pursuit-like eye movements were not found. The existence of this reflex was tested in various chickens by moving, by hand or with a galvanometer, small and high contrast visual targets in various directions. The lack of smooth pursuit could be related to the "panoramic" retina of chickens. Also *flicks* and *impulses* (Nye, 1969; Steinbach, Angus and Money, 1974) were not observed. In hundreds of hours of recording fewer than 10 of such events were observed. Perhaps *flicks* and *impulses* were themselves artifactual as they were described in a semi anesthetized preparation where the nictitating membrane was cut. The complex trajectory of the eye during saccades is not a simple function of the initial and final positions. Saccades with the same starting and finishing positions can have totally different trajectories as the direction of the first subphase as well as the number of cycles could be different.

In the chicken, most saccades are small: 85% of them move the eye less than 3 ° and almost a fifth of saccades leave the eye in the same initial position. Furthermore the real change in gaze direction is less than the

saccade amplitude because the latter includes changes in torsional position which leave gaze direction unchanged. In fact the median change in gaze direction is 2° (while the median saccade amplitude is 3.1°). Thus 75% of saccades change the direction of gaze by 4° or less (figure 2.39). The low amplitude of chicken saccades is not an intrinsic property of their oculomotor system as 15° OKN quick phases demonstrate. This small average amplitude of chicken saccades has profound implications for understanding the functional role of avian saccades. The small amplitude of chicken saccades is not compatible with them being part of a mechanism to increase the resolution (acuity) of the visual image. The uniform retina of chickens is such that a 2-3° change in gaze direction does not change dramatically the grain of the retinal image (figure 1.5). For example, a 3° change in gaze direction changes the density of ganglion cells of the retinal patch receiving the visual image by 8% only. An equivalent change in gaze direction in primate changes the density by 50%. Furthermore, qualitative but extensive observations indicate that the presentation of visual objects does not trigger a saccade directed toward them in chickens. Thus it must be concluded that avian saccades, at least in the head-fixed preparation, could not be part of an oculomotor strategy that optimizes the resolution of the images of "interesting" objects. Perhaps saccades are part of a "foveating" mechanism in the unrestrained subject in conjunction with head movements.

Saccade duration.

Almost all chicken saccades last more than 100 msec and are much longer than their counterparts in primates. Furthermore chicken saccades are such that their duration is not a function of their amplitude. Small saccades can last as long as large saccades. The duration is a strict function of the total numbers of oscillations, not of the saccadic displacement, which is in general very small. Interestingly the same lack of relation exists for OKN quick phases. Finally, it seems that saccade duration might be influenced by attentional mechanisms as the mean saccade duration can change for a chicken in between recording sessions. However the difference in duration is totally due to the difference in the numbers of oscillatory cycles in each saccade and not to the duration of each cycle.

Properties of saccadic oscillations.

Saccadic oscillations are an integral part of chicken's saccades and quick phases. The temporal organization of oscillations shows little variation within or between chickens. While the data collected does not clearly solve the outstanding problem of the function of oscillations it clarifies the motor mechanisms producing oscillations.

Mechanism of production of oscillations.

Four lines of evidence indicate that saccadic oscillations are actively produced by the two oblique muscles: a) the lesion experiments in which one or the two obliques were disabled, b) the recording of the tension produced by the superior oblique during saccades, c) the instantaneous axis of rotation during saccades and its similarity with the (calculated) axis of rotation of a pure contraction of the obliques and d) the symmetry between intorsional and extorsional subphases. The most direct evidence is the almost total disappearance of oscillations when the four recti are left intact and the two obliques disabled. Furthermore, at least in the case of the superior oblique, the pattern of force developed during oscillations has the same temporal structure as saccadic oscillations. The final argument concerns the geometrical disposition of the obliques. The mean axis of rotation during saccades, a line close to the optic axis, corresponds approximately to the line of action of the obliques (table 2.10). These facts when taken together show that oscillations reflect contraction/relaxation pulses of both obliques occurring 18 msec apart from each other during saccades (figure 2.40). Intorsional subphases are produced by contractions of the superior oblique, extorsional subphases by contractions of the inferior oblique.

The fact that all saccadic oscillations have vertical and horizontal components may depend on the geometrical disposition of the obliques. For example, the plane containing the origin and insertion of the superior oblique is not perpendicular to the optic axis, thus when the superior oblique contracts it also elevates and abducts the eye. A concordant piece of evidence is the relation (angular offset) between the average instantaneous axis of rotation and the torque produced by the superior oblique. The moments produced by the superior oblique give directly the rotation axis

induced by its contraction: $\vec{L}_{oblique} = 0.71\vec{i} - 0.63\vec{j} + 0.3\vec{k}$. The average instantaneous axis of rotation $\vec{L}$ calculated using kinematical data is ($\vec{L} = 0.9\vec{i} - 0.4\vec{j} + 0.15\vec{k}$), thus he angle between these two axes is: α=19°. Thus the contraction of the superior oblique gives the correct qualitative direction of the axis of rotation (intorsion, elevation, abduction) but with an offset of 19°.

It must be concluded that all six extraocular muscles do not contribute equally to the production of saccadic oscillations. When the two obliques are disabled (figure 2.35) the oscillations lose 95% of their amplitude. The small oscillations left could be due to a) partial reattachment of some muscle fibers of the inferior oblique or b) small contributions of the four recti. While the experiments described in this chapter did not resolve the issue of the contribution of the recti to saccadic oscillations completely, results reported in Chapter 3 will support the option that a small contribution is made by the recti. The imbalance between the contributions of the obliques and the recti could be explained in part by the larger size (muscular volumes) of the obliques relative to the recti (personal observations). Thus the minor contribution hinted by figure 2.35 could reflect the different size of the obliques relatively to the recti rather than qualitatively different mechanical contributions to the movement of the eye during saccadic oscillations. Another fact that hints to a participation of the four recti in generating oscillations is the change in the relative amplitudes of the torsional, vertical and horizontal components as each saccade progresses (figure 2.18). For example, the ratio of the torsional amplitude to the vertical amplitude diminishes; one would expect that if the oscillations were due to the obliques only this change would not occur, but the same ratio would be maintained throughout the saccade. One explanation is that the recti generate a small oscillatory component that is initially masked by the large torsional component. But it is important to emphasize that the heavy numerical treatment of the eye position data (i.e. the correction for "kinematic" errors) could be responsible for the observed change in the amplitude ratio. As the contribution of the recti to the oscillations is an important point to clarify it should be studied further with specially designed experiments. In any case, the result of disabling the obliques (figure 2.35)

shows that mechanically the obliques contribute at least 95% of the power of oscillations. Although the preeminent contribution of the obliques can not be denied, it is possible that the recti generate some 5-10% of the amplitude of oscillations.

A particularly intriguing property of saccadic oscillations is that they seem to be as fast and biomechanically efficient, as the biophysics of muscle contraction permits. Each oscillatory cycle results from activity in one oblique followed half a cycle later (18 msec) by activity in the antagonist oblique. It would be desirable to avoid having one member of the pair stretch the still contracting antagonist: otherwise a part of the energy spent in contracting one muscle would be spent in stretching the active antagonist muscle rather than moving the eyeball. If the duration of a twitch contraction in the chicken superior oblique were similar to that reported for cats, 19 msec (Nelson, Goldberg and McClung, 1986), the 18 msec interval between the contraction of obliques during one oscillatory cycle might be the shortest time to avoid the stretching of an actively contracting muscle (figure 2.41).

Structure of the neural command.

As saccadic oscillations reflect primarily the activity of the obliques details of the neural mechanism controlling these extraocular muscles can be deduced from kinematic eye data. Two mechanisms appear to determine the state of contraction of each oblique. One defines the contraction state during the periods of fixations (*Tonic mechanism*), the other produces saccadic oscillations (*Phasic mechanism*). While these two mechanisms are briefly operative during saccades they seem to be independent or very weakly linked.

Their independence is suggested by the stereotyped nature of saccadic oscillations. Many saccades barely move the eye (i.e. the final and initial positions differ by less than 1 degree), but they show 10-12° oscillations similar to oscillations found in 10° quick phases. Furthermore quick phases that move the eye 15° in the intorsional direction have oscillatory patterns very similar to quick phases that move the eye 15° extorsionally. If the tonic mechanism that produces the net displacement of the eye were to be coupled

to the phasic mechanism greater differences between oscillations in quick phases moving the eye in opposite directions should be expected.

The time course of quick phases provides a second argument in favor of independence between the tonic and phasic mechanisms. During OKN, quick phases (figure 2.33) a slow change in eye position superimposed on oscillations can be detected. This monotonic and slow change in eye position is usually hidden, or absent, during spontaneous saccades as the eye barely moves. Furthermore the amplitude of subphases during quick phases is changed in a particularly informative fashion. When the subphase is in the same direction as the overall pull of the quick phase its amplitude is larger than normal. On the other hand, when the subphase is in the opposite direction than that of the quick phase its amplitude is less than normal (figure 2.32). The above argument can be put in more quantitative terms by plotting the average peak displacement from the initial eye position for spontaneous saccades and quick phases (figure 2.33). For each saccade the displacement between successive peaks and the initial eye position is a coarse measure of the overall eye displacement as the saccade progresses. Figure 2.33A shows that for peak #3 the eye is 3° more intorsional in quick phases than during spontaneous saccades. This difference grows to 6° and 10° for the fifth and seventh peaks respectively. One interpretation of figure 2.33 is that the slow change in eye position found in OKN quick phases is due to a slow increase in the strength of the tonic mechanism that slowly increases the average force developed by the superior oblique. Oscillations are the by-product of the phasic mechanism and their temporal features are affected in a trivial way by the tonic mechanism. Thus, symbolically we can write:

Observed oscillation=(True oscillation) +/- (slow eye mov..)

The lack of correlation between saccade duration and net eye displacement also suggests the independence of the two mechanisms (see figure 2.17). Saccade duration is defined by the number of oscillations found in the saccade or the quick phase; thus it is a parameter that depends on the phasic mechanism. On the other hand the saccadic displacement is the manifestation of the tonic mechanism.

Finally, the fact that oscillations, but not saccadic displacements are yoked for the two eyes also argues for the independence of these two mechanism. Saccadic oscillations in the two eyes begin within 2-6 msec of each other, have the same number of cycles, are always mirror images of each other even when the net eye displacement is not always correlated.

These observations suggest that the tonic and phasic mechanisms need not to be coupled. Some inferences about the signal structure of the motor commands controlling the obliques can be made:

a) The phasic input arriving at the superior oblique and the **contralateral** inferior oblique appear to be the same. They are temporally similar as they begin and end at the same moment and appear to induce oscillations of similar amplitudes in both eyes.

b) The phasic component arriving at the superior oblique consists of pulses separated by intervals of about 36 msec on average. The pulses have a microstructure. They are not identical. First, the strength of pulses must be correlated with oscillation amplitude, at the same time that the timing between successive pulses must vary to explain the increase in acceleration hinted by figure 2.27.

c) The tonic mechanism is the only mechanism active during fixations.

d) The tonic mechanism is also active during saccades and controls the net eye displacement. During intorsional saccades it is gradually engaged, it produces small displacements for peaks 1 and 2 but corresponding larger displacements are produced for peaks 3,4, etc.. (figure 2.33).

All these features point to an organization of the avian oculomotor system that substantially differs with respect to mammals. This conclusion is different from the one found by McVean and Stelling (1986). These authors conclude, after analyzing eye movements induced by electrical stimulation of the abducens nucleus in the anesthetized pigeon, that pigeons have an oculomotor organization similar to cat's. But, in light of the data

just presented, electrical stimulation of the abducens nucleus of anesthetized subjects would left untouched the neurons involved in producing oscillations, as they are present in the motor pools controlling the obliques.

Hint of a central pattern generator.

One possible explanation of the stereotyped temporal course of saccadic oscillations is that a **CENTRAL PATTERN GENERATOR (CPG)** is involved in their generation. Saccadic oscillations have three characteristics consistent with a CPG: a) alternate contraction of agonist/antagonist muscles, b) stereotyped behavior and c) relative immunity to sensory input. Further evidence of a CPG is the strict yoking of the two eyes during oscillations.

Saccadic neural command is affected by visual and auditory inputs.

An important property of avian saccades is their modifiability by sensory stimulation in midcourse. In cats a similar modifiability exists, a strong flash given during saccades near the area centralis stops saccades in midcourse (Evinger, Kaneko and Fuchs, 1982). This stopping action appears to be due to the visual properties of omnipause neurons located in the brainstem, which inhibit the saccadic machinery (Scudder, 1988). However, in humans and monkeys saccades appear to be less susceptible to midcourse modification. Target disappearance or flash presentation of a new target do not modify an already outgoing saccade (Hallet and Lightstone, 1976). In double steps experiments where the first step is short, saccades appear to be modifiable in humans (Lévy-Schoen and Blanc-Garin, 1974), but it have been argued that this situation is due to 2 successive saccades happening with no intersaccadic interval (Becker and Jürgens, 1979) rather than an "on flight" modification of the initial saccade. The difference in this respect between primate and cat saccades could be due to different properties of Omnipause neurons in those species; in primates these neurons are not visually sensitive (Evinger, Kaneko and Fuchs, 1982; Sparks, Mays and Porter, 1987). Perhaps the difference between chickens and primates with respect to the "in flight" modifiability of saccades is a reflection of the longer duration of avian saccades. In primates almost all saccades are executed in less than 80 msec, thus when visual retinal activity arrives to the oculomotor machinery the saccade is already finished. In

chickens, where the average duration of saccades is 180 msec, visual activity can interact with the saccadic machinery.

The shortening of chicken's saccades when the visual world is transiently moved during saccades (figure 2.37) shows that their visual system can detect a small movement superimposed upon the larger optic flow induced by the oscillations. One interpretation of the shortening of saccades is that the visual system detects a small movement in the scene. As this movement was not present at the onset of the saccade, the appearance of this sudden movement is interpreted as an abnormal situation and the chicken stops the saccade to "check" the situation.

The "in flight" modifiability of chicken saccades suggests several interesting points. First, the idea of a central pattern generator commanding the saccadic oscillations should be modified. The central command interrupting the saccadic machinery could be triggered by perceptual events. The fact that a small rotation of the visual field, during saccades, is perceived by the chicken is interesting by itself. During these experiments the angular speed of the drum was 10% of the maximal speed reached by the eye during oscillations. It could be that the visual system of the chicken detects the movement of the drum during the brief periods in each oscillation where the speed of the eye approaches 0 deg/sec (i.e. at the peak of each oscillation). Another possible explanation is that the visual system of the bird is equally sensitive to movement all along during each saccadic oscillation and somehow it manages to extract from the optical flow the components induced by a real movement of the world from the one endogenously produced by the oscillation of the eyeball. This fact will be used in Chapter 3 to construct a theory about the physiological role of saccadic oscillations.

CHAPTER THREE

MOTOR ORGANIZATION OF THE TROCHLEAR MOTOR POOL IN THE CHICK

Introduction

Avian saccadic oscillations are mostly produced by a sequential series of contractions/relaxations between the two oblique extraocular muscles. This is the main result derived from the previous chapter. The sequence of contractions that every oblique undergoes during saccades cannot be produced by motoneurons having the "pulse and step" activity profile found among mammalian, or teleostian, extraocular motoneurons. To investigate the properties of the avian motoneurons generating saccadic oscillations, recordings from trochlear motoneurons in awake chickens were made.

The results obtained in this chapter clearly indicate that two functionally distinct types of motoneurons exist in the chicken's trochlear nucleus. One class of motoneurons controls the eye during the periods of fixation, or when the eye moves at low speeds. The second class is only involved in the generation of saccadic oscillations. "Pulse and step" (i.e., "burst-tonic") responses were not found inside the chicken trochlear nucleus. This strict and clear functional segregation found among trochlear motoneurons has at least two important theoretical consequences. One consequence concerns the input homogeneity implicit in the size principle. A unifying principle of vertebrate motor control states that all the motoneurons belonging to the same motor pool are "essentially identical" in their activity profile; a fixed and invariant recruitment order exists among the motoneurons forming a motor pool. No functional segregation of motoneurons exists. The second consequence concerns the physiological organization and anatomical connectivity of brainstem neural circuits controlling fast eye movements. The existence of two apparently functionally disconnected populations of motoneurons to control a single muscle renders inapplicable to birds one of the principal results deduced from mammalian data that the "step" component of a response is the integral, in the mathematical sense, of the "pulse" component (figure 1.5).

While the results and interpretations obtained in this chapter can be focused in the framework of oculomotor organization only, a more interesting path is to interpret them in the expanded framework of motor control. In effect, the study of the extraocular muscle system is an example of how coordination is achieved between many muscles to produce a coherent behavior.

Vertebrate motor control.

The problem of motor control can be subdivided in two parts: a) the control of the force produced by a single muscle and b) the temporal and functional coordination between synergistic muscles to produce a coherent movement.

Control of the force developed by a muscle.

The control of the force produced by a single muscle is based on a strategy of activating the muscle fibers in an invariant order. Every skeletal muscle is composed of many motor units. Each motor unit is driven by a single motoneuron and contains many muscle fibers not necessarily anatomically contiguous. The overall active force developed by the muscle is the sum of the individual forces produced by each muscle unit. Not all muscle units are similar; they differ in the number and type of muscle fibers they contain (Burke, 1990; Nemeth, 1990). These anatomo-physiological differences imply that at supramaximal stimulation not all motor units produce the same level of force. The great number of motor units in a muscle and their intrinsic variability with respect to force generation and fatigue resistance indicate that the total force produced by a muscle could be produced by activating different sets of motor units at different levels of stimulation. The set of states that a muscle can adopt is, in theory, staggeringly large. If a muscle contains N motor units and the firing rate of each motoneuron can be controlled in **m** steps between 0 and the maximal stimulation, then $\sum_{k=1}^{Nm} \frac{Nm!}{k!(Nm-k)!}$ states are possible. A small muscle with 10 motor units, each of which can be stimulated in 10 steps would have 10^{30} states. Of course many of these states would be equivalent with respect to

the force output, as many combinations of motor units and their level of innervation would be equivalent.

Of this vast universe of states, each muscle adopts only a small fraction. In effect, a fixed order exists in the use of motor units. When the muscle goes from 0% to 100% of the maximal force, a definite order exists in the activation of motor units, a phenomenon called "orderly recruitment". As a first approximation, the output force is increased by activating motor units in a strict and unchanging sequence. The force output is decreased by deactivating motor units in the inverse sequence. Force output can also be changed by varying the frequency of the motoneuron driving each motor unit. This strategy (called "rate modulation") is superimposed on the orderly recruitment of motoneurons and plays a second order effect in spinal muscles. How the nervous system implements a single strategy to control every muscle is not clear, but the combinatorial problem of controlling the motor units individually is solved by the use of a control strategy relying on a single activation order among motor units.

Organization of spinal motor pools

Mammalian skeletal muscles are organized in such a way that each muscle fiber is only innervated by one and only one motoneuron. Thus the activation state of the muscle fibers in a motor unit is a direct consequence of the stream of action potentials travelling on the axons of the motoneuron innervating the muscle fibers. Thus recruitment can be studied at the level of the activation of the motor pool controlling a given muscle. The best studied examples are among "segmental muscles"(i.e. muscles belonging to the limbs and which have their motoneurons in the spinal cord).

Spinal motoneurons receive three afferent systems: a) the direct proprioceptive input, b) the input from spinal interneurons and c) the input from central (descending) sources. These three inputs form the *total activation* received by motoneurons. It has been postulated (Henneman, Somjen and Carpenter, 1965) that the uniform order of recruitment is a consequence of: a) the homogeneity of the input received by all motoneurons in a given pool and b) the different soma sizes among motoneurons. In this scheme all motoneurons receive the same total

activation (i.e. an identical sum of excitatory and inhibitory signals). Motoneurons with a small soma size would be activated before larger ones as their input resistance is larger. A most important consequence of this formulation is the implicit consequence that motoneurons are not functionally subdivided.

Pattern generators in the spinal cord.

The functional and temporal coordinations of muscle groups, the "second" problem of motor control, are produced by local spinal circuits based on networks of interneurons. These networks generate the fundamental rhythms in movements like walking, running and scratching without the participation of proprioception or descending commands. Thus these spinal networks are an example of neural circuits that are able to generate complex repetitive patterns of activity by themselves; PATTERN GENERATORS (PGs).

Pattern generators are important in our conceptual models of segmental and non-segmental motor systems because they provide the fundamental framework to explain the origin of coordination between many muscles. Initially, it was thought that such coordination was produced by a chain, or chain of chains, of reflexes. Each reflex in such a chain would provide the triggering stimuli for the next reflex in the sequence. Lesion experiments, in which the proprioception for all muscles involved in a given "coordination" was abolished without affecting the overall movement, demonstrated the "chain reflex" model to be incorrect. This simplistic view was replaced by the idea of "organizing centers" that would provide the correct sequence of commands to the different muscles without requiring sensory inputs. Ideally, pattern generators should have the following properties: a) each PG must be made of various interrelated "neural centers", b) some of these neural centers must be active during one phase of the movement and silent for others, c) other centers should have the opposite pattern of activity, d) the pattern of activity of the centers forming the PG must be similar in duration, not only temporally locked, to the different phases found in the movement, e) the PG activity pattern must be modifiable by sensory and descending signals and f) the PG activity must be necessary for the movement to occur and not a reflection of efference copy signals

produced by other neural centers. In vertebrates, the existence of PG has not been proved unequivocally, but solid evidence points to their existence in the spinal cord. Although PGs explain the generation of the basic rhythm found in many real movements (walking, breathing, running, scratching) the synthesis of non-repetitive and novel movements is still unclear. The deciphering of such coordination requires an understanding of how descending signals interact with the spinal interneuronal networks in dynamically shaping the neural output of spinal PGs (Grillner, 1991). It is exactly in the study of this interaction between many muscles that the study of the extraocular system can be very rewarding.

Motor control of mammalian extraocular muscles.

The neural control of mammalian extraocular muscles is similar to segmental muscles but important differences exist. The principal similitude between segmental and extraocular systems is the existence of a single functional type of motoneuron innervating extraocular muscles. As mentioned in Chapter 1, all extraocular motoneurons have the "pulse and step" pattern of activity during saccades (figure 1.2) (Fuchs and Luschei, 1970; Robinson, 1970; Schiller, 1970).

Activity of mammalian extraocular motoneurons.

Recording the activity of individual cranial neurons in awake mammals has been possible since the mid-60's. The results of such recordings are highly informative as it is possible to correlate precisely the electrical activity of neurones with behavior or muscle activity under normal physiological conditions. This electrophysiological technique has been fundamental to understanding the mammalian oculomotor system.

All extraocular motoneurons show the "pulse and step" pattern but the details of their activity profiles vary among the members of a given motor pool. The main difference is a scaling factor relating eye position and activity, but qualitatively the response patterns are similar. In presenting the physiological characteristics of extraocular motoneurons relating their firing with eye position it is necessary to point to the peculiar way that data is usually presented in the oculomotor field. While any eye position is the

outcome of the activity of many motoneurons, the experimental data is presented in an opposite way as if the firing rate of a motoneuron were a function of eye position. This choice reflects the fact that eye position is a parameter than can be easily controlled, and measured, by the experimenter while the real input to motoneurons, the sum of all afferences, is an unknown quantity.

The discharge rate ($f(t)$) of extraocular motoneurons during fixations and slow speed movements (i.e.non-saccadic movement like OKN and VOR) is approximately a linear combination of eye position ($E(t)$), speed ($E'(t)$) and acceleration ($E''(t)$) (Keller, 1973), thus the following equation can be written:

$$f(t) = k(E(t) - \Theta) + rE'(t) + mE''(t) \qquad \text{Eq. (1)}$$

Θ = eye position threshold

Not all motoneurons in a given pool are identical; they differ in the values of the four parameters k, r, m, Θ; not all motoneurons have the same threshold or the same constants **k** and **r**. For example, when the eye is in the primary position about 75% of abducens motoneurons are active while at +20° (towards the "on" direction) 100% have been recruited. The other three parameters show a wide range: 1-10 for **k** and 1-5 for **r** (Delgado-Garcia, Del Pozo and Baker, 1986). **Eq. (1)** is the formalization of the fact that all extraocular motoneurons belonging to a given pool have the same (qualitative) behavior. While some members of a motor pool have greater sensitivity to position than to speed (i.e., **k** bigger than **r**) motoneurons devoted to only one task (i.e., active during saccades only) do not exist. Thus, **Eq. (1)** is a phenomenological description of the empirical relation between eye position and the activity in a given motoneuron, but it is not a complete description of the relation between the activity of the motor pool and eye position.

The fact that eye position is the outcome of the operation of a heterogeneous neural group is not addressed by **Eq. (1)**. A complete explanation of how an eye movement is specified by extraocular motoneurons would require to consider the overall behavior of many (hundreds) equations like **Eq. (1)**.,

one for each motor unit. Furthermore, it is known that the linear model of **Eq (1)** is incomplete; the firing rate of motoneurons show hysteresis, as it also depends on the direction of the movement used to arrive to that position (Goldstein and Robinson, 1986). Powerful experimental reasons induce the recording of only one dimension of eye position in these experiments. The dimension which is recorded reflects the principal action of the motor pool under study. For example when recording from the abducens nucleus, which innervates the lateral rectus, the horizontal eye position is measured. This *one-dimensional analysis* obscures the fact that the six extraocular muscles act in synergy to specify eye position. Thus in strict rigor eye position, **E(t)**, should be a vector and not a simple scalar quantity as in **Eq. (1)**.

During saccades the temporal pattern of activity of mammalian extraocular motoneurons is approximately described by **Eq (1)**, but important non-linearities appear. Motoneurons participating in an "on" saccade show an intense burst of activity temporally locked to the saccade. The pulse precedes the physical eye movement by 4-12 msec and has a firing rate that is not constant. After reaching its maximal frequency, that coincides with peak saccadic velocity, the burst decreases with an exponential decay of about 80 msec (Delgado-Garcia, Del Pozo and Baker, 1986) and lasts a variable amount of time that depends on saccade amplitude. The duration, and number of spikes, of the pulse are related to saccade amplitude (Fuchs and Luschei, 1970; Kaneko, Evinger and Fuchs, 1981). The principal non-linearity is that the eye speed is so high during saccades that motoneurons show saturation effects in their firing rate. The mechanism producing the pulse is calibrated in such a way that after saccade completion the eye stays in the final position.

Premotor circuits controlling extraocular motoneurons.

The exploration of premotor brainstem circuits to the extraocular motor nuclei shows one important advantage of working on the oculomotor system. In this system it is possible to record from many putative premotor groups in awake animals and to construct detailed models of the physiology and connectivity of premotor and motor groups. While many uncertainties remain, it appears clear that three main types of neurons constitute the main

portion of the premotor circuit (van Gisbergen, Robinson and Gielen, 1981; Scudder, 1988). For the abducens muscle these three types are (figure 3.1)

a) *Excitatory Burst neuron* (EBN, ipsilateral)

b) *Tonic neuron* (TN, ipsilateral)

c) *Inhibitory Burst neuron* (IBN, contralateral)

Current models of the saccadic machinery (Robinson, 1975; Scudder, 1988) suppose that the amplitude of a saccadic movement is encoded in the activity of EBN, which are silent during fixations and fire a short burst 9 msec before saccade onset. The total number of spikes in the burst of EBN defines the eye displacement, and it is directly fed to motoneurons making the "pulse" component. The EBN burst also arrives at TN, which directly, by use of recurrent positive excitation, or indirectly, by use of a neural network (Cannon and Robinson, 1985), perform an integration and produce the "step" component. This relation between the activity of EBN and TN is crucial for our current models of saccadic machinery as it indicates that the "pulse" and "step" components are not independent from each other and that the"step" component is perfectly matched to the "pulse". This relation explains why some saccadic parameters, like duration or peak velocity, depend on the net eye displacement (saccade amplitude) (see figure 2.2). IBN are inhibitory cells that play a fundamental role producing the pause during "off" saccades.

The correct temporal interplay between the EBN, IBN and TN neuronal populations requires other neuronal groups (figure 3.1). Two are particularly relevant:

a) *Omnipause neurons* (OPN)

b) *Long Lead Burst neuron* (LLBN)

These two classes of neurons are essential for the correct functioning of the overall saccadic machinery. LLBN, which provide the output to EBN, receive two signals, a' (a collicular signal reflecting the desired eye position) and e' (efference copy signal from TN), and produce a high gain

version of their differences (LLBN=a'-e'). Thus the output of LLBN is an error signal between desired and actual eye position. The operation of LLBN cells is the central aspect of the models of Robinson (1975), van Gisbergen (1981) and Scudder (1988) ("bang-bang" models) as it embodies the core of a feedback regulated amplifier. OPN neurons, which inhibit EBN, have a steady, and invariant discharge rate during fixations and stops for all saccades. Thus when the trigger signal arrives and OPN stop briefly, the saccadic mechanism begins to operate in a high gain mode until a'-e' =0. The pause is further maintained by a circuit involving EBN and IBN as OPN are inhibited, indirectly, by EBN.

The simplified model of the saccadic machinery presented depends on two "descending" signals, the *desired eye position* and the *trigger*, to operate correctly. If these two signals disappear the remaining circuit does not operate correctly, it does not even show a qualitatively correct behavior. In this respect, segmental and extraocular muscles are controlled differently. After spinal transection, movements like walking or swimming, are not totally abolished because spinal pattern generators, without central signals, are able by themselves to produce some fundamental coordinations between muscles (Koshland and Smith, 1989). While similar lesion experiments are impossible to perform in the brainstem, the "bang-bang" model suggests that once the desired eye position signal is absent, the motor error signal would be inadequate all the time, the premotor elements of the saccadic machinery (EBN, TN, IBN) are unable to generate by themselves any meaningful saccadic motor pattern.

The other important difference between segmental and extraocular muscles concerns the role of proprioception and of Renshaw's type inhibition. In segmental muscles, proprioceptors project directly to their homonymous muscle and the local spinal network. Usually this anatomical projection is used as part of a physiological stretch reflex circuit (the muscles of the neck are an exception (Spencer and Porter, 1988; Abrahams, Rose and Richmond, 1990)). Extraocular muscles although possessing neuromuscular spindles appear not to have a classical stretch reflex (Keller and Robinson, 1971). In the same realm of phenomena, extraocular muscles lack the "feedback" mechanism based on axon collaterals. In the spinal

cord, motoneurons are inhibited by Renshaw's cells which are driven by axon collaterals from the same motoneurons (recurrent inhibition). It appears that extraocular motor pools instead of using muscular (i.e proprioceptive) or motoneuronal (i.e. collateral) signals to control their activity rely on efference copy signals generated by premotor circuits.

Although the oculomotor system of primates can not be considered "typical" from the point of view of motor control, it shares one fundamental characteristic with spinal motor systems: motoneurons are not functionally segregated and an uniform order of activation is used in their activation.

The extraocular system in chickens.

The active production of saccadic oscillations in chickens, as it was shown in Chapter 2, suggests immediately the participation of pattern generators in producing these stereotyped movements. The stereotyped nature of saccadic oscillations indicates that that the avian oculomotor system contains PGs similar to the PGs predicted in the generation of rhythmic movements in vertebrates. Furthermore, results from Chapter 2 show that the amplitude of saccadic oscillations is independent of the net eye displacement; for example saccadic displacement is uncorrelated with the amplitude of oscillations. This independence constitutes a fundamental difference between the neural organization of the saccadic machinery of mammals and birds. In this respect, the principal result to have in mind is the similarity of the oscillatory pattern for saccades that move the eye less than 1° and for saccades producing a 10° shift in eye position. Thus the "bang-bang" model, and its derivatives, all of which have the property that the "step" component of the motor saccadic command is the integral of the "pulse" component must be inapplicable to birds.

To answer how avian saccades are generated the most important piece of evidence is the pattern of activity of extraocular motoneurons during saccades. Although the first recordings of extraocular motoneurons in mammals were done more than 20 years ago, similar recordings have not been done in birds until now. The only physiological study of an avian extraocular motor pool has been the microstimulation of the abducens nucleus in anesthetized pigeons (McVean and Stelling, 1986). Using this

preparation the authors, incorrectly, concluded that oscillations were passive and that mammalian and avian saccadic machinery were similar. In this thesis recordings of single motoneurons will be presented. Clearly of all the motor pools involved in eye movements the torsional nature of saccadic oscillations indicates that the trochlear nucleus and the ventro-medial subdivision of the oculomotor complex, which innervate the superior and inferior oblique, respectively, are the prime candidates to be explored. Also explorations of brainstem areas would add to our understanding of the premotor circuits involved in saccade production.

Methods.

All experiments reported were done in 3-4 week-old normal White Leghorn chicks (*Gallus gallus domesticus*) hatched in the laboratory of Dr. Josh Wallman at City College of New York. Chicks were maintained in temperature controlled brooders under a 14L/10D day cycle.

Recording of neural activity and eye position.

In primates or cats, the technique for recording neural activity in awake subjects involves the placement of a metal headpiece attached to the skull by screws. This headpiece serves to fix the animal head without the discomfort of ear bars, and as a base to attach a micro-electrode advancer. A similar technique was developed in this project to record the activity of craneal neurons in awake chickens. The method differs from common practice with cats or primates, in that the headpiece holds the chicken head fixed to a stereotaxic device to which the electrode advancer is attached.

Surgical procedures

The construction and installation of the headpiece was as described in Chapter 2, but a small recording chamber was added behind the headpiece. All chickens were placed in the same standard position in the stereotaxic device before attaching the headpiece. A line connecting the auricular orifice with tip of the beak was 10-15° below horizontal. The recording chamber consisted of a hollow lucite cylinder, 10 mm i.d. and 4 mm deep, with its bottom carved to match the contour of the skull and was secured to the skull with dental acrylic. A reference point, placed in the intersection of the midline with the vertical plane passing through the middle of both auricular orifices, was put on the exposed bone to serve as landmark for all microelectrode penetrations (figure 3.2). The recording chamber was closed, first by a layer of absorbable sterile sponge (Upjohn, GELFOAM), a thick layer of bone wax (Ethicon), and finally a layer of low melting point wax. Birds recovered from these procedures by the next day.

On the first recording day, usually two days after installation of the headpiece, chickens were anesthetized with a gas mixture (20% Oxygen,

80% Nitrous Oxide and 0.8 % of halothane). The recording chamber was opened and a craniotomy was performed using a small dental drill. The excised piece of skull bone was stored in cold saline. The craniotomy did not cross over the midline, as the central sinus is located just beneath, and it is easy to damage it while drilling. When metal microelectrodes were used, the dura was left untouched, as almost all types, except Wood's metal electrodes, were able to penetrate it without damage. In the case of glass pipets, the dura was opened with fine forceps and scissors.

After two hours of recovery from the gas anesthesia, the chicken was put inside a sock and attached to the stereotaxic instrument by the headpiece. The exposed surface of the brain was kept moist by a small piece of wetted gelatin sponge periodically placed in the recording chamber.

At the end of each recording session the recording chamber was sealed. Under gas anesthesia the craniotomy was covered by the piece of bone stored in cold saline. Cloramphenicol and anti-fungal creams were applied over the bone, and layers of absorbable gelatin sponge (Gelfoam, Upjohn), bone wax and low temperature wax were applied. This sealing procedure greatly helped in controlling the outgrowth of connective tissue over the exposed dura mater.

The incision on top of the eye, used to attach eye coils, was cleaned. Cloramphenicol and anti-fungal creams were applied on the back and top of the eye and the skin incision closed with surgical suture.

Microelectrodes and electronics.

Eye position was monitored with a search coil system as described in Chapter 2. Most of the time only the torsional component of eye position was recorded, but in some experiments the horizontal and vertical components were also recorded. In all experiments, care was taken to obtain accurate measurements of eye position but kinematic errors were not compensated. Fortunately, as explained in figure 2.13, the correction for these errors is usually small.

Unitary activity was monitored with metal microelectrodes having a shaft diameter of 200-250 μm. Hand made tungsten in glass microelectrodes

with an exposed tip of 10-30 μm were usually used (Merrill and Ainsworth, 1972), as they isolate single units inside the trochlear in a consistent way. Stable extracellular recordings for 3-5 minutes were obtained on a regular basis. To avoid frequent contractions of the neck muscles, which produced enough brain movement to decrease the stability of recordings, the bird was maintained in a comfortable position. Recording sessions were between 4 and 8 hours long. A precise description of all microelectrode penetrations was logged in a notebook. For each penetration the following details were logged: type of electrode, angle of electrode with respect to the vertical, coordinates of the microelectrode entry point (with respect to the reference mark placed on top of the skull), microelectrode advancer reading when the electrode first entered the brain, type of background responses, type (and advancer reading) of units recorded, position and intensity of electrolytic lesions.

Three areas were explored. The main effort was devoted to the trochlear nucleus. The coordinates of the entry point of the microelectrode on the surface of the telencephalon to reach the trochlear were: Anterior→Posterior=-600 → -1200 μm, Medial→Lateral= 1800→ 2600 μm, Depth=8.5 mm (microelectrode inclined 10° toward the midline). The oculomotor complex is immediately anterior to this area. The second area was the vestibular complex, its coordinates were: Anterior→Posterior= -2000→ -3500 μm, Medial→Lateral= 1500→ 3000 μm, variable depth (electrode perpendicular). The third area was the Infracerebellar nucleus, its coordinates were: Anterior→Posterior: -3000→ -3500 μm, Medial→Lateral: 2500→ 3200 μm, Depth=6.5 mm (electrode perpendicular).

The electronics involved in recording action potentials were conventional. The only novel aspect was a high quality lowpass filter specially designed to attenuate the 29KHz sinusoidal "noise" created by the magnetic fields surrounding the bird. Eye position and neural activity signals were stored in a FM tape recorder for subsequent "off-line" analysis.

Histological identification of microelectrode tracks.

The localization of recording sites was a problem because of the small dimensions of the trochlear (800 μm diameter). Such small size

precluded making more than a few marking lesions without noticeably affecting the physiology of the nucleus. Lesions were made, using the recording microelectrode, by passing a total charge of 5 μAmpx4sec (microelectrode negative). To avoid the deleterious effect of too many lesions, they were made in a few tracks only. They were easily visualized by Nissl stain after survival time of 1-2 days following the lesion. Four or five tracks could be made and recognized histologically in the trochlear nucleus. Generally two to four separated recording sessions, separated by two days each, were performed in the same chicken.

At the end of the last recording session chickens were given an overdose of sodium pentobarbital and perfused via both carotids. The perfusion sequence was: a) 300 ml of cold avian saline, b) 300 ml of 10% formalin and c) 500 ml of 10% sucrose and 5% formalin. The brain was excised from the skull, left overnight at 4° C in 30% sucrose and cut in 40 μm sections with a freezing microtome. The sections were then processed with a Nissl stain. The localization of lesions was done with a microscope fitted with a camera lucida optical assembly.

One crucial experimental advantage of working in the trochlear nucleus of chicks, as opposed to the other two motor nuclei innervating extraocular muscles, is its lack of interneurons. Thus all neurons found inside the trochlear nucleus <u>are</u> motoneurons (Sohal and Holt, 1978; Sohal et al., 1985). This fact implies that is not necessary to antidromically stimulate neurons in order to classify them as motoneurons. Instead, the anatomical position is enough to correctly classify responses. Thus special care was taken to assure the correct localization of responses. The information provided by the localization of lesions was complemented by the information contained in the log protocol notebook on the various electrode penetrations. These two types of information were used to reconstruct almost all the electrode penetrations and to spatially localize the units recorded. Because the localization of a response constituted such an important step, units which were not unambiguously ascribed to the trochlear nucleus were not considered in this study.

Pathway tracing with HRP.

The afferent pathways to the trochlear nucleus were traced by horseradish peroxidase (HRP) labelling. In chickens prepared for simultaneous recording of eye movement and neural activity, HRP was deposited in the trochlear nucleus. A glass micropipete, 4 μm of tip diameter and filled with 0.8% NaCl and 4% HRP, served as recording and iontophoresis electrode. Because extracellular recording was possible, the electrode tip was placed close or into the trochlear minimizing the injection of tracer in other adjacent areas. Once the pipette was in the trochlear nucleus, HRP was iontophoretically injected by passing current pulses of 7 μAx20secs (50% duty cycle) for 40 minutes. After this period the micropipette was withdrawn and the craniotomy closed. After a survival time of 36-48 hours, birds were sacrificed with an overdose of sodium pentobarbital and perfused. The perfusion protocol for HRP was as follows: a) 300 ml of cold avian saline, b) 300 ml of 2% glutaraldehyde + 1.7% paraformaldehyde in 0.1M pH=&.4 phosphate buffer and c) 200 ml of 20% sucrose. The brain was excised, cut in 40 μm sections and processed for tetramethyl benzidine histochemistry (Mesulam, 1978). Stained sections were mounted in gelatinized microscope slides, dried and counterstained with 1% neutral red. The nomenclature of Wold (1976) was used to distinguish between the various subdivisions of the chicken vestibular complex.

Injection of HRP in single neurons and axons.

HRP was injected into single neurons and axons to investigate morphological aspects of trochlear motoneurons and their afferents. Chickens prepared for eye position and neural recording were used. Glass microelectrodes, 1-2 μm tip diameter and 10-30MΩ, filled with 2 M NaCl and 10% HRP were used. A flap of dura mater was removed, as glass microelectrodes were unable to traverse the dura without damage. Once the microelectrode tip was in the trochlear nucleus some neurons were impaled and HRP injected into them. The current parameters were approximately 5-10nAx60 secs (50% duty cycle). The inherent conditions of experiments in awake chickens were such that intracellular recordings were very labile,

never lasting for more than 2 minutes. Thus the quality of the injection was not uniform and a very incomplete picture of the synaptic potentials was obtained. But even these small periods of intracellular recording permitted the classification of responses. Two hours after the first HRP injection the animal was given an overdose of sodium pentobarbital and perfused as described in the previous section. The brain was left overnight in 30% sucrose and cut with a freezing microtome, in 80 μm sections. The sections were stained according to the DAB HRP protocol. The sections were mounted in gelatinized slides, covered and analyzed under x100-400 power microscope.

Data analysis.

Eye position and neural activity were stored in a FM magnetic tape during the experiment. Analysis was carried out later "off-line." The raw analog data was processed in three steps: a) digitized, b) checked and time-marked and finally c) numerically processed. The first step consisted in sampling 1024 points centered around each saccade. Spikes were converted into standard TTL pulses before sampling. To isolate the response of a single unit the raw neural activity was fed into an amplitude discriminator. An analog delay line was used to monitor continuously the quality of spike selection (Bak and Schmidt, 1977). Depending on the type of the units, the sampling rate was 1 KHz or 5 Khz. In the second step the digitized eye position and spike signal were displayed on an oscilloscope screen. Under visual control a cursor was moved over the traces to mark special points such as the beginning and end of saccades. This step was also used to reject spurious events. The third and final step used information provided by the time marks to calculate various parameters relating eye position to spike frequency. The eye position data in this chapter only reflects the approximate torsion and not the exact torsion used in Chapter 2. The difference is that no attempt was made to compensate for "kinematic" errors. The sign of saccades was defined as follows: plus (+) saccades begin with an intorsional subphase, minus (-) saccades begin with an extorsion. The software to implement the various steps was specially made for this project and implemented on PDP-11/73 and VAX platforms using Fortran and

assembler. Photographic plates of neural activity were obtained by a Grass oscilloscope camera.

Results

Types of responses in the trochlear nucleus.

As soon as the microelectrode entered the trochlear nucleus the background neural activity recorded became a distinct mixture of tonic and phasic components that served as a "signature" of the nucleus. The phasic component was time locked to saccades while the tonic component had a brief pause, also time locked with saccades. The appearance of such characteristic background served as a diagnostic element to know if the microelectrode was inside the trochlear or the oculomotor complex. From histological data the thickness of the nucleus was estimated to be 800 μm and the tonic/phasic background mixture spanned an equivalent length. The high level of background neural activity made isolation of single units difficult (see figure 3.3D). The dimensions and shape of the tip of the microelectrode were important in achieving successful isolation, exposed conical tips of 7 μm in the base and 20 μm long were found to be adequate. All the units isolated inside the anatomical limits of the trochlear nucleus were interpreted as belonging to motoneurons. The non-existence of interneurons in the chicken's trochlear is a crucial technical detail that has been clarified using two different techniques. First, the number of neurons in the trochlear is similar to the number of axons contained in the trochlear nerve; 743 neurons versus 861 nerve fibers, data from Sohal et al. (1985). Second, after HRP injections into the superior oblique muscle, all trochlear neurons are stained (Dr. Craig Evinger, personal communication).

One of the principal results of this thesis is the elucidation of the real structure of the background activity found in the trochlear. Two types of motoneuronal responses were found interspersed in approximately equal numbers in the trochlear nucleus. These two class differed in their firing pattern with respect to eye position. One class ("Tonic") showed a steady discharge during fixations, provided that the eye was beyond the threshold position ("on" region), increased its firing frequency as the eye took more intorsional eye positions, paused during saccadic oscillations and lacked any high frequency component during saccades regardless of saccade direction (figure 3.3A and figure 3.3D). The other class ("Phasic") was always silent during fixations and discharged a short train of spikes in association with

each saccadic oscillation (figure 3.4A,B and C). "Pulse and step" responses, such as those seen in mammalian extraocular motoneurons, were not found in the trochlear nucleus. Phasic and Tonic responses were not spatially segregated in the trochlear nucleus. The lack of spatial segregation, in the dorso-ventral axis, was deduced from the fact that at any given depth in the trochlear nucleus Phasic and Tonic responses were recorded with the same probability (figure 3.5).

Tonic responses.

The discharge frequency of Tonic motoneurons was related both to eye position and eye speed. Like primate extraocular motoneurons Tonic motoneurons showed a position threshold, in that they ceased to fire at some extorsional position of the eyeball ("off" region) and their discharge increased when the eye took progressively more intorsional positions (figure 3.6). Tonic Motoneurons had also a speed sensitivity, an example is shown in figure 3.3C, in which the unit stopped firing during extorsional slow phases of OKN even when the eye was in the "on" region. Tonic motoneurons stopped firing at the beginning of each saccade, regardless of saccade direction, for a period correlated with saccade duration but unrelated to saccade direction.

The pausing exhibited by Tonic motoneurons was present in all saccades and had a variable duration correlated with saccade duration (figure 3.7). In general, longer saccades were associated with longer pauses. Another factor controlling pause duration was the total saccadic displacement. During saccades with a sizeable intorsional net movement, pauses were shorter. Pausing began before saccade onset and lasted at least 35 msec. In all cases, Tonic motoneurons ceased to fire 20 msec before the saccade (figure 3.8). Thus Tonic motoneurons exhibited pauses of 200 or 50 msec, but never a pause of 35 msec or less (figure 3.9).

In some situations Tonic motoneurons exhibited a very different behavior and no pausing was seen. If the eye was in the "off" region for a given Tonic motoneuron, that cell was silent during the fixation period antecedent a saccade. If the saccade moved the eye from the "off" region into the "on" region for that Tonic motoneuron, the cell began to fire during

the saccade. If the final eye position stayed in the "on" region, the Tonic motoneuron continued to fire at a steady level for the next period of fixation. If, as it the usual case during OKN quick phases, the saccade was followed by a slow phase towards the "off" region the motoneuron stopped firing when the eye reached the "off" region. In all these cases, motoneurons began to fire after the onset of the saccade (figure 3.10).

In twenty seven Tonic motoneurons the relation between static torsional eye position and firing frequency was quantified. An absolute standard measure of torsion was not possible in these experiments. Thus, using results from Chapter 2 concerning the range and distribution of torsional eye positions, torsional eye positions were standardized across birds by subtracting from the torsional data the median value of torsion for 100 fixations. The firing frequency increased towards torsional eye positions for 25 cells, two had a flat response and none decreased its firing as the eye took more intorsional eye positions. The functional relation between torsional eye position and frequency was estimated using a weighted regression method (Cleveland, 1979) which uses a sliding procedure in which the contribution of points decreases with distance from the point considered. Representative curves of this procedure are shown in figure 3.11. For 24 units it was possible to behaviorally measure (i.e. to obtain eye positions in various parts of the "off" region) or to extrapolate (in the case of motoneurons that never went into the "off" region) the threshold and to approximate the frequency-position curve by a straight line. The threshold ranged from 30° extorsional to 4° intorsional and the slopes (**k** from **Eq. (1)**) ranged from 0.92 to 7.24 spikes/sec per deg (table 3.1). Thresholds and slopes appeared to be uncorrelated (r^2=0.38, N=22). Half of the units were recruited at -15° (15 ° extorsional) and no units were found with a threshold greater than +10° intorsion. Almost all cells were recruited when the eye was in the median torsional position. Five cells showed a "dual" behavior, in the range between their threshold and the median torsional position they increased their activity almost linearly (figure 3.11 curve **b**) but maintained a flat activity in the range between the median eye position and the extreme intorsional position tested.

The previous analysis while providing a first approximation for the dynamics characteristic of motoneurons has an important problem. The chicken used were not trained to produce specific eye movements with a given speed (or amplitude) profile. Thus sometimes the period of fixation contained "glissades" or low velocity periods and as motoneurons have speed as position sensitivity (see **Eq. (1)**) the position sensitivity of motoneurons was obscured in this analysis by their speed sensitivity. Also, as the eye movements were spontaneous (or induced via OKN), the complete range of positions was not examined for every motoneuron. To reveal both the position and speed sensitivities of motoneurons a different approach was used.

Simultaneous determination of *k* and *r*.

In a subset of trochlear Tonic Motoneurons (5 cells) a more detailed analysis of their response as a function of eye position and speed was made. As previously stated, during saccades the firing frequency of Tonic motoneurons appears to be unrelated to saccadic oscillations, thus the following procedure was used to "extract" a slow eye position component from the eye movement record. During saccadic oscillations the stereotyped 28Hz oscillations were eliminated by piecewise linear interpolation. For each saccade the midpoints between successive peaks plus the beginning and end of saccade were manually selected, this subset of points was then used to calculate via linear interpolation, a "slow" eye trajectory (figure 3.12A). The net effect of this procedure is to eliminate the oscillations from the eye position data. This procedure implicitly affirms that the eye trajectory during saccade is the direct sum of two non-interacting components: 28 Hz oscillations and a slow eye movement revealed by the interpolation procedure.

A multivariate fit between the interpolated eye position ($\mathbf{E}(t)$) and the corresponding eye velocity ($\mathbf{E}'(t)$) as the independent variables and the motoneuronal activity ($\mathbf{f}(t)$) as the dependent variable was calculated. Based on previous work done in mammals the following quasi-linear model was adopted for the fitting. The non-linearity reflects the fact that the firing frequency of a MN is always a non-negative number.

Quasi-linear model used:

$$F_{pred}(t) = k(E(t) - \theta) + rE'(t)$$

$$F_{pred}(t) \geq 0 \quad \text{for all } t \qquad (\theta = \text{threshold})$$

The procedure described above differs from the determination of the position (k) and speed sensitivity (r) constants done in mammals (Fuchs and Luschei, 1970; Delgado-Garcia, Del Pozo and Baker, 1986) and teleosts (Pastor and Delgado-Garcia, 1992) in an important aspect. In these previous determinations of k and r the fitting was done for discrete sets of data where each data point was obtained from a different intersaccadic period. Some of these periods were fixations, others were OKN or VOR slow phases. Each period of fixation provided one data point only consisting in three values: an eye position, an eye speed and a local average of the firing frequency of the motoneuron. The timing of these values was unimportant as far as they were obtained at the same moment.

The analysis performed here on the discharge frequency of Tonic motoneurons is different. Instead of using a single data item (made of three numbers representing eye position, eye velocity and frequency) for each intersaccadic period, a fitting between the position and speed curves on the one hand and the frequency curve on the other was done. Thus instead of having one data point per fixation the fit was done between three curves having between 600 and 1000 data points. The time interval chosen contained data encompassing three periods: a pre-saccadic state (200-400 msec), the saccadic event (100-250 msec) and a post-saccadic state (200-400msec). A linear polynomial $F_{pred}(t)$ on variables $E(t)$ and $E'(t)$ with coefficients k and r was evaluated. The coefficients k and r were then recursively changed until the difference between the actual frequency data ($f(t)$) and the predicted frequency ($F_{pred}(t)$) was minimal. For each Tonic motoneuron values of k and r were obtained by averaging the values found across 15-20 saccades, thus for each Tonic motoneuron a 95% range was found for k and r values. The procedure used to arrive at the values of k and r searched through the (k,r) parameter space, as opposed to a calculation via an error minimizing technique. This heuristic method should be applied with caution as it presents all the problems associated with multi-

dimensional optimization, for example, sometimes the algorithm discovers false solutions or wanders too long in search of a possible solution.

The k and r obtained (figure 3.12D and Table 3.2) are of the same order of magnitude as the corresponding values in monkeys (k=4.0, r=0.95 (Robinson, 1981)), cats (k=8.7, r=1.31 (Delgado-Garcia, Del Pozo and Baker, 1986)) and goldfish (k=7.1, r=0.96 (Pastor and Delgado-Garcia, 1992)). Interestingly a relation appeared to exist between k and r. The fit between the predicted and actual frequencies curves was sometimes very close (figure 3.12A and B), thus it can be inferred that the frequency discharge of Tonic motoneurons is better correlated with the "slow" component than with the actual oscillations.

Although the quasi-linear model used here appears to predict the discharge pattern of Tonic Motoneurons it is obvious that the relation between eye position and frequency is more complex. In addition to a functional relation linking eye position and frequency another factor exists. This extra factor is reflected in the characteristic pause in the discharge of Tonic motoneurons.

Figure 3.12C shows the implications of the pausing for the linear model, the saccade depicted is an "on" directed saccade that begins and ends inside the "on" region for that motoneuron. During the saccade the eye position is always inside the "on" region and the speed is always positive, these two constraints would impose an increase in the firing frequency if the linear model were a complete description of the situation. The decrease in firing just after saccade onset shows that another factor must be controlling the firing. The linear model can be used, but the value of r obtained is a negative number and by physiological considerations this mathematically correct result must be rejected. Thus the presence of a extra factor beside eye position in controlling the firing of Tonic motoneurons, must be taken into account when building Table 3.2. To calculate the values of k and r the first 80-120 msec of a saccade where not taken into account in calculating the linear fit if including this interval made the value of r negative.

Phasic Responses.

Phasic motoneurons, in contrast, were totally silent during fixation, even when the eye was at extreme intorsional positions. They discharged during every saccade with bursts of spikes time-locked to the intorsional subphase of oscillations. The response of trochlear Phasic motoneurons was extremely stereotyped. One burst was always associated with every intorsional oscillatory subphase. Phasic motoneurons fired for nearly every oscillatory cycle of every saccade or OKN quick phase. Beside being silent for every fixation, Phasic motoneurons were also silent during slow phases of OKN when the eye was moving at less than 20°/sec, slow phases with velocities > than 20°/sec were not explored.

The number of spikes in each burst, for each Phasic motoneuron, varied in a small range. Some cells fired bursts containing 2-9 spikes, others had only 1-3 spikes per burst (figure 3.13). In very few cases, less than 1%, Phasic motoneurons did not fire during an intorsional subphase. Thus, every Phasic motoneurons fired for all saccades and for nearly all oscillations.

Bursts lasted between 1.7 msec and 10 msec. The rate of firing during bursts was very high, reaching levels of 500-1000 spikes/sec. On a few occasions interspike intervals of 0.8 msec were observed. (However it must be remembered that spikes were sampled with an accuracy of only 0.2 msec.) The number of spikes in a burst and burst duration were related. The number of spikes increased with the duration of bursts (figure 3.14). The mean frequency of discharge (number of spikes in burst/burst duration) was 600 spikes/sec.

The timing of bursts with respect to the beginning of each intorsional subphase was itself stereotyped. For "+" saccades (i.e. saccades beginning with an intorsional subphase), the first burst preceded the eye movement by 4.6 msec. For the next subphases, bursts lagged the intorsional subphase with a median delay of 4-6 msec. For "-" saccades (i.e. extorsional first subphase), bursts were usually delayed with respect to the beginning of the movement (figure 3.15). This time delay between the onset of the movement and the origin of bursts was found in all Phasic motoneurons studied (figure 3.16). For example, bursts began 3.8 msec after the

beginning of the second intorsional subphase. For "minus" saccades, the first burst lagged behind the initiation of intorsional subphases by 3.2 msec (figure 3.17). Thus, with the exception of the first subphase of saccades beginning with an intorsion, bursts lagged behind the initiation of intorsional subphases by a median of 3-5 msec.

The torsional amplitude of oscillations covaried with the number of spikes in each burst. Figure 3.18, where the median subphase amplitude and the median number of spikes were plotted against the burst number, shows some examples of this correlation for different Phasic motoneurons. Saccades were separated according to their "flavor" i.e. saccades beginning with an extorsional subphase (left side of figure 3.18) or with an intorsional subphase (right side of figure 3.18). For two cells (A and B) of figure 3.18 the correlation between subphase amplitude and number of spikes in the corresponding burst is very good. This correlation is not always found (C). The correlation between subphase amplitude and number of spikes failed completely for the initial subphase of "plus" saccades (figure 3.18 right). During these saccades the initial burst of Phasic motoneurons is as intense as the second or third but the amplitude of the movements is only half (i.e. 4-5°) of the second or third subphase (i.e. 10-12°, see Chapter 2). Thus, in the case of "+" saccades, the first oscillatory cycle is a special case because the amplitude of that cycle is half of the amplitude of subsequent cycles at the same time that the number of spikes in the corresponding burst is similar to the second or third bursts.

The relation between amplitude of oscillations and the number of spikes in bursts can be also visualized by plotting the median amplitude of subphases as a function of the number of spikes. In figure 3.19 the median amplitude of subphases was plotted against the number of spikes in the burst with the only exception of the first subphase of "plus" saccades. The data used in this figure is exactly the same as the data used in figure 3.18 but it has been rearranged according to the number of spikes in each burst instead than time. Of the five examples presented, four show an increase in amplitude when the number of spikes in the burst increases. For 27 Phasic motoneurons the correlation coefficient and the slope of a linear fit (figure

3.20) were calculated. In 22 of them (80%) a correlation coefficient greater than 0.6 was found. The median slope was 0.9 °/spike.

Tonic and Phasic motoneurons are quite distinct and there are no motoneurons with intermediate properties. Recordings done in the oculomotor complex indicated that a similar task segregation exists among Inferior Oblique motoneurons, suggesting that saccadic oscillations probably result from the alternate activation of the motor pools of the two antagonist muscles. In some cases clear recordings were made from the oculomotor ventro-lateral subdivision, which innervates the inferior oblique. Phasic responses similar to trochlear Phasic responses were found and their responses were time locked with extorsional subphases.

Morphology of trochlear motoneurons and vestibular afferents to the trochlear nucleus.

Twelve motoneurons from the trochlear nucleus and the oculomotor complex were physiologically identified and intracellularly stained with HRP. Five were Tonic and seven were Phasic. Some anatomical distinctions were present between motoneurons innervating different extraocular muscles, and no dissimilarities existed between Tonic and Phasic motoneurons. Trochlear motoneurons had a nearly circular cell body with six to nine primary dendrites (figure 3.21). The soma diameter of four motoneurons ranged form 34 to 44 μm. The dendrites extended approximately 1 mm laterally, well outside the trochlear nucleus as defined by Nissl staining. Dendrites also projected laterally into the reticular formation and ventrally into the medial longitudinal fasciculus. At the midline, the dendrites turned downward and never crossed the midline. In no case did the dendrites extend into any other pool of extraocular motoneurons. No axons collaterals were present. The inferior rectus motoneurons had a globular cell body, with a soma size ranging from 34-39 μm. The dendrites of these motoneurons projected outside the dorsolateral subdivision of the oculomotor complex reaching into the other subdivisions of the oculomotor nucleus or the trochlear nucleus. No axons collaterals were present on these motoneurons. Medial rectus motoneurons were smaller than superior oblique or inferior rectus motoneurons. Their soma size ranged from 29-35 μm and had 5 or 6 primary dendrites. The dendrites

of medial rectus motoneurons did not project outside the dorso-medial subdivision of the oculomotor complex.

The medial longitudinal fasciculus and reticular formation lateral to the oculomotor nuclei contained axons whose discharge patterns were similar to that of Tonic and Phasic motoneurons. Six axons, which terminated in the oculomotor nuclei, were physiologically characterized and intracellularly stained. Three of the axons exhibited a tonic discharge pattern and remaining three had a phasic pattern. Five of the axons travelled in the medial longitudinal fasciculus and the sixth arose from the tectum. The axons having "tonic" patterns appear to be similar to mammalian secondary vestibular axons. For example, one axon terminated in the trochlear and in the dorso-lateral subdivision of the oculomotor nucleus. Phasic axons tended to have a more restricted terminal field than tonic axons.

Small HRP injections were made into the right trochlear of 6 chickens. In five of them the injection site, as revealed by TMB histochemistry, was circumscribed to the trochlear nucleus or its immediate vicinity. From anterior to posterior, labelled cells were found in the following structures. Few labelled neurons were found in the ipsi- and contralateral nucleus pontis caudalis. In some animals, some labelled neurons were found in the contralateral abducens nucleus. The most intense labelling was found in the vestibular complex. Using the nomenclature of Wold (1976) labelled neurons were found in the following subdivisions of the vestibular complex: a) contralateral vestibularis medialis, b) ipsi and contralateral vestibularis superior and c) contralateral tangentialis. Labelled neurons were also found in the contralateral nucleus, above the superior vestibularis. (figure 3.22 and figure 3.23). Labelled neurons were not seen in the following subdivisions of the vestibular complex: Deiters ventralis, Deiters dorsalis, group cell A or group cell B. The most clearly labelled group was the contralateral tangentialis. In this case, labelled neurons were found, 22 neurons in average per animal, in between the fibers of the vestibulo-cochlear nerve. According to the classification of Puesner (Puesner and Morest, 1977) labelled tangentialis neurons were "*principal*" cells. The second most numerous group was in the superior vestibular. In

two chickens HRP was deposited approximately 500 μm caudal to the trochlear. In these cases no labelled neurons were detected in the vestibular complex, the abducens, or the infracerebellaris nucleus.

Saccade related responses in vestibular complex and infracerebellaris n.

In five chickens extracellular recordings were done in the following three areas: the tangentialis, the superior vestibular nucleus and the infracerebellaris nucleus. In the tangentialis/medialis border two types of responses were found (figure 3.24). One type of neurons had a high (100 sp/sec) steady discharge during fixations and paused for every saccade. The pausing was independent of saccade direction or amplitude and their discharge during fixations was not related to eye position. The pause began about 12 msec before saccade onset and these neurons resumed firing at the end of the saccade. The second type was totally silent during fixations and fired a continuous "train" of spikes for each saccade independently of amplitude and direction. These units did not fire bursts like Phasic motoneurons. They fired a train of spikes, starting 5-10 msec before saccade onset, with a frequency of 20-40 sp/sec for the complete duration of the saccade.

In the superior vestibular nucleus, tonic cells with a variable discharge rate were found. These cells increased their discharge with intorsional eye positions and stopped for saccades. Eye movement related responses were not found inside the infracerebellaris nucleus.

Discussion.

Trochlear motoneurons in chickens are divisible into two non-overlapping, functionally distinct classes. Tonic motoneurons are active during fixations or when the eye moves smoothly at low speed, and pause for a variable interval during all saccades, even those in the "on" direction. Phasic motoneurons fire during every saccade with a brief burst of spikes time-locked with each intorsional phase of saccadic oscillations, regardless of initial direction, amplitude or duration of the saccade. Because Phasic motoneurons never fire during fixations, even at extreme intorsional positions, they are not like mammalian extraocular tonic-phasic motoneurons with a high position threshold (Henn and Cohen, 1975). The fact that the trochlear nucleus receives inputs that are themselves segregated into tonic and phasic classes suggests that the functional difference between Tonic and Phasic types is based on an inhomogeneous input to these two classes rather than different biophysical properties. Most certainly "phasic" and "tonic" axons travelling in the medial longitudinal fasciculus (mlf) make differential contacts with different types of trochlear motoneurons creating the strict dichotomy seen. This functional segregation, at the level of trochlear motoneurons, has deep implications for our understanding of the avian oculomotor system. This segregation proves that the model of neural circuits involved in saccade generator used for mammals, where the input to the motor nucleus is homogeneous, can not be directly applied to birds. To accomodate the existence of two types of motoneurons a fundamentally new model must be built for the avian saccadic machinery. But before building such a model a careful analysis of the data must be undertaken.

An experimental problem in this thesis was the unsystematic exploration of the EYE POSITION/EYE SPEED space for each motoneuron. The chickens used in this study were not trained to produce specific eye movements with a given combination of eye position and speed. Thus spontaneous movements and OKN quick and slow phases were used instead. Unfortunately, as shown in Chapter 2, the spontaneous eye movements of chickens are restricted. many spontaneous saccades barely move the eye and OKN quick phases, while inducing larger eye displacements, present another problem. The visual stimulation necessary to

induce OKN is an unsettling experience for chickens, after 1 minute they become agitated and attempt evading behaviors such as contraction of neck musculature or opening and closing the beak. In these circumstances, the unit under study is lost as the movements make the brain to vibrate. Thus the experimental approach used in this thesis explored subsets of the position and velocity spaces. To expand these subsets further it would be necessary to use trained birds. It is still an open question whether chickens can be trained to make specific eye movements. In addition, the results of Chapter 2 indicate that chickens do not have smooth pursuit, thus the only method available to obtain periods of low speed is via OKN. In this case, techniques would have to be developed to obtain better mechanical stability of the microelectrode.

Oscillations are the direct consequence of Phasic motoneurons.

Although most of the data on this chapter concerns the trochlear nucleus, a similar task segregation exists in the Inferior Oblique subdivision of the Oculomotor complex (ventro-lateral subdivision). This sub-nucleus contains the motor pool controlling the inferior oblique. First, as the trajectories of saccades suggest that their oscillations are principally generated by the obliques, and as oscillations have similar intorsional and extorsional velocity profiles, therefore both oblique muscles probably undergo the same sequence of contractions but out of phase by a half cycle during each oscillation. Specifically, because saccadic oscillations have a frequency of 28 Hz, the activity in trochlear Phasic motoneurons must be followed approximately 18 msec later by Phasic activity in motoneurons innervating the inferior oblique. Second, the symmetry of the effects of disabling the obliques implies that the motor pools controlling the obliques share a common organization. Finally, some recordings were made in the ventro-lateral subdivision of the oculomotor nucleus where both Phasic and Tonic responses were isolated.

The amplitude of oscillations, to a first approximation, is totally controlled by the activity of Phasic motoneurons. This amplitude control is not done by "recruitment". As all Phasic motoneurons are active for every oscillatory cycle of every saccade, it is obvious that recruitment is not used to control the output of the Phasic motor pool. On the contrary it appears

that a method based on "rate modulation" is used instead. As figure 3.18 shows it is the mean number of spikes that is correlated with amplitude. Thus during any saccade, Phasic motoneurons begin firing bursts with a maximal number of spikes, as the saccade progresses each burst has fewer and fewer spikes. The only exception to this rule is the relation between the intensity of the first burst and the amplitude of the first subphase of "plus" saccades which on average have 50% of the amplitude of subsequent subphases. The reason for this discrepancy might be found in the physiology of muscle contraction. It is known that the isometric force developed by a muscle is a function of its operating length and that there are a length at which the muscle develops the maximal tension. Thus the force developed by the muscle fibers innervated by Phasic motoneurons depends on the length of the superior oblique at the moment of firing.

In the mammalian extraocular system the amplitude of a movement is controlled by a combination of recruitment and rate modulation whereas in chickens the firing pattern of Phasic motoneurons appears to be independent of the net displacement of the eye. The pattern of discharge of Phasic motoneurons was studied to see if correlations existed with the total eye displacement produced by saccades. The number of spikes in different bursts (i.e., second, third, fourth) or the number of spikes in different combinations of bursts (i.e., second and third or second and third and fourth or third and fourth) was correlated with the total saccadic displacement for spontaneous saccades. No significant correlations were detected. For example, the total number of spikes in bursts 2, 3 or 4 appears independent of the total eye displacement. Similarly, the total number of spikes fired during a saccade shows no correlation with eye displacement. These results suggested that Phasic motoneurons show the same pattern of activity for small saccades (i.e. small net eye displacement) as well as for larger saccades: they are unmodulated by the total eye displacement.

Phasic motoneurons are under a precise temporal control. During saccades the intensity and temporal profile of the activity of Phasic motoneurons are precisely controlled. With the exception of the first burst of "plus" saccades, all Phasic motoneurons fire their bursts after the intorsional phase of each oscillation has began (figure 3.16). Thus during

the first msecs of each intorsional subphase the force applied by the superior oblique is only due to its spring like characteristics. This peculiar timing can be seen in the eye trajectory as an inflexion point, which is in fact an acceleration of the movement of the eye (figure 2.27). The larger duration of subphases as saccades progress (from 17 to 19 msec, figure 2.23) has a parallel on the delay between bursts and the beginning of intorsional subphases (delay = 4.0 msec for the second burst, delay=6.0 msec for burst #5, see figure 3.16).

As mentioned in Chapter 2, the timing between bursts produced by Phasic motoneurons in the superior and inferior oblique motor pools appears to be optimized for saccadic oscillations to be maximally rapid. The temporal data of figures 3.16 and 3.17 show that Phasic motoneurons that control the inferior and superior oblique are never co-activated. As each subphase lasts approximately 18 msec (measured from one peak to the next peak) and oscillations are approximately symmetric the relative timing between agonist and antagonist Phasic motoneurons can be deduced. For an intorsional subphase Phasic motoneurons fire during the firsts 10 msec of the subphase (figure 3.16), thus during the last 8 msec of the subphase the muscle fibers innervated by Phasic motoneurons have time to contract and to begin their relaxation. As mentioned in Chapter 2, this timing appears to be optimal to generate the fastest oscillations. The possibility that natural selection has in this way maximized the frequency of saccadic oscillations is consistent with two hypotheses about their function: that saccadic oscillations function in saccadic suppression (Brooks and Holden, 1973), or that they facilitate the stirring of the vitreous humor (Pettigrew, Wallman and Wildsoet, 1990).

Tonic motoneurons control the eye during fixations and slow speed eye movements. Tonic motoneurons have an activity proportional to eye position and speed, and exhibit a period of total silence beginning 20 msec before the onset of saccades and lasting at least 35 msec, thus at least the pausing period extends 15 msec into each saccade. In the big majority of cases the pause is much longer. The pausing period is not "hardwired" into the physiology of each Tonic motoneuron. A great variability is seen. The pausing is correlated with saccade duration but the net eye displacement also

influences pause duration. A tonic motoneuron that shows a 150 msec pause during a 180 msec saccade that barely moves the eye might have a 70 msec pause during a 180 msec saccade that moves the eye 12° intorsionally. On the other hand, during a 12° extorsional saccade lasting 180 msec the same Tonic motoneuron might have a pause much larger than the saccade duration.

The main conclusions about the firing of Tonic Motoneurons is that as it is the case in mammals their discharge can be approximated by a polynomial expression containing eye position and eye speed as variables. This approximation is valid during the periods of fixations but it fails during saccades as the discharge frequency is uncorrelated with saccadic oscillations. Extensive numerical tests failed to reveal any modulation of their discharge patterns by a 28 Hz wave. Futher indication of the lack of relationship between oscillations and Tonic discharges is the relatively good fit obtained between eye position and firing when the 28 Hz oscillations are extracted from the eye position record (Table 3.2 and figure 3.12) But even with this replacement the linear model relating eye position (slow) with the activity of Tonic Motoneurons consistently fails during the first 50-100 msec of saccades. In that period, the pausing in discharge so characteristics of Tonic motoneurons reveals the existence of another factor, different from eye position or eye speed, controlling the firing of Tonic Motoneurons. This extra factor creates the almost mandatory pause exhibited by Tonic Motoneurons and reflects the existence of an active inhibitory wave reaching this type of motoneuron.

The k values (position sensitivity) of Tonic motoneurons (mean=4.5) were similar to the values obtained in monkeys (mean=3.7 (Fuchs and Luschei, 1970)), cats (mean=6.2, (Fuchs, Scudder and Kaneko, 1988)) and goldfish (mean=7.1, (Pastor and Delgado-Garcia, 1992)). Also the r values were similar (mean=0.35) to the values obtained in monkeys (mean=0.95 (Fuchs and Luschei, 1970)), cats (mean=1.31, (Fuchs, Scudder and Kaneko, 1988)) and goldfish (mean=0.96, (Pastor and Delgado-Garcia, 1992)). However chickens' values were the lowest. A relation appear to exist between k and r, motoneurons with large ks also have large rs (figure 3.12D). Similar dependencies have been reported in monkeys (Fuchs,

Scudder and Kaneko, 1988), cats (Delgado-Garcia, Del Pozo and Baker, 1986) and goldfish (Pastor et al. *in press)*). While it can be argued that the mathematical method used to obtain the k and r values has an intrinsic propensity to produce a relation between these two parameters it must be concluded that the relationship reflect a real dependency. As said, a similar dependency has been found in other species and the method used is similar to the method employed by Pastor et al. On the other hand, no clear relationships are visible between *k* or *r* with threshold. In cats, primates and goldfish *k* (and also *r*) is linearly related to the threshold, and this relation is taken as a manifestation that recruitment follows the size principle (Henneman, Somjen and Carpenter, 1965).

Functional implications of segregation among trochlear motoneurons.

The separation of motoneurons within a motor nucleus into tonic and phasic subpopulations implies significant differences in the organization of the avian saccadic system from that of mammals. First of all, because all avian Phasic motoneurons are activated for all saccades, the direction of the saccadic displacement cannot be encoded by which Phasic motoneurons are recruited. This situation contrasts with the mammalian case in which the direction of the saccade is encoded by the the pulse component of the motor command produced by extraocular motoneurons. Second, in mammals the saccade metrics are thought to be encoded by the phasic component of the "on"-direction neurons of the premotor saccadic burst generator and the tonic component obtained by integration of this phasic signal. In birds, it is not obvious that the saccade metrics could be encoded in the activity of such premotor phasic neurons, or that integration of this premotor activity would yield the correct tonic signal unless the premotor activity impinging on the Phasic motoneurons innervating the opposite muscle were subtracted. Rather, it appears that the pattern of oscillations must be the result of the operation of a central pattern generator that produces the appropriately timed bursts among the Phasic motoneurons innervating the superior and inferior obliques. This is suggested (and the alternative possibility that the oscillations are produced by the stretch of a muscle triggering the contraction of its antagonist by proprioceptive feedback ruled out) by our finding that neither denervating the superior oblique nor cutting the inferior oblique interferes with the pattern of contractions produced by the intact

member of the pair. Further evidence of a central pattern generator is that saccadic oscillations in the two eyes are tightly yoked even during saccades in which the two eyes move in opposite directions (figure 2.22).

The existence of a central pattern generator that drives the Phasic motoneurons would have implications for the control of saccadic trajectory. In mammals, excitatory burst neurons fire at high rates during saccades and drive those motoneurons that move the eye in the direction of the saccade; they are thought to stop firing when the oculomotor system's internal representation of eye position coincides with the internal representation of target position. In birds, this scheme could only work if the burst neurons acted not on the motoneurons but on the central pattern generator, stopping the oscillations when the target was reached. Alternatively, one could treat each saccadic oscillation as though it were a separate saccade as it has been done for human voluntary nystagmus (Shults et al., 1977). Even according to this view, the mammalian scheme would not account for the avian firing patterns because the phasic neurons only fire at the start of each oscillation. It is not yet known whether the premotor input to the Phasic motoneurons encodes the desired saccade size and direction. The fact that those chicken saccades resulting in negligible change in position have oscillations of normal amplitude argues for the existence of some input related to the oscillations themselves.

Another implication of the Phasic motoneurons being driven by a central pattern generator is that the inputs received by Tonic and Phasic motoneurons must be different. Specifically, the fact that Tonic motoneurons pause during saccades, when Phasic motoneurons are active, indicates that the excitatory or the inhibitory part of their input differs. Indeed, in a separate study, we found that medial longitudinal fasciculus fibers, identified by intracellular HRP as trochlear afferents, were divided into Phasic and Tonic types (Letelier, Evinger and Wallman, 1987).

Although avian oculomotor motoneurons are extreme in their functional segregation, previous work has suggested some functional segregation among other motoneurons of the vertebrate oculomotor system. In the primate oculomotor nucleus some motoneurons with extreme position thresholds are active mostly during saccades, thereby behaving as "de facto"

phasic motoneurons (Henn and Cohen, 1975). In frogs, "position" and "velocity" abducens motoneurons have been recorded, but their functional segregation is not complete (Dieringer and Precht, 1986). Finally, in the goldfish abducens nucleus there are neurons, perhaps motoneurons, which have been described as having either "tonic" or "tonic-burst" characteristics (Gestrin and Sterling, 1977). But this last result was not obtained in a more recent study (Pastor et al, *in press*) where only a single type of tonic-phasic response was found in the abducens of the goldfish.

There are indications of functional segregation in other motor pools as well. Three populations of cat sartorius motoneurons exist, but the muscle is compartmentalized into three subdivisions that are involved in different movements (Hoffer et al., 1987). Central partitioning has been also hinted at for the cat stapedius motoneurons (McCue and Guinan, 1988), the motor pool of which is spatially divided. Our results are interesting because the functional segregation is absolute (unlike the situation in the sartorius or the stapedius) and the two types of motoneurons are not anatomically separated as in the stapedius. How the inhomogeneous distribution of premotor terminal arborizations among trochlear motoneurons is achieved is not clear. The function of this motor organization is likewise unclear, but may be related to functions of the saccadic oscillations other than redirecting gaze.

Although these examples argue that some parcellation within motor pools exists in other systems, the functional segregation of avian superior oblique motoneurons into tonic and phasic subpopulations is a more extreme departure from the principle of uniform recruitment order in that entirely different inputs are sent to the two subpopulations of motoneurons. Because both the inputs and the motoneurons are so distinctly segregated into tonic and phasic types, it can be speculated that perhaps this parcellation extends to the synapsing of each type onto muscle fibers with different properties, as has been proposed, but never found, in mammalian extraocular muscles (Jampel, 1967). As some functional heterogeneity exists among primate extraocular motoneurons, the avian oculomotor system may present an exaggeration of trends present in mammals, rather than an entirely different organization. The study of systems with such extreme task segregation

might facilitate our understanding of how motor pools become organized during development and evolution.

Anatomical considerations about the site of origin of the phasic command.

Retrograde labelling of the trochlear revealed the same afferents that have been described previously (Wold, 1976; Wold, 1978; Labandeira-Garcia et al., 1989). These three studies produced big injection sites centered in the oculomotor complex. The method employed in this thesis permitted a more precise deposition of HRP specifically on the trochlear. Label was found in the vestibular complex, the abducens nucleus, the reticular formation and the infracerebellaris nucleus. The results are almost identical to ones reported in (Labandeira-Garcia et al., 1989). Labelling was very prominent in the tangentialis, the superior vestibular and the infracerebellaris nucleus. Because it was supposed that the premotor neurons which control Phasic trochlear motoneurons must be large, the previous three groups were explored with extracellular recordings. Furthermore the tangentialis group seemed specially interesting because this nucleus is unique to birds and its mammalian homologue (interstitial nucleus of the vestibular nerve) does not project to any oculomotor nuclei. This characteristic made it an interesting candidate for producing the bursts received by phasic motoneurons.

Recordings from the vestibular complex failed to reveal responses that could unambiguously be the origin of the "burst" signal received by phasic motoneurons. For example the "train" cells found in the tangentialis/medialis border could not be the immediate excitatory inputs to phasic motoneurons. Because the tangentialis nucleus was exhaustively explored, it must be concluded that the origin of the "burst" is not located inside the tangentialis. Similarly, the group of labelled neurons found in the infracerebellaris nucleus, above the superior vestibular nucleus, did not contain "burst" signals.

Perhaps the origin of the phasic command is in the pontine reticular formation. In mammals, excitatory burst neurons are located in the paramedian pontine reticular formation, just anterior to the abducens nucleus, and are responsible for encoding the saccadic step. As mentioned,

in chickens, neurons from the pontine reticular formation project to the trochlear. Unfortunately, no systematic extracellular recordings were done in this area and this project would be an excellent topic for further study.

Model of saccadic circuitry in chickens.

The experimental evidence gathered to construct a model of the chicken's saccadic machinery is incomplete. Such a project requires the systematic exploration of brainstem regions. But the scant amount of data collected on premotor areas combined with the properties of trochlear motoneurons and the knowledge of eye movements permit the construction of a first order model. The principal facts to have in mind constructing such model are:

a) Oscillations in both eyes occur simultaneously (figure 2.22)
b) The time course of oscillations is, approximately, the same in both eyes (figure 2.22)
c) The pattern of oscillations is very stereotyped and seems unrelated with the net saccadic displacement (figure 2.23; 2.24; 2.19)
d) The number of oscillatory cycles in a saccade is decreased by visual and auditory stimuli (figure 2.37)
e) Oscillations are produced by Phasic motoneurons (figure 3.4)
f) Tonic motoneurons appear to be briefly inhibited during the initial portion of each saccade (figure 3.3; figure 3.12)
g) The activity pattern of Phasic motoneurons is very stereotyped (figure 3.17)
h) Phasic and tonic signals are found in the medial longitudinal fasciculus, enter the trochlear nucleus and probably synapse onto trochlear motoneurons
i) Omnipause-like neurons exist in the brainstem below the trochlear nucleus.

A simple model of the saccadic circuits would assume the existence of a *bona fide* pattern generator involved in the production of oscillations

(figure 3.25). This pattern generator would consist of two centers, one for each side of the brain, mutually interconnected by inhibitory connections. The amplitude of oscillations would be controlled in a stereotyped way by the putative pattern generator. Once the pattern generator were turned "on" it would go through a sequence of states internally generated. The only external influence upon the pattern generator is a gate signal which would inhibit their activity during the periods of fixation but also could interrupt their activity in the middle of a saccade. In this model the amplitude of the signal arriving at Phasic motoneurons would not be used by Tonic motoneurons. In the language of the "bang-bang" models, the "step" component is independent of the "pulse" component. It is exactly in this respect that the avian model differs the most from the mammalian saccadic circuits. As in the case of mammals the optic tectum is supposed to specify the final eye position. The output of the optic tectum is a signal describing eye position most probably in craniocentric coordinates. Again this schema differs in a fundamental way from the mammalian one in which the tectal output encodes the vectorial representation of the saccadic movement not final eye position.

Theories about the functions of saccadic oscillations.

Saccadic oscillations have a still elusive functional significance. Many theories have been advanced concerning their possible functions. Perhaps the first question is whether oscillations must have a function and if they are not a curious epiphenomena with no physiological relevance to the organism.

Two factors seem to indicate that oscillations are relevant to the physiology of birds. The first is their apparent universality. While precise measurements of eye movements have been done in only a few species (pigeon (*Columba livia*) (Nye, 1969); Great horned owl (*Bubo virginatus*) (Steinbach, Angus and Money, 1974); Chicken (*Gallus domesticus domesticus*) (Turkel and Wallman, 1977); Tawny frogmouth (*Podargus strigoides*); Bookbook owl (*Ninox novaeseelandiae*); Bush thick-knee (*Burhinus grallarius*) and the laughing Kookabura (*Dacelo gigas*) (Wallman and Pettigrew, 1985; Pettigrew, Wallman and Wildsoet, 1990)), it is striking that in all these species saccadic oscillations exist. This apparent

universality is not compatible with the distribution of a "neutral" character as these would tend to be absent in some species. The second factor is that saccadic oscillations seem to be "calibrated" to be the fastest and energetically efficient movement that the obliques extraocular muscles can produce. These two features lead to the conclusion that the temporal course of saccadic oscillations is under the influence of selective forces and thus must have a functional role.

Some theories assert a perceptual, visual, function (Brooks and Holden, 1973; Turkel and Wallman, 1977), while other theories ascribe vegetative, non-perceptual, roles for saccadic oscillations (Nye, 1969; Pettigrew, Wallman and Wildsoet, 1990). The author who described saccadic oscillations first (Nye, 1969) observed that they occur in conjunction with nictitation (i.e, movement of the nictitating membrane). Thus he supposed that saccadic oscillations serve to clean the cornea by rubbing the front of the eye against the nictitating membrane and named them "polishing eye movements". A similar point of view was taken by the authors who described the eye movements in the Owl (Steinbach, Angus and Money, 1974), this hypothesis does not explain why at least 50% of saccades are performed without a movement of the nictitating membrane (personal observation). If the purpose of saccadic oscillations were to clean the cornea it seems difficult to interpret the fact that in half the occasions the movement would be done in vain.

Another theory concerning a vegetative function is expressed in (Pettigrew, Wallman and Wildsoet, 1990). According to these authors the torsional oscillations, which have a very high acceleration, would help the transport of nutrients from the *pecten oculi* to the vitreous humor. During saccadic oscillations the vitreous humor would move, quite quickly, with respect to the *pecten.* In Chapter 2 a concordant fact was found (figure 2.34). The relative position of the Ω region with respect the tip of the pecten seems optimal to enhance the passage of substances from the pecten to the vitreous during saccadic oscillations. While this theory is compelling, more data is necessary to assess its validity.

A perceptual role for oscillations was first advanced with respect to "saccadic suppression" (Brooks and Holden, 1973). According to these

authors the fast retinal slip, in the range of hundreds of degrees per second, induced by oscillations would blur the image creating thus a non-central mechanism for suppression. Two of the results reported in this thesis are incompatible with this theory. The first is that the geometrical nature of oscillations, as the axis of rotation is within a 15° angle from the optic axis (see Chapter 2) the central retinal area (circle of 10° in diameter) experiences low speeds; on the order of 25 °/sec. The modifiability of saccades by visual stimuli provides the second reason, as it shows that "saccadic suppression" must be very weak in chickens, as they are able to detect an object moving at 10% the speed of the maximal speed reached during oscillations.

A new theory: Oscillations help visual perception of moving objects

A new hypothesis concerning a perceptual function of saccadic oscillations is presented. This theory proposes that the detectability of slow moving borders, by the retino-tectal pathway, is increased by oscillations. The model is based on the following two facts:

a) Tectal cells, in birds, are mostly movement sensitive (Jassik-Gerschenfeld and Guichard, 1972; Frost and DiFranco, 1976). Their receptive fields are not concentrically organized and their velocity sensitivity is like the ideal curve shown in figure 3.26.

b) Saccadic oscillations produce a peculiar optical flow in the retina (figure 3.27). At every point, located at an eccentricity **x**, a tangential speed **S(x)** is felt during oscillations. Near the Ω region the speed is zero and it increases linearly with eccentricity.

Suppose that a tectal cell with a receptive field at eccentricity **y** and an object is moving with a speed v in the receptive field. During oscillations the relative speed between the moving object and the receptive field would change from v-**S(y)** to v+**S(y)** (figure 3.28A). If the tectal cell acts normally during saccades, i.e. with no saccadic suppression, it would produce responses **Ri=R(**v-**S(y))** and **Re=R(**v+**S(y))**, both responses will not occur at the same time but will be delayed by half an oscillatory cycle (18 msec) with respect to each other. Now another neural element must be added to the model: a cell (or set of cells) that "somehow" stores one response and

subtracts one response from the other (figure 3.28B). The response of this element would then be equal to:

$$O=H(Ri,Re)=Ri-Re=R(v-S(y)) - R(v+S(y)) \qquad \text{Eq. (3.1)}$$

This arrangement will automatically cancel any signals produced only by the fictitious retinal slip induced by saccadic oscillations ($v=0$ for all borders). On the other hand, it will substantially increase the signal from slow moving borders because **Ri-Re** would be different from zero for all moving borders. For example, if we assume a linear relation between speed and response (i.e. $R(v) = av+b$) a border moving at a subthreshold speed $v=\varepsilon$ would generate a response, according to equation 3.1, of the order to $2a\varepsilon$. Thus the response to a subthreshold moving border will be multiplied by the sensitivity (i.e. **a** which has units of spikes/(°/sec)) of the tectal cell. The model would work differently if the velocity response curves were non-linear. Quadratic non-linear responses (i.e. $R(v) = -a(v-m)^2$) would produce a response **O** depending on ε^2 allowing a more precise discrimination of low speeds. In summary, the overall sensitivity of the mechanism would depend on tectal cells that give different responses to stimuli moving at slightly different velocities. Also, because the radial velocity induced by oscillations increases towards the periphery it should be expected that the range at which tectal cells involved in this mechanism operate also increases with eccentricity. Unfortunately few quantitative descriptions of the velocity sensitivity of avian tectal cells exist, thus it is currently difficult to validate the model presented here. The data available on the speed sensitivity of avian tectal cells (Frost and DiFranco, 1976) shows tectal cells with a quadratic response profile like as in figure 3.26 and an optimal speed of 30 °/sec. The application of the model embodied in Eq. 3.1, for that data, shows that the response **O** to a 0.5°/sec moving border could be increased 50 times during oscillations, but if the border moves at 1°/sec the mechanism only increases its detectability 5 times. Interestingly, some data indicates that the optimal speed of tectal cells increases towards the periphery Gutsu (1970) as cited by Hughes and Pearlman (1974). This fact, if confirmed by new studies, is consistent with the model and with the fact that the tangential speed created by oscillations increases toward the periphery, thus at different eccentricities tectal cells should have different optimal velocities. In

summary the mechanism proposed here asserts that the detection of moving objects will be enhanced by adding a "fictional" speed to a border. Tectal cells would detect (or detect better) the moving border and "somehow" the artificial part of the neural response due to the internally originated movement would be removed.

The stereotyped nature of saccadic oscillations can be a necessary consequence of the model just explained. In effect the model asserts that the final output of some class of tectal detectors would be equal to:

$$O = H(Ri, Re) = H(\int F(v, mi(t))dt, \int F(v, me(t))dt) \qquad \text{Eq. (3.2)}$$

where **H** is a function of the responses obtained during the intorsional (**Ri**) and extorsional (**Re**) subphases. In the outline just given **H** is assumed to be simply the subtraction of these two responses, but this theoretical scheme can be made to work under a great number of conditions. For example the functions that describe the velocity of the receptive field during the intorsional and extorsional subphases of each oscillations, $me(t)$ and $mi(t)$, are not necessarily mirror images of each other, and they could change from oscillation to oscillation and from saccade to saccade. The price of such plasticity would be to make the function **H** complex and plastic as it would have to change constantly to compensate the changes made by $me(t)$ and $mi(t)$. While not denying that such "fluid" control mechanism could exist, it appears advantageous to have a pre-wired neural population that will calculate **O** based in only one set of functions $me(t)$ and $mi(t)$ in a fast and efficient manner. Because the functions $me(t)$ and $mi(t)$ depend ultimately of the eye movement during oscillations, a requisite for their invariance is an invariance of saccadic oscillations themselves.

The most unusual part of this model is the operation of the "storage/subtraction" subsystem, but the idea of storing (or delaying) a signal, is similar with the one put forward in current models of movement detection (Reichardt, 1987). The stereotyped temporal course of saccades appears now as a requisite for such a model, in effect, implicit in the equation (Eq. 3.1) is that the visual system knows if the eye is moving intorsionally or extorsionally. As previously noted the visual responses of

tectal cells are not treated identically, one is "stored" (or delayed) for 18 msec. Thus the visual system must be "clocked" (or synchronized) by a mechanism that really reflects the true eye movement. Three sources of eye position are available: a) proprioception, b) visual and c) efference copy. A proprioceptive origin seems unlikely to operate in the model proposed. If data from the segmental motor system of mammals is extrapolated to the avian oculomotor system, it is found that 20-30 msec lags would exist between the state of contraction of a muscle (hence eye position) and the proprioceptive signal. This lag (equal to 75% of an oscillatory cycle) seems incompatible with a fast velocity determination task. This last argument can be rephrased in terms of the low frequency response of stretch receptors (10Hz) when compared with saccadic oscillations (28Hz). But proprioception could be used in other tasks in the oculomotor system. Although in mammals a stretch reflex seems absent in the oculomotor system (Keller and Robinson, 1971) inflow from extraocular muscles has been implicated as source of eye position information (Skavensky, 1972). Visual signals, derived for example from an analysis of the complete optical flow to determine if the eye is moving intorsionally or extorsionally, would also lag eye movement as the retinal processing time is equal to one oscillatory cycle. Thus it seems that the only alternative is the existence of "internal" corollary signals that reflect eye movements. Recent experiments on the centrifugal visual system of birds (Marin, Letelier and Wallman, 1990) show that almost certainly saccade related signals must exist at least in the stratum griseum et fibrosum superficialis near the junction of sublaminae *h* and *i* of the optic tectum (Crossland and Hughes, 1978). It is possible to speculate that precise neural signals reflecting not only the presence or absence of a saccade but the phase (or sense) of saccadic oscillations are available in the optic tectum as well. Finally it must be mentioned that the use of saccades for enhancing certain attributes of an image have been suggested and experimentally supported in the human visual system (Deubel and Elsner, 1986). These experiments showed that patterns with low spatial frequency or which were flickering at high temporal frequencies had a greater detectability after a saccade.

To assess the validity of the model presented here, recordings of tectal cells in awake birds should be done. Specifically the dynamic properties of

their receptive fields should be correlated with eye movements. The model predicts that some tectal cells should be active during saccadic oscillations. Another area for further study is the clarification of the premotor circuits controlling oscillations. Preliminary observations have shown that saccade related signals are widespread in the brainstem. The manner in which this multitude of signals interacts is an open question.

APPENDIX - A

Three Dimensional kinematics of the eyeball: an explained formulaire

1) How to specify rotations.

Different methods exist to specify eye positions and eye rotations. Some of these methods are: Quaternions (Tweed and Vilis, 1987), "orientation vector" (Daunicht, 1988), "rotation vector" (Haustein, 1989). In this appendix another method, based on the matrices representing coordinate transformations between two rotated references frames, will be introduced. Recognizing the computational advantage of quaternions for representing rotations, matrices are still the method of choice as they have a close relation with the search coil method used to record eye position. Rotation matrices also serve to elucidate the correction technique used to compensate for the unavoidable misplacement of the eye coils (Ferman, Collewjin and Van Den Berg, 1987).

2) The problem of the description of eye position inside the orbit.

The movement of the eye inside the orbit is equivalent, to a first approximation, to the rotation of a sphere about a fixed center of rotation. A mathematical model of this physical situation supposes that a cartesian (right-handed) reference frame (**XYZ**) is fixed and attached to the eye orbit. Another such system (**X'Y'Z'**) is attached to the eye and moves with it (conventions as in the methods section of Chapter 2). Furthermore both reference frames are attached at their origin O, which is the center of rotation of the eye and the center of the orbit. At any given moment the system **X'Y'Z'**(representing the eyeball) is "rotated" with respect to the fixed system **XYZ**. The aim is to express this rotation in manageable terms.

In order to create a common language, the transformation of coordinates between these two reference frames must be deduced (figure A.1).

Basic theory.

Let two coordinate systems, **XYZ** and **X'Y'Z'**, have the same origin **0**, but are rotated with respect to each other. Their basis are the vector sets $\{\vec{i},\vec{j},\vec{k}\}$ and $\{\vec{e}_1,\vec{e}_2,\vec{e}_3\}$ respectively. Let $\vec{x}$ a vector with coordinates (x',y',z') in the system **X'Y'Z'**; $\vec{x} = x'\vec{e}_1 + y'\vec{e}_2 + z'\vec{e}_3$. The coordinates (x,y,z) of $\vec{x}$ should be expressed in system **XYZ**.

Using the definition of cosine between vectors:

$$\vec{e}_1 = \cos(\vec{e}_1,\vec{i})\vec{i} + \cos(\vec{e}_1,\vec{j})\vec{j} + \cos(\vec{e}_1,\vec{k})\vec{k}$$
$$\mathbf{a}_{11} \qquad\qquad \mathbf{a}_{12} \qquad\qquad \mathbf{a}_{13}$$
$$\vec{e}_2 = \cos(\vec{e}_2,\vec{i})\vec{i} + \cos(\vec{e}_2,\vec{j})\vec{j} + \cos(\vec{e}_2,\vec{k})\vec{k}$$
$$\mathbf{a}_{21} \qquad\qquad \mathbf{a}_{22} \qquad\qquad \mathbf{a}_{23}$$
$$\vec{e}_3 = \cos(\vec{e}_3,\vec{i})\vec{i} + \cos(\vec{e}_3,\vec{j})\vec{j} + \cos(\vec{e}_3,\vec{k})\vec{k}$$
$$\mathbf{a}_{31} \qquad\qquad \mathbf{a}_{32} \qquad\qquad \mathbf{a}_{33}$$

$\vec{x}$ can be rewritten as:

$$\vec{x} = x'(\mathbf{a}_{11}\vec{i} + \mathbf{a}_{12}\vec{j} + \mathbf{a}_{13}\vec{k}) + y'(\mathbf{a}_{21}\vec{i} + \mathbf{a}_{22}\vec{j} + \mathbf{a}_{23}\vec{k}) + z'(\mathbf{a}_{31}\vec{i} + \mathbf{a}_{32}\vec{j} + \mathbf{a}_{33}\vec{k})$$

rearranging terms then

$$\vec{x} = (x'\mathbf{a}_{11} + y'\mathbf{a}_{21} + z'\mathbf{a}_{31})\vec{i} + (x'\mathbf{a}_{12} + y'\mathbf{a}_{22} + z'\mathbf{a}_{32})\vec{j} + (x'\mathbf{a}_{13} + y'\mathbf{a}_{23} + z'\mathbf{a}_{33})\vec{k}$$

The relations between the coordinates (x,y,z) and (x',y',z') are then

$$\begin{cases} x = x'\mathbf{a}_{11} + y'\mathbf{a}_{21} + z'\mathbf{a}_{31} \\ y = x'\mathbf{a}_{12} + y'\mathbf{a}_{22} + z'\mathbf{a}_{32} \\ z = x'\mathbf{a}_{13} + y'\mathbf{a}_{23} + z'\mathbf{a}_{33} \end{cases}$$

These relations can be expressed in term of a matrix equation.

$$\begin{pmatrix} x \\ y \\ z \end{pmatrix} = \underbrace{\begin{bmatrix} a_{11} & a_{21} & a_{31} \\ a_{12} & a_{22} & a_{32} \\ a_{13} & a_{23} & a_{33} \end{bmatrix}}_{\substack{\text{Transformation} \\ \text{matrix} \\ M}} \begin{pmatrix} x' \\ y' \\ z' \end{pmatrix}$$

$$\vec{x} = M\vec{x}'$$

This matricial equation relates the coordinates of a vector in the moving frame **X'Y'Z'** with its coordinates in the fixed frame **XYZ**.

The matrix **M** totally describes the rotation between the two coordinate systems. **M** is a 3x3 matrix composed of 9 numbers, but because the a_{ij} represent direction cosines between the principal axis of **XYZ** and **X'Y'Z'** they are not independent. They comply with orthogonality conditions like:

$$a^2_{11} + a^2_{21} + a^2_{31} = 1$$

The set of 9 numbers $\{a_{11}, a_{12}, \ldots, a_{33}\}$ is in fact specified by only three numbers, for example $\cos(\vec{i}, \vec{e}_1)$, $\cos(\vec{i}, \vec{e}_2)$ and $\cos(\vec{k}, \vec{e}_3)$.

Instead of using three independent a_{ij} to totally describe **M** another method is usually used. This method is an operational procedure that depends on the crucial fact that any position of the system **X'Y'Z'** can be reached (or decomposed) in three elementary rotations. Each of these elementary rotations is a rotation around some special axis starting from "zero" (i.e. a situation where both reference frames are superimposed).

Because the selection of axes around which these "elementary" rotations are done, and the order in which they must be carried out, are not unique, the matrix **M** can be obtained in more than one way. Three of these procedures will be reviewed.

3) Angles of Euler, Helmholtz and Fick.

In this section the matrix **M** will be expressed in terms of the angles defined by each of these methods. In each of these three procedures the attitude, or position, of the moving system **X'Y'Z'** is defined by a set of three angles and by an implicit order in which the three rotations are done. Thus, the three methods only differ around which axes, and in which order, these elementary rotations are performed.

Euler angles.

The Eulerian angles are defined as follows: the transformation is carried out by means of three successive rotations. Suppose that 2 identical reference frames {(X,Y,Z) and (X",Y",Z")} are initially perfectly superimposed. The sequence begins by rotating ϕ radians about the Z axis. After this rotation the axis X" no longer coincides with axis X. The second rotation is θ radians around axis X", now the axis Z" does not coincide with axis Z. The final operation is done by rotating ψ radians around axis Z". The last position of the system (X",Y",Z") can be thought as the reference frame of the eyeball (X',Y',Z'). These three operations are summarized by:

1) a rotation of ϕ radians around the axis Z: $XYZ \rightarrow X''Y''Z$

2) a rotation of θ radians around the axis X": $X''Y''Z \rightarrow X''Y'''Z'$

3) a rotation of ψ radians around the axis Z": $X''Y'''Z' \rightarrow X'Y'Z'$

As it is difficult to visualize all these different axes it is advisable to consult a figure at this point. The discussion found in (Goldstein, 1965) (figure 4-6 page 107) is particularly clear and also explains the different definitions of Eulerian angles found in the literature.

Using a well known result of linear algebra, **M** can be calculated as the product of three matrices, each of which represents an elementary rotation (Goldstein, 1965)

$$\mathbf{M} = \begin{pmatrix} \cos\phi & -\sin\phi & 0 \\ \sin\phi & \cos\phi & 0 \\ 0 & 0 & 1 \end{pmatrix} \begin{pmatrix} 1 & 0 & 0 \\ 0 & \cos\theta & -\sin\theta \\ 0 & \sin\theta & \cos\theta \end{pmatrix} \begin{pmatrix} \cos\psi & -\sin\psi & 0 \\ \sin\psi & \cos\psi & 0 \\ 0 & 0 & 1 \end{pmatrix}$$

thus

$$\mathbf{M} = \begin{pmatrix} \cos\psi\cos\phi - \cos\theta\sin\phi\sin\psi & \cos\psi\sin\phi + \cos\theta\cos\phi\sin\psi & \sin\psi\sin\theta \\ -\sin\psi\cos\phi - \cos\theta\sin\phi\cos\psi & -\sin\psi\sin\phi + \cos\theta\cos\phi\cos\psi & \cos\psi\sin\theta \\ \sin\theta\sin\phi & -\sin\theta\cos\phi & \cos\theta \end{pmatrix}$$

Euler angles are widely used in physics but they are not in oculomotor research. Two factors make Eulerian angles unsuitable: a) the direction of the optic axis (axis OX' in our model) is not readily obtainable from them and b) two of the rotations (the first and the third) are done around the axis 0Z' and none around the axis 0Y'. These two reasons make preferable a description of eye position in terms of the angles of Fick or Helmholtz. These two conventions permit a quick specification of the orientation of the optic axis.

Helmholtz angles.

The Helmholtz angles (λ,μ) are defined by the following sequence of rotations:

1) a rotation of λ radians around the axis Y: XYZ → X″YZ″
2) a rotation of μ radians around the axis Z″: X″YZ″ → X′Y′Z″

Fick angles.

The angles in the Fick system differ from the Helmholtz only in the order in which the elementary rotations are executed;

1) a rotation of ϕ radians around the axis Z: XYZ → X″Y″Z
2) a rotation of θ radians around the axis Y″: X″Y″Z → X′Y″Z″

In general a third rotation is not included in these two conventions. The amount of torsion, that is the amount of rotation around the optic axis, is not a free parameter in primates (Donder's law). The degree of torsion is a precise function of λ and μ (or ϕ and θ). In strict rigor the following rotation should be included in both procedure:

3) a rotation of ψ radians around the axis X′: X′Y‴Z″ → X′Y′Z′

As it was done for Eulerian angles, the matrix M can be expressed in functions of Helmholtz or Fick angles.

For Helmholtz angles:

$$\mathbf{M} = \begin{pmatrix} \cos\lambda & 0 & \sin\lambda \\ 0 & 1 & 0 \\ -\sin\lambda & 0 & \cos\lambda \end{pmatrix} \begin{pmatrix} \cos\mu & -\sin\mu & 0 \\ \sin\mu & \cos\mu & 0 \\ 0 & 0 & 1 \end{pmatrix} \begin{pmatrix} 1 & 0 & 0 \\ 0 & \cos\psi & -\sin\psi \\ 0 & \sin\psi & \cos\psi \end{pmatrix}$$

and for Fick angles:

$$\mathbf{M}(\phi,\theta,\psi) = \begin{bmatrix} \cos\phi & -\text{sen}\phi & 0 \\ \text{sen}\phi & \cos\phi & 0 \\ 0 & 0 & 1 \end{bmatrix} \begin{bmatrix} \cos\theta & 0 & \text{sen}\theta \\ 0 & 1 & 0 \\ -\text{sen}\theta & 0 & \cos\theta \end{bmatrix} \begin{bmatrix} 1 & 0 & 0 \\ 0 & \cos\psi & -\text{sen}\psi \\ 0 & \text{sen}\psi & \cos\psi \end{bmatrix}$$

The final expression for M, using the convention of Fick, is:

$$\mathbf{M}(\phi,\theta,\psi) = \begin{bmatrix} \cos\theta\cos\phi & -\cos\psi\sin\phi + \sin\psi\sin\theta\cos\phi & \sin\psi\sin\phi + \cos\psi\sin\theta\cos\phi \\ \cos\theta\sin\phi & \cos\psi\cos\phi + \sin\psi\sin\theta\sin\phi & \cos\psi\sin\theta\sin\phi - \sin\psi\cos\phi \\ -\sin\theta & \sin\psi\cos\theta & \cos\psi\cos\theta \end{bmatrix}$$

In deriving this matrix it is important to note that an implicit right-hand reference frame is used and that a positive angle θ represents a depression of the eyeball, not an elevation. Also it must be noticed that $\mathbf{M}(\phi,\theta,\psi)$ is nothing more than a rotation matrix that represents how coordinates (or vectors) are transformed when a reference frame is rotated with respect to some arbitrary system considered as fixed in space.

$$\vec{\mathbf{V}}_{(orbit)} = \mathbf{M}(\phi,\theta,\psi)\vec{\mathbf{V}}_{(eye)}$$

It must be emphasized that the triplet (ϕ,θ,ψ, Fick's angles) determines a different frame X'Y'Z' from the triplet (ϕ,θ,ψ, Helmholtz's angles). In other words: the same triplet of angles determine very different eye positions if they are interpreted as Fick's or Helmholtz's angles. While both procedures can be used to specify eye position, in this thesis the Fick's convention will be used to specify eye position.

The Fick's angles (ϕ,θ,ψ) unambiguously describe a "position" of the eyeball in the orbit. Sometimes it is preferable to specify the "eye position"

by the associated rotation matrix $\mathbf{M}(\phi,\theta,\psi)$. This representation is adequate because it allows for an easy calculation of the true magnitude of changes in eye position during saccades. Also this representation allows the instantaneous axis of rotation during saccades to be found and the formulas to compensate for the misalignment between the reference frame of the eye coils and the eye to be developed.

Calculation of M, and Fick's angles (ϕ,θ,ψ), from raw data.

The search coil method gives immediately three of the a_{ij} that completely specify the matrix **M**. Two different situations will be explored. In one situation the two eye coils C1 and C2 are in the planes **Y'Z'** and **X'Z'** respectively (Robinson, 1963; Ferman, Collewjin and Van Den Berg, 1987). In the other situation the eye coil C2 lies in the plane **X'Y'**. The outputs of the three phase detector circuits have different meanings in these two situations.

i) <u>C1 in Y'Z', C2 in X'Z'</u>

As explained in the methods section (Chapter 2) the three phase detectors produce outputs that are directly related to matrix **M**.

$$O_1 = \alpha\cos(\vec{e}_1,\vec{k}) = \alpha a_{13} \quad \text{"vertical signal"}$$

$$O_2 = \alpha\cos(\vec{e}_1,\vec{j}) = \alpha a_{12} \quad \text{"horizontal signal"}$$

$$O_3 = \alpha\cos(\vec{e}_2,\vec{k}) = \alpha a_{23} \quad \text{"torsional signal"}$$

α ="gain" of recording system

By identifying the values of a_{13}, a_{12} and a_{23} with their expression in $\mathbf{M}(\phi,\theta,\psi)$ the values of (ϕ,θ,ψ) can be calculated.

$$\theta = \mathrm{A}\sin(-a_{13}) = \mathrm{A}\sin(-O_1(t)/\alpha)$$

$$\phi = \mathrm{A}\sin(a_{12}/\cos\theta) = \mathrm{A}\sin(-O_2(t)/(\alpha\cos\theta))$$

$$\psi = \mathrm{A}\sin(a_{23}/\cos\theta) = \mathrm{A}\sin(-O_3(t)/(\alpha\cos\theta))$$

A sin = inverse sin

These three equations can be implemented in computer routines that extract from the steam of raw data $(O_1(t),O_2(t),O_3(t))$ the stream of Ficks angles $(\theta(t),\phi(t),\psi(t))$.

ii) C1 in Y'Z', C2 in X'Y'.

If coil C2 lies in the X'Y' plane and its emf is "phase detected" against a magnetic field in the direction OY the output O_3 is more complex. In effect, the torsional signal is:

$$O_3 = \alpha\cos(\vec{e}_3,\vec{j}) = \alpha a_{32} \quad \text{"torsional signal"}$$

Thus the torsional angle can be found from:

$$O_3 = \alpha(-\sin\psi\sin\phi + \cos\theta\cos\phi\cos\psi)$$

Because the signals O_1 and O_2 are the same as previously, they can be used to calculate θ and ϕ first and then to calculate ψ using this last equation.

These two examples show how important it is to realize which search coil configuration (i.e. orientation of eye coils and the reference signals used for "phase detection") is being used in order to correctly calculate the Fick angles (ϕ,θ,ψ).

Numerical correction for misalignment of eye coils.

All the analysis presented supposes that the implicit reference frame defined by the eye coils C1 and C2 is the same reference frame defined by the optic axis and the equatorial plane of the eye. In other words it assumes that coil C1 is concentric with the optic axis. Experimentally this condition is never fulfilled. Always a misalignment exists between these two reference frames. The effect of this misalignment is not only to "offset" the angles (ϕ,θ,ψ) by a constant amount. The error introduced by this offset continuously changes because it is a function of eye position.

If it is assumed that the misalignment is constant during an experiment (no movement of the eyecoils after they have been attached) the eye position, with respect to the orbit can be calculated from the raw data. In effect, let

$(\theta_m, \phi_m, \psi_m)$ be the triplet that describes the rotation existing between the eye and eye coils reference frames. This triplet has a matrix associated $M(\theta_m, \phi_m, \psi_m)$ that represents the rotation between the two frames:

$$\vec{V}_{(eye-coils)} = M(\theta_m, \phi_m, \psi_m)\vec{V}_{(eye)}$$

The angles $(\theta_m, \phi_m, \psi_m)$ should be determined during the experiment by means of another procedure. In this thesis a photographic method based on an idea of Hamada was used (Hamada, 1984). If the subjects could be instructed to foveate at specific targets the angles $(\theta_m, \phi_m, \psi_m)$ could be easily measured.

Furthermore the analysis just carried out shows that the relation between the reference frame of the orbit and the eye coils is:

$$\vec{V}_{(orbit)} = M(\phi', \theta', \psi')\vec{V}_{(eye-coils)}$$

Where $M(\phi', \theta', \psi')$ is the transformation matrix associated with the Fick's angles (ϕ', θ', ψ') as determined by the outputs $(O_1(t), O_2(t), O_3(t))$. Thus, the outputs $(O_1(t), O_2(t), O_3(t))$ perfectly describe the position of the eyecoils with respect to the laboratory.

The last two equations can be combined to express the transformation between the orbit and the eye:

$$\vec{V}_{(orbit)} = M(\phi', \theta', \psi')M(\theta_m, \phi_m, \psi_m)\vec{V}_{(eye)}$$

The matricial product $M(\phi', \theta', \psi')M(\theta_m, \phi_m, \psi_m)$ defines a new transformation matrix that relates the reference frames of the orbit and the eye. The final Fick's coordinates of the eyeball with respect to the lab $(\theta_r, \phi_r, \psi_r)$ are obtained as follow:

Let Q be the a_{13} component of $M(\phi', \theta', \psi')M(\theta_m, \phi_m, \psi_m)$ then

$$\theta_r = A\sin(-Q)$$

Similar procedures give the other two angles by considering the components a_{12} and a_{23}.

Description of rotations

The symbolism of rotation matrices can also be used to describe not only static eye positions but also all eye movements. The idea behind the method is simple.

At the beginning of a saccade eye position is described by a rotation matrix $\mathbf{M}_b$ and by matrix $\mathbf{M}_e$ at the end. To simplify notation all the references to Fick's angles have been dropped. Matrices $\mathbf{M}_b$ and $\mathbf{M}_e$ are rotation matrices and it is irrelevant if they are built using the conventions of Euler, Fick or Helmholtz. A property of rotation matrices is a unique rotation matrix $\mathbf{M}_{rot}$ fulfills the following equation:

$$\mathbf{M}_e = \mathbf{M}_{rot}\mathbf{M}_b$$

the matrix $\mathbf{M}_{rot}$ can be calculated by:

$$\mathbf{M}_{rot} = \mathbf{M}_e\mathbf{M}^{-1}_b$$

This mathematical result is equivalent to the theorem of Euler-D'Alembert that states that any pure rotation is a rotation around some axis. The matrix $\mathbf{M}_{rot}$ specifies the direction of such axis and the amplitude of the rotation.

Amplitude of saccades.

In the analysis of eye movements in only one dimension, for example the horizontal component, it is natural to measure "the amplitude" of a saccade as the change in the horizontal component between the beginning and the end of the saccade. In 3 dimensions the method can not be generalized to something like:

$$\textbf{amplitude} = \sqrt{\Delta\psi^2 + \Delta\theta^2 + \Delta\phi^2}$$

where $\Delta\psi, \Delta\theta, \Delta\phi$ are the algebraic differences for all three Fick's components of eye position between the beginning and the end of a saccade.

The euclidean distance valid for two points in R^3, does not represent the "distance" (or amplitude) between rotations because angles do not behave like scalars at this respect. One solution to calculate the "true" amplitude of a movement is to use the Euler-D'Alembert theorem and the properties of matrix $\mathbf{M}_{rot}$.

The crucial point is that $\mathbf{M}_{rot}$ is a rotation matrix. Rotation matrices can always be written in an special simple form. If the implicit coordinate system where the matrix $\mathbf{M}_{rot}$ is expressed is changed to another coordinate system where one of the axis (for example the Z axis) coincides with the axis of rotation it can be written as:

$$\mathbf{M}_{\bullet} = \begin{bmatrix} \cos(\alpha) & \sin(\alpha) & 0 \\ -\sin(\alpha) & \cos(\alpha) & 0 \\ 0 & 0 & 1 \end{bmatrix}$$

Where α is the amplitude of the rotation.

$\mathbf{M}_{rot}$ and $\mathbf{M}_{\bullet}$ represent the same physical rotation, they are only expressed in different coordinate systems. Technically speaking it is said that both matrices are SIMILAR. This means that a matrix B exists that has the following property:

$$\mathbf{M}_{\bullet} = \mathbf{B}\mathbf{M}_{rot}\mathbf{B}^{-1}$$

An important matrix operator appears now on the scene: The trace operator.

$$tr(M) = \sum_{i=1}^{i=3} M_{ii}$$

In other words the trace is the addition of the diagonal elements in matrix M. A well known theorem states that the trace of two similar matrices is the same, then:

$$tr(\mathbf{M}_{rot}) = tr(\mathbf{M}_{\bullet}) = 2\cos(\alpha) + 1$$

Given $\mathbf{M}_{\bullet}$ and $\mathbf{M}_{b}$, $\mathbf{M}_{rot}$. can be calculated Usually $\mathbf{M}_{rot}$ would not have the simple form of matrix $\mathbf{M}_{\bullet}$, but this does not matter. Because the trace is invariant under similarity operations:

$$\mathbf{tr(M_{rot}) = 2\cos(amplitude) + 1}$$

Thus the amplitude of the saccade is:

$$\mathbf{amplitude} = \cos^{-1}\left(\frac{\mathbf{tr(M_{rot}) - 1}}{2}\right)$$

Determination of the instantaneous axis of rotation.

During a saccade the movement of the eye can be described in many ways. One method is to specify the set of points

$$\{(\psi(t), \theta(t), \phi(t)); t \in [t_{begin}, t_{end}]\}$$

That represent the succession of eye positions expressed in Fick's coordinates. While this description is perfectly adequate it is possible to use an elaboration of the Euler-D'Alembert theorem to calculate the instantaneous vector of angular speed $\vec{\Omega}(t)$. This vector specifies the instantaneous axis of rotation and the speed of the rotation.

Let $\mathbf{M(t)}$and $\mathbf{M(t+1)}$ be two consecutive eye positions measured about 1 msec apart: A rotation $\mathbf{D(t)}$ that changes $\mathbf{M(t)}$ into $\mathbf{M(t+1)}$ exists. As was done for the amplitude of saccades the following equation can be written:

$$\mathbf{M(t+1) = D(t)M(t)}$$

This implies that $\mathbf{D(t)}$ is equal to:

$$\mathbf{D(t) = M(t+1)M^{-1}(t)}$$

Because the time between t and t+1 is usually small $\mathbf{D(t)}$ is a peculiar matrix as it represents an "infinitesimal" rotation, this implies that it can be written as:

$$\mathbf{D(t) = I + \varepsilon(t)} = \begin{bmatrix} 1 & 0 & 0 \\ 0 & 1 & 0 \\ 0 & 0 & 1 \end{bmatrix} + \begin{bmatrix} 0 & \mathbf{a} & \mathbf{-b} \\ \mathbf{-a} & 0 & \mathbf{c} \\ \mathbf{b} & \mathbf{-c} & 0 \end{bmatrix}$$

where $\varepsilon(t)$ is an antisymmetric matrix. From matrix $\varepsilon(t)$ the vector $\vec{\Omega}(t)$, which represent the instantaneous angular speed vector, can be found by simple inspection. In effect:

$$\vec{\Omega}(t) = \varepsilon_{32}(t)\vec{e}_1 + \varepsilon_{13}(t)\vec{e}_2 + \varepsilon_{21}(t)\vec{e}_3$$

The instantaneous speed at time t is:

$$\left\|\vec{\Omega}(t)\right\| = \sqrt{\varepsilon^2{}_{32}(t) + \varepsilon^2{}_{13}(t) + \varepsilon^2{}_{21}(t)}$$

and the direction of the instantaneous axis of rotation is given by the unitary vector $\vec{n}(t) = \vec{\Omega}(t) / \left\|\vec{\Omega}(t)\right\|$. Then a trajectory of the eye between two points is perfectly described by the vector sequence

$$\Gamma = \left\{\vec{\Omega}(t), t \in [t_{begin}, t_{end}]\right\}$$

APPENDIX - B

A method to discover the existence of a functional relation among three variables.

This appendix describes a simple and intuitive method to solve the following problem. Let $S = \{(x_1,y_1,z_1),(x_2,y_2,z_2),.....,(x_n,y_n,z_n)\}$ be a set of measurements of three variables (X,Y,Z). The problem is to find if a functional relation exists among (X,Y,Z). In analytical terms, to explore if a function such that $z = \Phi(x,y)$ exists.

Two factors make the answer to such question difficult: a) the putative relationship between the variables can be very complex, not a simple plane in space as in $z = Ax + By$ and b) real measurements are not perfectly determined, an imprecise amount of "noise", which obscures any functional relationship, is added to the data.

In some statistics textbooks (Mandel, 1964) an answer to this problem is given if the type of relationship is known. In this case a fitting of the data points can be attempted according to a pre-existing model. It would be desirable to have a method that, without assuming any "a priori" information about Φ would determine if such function exists, or if X,Y,Z are mutually independent variables.

An approximate method relies on the fact that if a functional relation exists, the points $(x,y,\Phi(x,y))$ represent a surface in space. In this case the original sample S would consist of n points drawn from that surface. By plotting all the data points in any 3-D computer program a qualitative answer can be generated. Two extreme situations are possible: 1) the points in S perfectly outline a surface, a perfect functional relation exists and 2) the points of S form a spherical "cloud" of points, the three variables are uncorrelated. While this qualitative method is easy to understand a quantitative method would be desirable.

Here a quantitative method is introduced. The idea behind the method is to analyze the variations of the density of points in S at different spatial scales. The algorithm is as follows:

Let

$S = \{(x_1,y_1,z_1),(x_2,y_2,z_2),.....,(x_n,y_n,z_n)\}$ the data set made of n independent samples. For every point j the following sequence of numbers is calculated.

$N(j,\alpha)$ = number of points located at a distance α or less from point j

It is convenient to choose for α a set of values on a geometrical sequence like

$$\left\{\frac{d_{max}}{2^P},\frac{d_{max}}{2^{P-1}},\frac{d_{max}}{2^{P-2}},\cdots,\frac{d_{max}}{2^0}\right\} = \{\alpha_0,\alpha_1,.....,\alpha_p\}$$

where d_{max} is the "diameter" of the cloud of points (i.e. the greatest distance between points in the set S) and P a small integer. If P is chosen to be 20 the analysis would cover 6 orders of magnitude. Next the average of the $N(j,\alpha)$ is calculated.

$$N(\alpha) = \frac{\sum_{j=1}^{j=n} N(j,\alpha)}{n}$$

$N(\alpha)$ represents the average number of points located inside a sphere of radius α centered in any point of S. The rationale of the method is that each time the diameter of the sphere is doubled (implicit by the choice of α) the volume of space increases by 8 but $N(\alpha)$ changes by a different amount depending on the spatial distribution of points in the sample.

If the points from S are extracted from a volume of space $N(\alpha)$ would also increase by the same factor of 8 when α is doubled. If the sample was taken from a surface $N(\alpha)$ will increase by a factor of 4 and by a factor of 2 if the points are from a curve in space.

The "dimensionality" of the set S can be analyzed by considering a plot of $Log(N(\alpha))$ vs $Log(\alpha)$ (figure B.A). In theory this graph should be a straight line, and the slope should give a cue about the nature of S. A slope of 3 indicates that the distribution of points in S varies as the volume: no

functional relationship exist between (X,Y,Z). A slope of 2 shows a strict correlation thus $Z = \Phi(X,Y)$. Finally a value of 1 would indicate that $Z = \Phi(X)$ and $Y = \Omega(X)$. Intermediate values (e.g. 2.3) imply that an imperfect functional relation exists and it is partially masked by noise: i.e. $Z = \Phi(X,Y) + \text{noise}$.. As the relevant parameter in this method is the slope in figure B.A a more intuitive way of plotting the data is to plot the following approximation to the derivative of $\text{Log}(N(\alpha))$.

$$\frac{[\text{Log}(N(\alpha_i)) - \text{Log}(N(\alpha_{i-1}))]}{\alpha_i - \alpha_{i-1}}$$

Figure B.C shows the two distortions that affect this method. First, at extreme scales, small and large values of α, the slope tends to 0. Second, the maximal slope is always less than the expected value. For example, for uncorrelated data points the maximal slope is 2.7 instead of 3.0. These two distortions are an unavoidable side effect of the finite size of the original sample S.

Because the sample size is finite, hence discrete, $N(j,\alpha)$ does not always change as α increases. As the points are isolated in space any increase in α by a quantity smaller than the minimal distance between points does not change $N(j,\alpha)$ or $N(\alpha)$. In other words $N(\alpha_0) = N(\alpha_1) = N(\alpha_2)$. At this small scale it appears that all the points are isolated in space without global structure. Thus the slope, toward the left of figure B.A and B.B is close to 0.

As the data is necessarily bounded, the change in $N(j,\alpha)$ is not as big as expected for large values of α. In effect, for large values of α a sphere of radius α will contains a sizable portion of points of S and of space "outside" the data cloud. Any increase on the value of α does not change $N(j,\alpha)$ appreciably. Thus at large scales, the data points seem to be collapsed into a small region of space, and the slope toward the right of figure B.A and B.B is close to 0.

For intermediate values of α, where the two effects just mentioned are less important, the slope of $\text{Log}(N(\alpha))$ vs $\text{Log}(\alpha)$ reflects the true dimensionality of the set S. Three sets of data are analyzed in figure B.C. One set, S_3, was made of 1000 points randomly chosen from the "cube" $[-1,1]^3$ another, S_2,

from 1000 points randomly from the surface $S_2 = \{z = \sqrt{x^2 + y^2}, x, y \in]-1,1[\}$, and 1000 points obtained from the line $\{(x,x,x); x \in]-1,1[\}$ S_1. The maximal slope for S_1 is 0.95, 1.8 for S_2 and 2.7 for S_3 (figure B.C). In all three cases the maximal slope is less than the predicted value (0.95 vs 1.0; 1.8 vs 2.0 and 2.7 vs 3.0). This is due to the finite sample size. The points located towards the boundary of the data clouds introduce a bias in $N(j,\alpha)$. For these points after a certain, intermediate, value of α the implicit sphere defined by $N(j,\alpha)$ contains an asymmetric distribution of points; a sizeable portion of the sphere is "outside" the data cloud. This implies that their contribution of the points in the periphery to the average $N(\alpha)$ is less than of those points located in the middle of the data cloud causing $N(\alpha)$ to varies less than the predicted value.

The method is fairly robust, for example in figure B.D we have a plot similar to figure B.C but for three different surfaces; a plane, a semi-sphere and a two dimensional gaussian The variations in the slopes are almost identical for all of them, indicating that the data sets were extracted from surfaces.

Table 2.1 Spontaneous oculomotor range in 14 chickens. For each component of eye position (expressed in Fick's coordinates) the range containing 95% of fixations is given. The torsional range of spontaneous fixations is as big as the horizontal and vertical components. In the conditions used in this thesis (i.e. head fixed) the eye moves in a "cube" of 15 ° approximately.

Chicken-ID	Torsional range (95% of fixations)	Vertical range (95% of fixations)	Horizontal range (95% of fixations)
c-10	10.0	14.8	7.2
c-11	12.3	16.9	15.0
c-12	16.4	16.3	19.5
c-01	10.9	14.9	13.4
c-02	9.5	20.6	10.7
c-03	9.2	12.6	5.3
c-04	13.4	15.2	8.6
c-05	9.2	15.2	8.8
c-08	15.7	19.2	19.1
c-09	13.9	13.4	17.5
c-13	16.2	24.4	20.6
c-14	14.7	25.1	18.8
c-15	16.8	20.1	14.6
c-16	20.6	22.2	13.1
Average (StDev)	13.5 (3.5)	17.9 (4.0)	13.7 (5.0)

Table 2.2. Mean duration of fixations. In 14 chickens (upper row of table) the mean duration of 1000 succesive fixations was obtained (lower row, in seconds). This data was obtained with a head fixed preparation.

c-10	c-11	c-12	c-01	c-02	c-03	c-04	c-05	c-08	c-09	c-13	c-14	c-15	c-16
1.9	1.1	1.5	1.2	1.7	1.5	1.5	1.6	1.4	1.3	1.7	1.5	2.1	2.0

Table 2.3 Mean duration of saccades. Saccades shorter than 70 msec are very rare in chickens. The duration of saccades seems to be influenced by attentional mechanisms and it can be manipulated by visual and auditory stimuli (see Tables 2.8). This table reflects the duration of spontaneous saccades with the head fixed, (population average=169 msec). As a comparison, saccades in primates last less than 80 msec.

Chicken-ID	Mean duration of saccades (msec) [StDev]
c-30	155 [31]
c-41	141 [30]
c-52	127 [36]
c-7	168 [50]
c-90	127 [29]
c-12	183 [57]
c-13	200 [47]
c-14	219 [68]
c-15	198 [39]
c-16	171 [35]

Table 2.4 Duration of subphases S2-S7 for 10 chickens. In each box the median duration of the subphase is given in msec and below the 95% confidence interval for the median. Subphases were not sorted according to their type. The duration of subphases is very constant, 18 msec approximately in all saccades and all chickens. This correspond to a frequency of 28 Hz.

	S2	S3	S4	S5	S6	S7
C-30	17.0 [16.7-17.3]	17.0 [16.7-17.4]	17.8 [17.3-18.2]	19.2 [18.8-19.5]	18.5 [18.0-18.9]	19.2 [18.7-19.7]
C-41	16.3 [15.8-16.9]	17.8 [17.5-18.0]	17.8 [17.5-18.0]	19.2 [18.9-19.4]	19.2 [18.8-19.6]	18.5 [18.0-18.9]
C-50	15.6 [15.4-15.8]	16.3 [16.1-16.5]	17.0 [16.8-17.2]	17.8 [17.5-18.0]	18.5 [18.3-18.7]	18.5 [18.2-18.7]
C-7	17.0 [16.8-17.2]	17.8 [17.6-17.9]	18.5 [18.3-18.7]	19.9 [19.7-20.1]	19.2 [19.0-19.4]	19.2 [18.9-19.4]
C-90	14.9 [14.6-15.2]	17.8 [17.4-18.1]	17.8 [17.3-18.2]	18.5 [18.2-18.7]	17.8 [17.5-18.0]	17.0 [16.5-17.6]
C-12	17.0 [16.7-17.4]	18.5 [18.0-19.0]	18.5 [18.2-18.7]	18.5 [18.1-18.8]	18.5 [18.2-18.7]	19.2 [18.8-19.6]
C-13	16.3 [15.8-16.9]	15.6 [15.3-15.9]	16.3 [16.1-16.6]	17.0 [16.9-17.1]	17.8 [17.6-17.9]	18.5 [18.3-18.7]
C-14	18.5 [18.3-18.6]	18.5 [18.0-18.9]	18.5 [18.1-18.8]	20.6 [20.2-21.0]	19.9 [19.5-20.2]	21.3 [21.0-21.6]
C-15	16.3 [15.7-16.9]	17.0 [16.6-17.5]	17.8 [17.4-18.1]	18.5 [18.5-18.5]	18.5 [18.2-18.8]	18.5 [18.3-18.6]
C-16	18.5 [18.0-19.0]	22.0 [21.6-22.4]	20.6 [20.3-20.8]	22.7 [22.4-23.1]	21.3 [21.0-21.6]	22.7 [22.3-23.2]

Table 2.5 Amplitudes of subphases (S2-S7). The median amplitude (in degrees) and the 95% confidence interval for the median are given for subphases S2-S7. The amplitude is the 3-dimensional amplitude. The second and third subphases are the largests with an amplitude of 10-12°. Subphases 4-7 are smaller but their decay in amplitude is not an exponential function of time.

	S2	S3	S4	S5	S6	S7
C-30	8.8 [8.5-9.2]	9.5 [9.2-9.7]	9.7 [9.5-9.9]	8.9 [8.6-9.2]	8.0 [7.7-8.4]	6.3 [5.7-6.9]
C-41	9.9 [9.6-10.2]	10.1 [9.8-10.4]	10.9 [10.8-11.1]	9.8 [9.6-10.0]	9.3 [9.0-9.6]	8.4 [7.4-9.4]
C-50	11.7 [11.5-11.8]	11.6 [11.4-11.7]	12.2 [12.1-12.4]	11.9 [11.7-12.1]	11.8 [11.6-12.0]	10.8 [10.4-11.1]
C-7	9.9 [9.7-10.2]	9.7 [9.5-9.9]	10.2 [10.0-10.4]	9.5 [9.2-9.7]	9.1 [8.8-9.4]	7.7 [7.1-8.3]
C-90	11.0 [10.9-11.1]	10.9 [10.8-11.0]	11.8 [11.7-11.9]	10.1 [9.9-10.3]	9.2 [9.0-9.5]	7.6 [6.8-8.4]
C-12	7.2 [6.7-7.7]	8.0 [7.7-8.3]	7.8 [7.6-8.1]	7.0 [6.6-7.5]	6.5 [6.0-7.0]	5.7 [4.9-6.5]
C-13	10.9 [10.6-11.2]	11.2 [11.0-11.4]	11.3 [11.2-11.5]	11.0 [10.8-11.2]	10.5 [10.2-10.7]	9.5 [9.2-9.8]
C-14	13.5 [13.1-13.9]	13.1 [12.9-13.4]	13.9 [13.6-14.1]	13.5 [13.2-13.8]	13.0 [12.7-13.3]	12.1 [11.6-12.5]
C-15	9.5 [9.3-9.7]	9.5 [9.3-9.7]	9.8 [9.6-10.0]	9.4 [9.0-9.7]	9.5 [9.2-9.8]	8.5 [8.0-8.9]
C-16	11.1 [10.8-11.4]	11.9 [11.7-12.0]	12.6 [12.4-12.8]	11.6 [11.4-11.8]	10.7 [10.4-11.0]	8.7 [8.2-9.2]

Table 2.6 Average speed during oscillations. The median of the average velocity (i.e. subphase amplitude/subphase duration) is given in deg/sec for subphases S2-S7, also the 95% confidence interval for the median. Saccadic oscillations are very fast, reaching peak velocities of 700 °/sec.

	S2	S3	S4	S5	S6	S7
C-30	541 [515-567]	546 [522-571]	563 [541-585]	476 [458-494]	427 [406-447]	342 [307-377]
C-41	624 [601-646]	584 [569-599]	604 [592-616]	506 [494-519]	492 [470-514]	435 [386-484]
C-50	763 [750-776]	720 [708-732]	722 [712-731]	657 [644-671]	644 [629-659]	583 [567-600]
C-7	590 [574-607]	544 [533-555]	557 [544-570]	490 [474-507]	481 [462-500]	392 [358-426]
C-90	720 [701-739]	630 [618-642]	671 [652-690]	546 [537-559]	498 [480-516]	434 [396-483]
C-12	417 [389-445]	419 [407-432]	440 [426-454]	374 [354-393]	347 [323-371]	292 [253-331]
C-13	716 [699-730]	708 [697-719]	688 [671-704]	635 [626-645]	590 [575-606]	524 [511-537]
C-14	748 [723-774]	709 [683-735]	737 [713-761]	660 [640-680]	653 [635-671]	571 [544-599]
C-15	607 [585-630]	541 [526-556]	547 [536-559]	517 [498-535]	527 [510-544]	451 [422-480]
C-16	591 [574-608]	546 [534-557]	624 [608-639]	512 [500-523]	504 [489-519]	378 [358-398]

Table 2.7 95% confidence intervals for the duration, amplitude and speed for the first subphase separated according to type. Extorsional subphases are larger, and faster than their intorsional counterparts.

	Amplitude (°)	Duration (msec)	Speed (°/sec)
Intorsional (N=596)	[4.8-5.1]	[17.6-17.9]	[478-502]
Extorsional (N=616)	[6.3-6.5]	[15.4-15.8]	[518-535]

Table 2.8A Movement detection during saccades. The rotation of the visual world (40 °/sec for 100 msec) during saccades produces a shortening of saccades. This table gives the duration of saccades in a normal situation (i.e.no rotation of outside visual field) and the duration of saccades in which the visual field was rotated during the saccade.

	Chicken #1	Chicken #2	Chicken #3
Control Saccades	dur=179 stdev=41, N=54	dur=175 stdev=49, N=64	dur=152 stdev=29, N=71
Motion during saccades	dur=131 stdev=31, N=66	dur=138 stdev=29, N=53	dur=135 stdev=22, N=85

Table 2.8B Saccade shortening by auditory stimulus. If a sound is given during saccades a shortening of the saccade is produced.

	Chicken #1	Chicken #2	Chicken #3
Control Saccades	dur=187 stdev=29, N=38	dur=137 stdev=22, N=44	dur=168 stdev=34, N=58
Sound during saccades	dur=128 stdev=32, N=40	dur=93 stdev=24, N=44	dur=114 stdev=22, N=36

Table 2.9: Geometrical parameters of some extraocular muscles.

The coordinates of the origins and insertions of three extraocular muscles were defined with respect to the highest point of the equatorial plane. The angle between the equatorial plane and the midline was defined as the angle between the line created by the intersection of the equatorial plane with the horizontal plane and the saggital plane of the head. The insertions of extraocular muscles in chickens, especially those of the superior rectus and superior oblique are very wide. Data concerning the medial and inferior rectus and the inferior oblique was not available because the insertions of those muscles were not visible. Data was obtained from 4 left eyes of 3-4 week old chickens, standard deviation given in parentheses.

Parameter name	X mm	Y mm	Z mm
Anterior part of insertion **Superior Oblique**	-3.1 (0.7)	2.3 (0.6)	1.3 (0.6)
Posterior part of insertion **Superior Oblique**	4.8 (1.0)	1.3 (1.6)	2.5 (0.4)
Origin **Superior Oblique**	-3.8 (0.5)	7.4 (1.1)	5.5 (0.4)
Anterior part of insertion **Superior Rectus**	-1.1 (0.3)	2.7 (0.5)	0.9 (0.3)
Posterior part of insertion **Superior Rectus**	4.6 (0.4)	0.6 (0.6)	2.2 (0.8)
Origin **Superior Rectus**	5.3 (0.5)	6.1 (0.4)	7.9 (0.9)
Dorsal part of insertion **Lateral Rectus**	6.3 (0.8)	-0.2 (0.3)	5.5 (1.5)
Ventral part of insertion **Lateral Rectus**	6.5 (0.8)	-0.2 (0.3)	9.1 (0.8)
Origin **Lateral Rectus**	6.1 (0.8)	5.3 (2.2)	7.2 (0.5)
Length **Superior Oblique** (mm)	9.4 (0.6)		
Length **Superior Rectus** (mm)	9.1 (0.4)		
Length **LateralRectus** (mm)	6.6 (0.4)		
Equatorial diameter (mm)	13.2 (0.9)		
Angle between equatorial plane and midline	19° (2)		

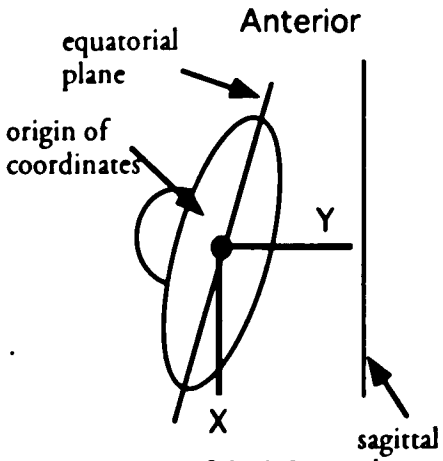

Top view of the left eye and the coordinate system used to obtain geometrical parameters of some extraocular muscles.

Table 2.10

Unit moments of the superior oblique, the superior rectus and the lateral rectus. The moments were calculated using the same convention as explained in the methods section of chapter 2 (right-hand coordinate system). Intorsions (Mx) and abductions (Mz) are positive numbers, while elevations (My) are negative numbers. Question marks denote situations where a qualitative assessment of the action of a muscle was not possible. Plus and minus signs denote situations where a qualitative assessment was possible. Thus the inferior oblique produces extorsions and depressions of the eyeball. Because moments were calculated for a vector of magnitude equal to the unity they are given without units. The interesting fact shown in the table is the relative value of the moments produced by the extraocular muscles. Thus, a contraction of the superior oblique produces, as primary action, an intorsion, the secondary action is an elevation (the minus sign in My results from the consistent definition of positive angles) and finally an abduction.

Convention:{(-)=extorsion, elevation, adduction}
{(+)=intorsion, depression, abduction}

	LR	MR	SR	IR	SO	IO
Mx (torsion)	-0.17	?	-0.38	?	0.71	-
My (vertical)	0.03	?	-0.92	+	-0.63	+
Mz (horizontal)	0.97	-	0.08	?	0.3	?

Table 3.1 "k" values and thresholds for 24 Tonic motoneurons.

Cell-ID	Slope spikes/s/deg	Threshold (deg)
1	3.44	-25
2	3.73	-17
3	1.52	-21
4	1.65	-13
5	1.87	-3
6	0.92	-35
7	3.53	-15
8	2.12	-25
9	4.7	-21
10	3.73	-14
11	6.48	-2
12	4.47	-4
13	3.75	-6
14	2.18	-14
15	4.71	-3
16	2.55	-12
17	1.5	-8
18	5.58	-1
19	3.96	2
20	1.83	-25
21	1.87	4
22	7.24	-13
23	4.98	-12
24	1.29	-25

Table 3.2 "k" and "r" values for 5 Tonic motoneurons
The procedure used to arrive at the values of *k* and *r* searched through the (*k*,*r*) parameter space, as opposed to a calculation via an error minimizing technique. For each Tonic motoneuron, average values of *k* and *r* were obtained by averaging the values found across 10 saccades. The calculation of k and r used a "smooth" (or slow) version of the real eye position trace, the oscillatory component was extracted from the original data. Also, in most saccades the initial 80-120 msec were ignored. During that period of time an active pause, not related to eye position or speed, controls the firing of Tonic motoneurons.

Cell-ID	k Position sensitivity spikes/s/deg	r Speed sensitivity spikes/s/deg/s
190	7.85(2.9)	0.47(0.26)
240	0.93(0.28)	0.13(0.18)
249	9.18(2.1)	0.8(0.36)
253	2.85(0.5)	0.19(0.1)
291	2.0	0.15

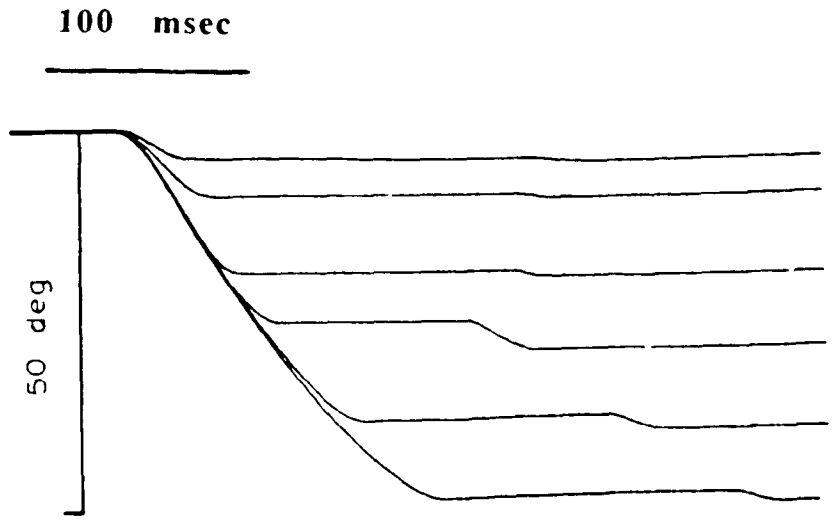

Figure 1.1
Examples of primates saccades. This family of six horizontal saccades was evoked by targets at 5, 10, 20, 30, 40 and 50 deg. The largest saccade lasts 140 ms and moves the eye 47 deg obtaining a mean speed of 340 deg/s. The maximal eye speed is about 430 deg/sec for large saccades and 160 deg/sec for the smallest. The sigmoidal time course is a common feature of all primate saccades.

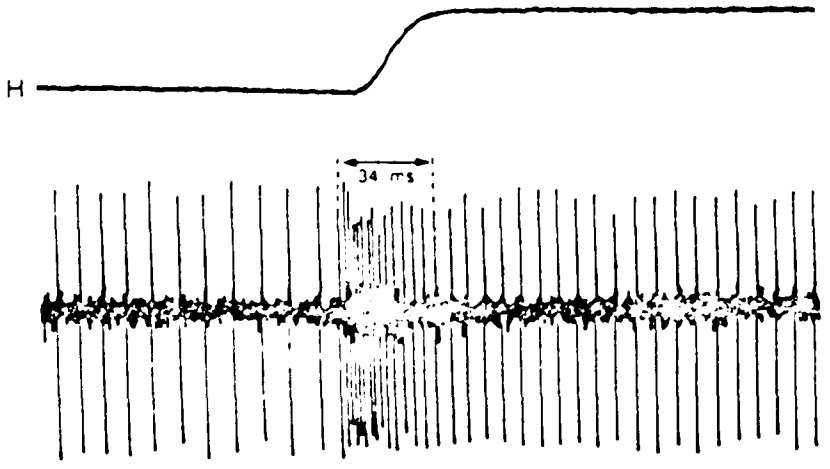

Figure 1.2
Discharge of a primate abducens motoneuron during a horizontal saccade. Top trace is eye movement, horizontal component, recorded by the magnetic search coil method. Lower traces is the extracellular activity of the neuron. The discharge during fixations changes from 120 spikes/s to 164 spikes/s according to a temporalward eye position change of 7 degrees (King et al., 1986). The burst of activity in the motoneuron precedes the saccadic eye movement by about 12 ms, reaches a discharge frequency of 411 spikes/s and last about the same time than the saccade. All extraocular motoneurons, in mammals, show this "burst-tonic" response pattern.

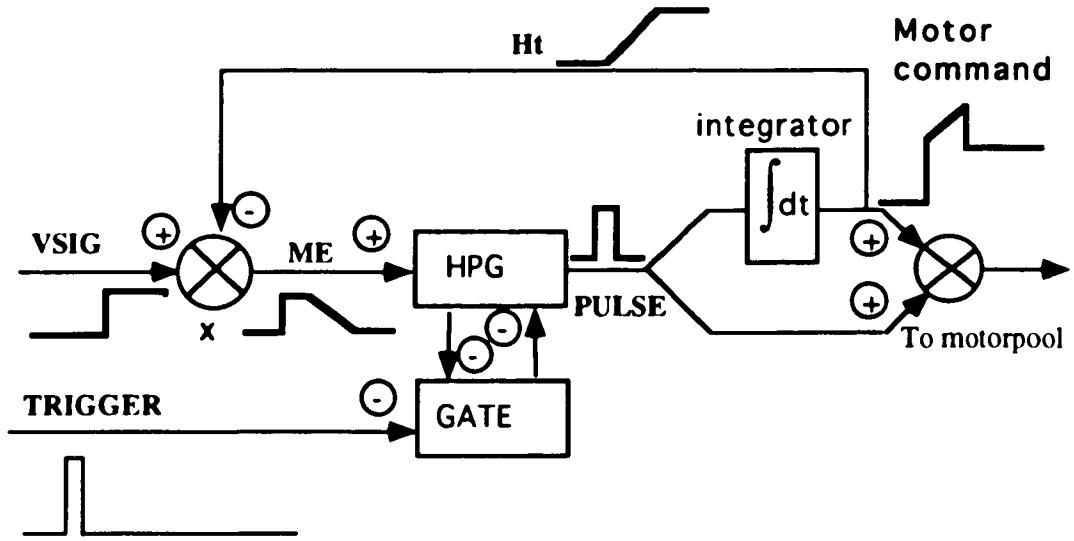

Figure 1.3
One dimensional Robinson model of the saccade generator. This model assumes that a visual signal (VSIG) is compared to an internal representation of eye position (Ht) at x. A motor error signal (ME=VSIG-Ht) is fed into the Burst neurons inside the HORIZONTAL PULSE GENERATOR (HPG). During fixations the activity of HPG neurons is inhibited by the action of pause neurons found in GATE. The mutual inhibition between HPG and GATE, assures that saccades achieve the desired target position. Once the ME signal is not zero, as it mut be at the beginning of each saccade, the GATE circuit is inhibited and the HPG can synthesize the correct pulse. At the end of each saccade, as ME approaches zero, the GATE circuit begins to inhibit HPG neurons again. The saccade generator is started by a signal (Trigger) that momentarily inhibits the GATE circuit. The onset of Trigger must be concomitant with a change in the VSIG. The transient output of HPG (Pulse) is integrated to produce the tonic signal Ht. Together these two signals are added and fed to the motor pool. The temporal profile of neural signals related to eye position are depicted in thick lines.

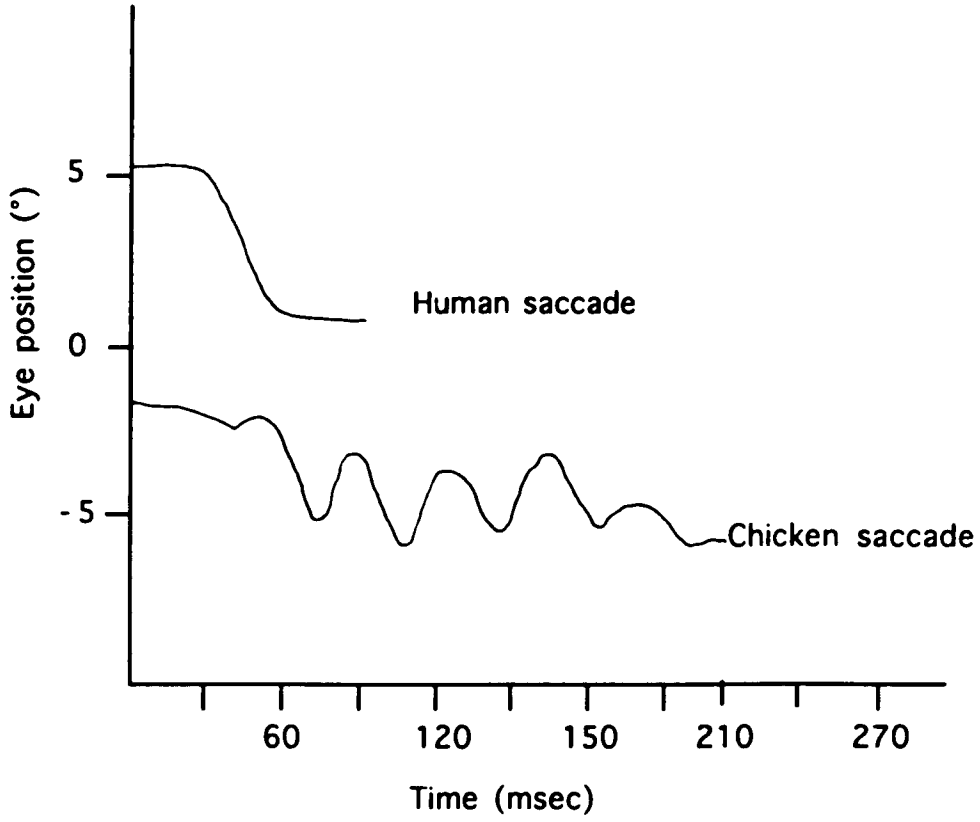

Figure 1.4A
Human and chicken saccades. This graph shows, at the same temporal and spatial scales, a chicken saccade and a human saccade (Dr. A. Fuchs). Both traces reflect the horizontal component of eye position. Note the prominent oscillations present in the case of the chicken. (data obtained from Dr. C. Harris and A. McPhun).

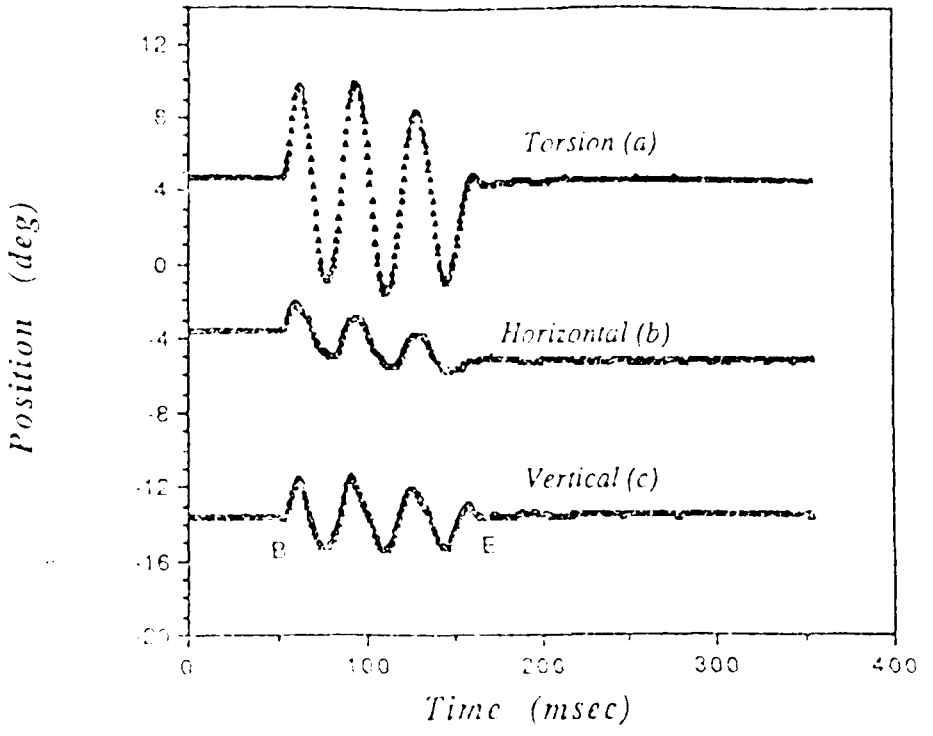

Figure 1.4B
Trajectory of a chicken saccade The saccade depicted has an amplitude of 2 degrees nasalward and consists of three oscillatory cycles (somewhat fewer than most), each one lasting 36 msec approximately. As is usual the torsional component is the largest, with an amplitude of 10-12 degrees. (Upward deflection, for traces a,b and c, means intorsion, temporalward, upward respectively. B= beginning of saccade, E= end of saccade). All traces were obtained by the 3-D magnetic search coil method and transformed into Fick's coordinates.

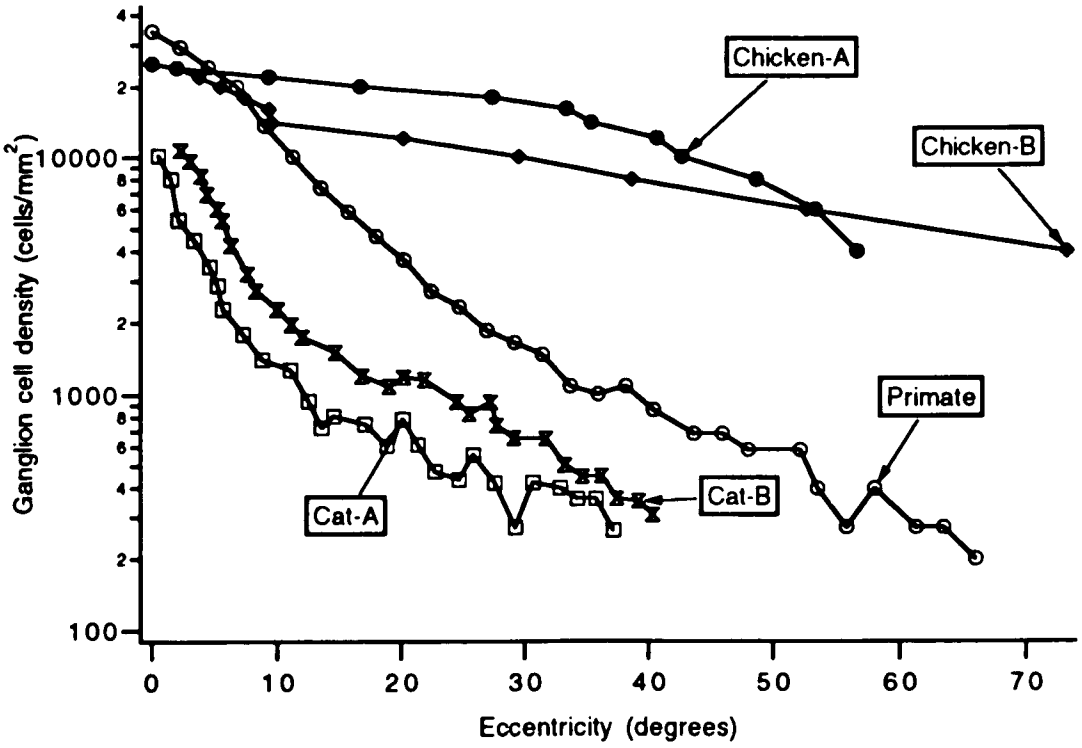

Figure 1.5
Ganglion cell density distribution in cat, monkey and chicken. The primate data is for the vertical meridian (Perry and Cowey, 1985). The ganglion cell distribution is approximately radially symmetric in primates, thus the data for the horizontal meridian is similar. Cat data is from (Wassle, Levick and Cleland, 1975). The cat's retina has a more assymetric distribution of ganglion cells, thus the distribution along two meridians (naso-temporal=Cat-A, vertical=Cat-B) was plotted. Chicken data is for the centre of the streak zone (Chicken-A) and for an orthogonal axis (Chicken-B) (Ehrlich, 1981). The density ratio, between the center and the periphery of the retina, is 150 for primates, 75 for cats and 7 for chickens.

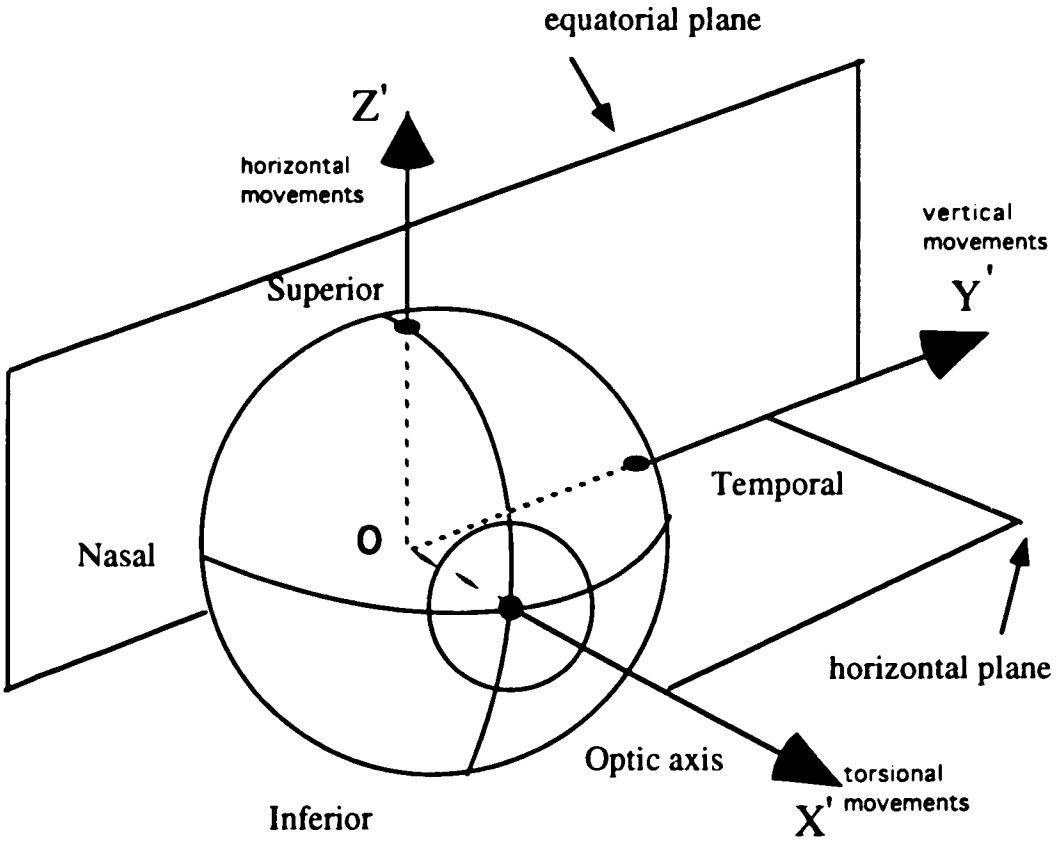

Figure 2.1
Model of the left eye and reference frame. Rotations around the optic axis produce torsional eye movements. Rotations around the vertical axis produce horizontal eye movements and rotations around the axis OY' produce vertical eye movements. The reference system X'Y'Z' moves with eyeball and is centered at the center of rotation. A similar, but fixed, reference frame is defined in the orbit. As a first approximation both reference frames coincide when the eye is in the primary eye position. Because both eyes are mirror images of each other the reference frame defined for the left eye cannot be applied without modifications to the right eye.

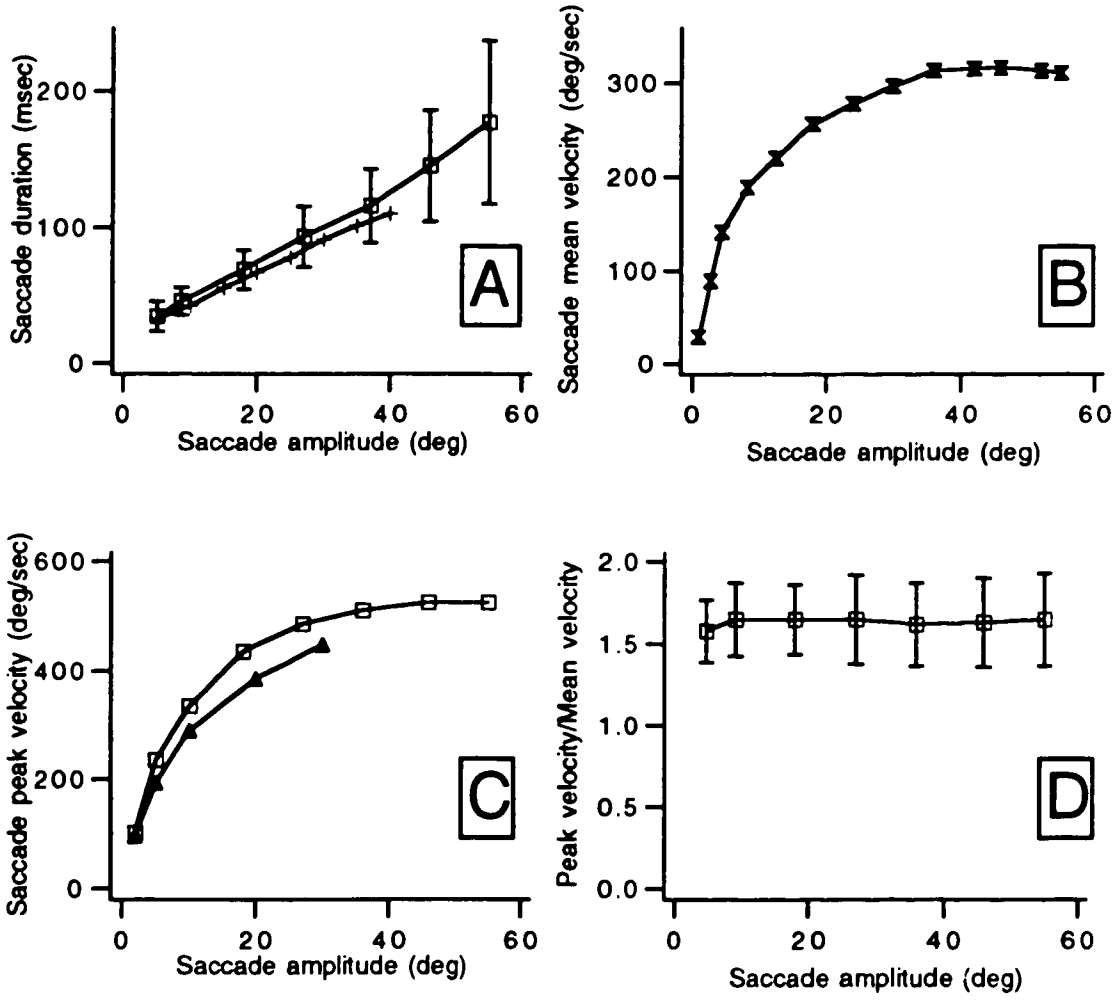

Figure 2.2
Basic parameters of human saccades.
(A) Duration of saccades as a function of saccade amplitude, data from (Robinson, 1964) (+) and (Becker, 1989)(□).
(B) Mean saccadic velocity as a function of amplitude. The mean saccadic speed increases rapidly and appears to have an asymptotic value of 350 °/sec, data from (Becker, 1989).
(C) Peak saccadic velocity. Peak velocity increases and then levels off, data from (Becker, 1989) (□) and (Boghen, 1974) (▲).
(D) Ratio between peak and mean velocity. The ratio stays close to a value of 1.6, data from (Becker, 1989).

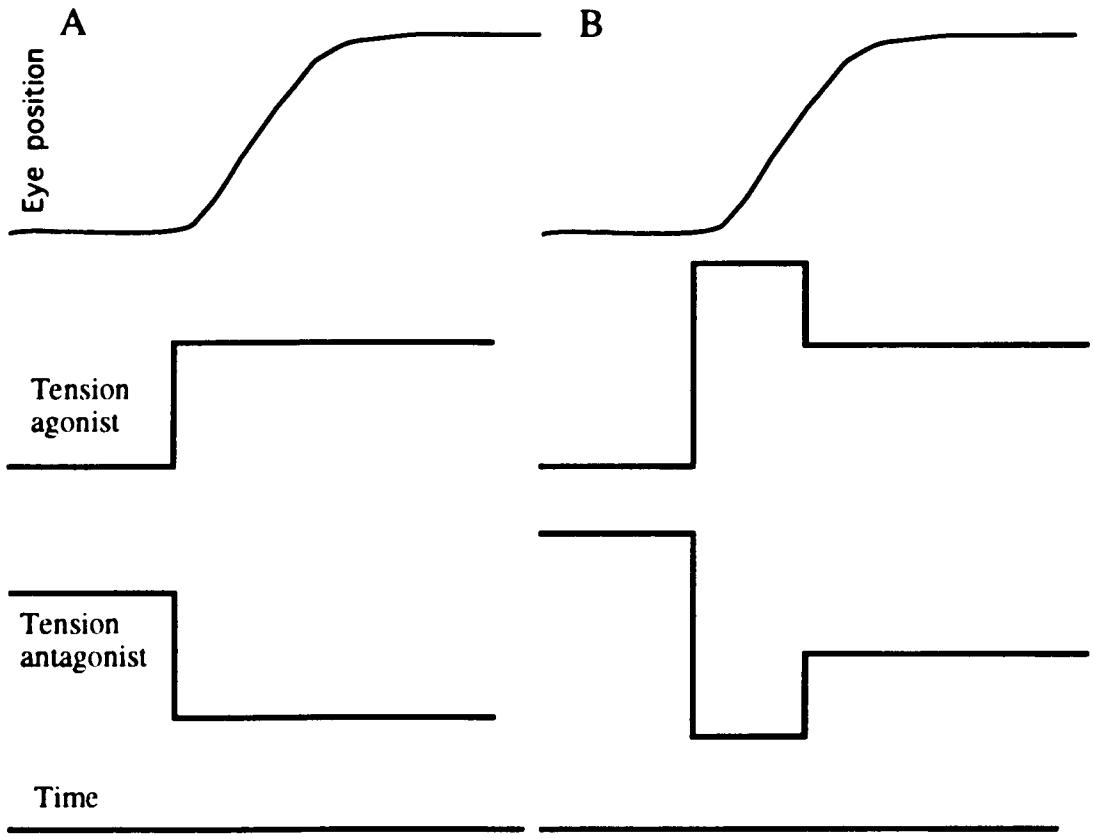

Figure 2.3
Force patterns produced by extraocular muscles during saccades.
(A) Pattern postulated by Westheimer (1954) and (B) Robinson (1964).
In Robinson's schema, which has received experimental confirmation,
the extra force produced during saccades ("the pulse") provides the high
acceleration of human's saccades.

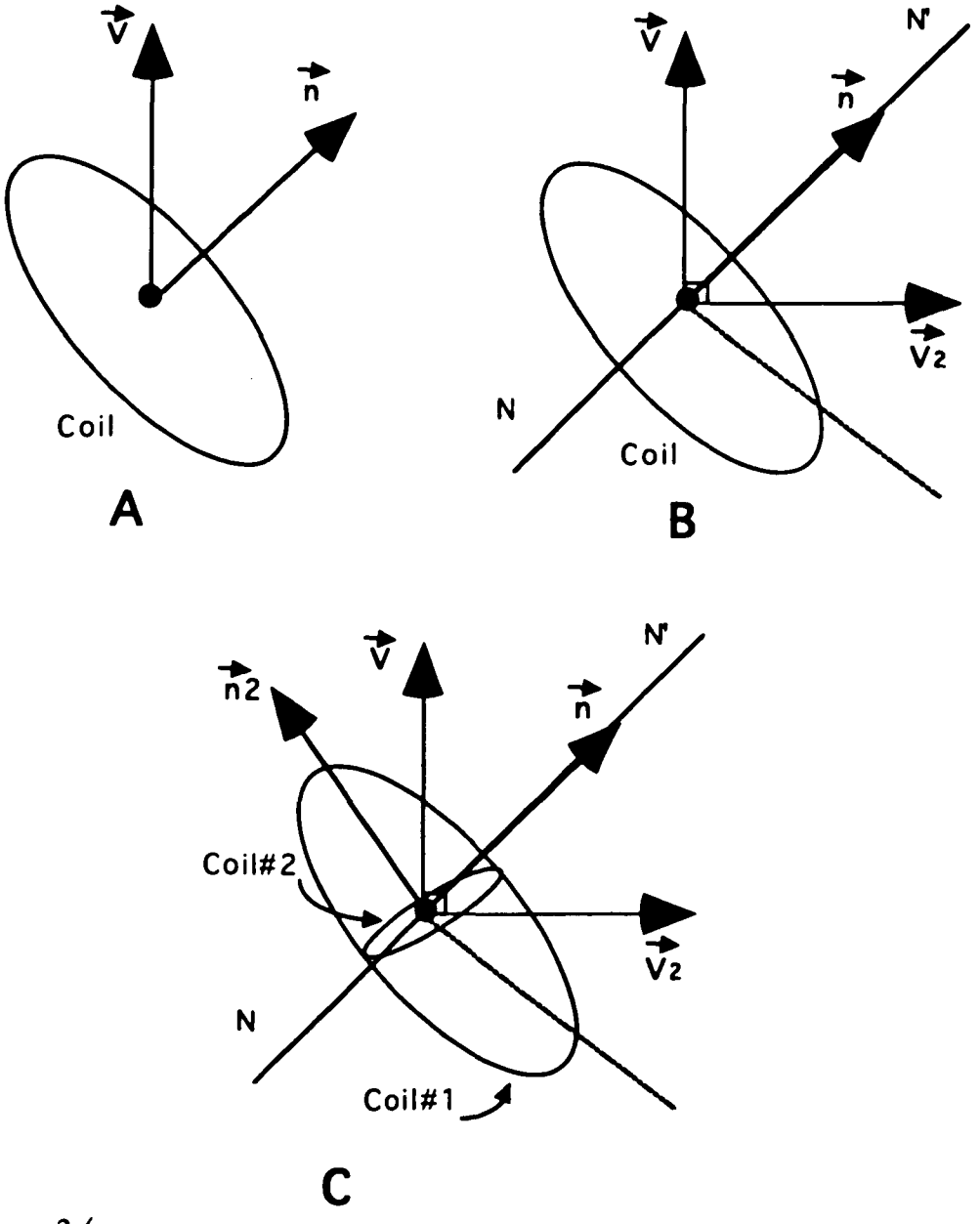

Figure 2.4
Magnetic fluxes across eye coils. (A) The most simple situation; one magnetic field, one eye coil. (B) Two magnetic fields, one eye coil. In this situation rotations around NN' are not detected. (C) Two magnetic fields, two eye coils. In this situation rotations around NN' do not change the flux across C1, but they change the flux across C2. (V,V_2,= direction of magnetic fields, **n**,**n2**= normal direction to coils C1 and C2). Appendix A describes the various mathematical transformations used to obtain eye position.

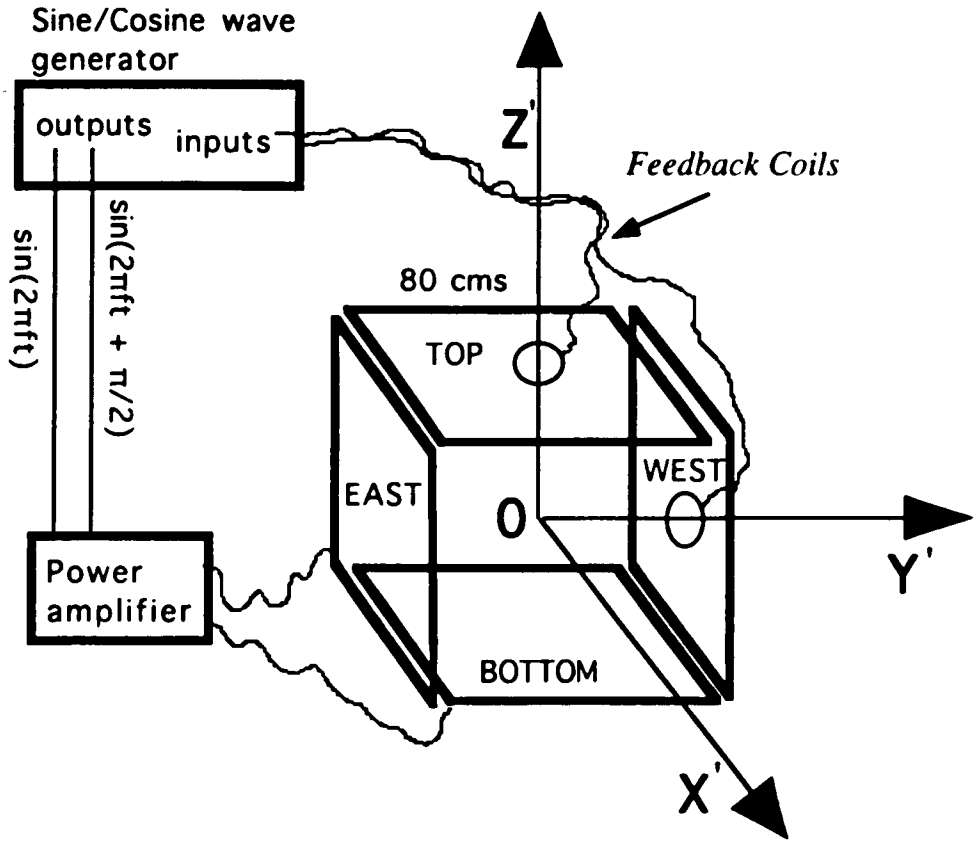

Figure 2.5
Simplified diagram of field coils set-up. Two pairs of helmholtz coils created the two magnetic fields. The chicken'e eye was positioned in location O. with its optic axis along the OX ' direction. The cables of the feedback coils, which sense both magnetic fields to ensure quadrature, must be shielded with mu-metal.

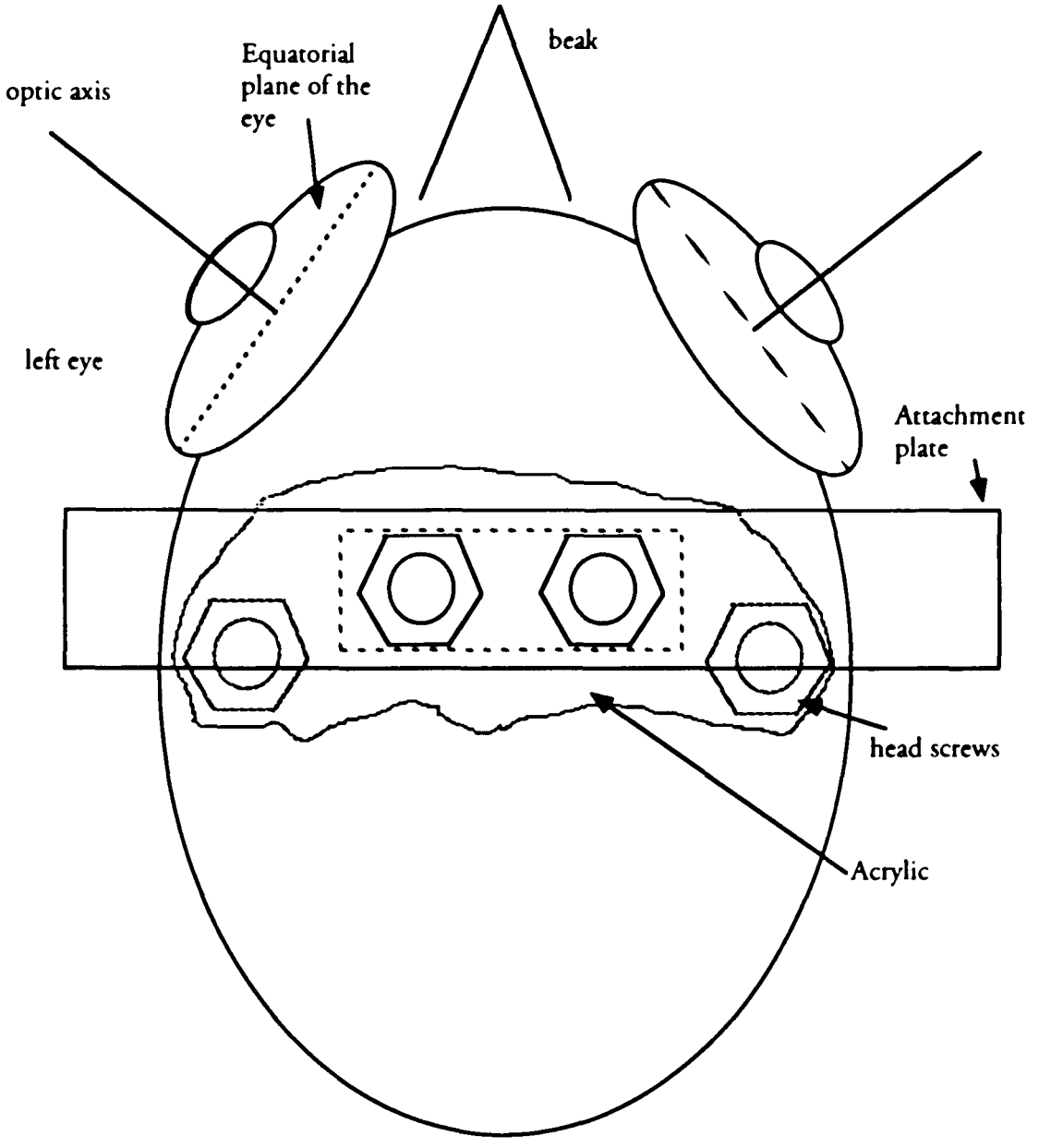

Figure 2.6A
Diagram of the top of chicken skull with headpiece installed. The head piece was installed on top of the skull. The eye coils, which were on top of the left eye never touched the attachment plate.

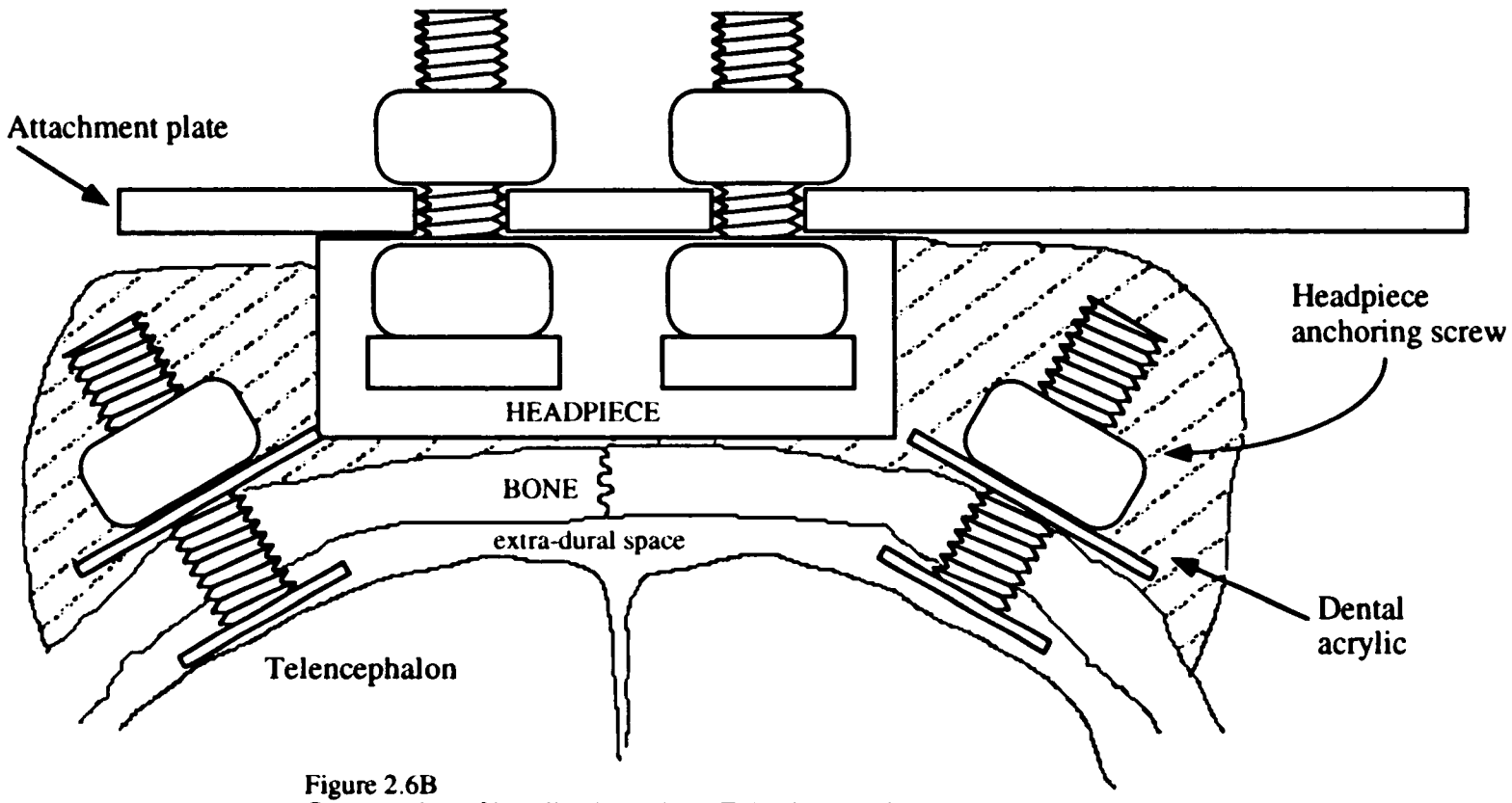

Figure 2.6B
Cross section of installed headpiece. This diagram shows the relative positioning of the head screws, the head holder and the attachment plate. This method provides a very convenient method of securing the head of the chicken.

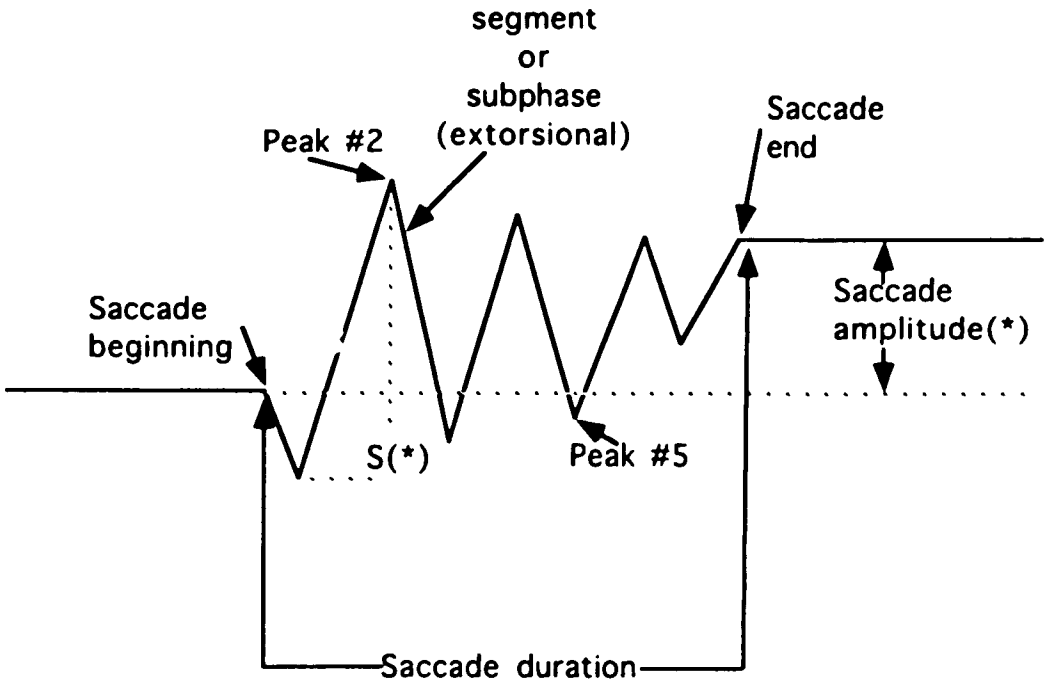

Figure 2.7
Diagram of a chicken saccade and definitions of terms. This diagram summarizes the definitions of the terms used in this chapter. S(*) represents the 3-D amplitude of a given subphase and it was calculated using the Euler-D'Alembert theorem (Appendix A).

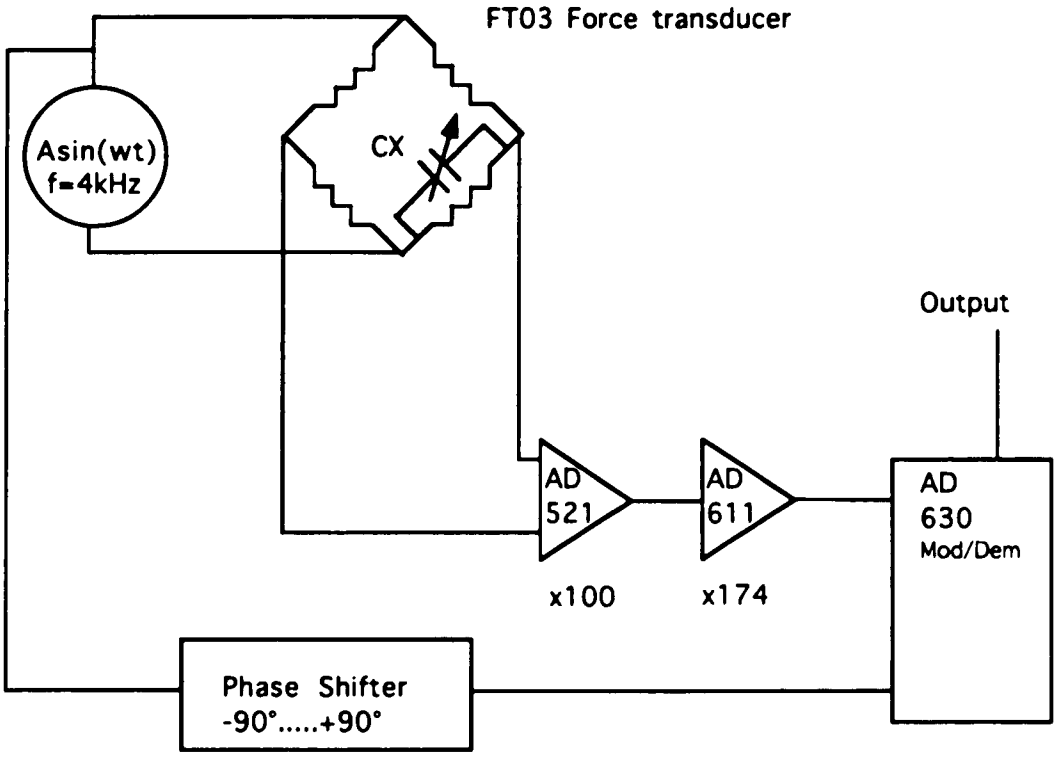

Figure 2.8
Simplified diagram of Phase-lock amplifier. This is the block diagram of the Phase-lock amplifier built in order to use the force transducer with a 330Hz resonant frequency. In that configuration the transducer is very "stiff" and a simple method, like D.C. amplification, does not work because the signal from the bridge is approximately 10 microVolts. The circuit built had an overall sensitivity of 3.0 Volts/gr and a respectable signal to noise ratio. The capacitor Cx is crucial, failure and success are separated by only a few picofarads on the value of Cx.

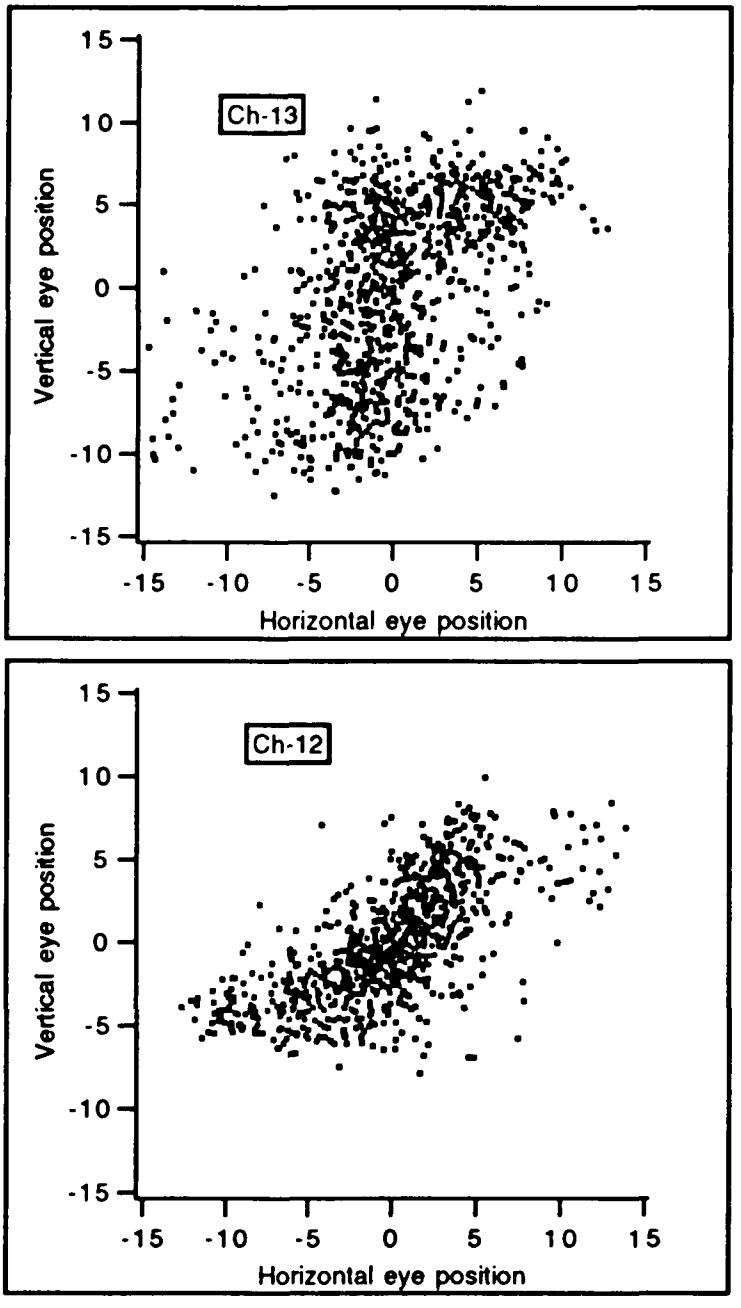

Figure 2.9
Projection of gaze direction. In two chickens (Ch-13 and Ch-12) the projection of the optic axis was plotted with respect to the visual field. The position (0,0) represents the projection of the optic axis in the "primary"position. The distribution of positions is not uniform. For subject ch-12, 50% of fixations stay in a 3.8° circle,while 75% stay in a 6.3° circle of the primary position (ch-13: 50% in a 6.0° and 75% in a 8.2° circle).

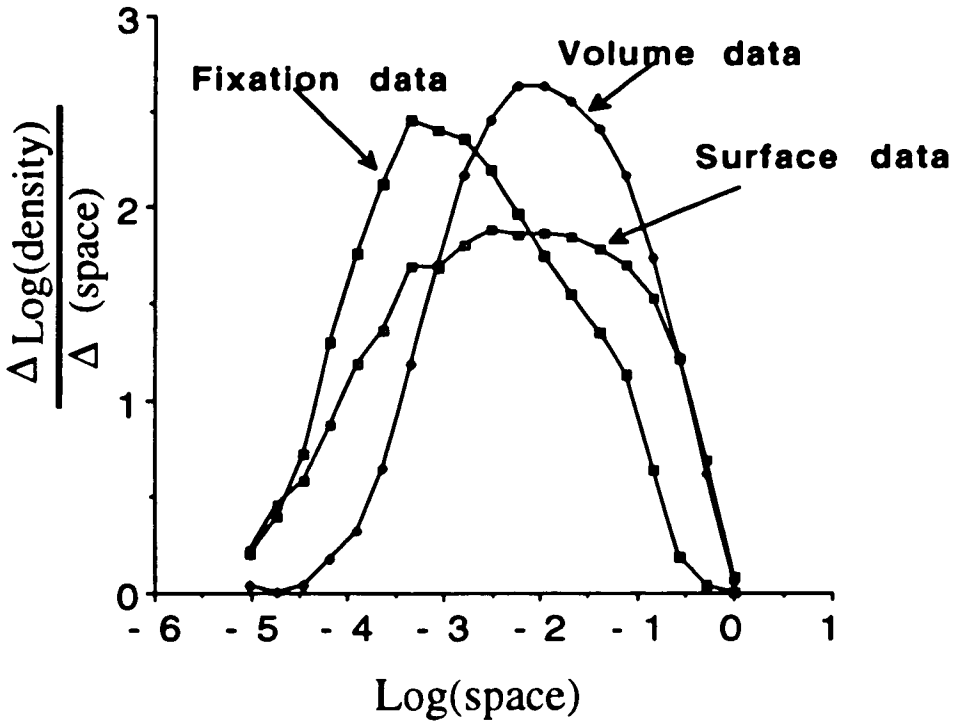

Figure 2.10
Donder's law does not hold for chickens. The method behind this figure, explained in Appendix B, calculates the dimensionality of a series of points representing positions in space. In theory the peak of the curve represents the dimensionality of the data set: 2 for a surface, 3 for a volume. In practice, because the samples are finite, this method gives somewhat lower values: 1.8 for a surface (SURFACE DATA), 2.83 for a volume (VOLUME DATA).
The X-axis represents the Log(base e) of the spatial scale, here the analysis covers 3 orders of magnitude. Thus for the fixation data the analysis goes from 0.1° to 15°. The Y-axis is the spatial derivative of the variation in density (see Appendix B). The idea behind the graph is to obtain a measure of the spatial variation of the density at different spatial scales.
The method, when applied to 999 positions of fixations, (FIXATION DATA) gives a value of 2.57 an indication of almost total independence between torsion and the direction of gaze. Similar results were obtained in four chickens for which this analysis was carried out.

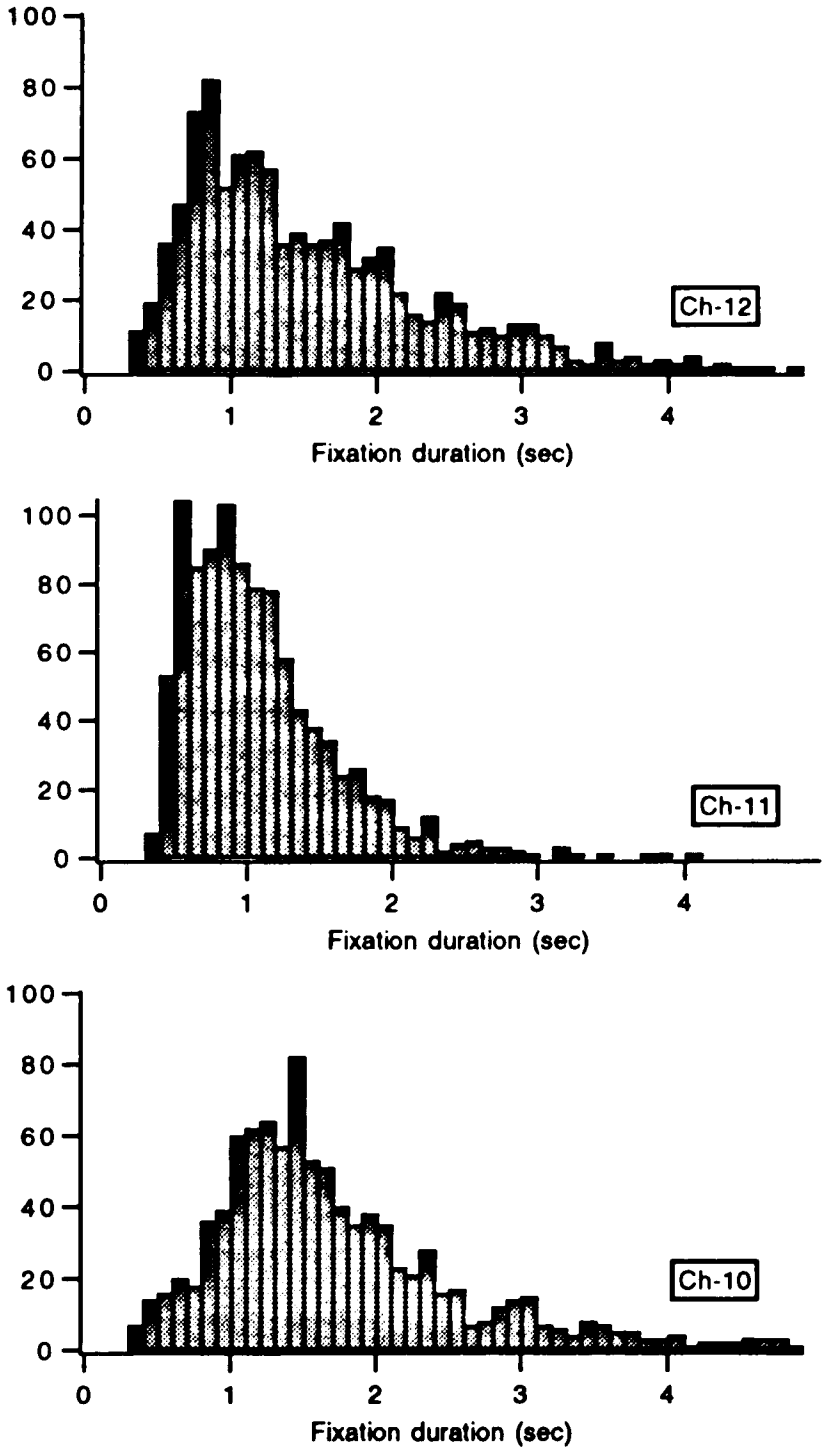

Figure 2.11
Distribution of duration of fixations. Three examples of the distribution of fixations. Fixations shorter than 400 msec are very rare as well as fixations in excess of 4.0 secs. The mean duration of fixations is 1.6 sec (14 chickens, 999 consecutive fixations per chicken).

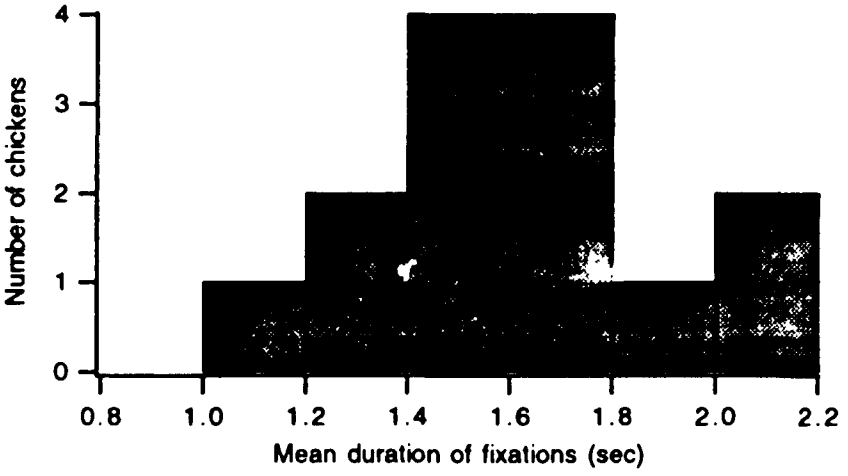

Figure 2.12
Distribution of average duration of fixations.
Histogram of the mean duration of fixations for
14 chickens during periods of spontaneous viewing.

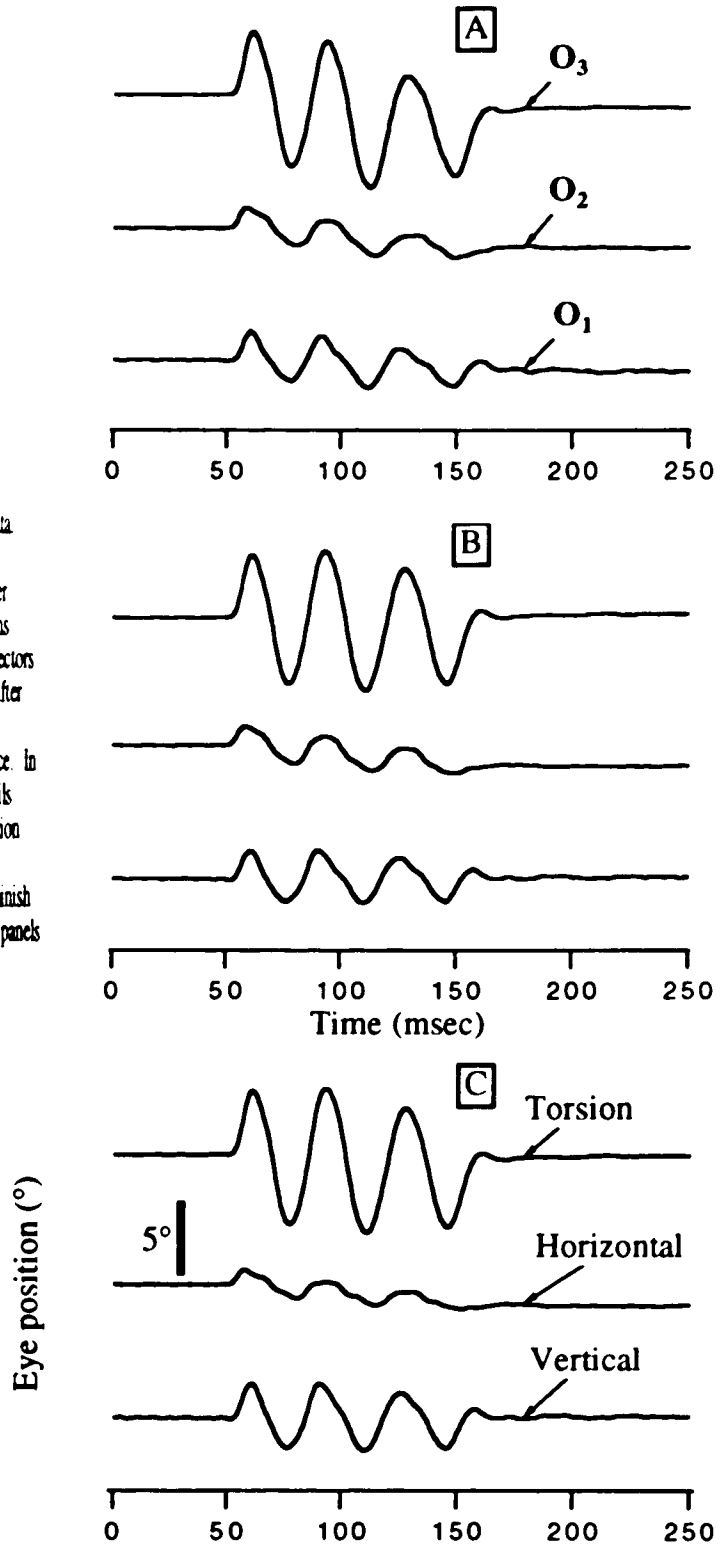

Figure 2.13
Effects of mathematical transformations on raw data. (A) raw, direct data taken directly from the three outputs of the three phase detectors. (B) Data after goniometrical transformations, these transformations take into account that the outputs of the phase detectors are not independent. (C) Data after step (B) and after compensation for "kinematics errors". This last transformation is a rotation of the frame of reference. In summary, (B) represents the position of the eye coils with respect to the lab and (C) represents the position of the eye with respect to the orbit.
The main effect of the last transformation is to diminish the value of the horizontal component. In all three panels the traces were shifted, the calibration bar is valid for all the traces in all three panels.

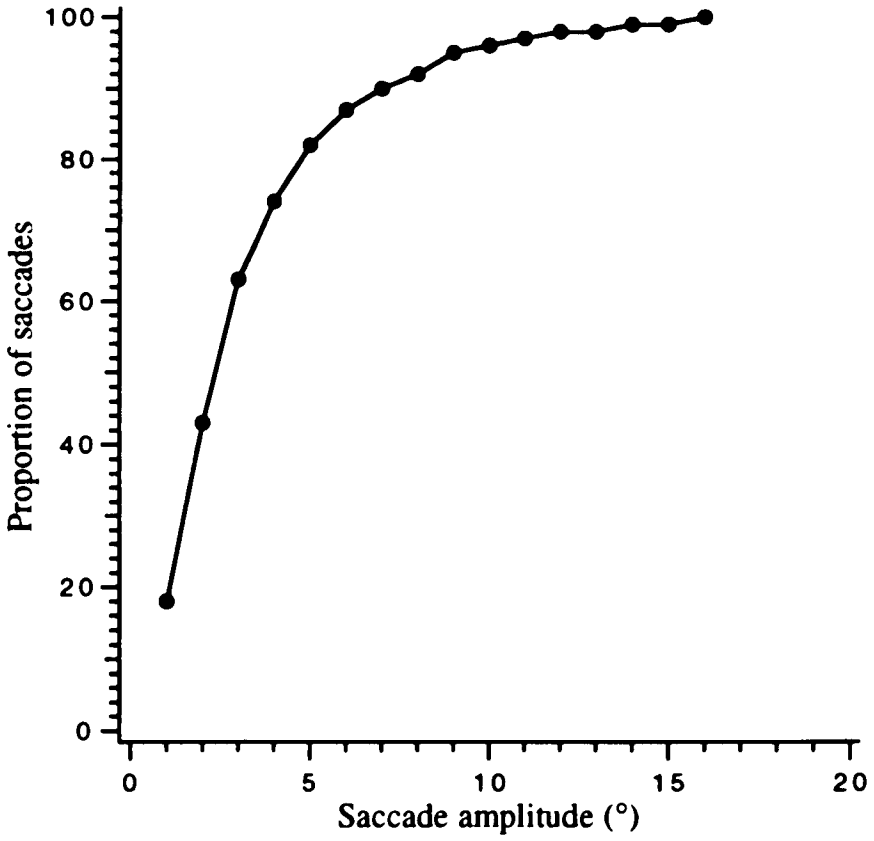

Figure 2.14
Distribution of saccade amplitude in chickens. Pooled data from 10 chickens, representing the relative distribution of saccade amplitude (or saccadic displacement).
The saccadic displacement was calculated as the true 3-D rotation of the eyeball. Half of saccades move the eye less than 3°.

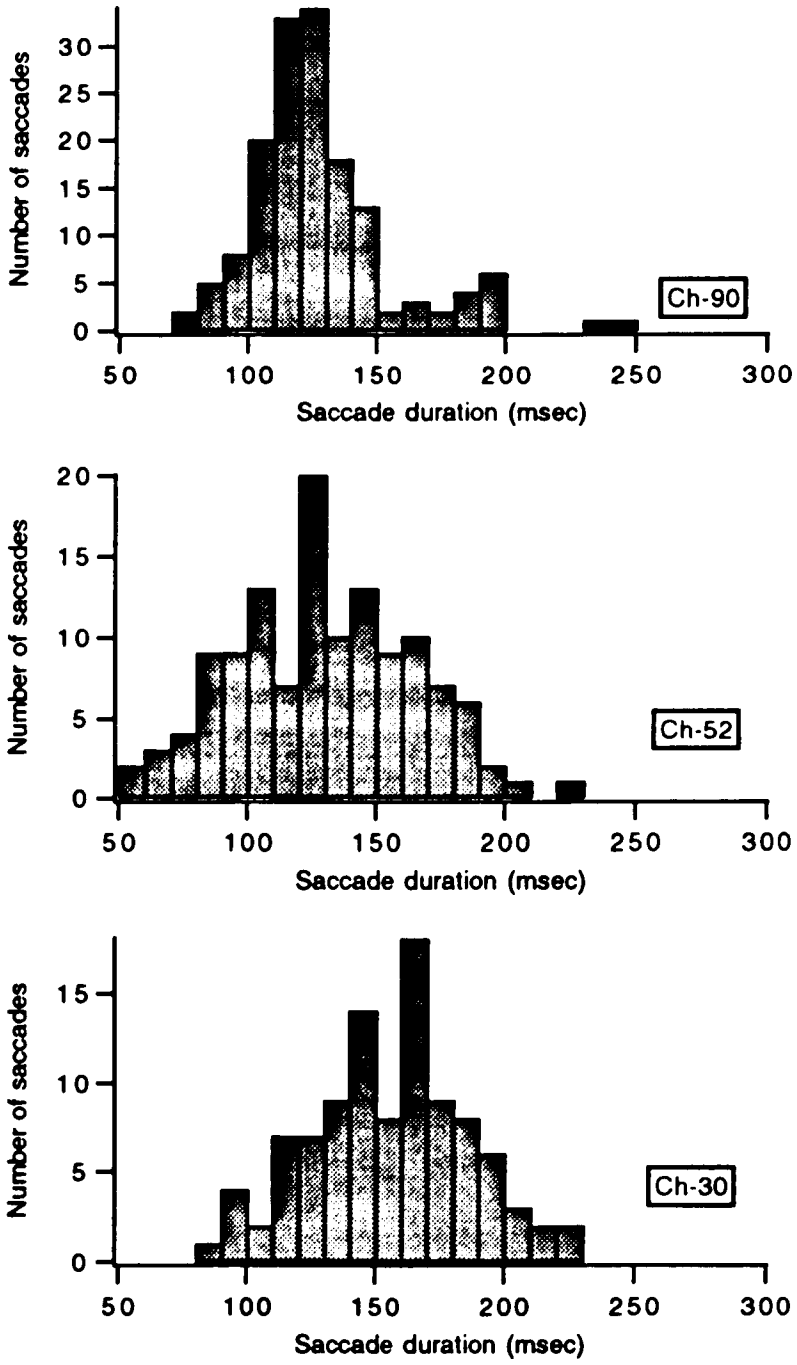

Figure 2.15
Distribution of saccade durations. Distribution of durations for spontaneous saccades in three chickens, as explained in the methods section eye oscillations served to measured the duration of saccades. Most avian saccades last 100-200 msec. Saccades shorter than 70 msec are uncommon.

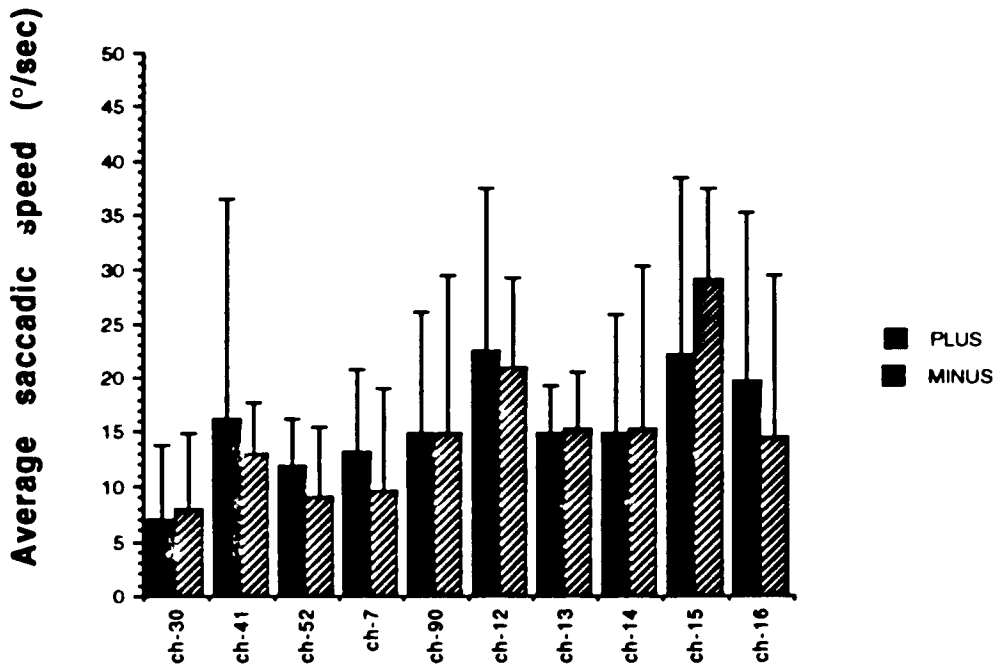

Figure 2.16
Average speed of saccades sorted according to saccade type. "Plus" and "minus" saccades have essentially the same average speed (error bars represent half of the 95% confidence interval). In 10 chickens the average speed was15°/sec. The low average speed, as well as the high variability, is a result of the small average amplitude of chicken saccades (see figure 2.14)

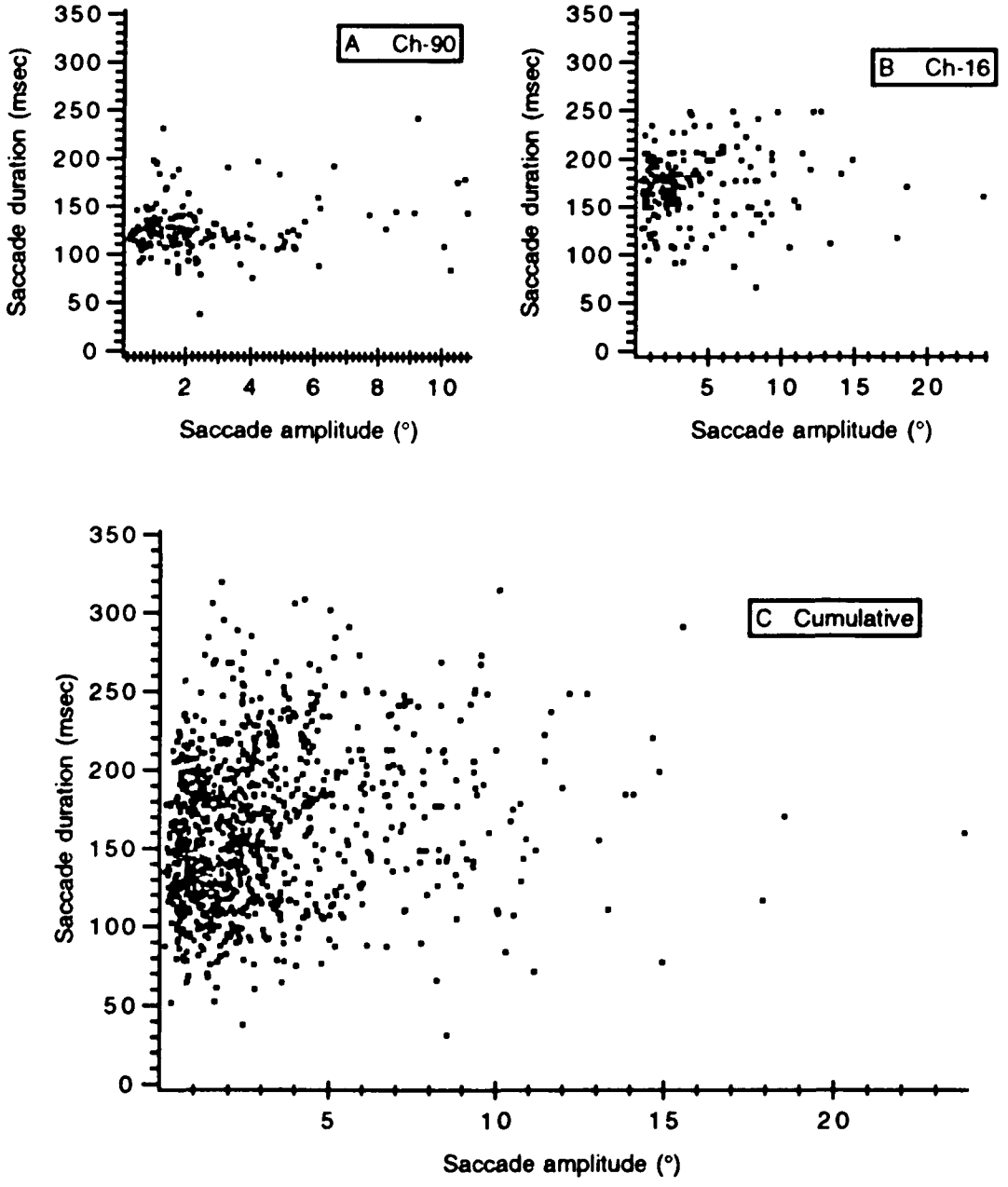

Figure 2.17
Independence between saccadic amplitude and duration. Plots showing the lack of relation between saccade duration and amplitude A and B for individual chickens, C for the cumulative data representing 10 chickens. The "cloud" of points centered at x=2,y=150 in C clearly shows the average amplitude and duration of spontaneous saccades.

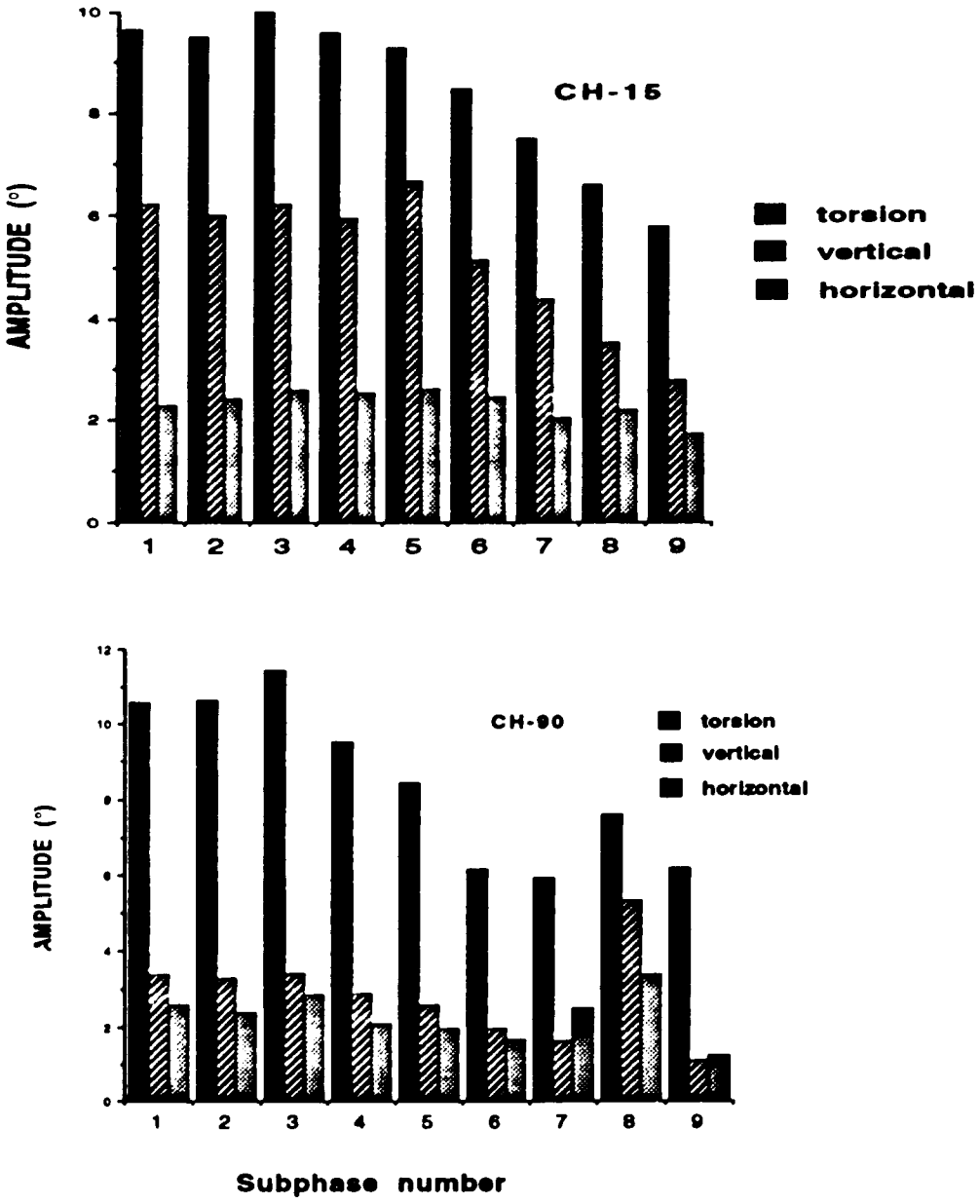

Figure 2.18
Amplitude of the three components in different subphases. Two examples showing the amplitude of the torsional, vertical and horizontal components. The torsional component is always the biggest reaching amplitudes of 10-12° by the second subphase. These two barplots show two extreme situations,usually the ratio found is 4/2/1 between the torsion, vertical and horizontal components respectively.

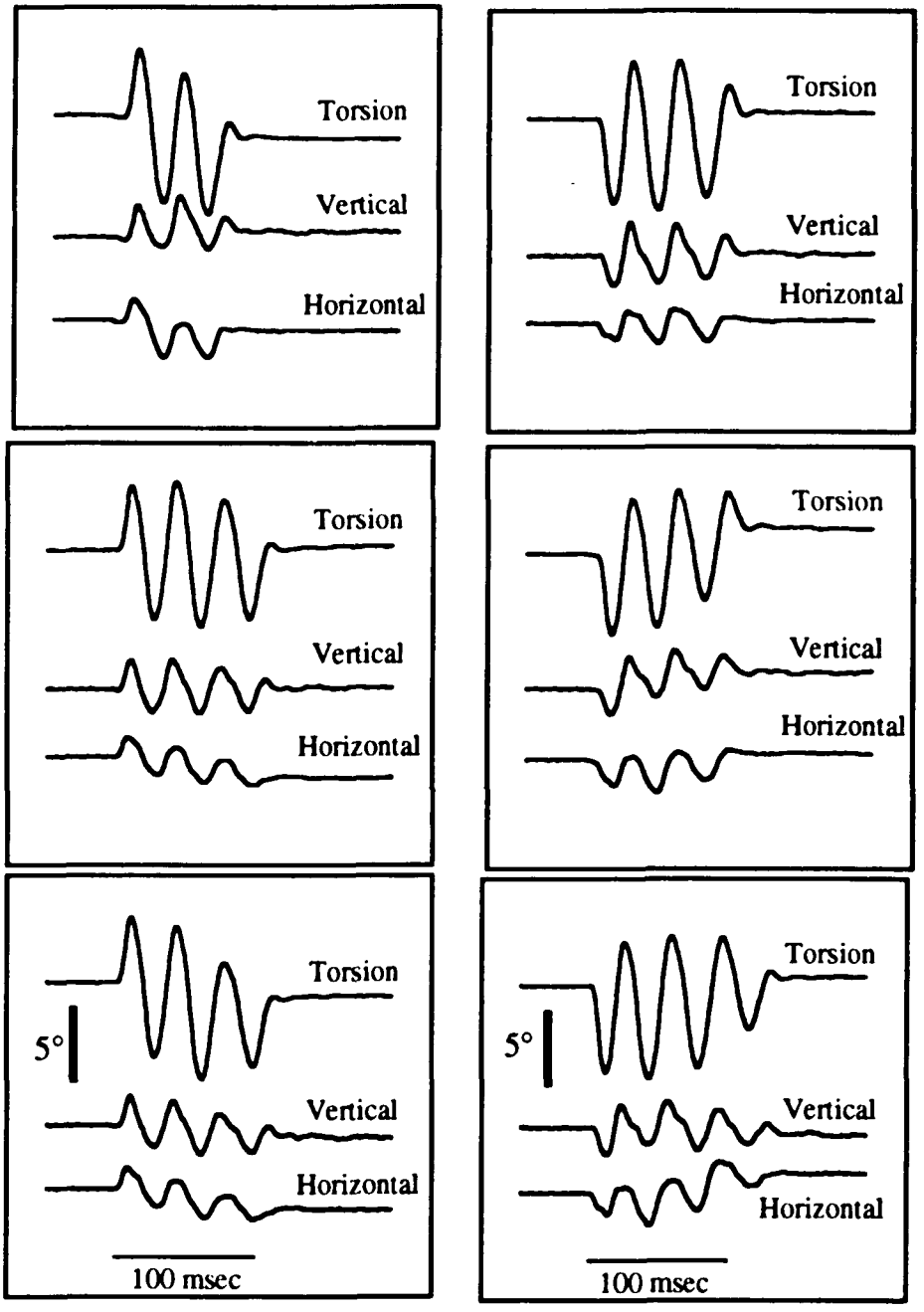

Figure 2.19
Relations between torsion, vertical and horizontal components during saccades. "Plus" saccades are depicted in the left column, "Minus" saccades in the right column. These two columns represent the only two "modes" of saccadic oscillations, other "modes" (intorsion, depression, abduction for example) were never seen. The time and position calibration marks are the same in all panels.

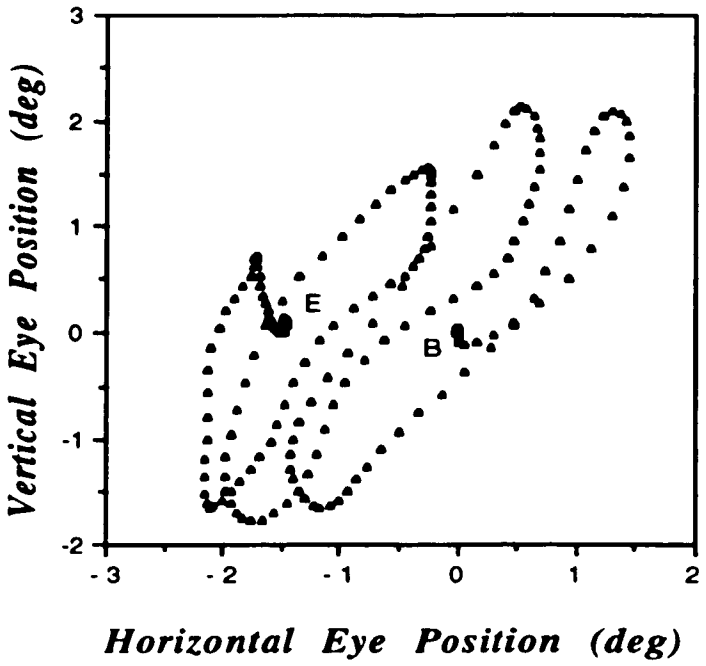

Figure 2.20
Example of gaze trajectory during saccade. The projection of the optic axis, the direction of gaze, follows a spiral-like movement during saccades. "Plus"or "minus" produce the same type of gaze movement. It should be noted that, as a result of oscillations, the optic axis scans the same region of the visual field many times during each saccade.
(B=projection of gaze at saccade initiation, E= at saccade end, each point is separated by 0.71 msec)

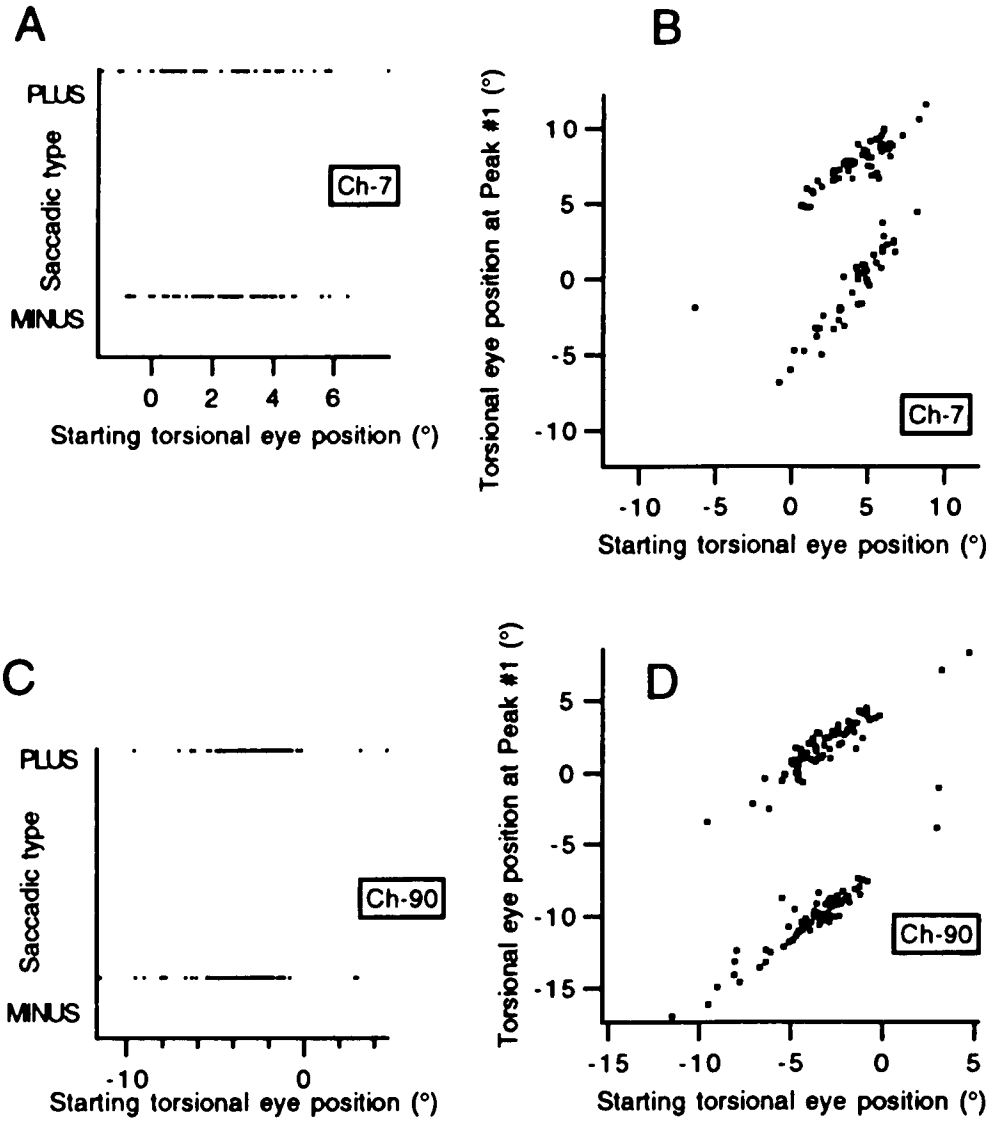

Figure 2.21
Saccadic type is independent of initial eye position. Two examples of the independence between the direction of the first subphase (saccadic type) and the initial eye position. In A and C the saccadic type was directly plotted against initial eye position, while in B and D the eye position during peak #1 was plotted against initial eye position. Thus in any eye position the eye has the same probability of beginning a sacccade with an intorsional or extorsional subphase.

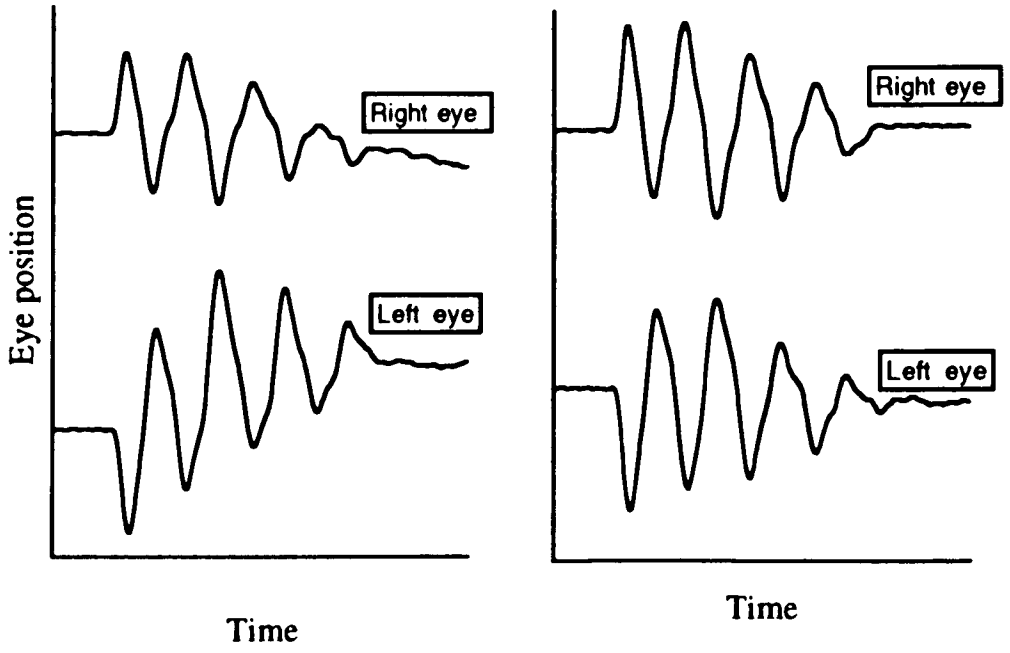

Figure 2.22
Simultaneous recording of saccades in both eyes. Saccadic oscillations in both eyes are strictly coupled, when one eye is in an intorsional subphase the other is performing an extorsion and vice-versa. The eye position traces in this figure do not represent torsion exactly, but an approximate combination of 3/4 torsion and 1/4 vertical.

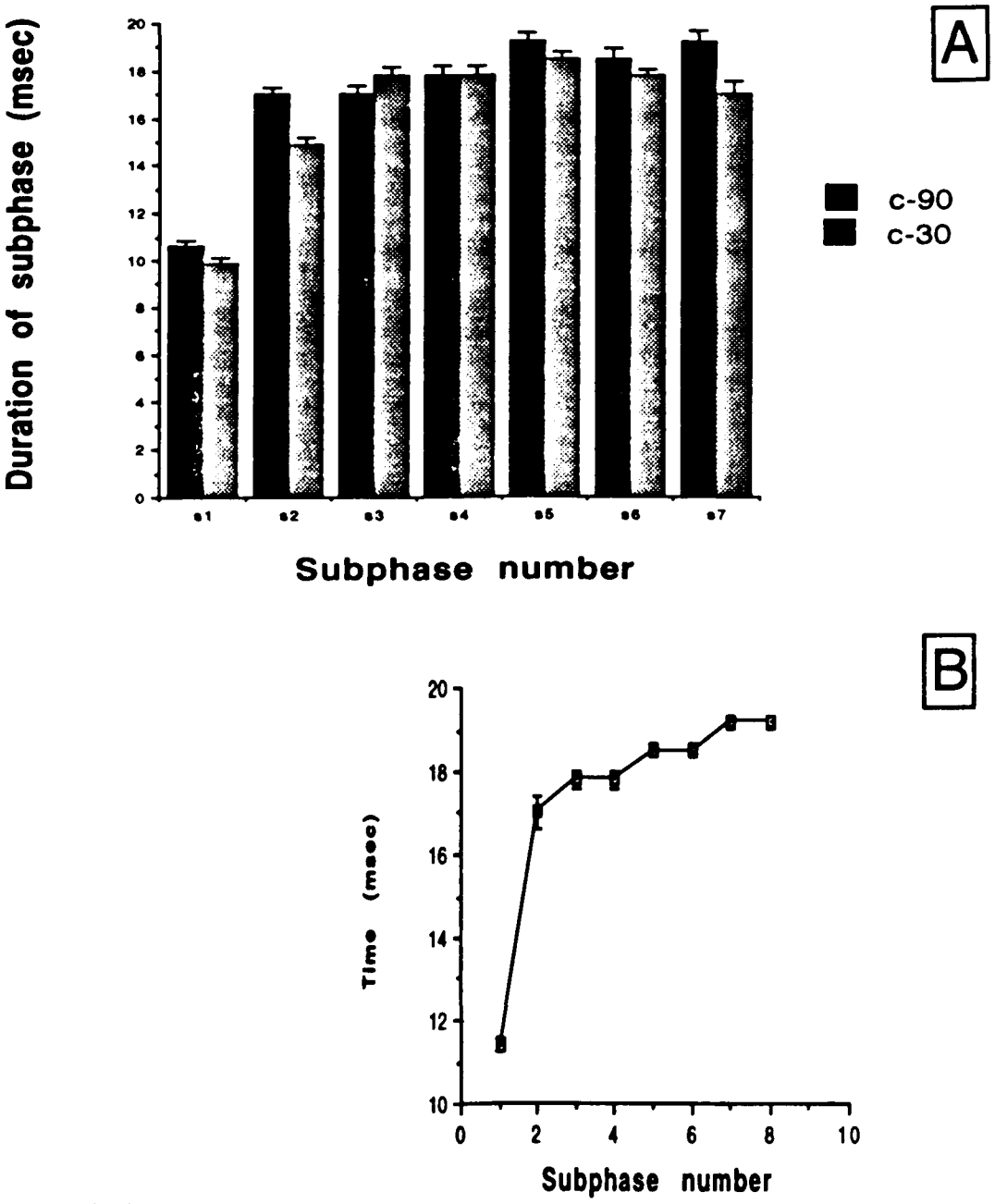

Figure 2.23
Duration of subphases. (A) Durations of subphases (1-7) for two chickens. Subphases 2-7 last in between 17-19 msec and they show very little variability. The almost invariant duration of subphases is one of the main stereotyped features of avian saccadic oscillations.
(B) Population average, across 10 chickens, of the duration of saccadic subphases. If the first subphase is excluded the average subphase duration is 18 msec (error bars= half of the 95% confidence interval for the median). A clear trend exists in that early subphases are 1 msec shorter than late subphases.

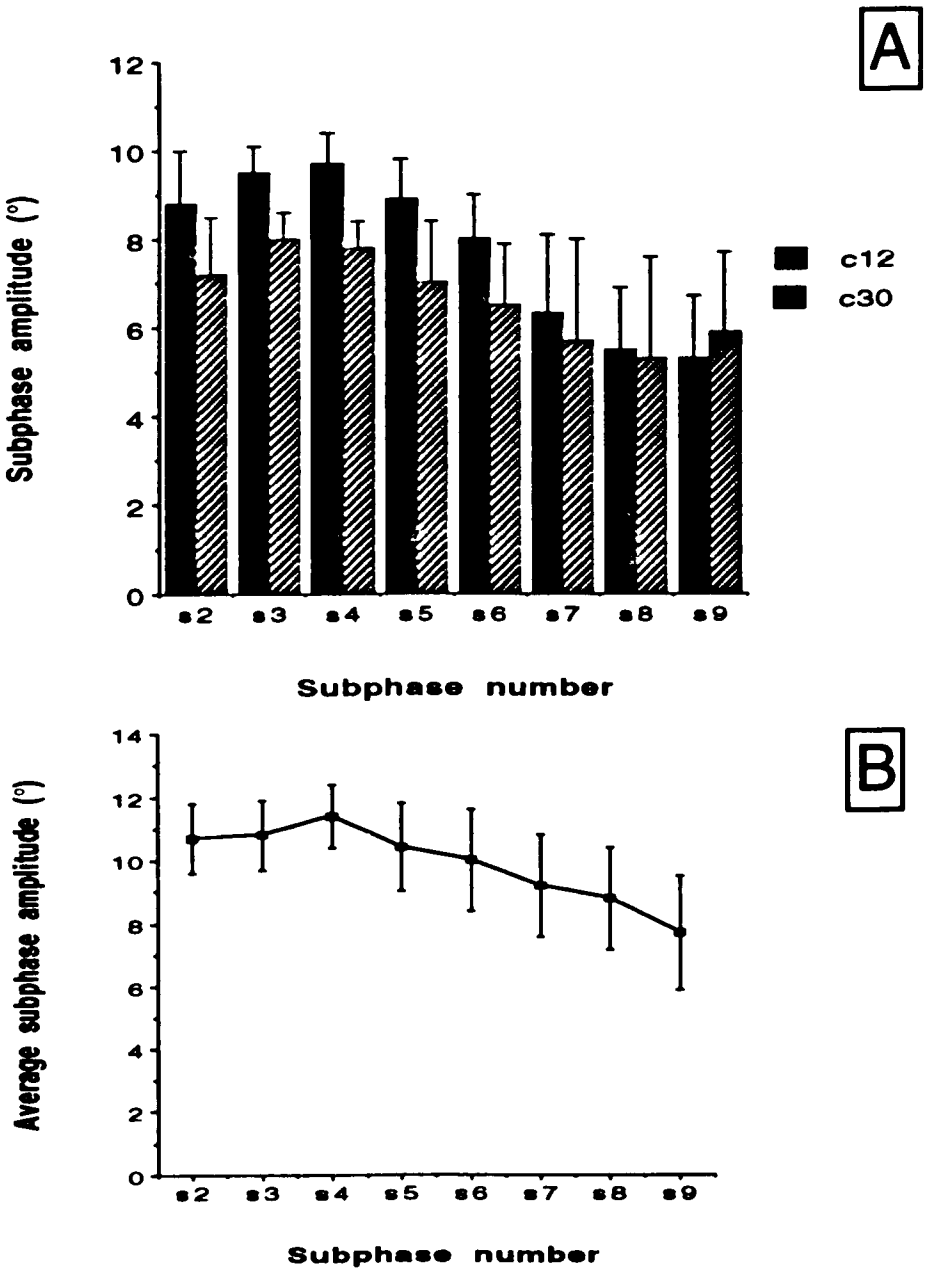

Figure 2.24
Amplitude of subphases. (A) Amplitude of subphases (2-9) for two chickens. Subphases 2-9 have an amplitude in between 12-5°. The largest subphase is the third or the fourth. The decay of subphases amplitude is very stereotyped, the first subphases have a 9-11 ° amplitude while the last subphases have an amplitude of 5-7° (error bars represent 95% confidence interval).
(B) Grand average, across 10 chickens, of the amplitude of saccadic subphases (error bars= 95% confidence interval for the median). Note that the decay in amplitude is not exponential with time, instead it appears to decrease linearly.

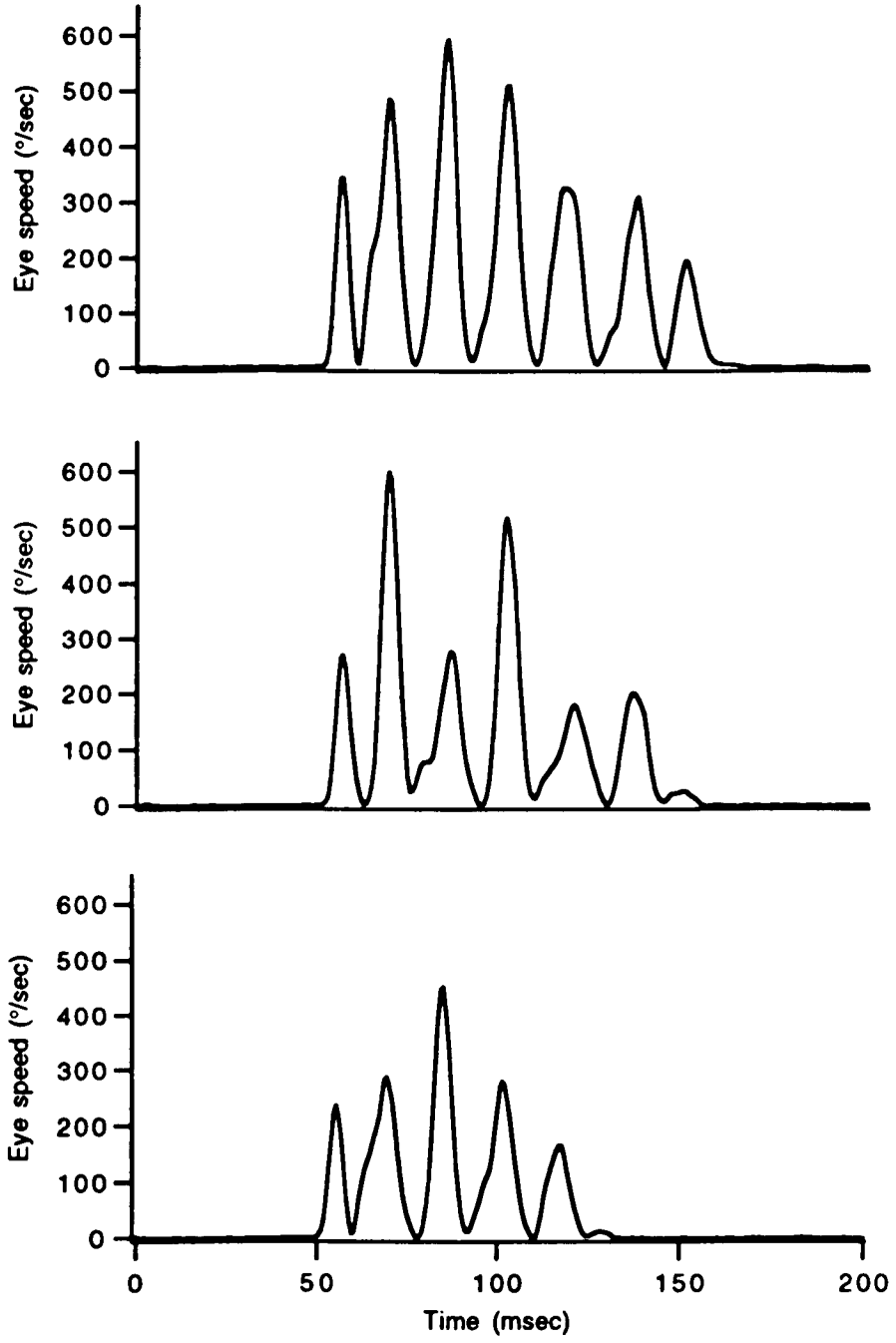

Figure 2. 25
Instantaneous speed during saccades. Three examples of the eye velocity (torsional component only). The peak velocity reaches 600 °/sec usually. The largest velocity is found in subphases 2-3. This graph understimates the instantaneous eye speed because the horizontal and vertical component of eye position were not used.

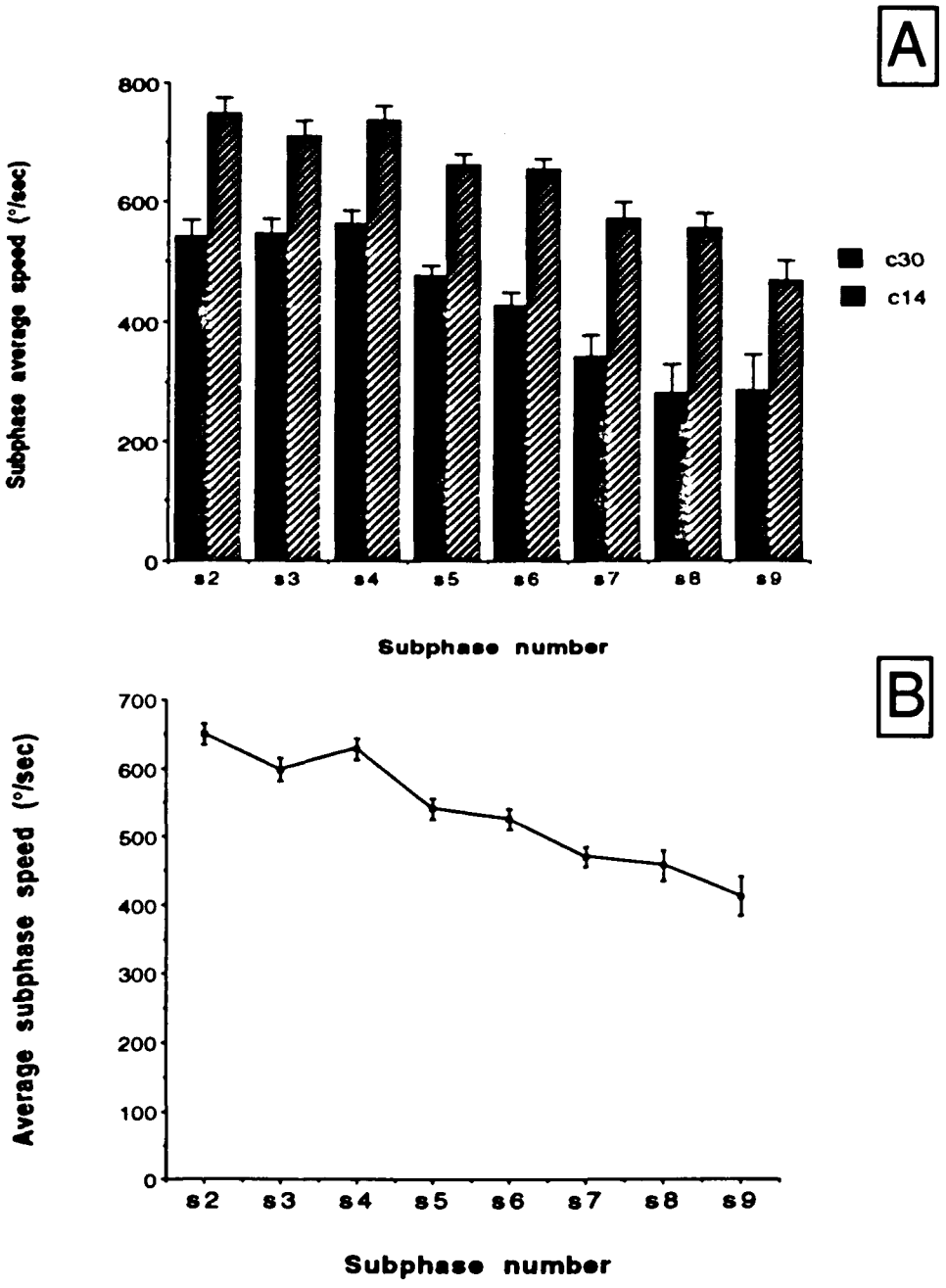

Figure 2.26
Average eye speed during oscillations. (A) Barplot of the average eye speed during subphases 2-9 for 2 chickens. Eye speed was computed by dividing the 3-D amplitude of each subphase by its duration (error bars= half of 95% confidence interval).
(B) Grand average of average eye speed during oscillations for a group of 10 chickens (error bars= 95% confidence interval). Eye speed does not change abruptly during saccades, the speed during subphase #9 being 70% of the speed of subphase #2. Mean speed was calculated using the total 3-D displacement of the eye.

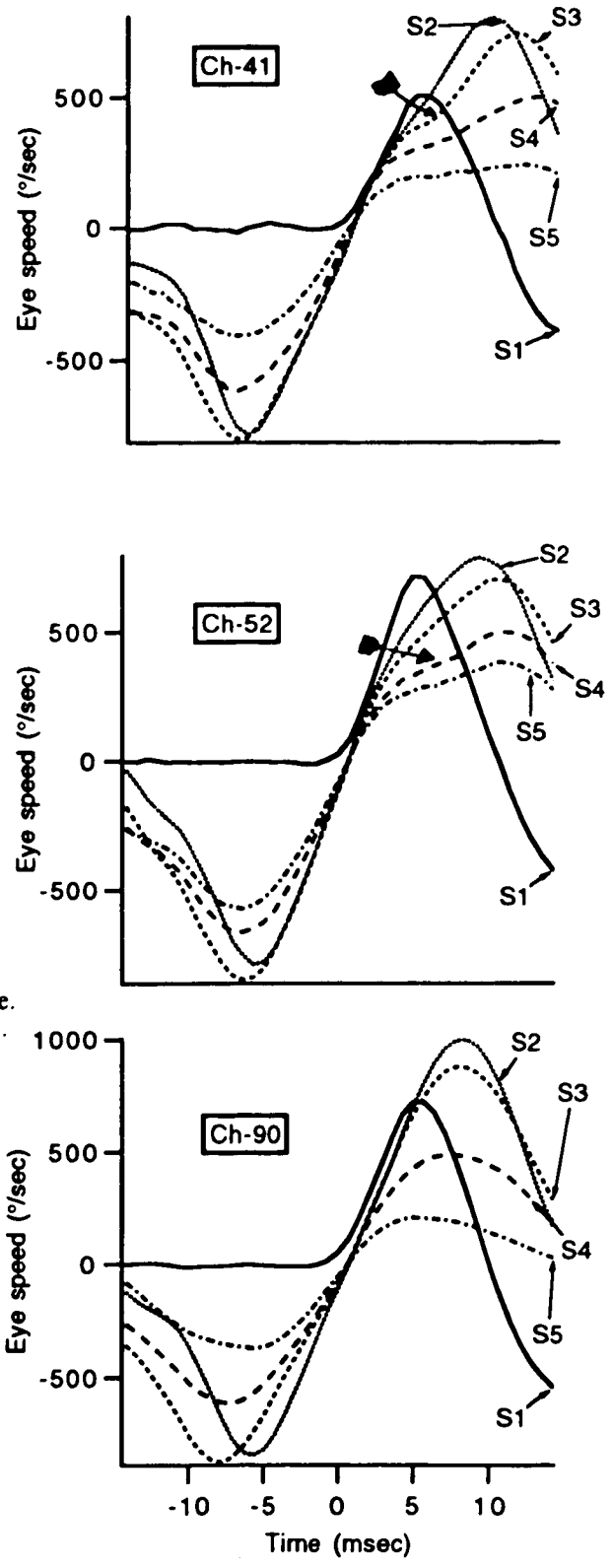

Figure 2.27
Average torsional speed profile for the first five subbphases. Three examples of the average speed for the first 5 subphases, only intorsional subphases were used. T=0 is the location of saccadic peaks, or the saccade beginning for S1. The maximal speed is not reached at the same moment in all subphases, it is reached 7-9 msec after the peaks for subphases 2-5, but only 5 msec after the initiation of the saccade. Also the presence of a "shoulder" (arrow) in some traces indicates the existence of an extra impulsive event after the beginning of the intorsional subhase. S1=first subphase, S2=second subphase, etc.. Each trace is the average of 5-10 saccades.

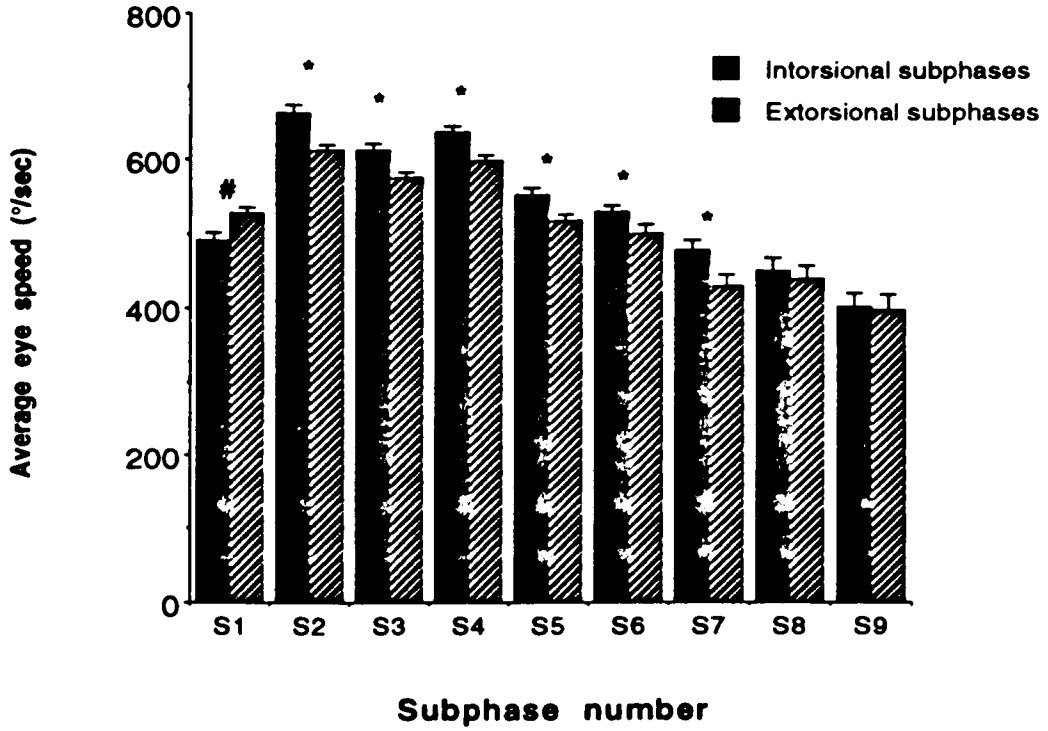

Figure 2.28
Speed asymmetry of subphases. Barplot of mean speed during subphases sorted according to subphase direction. Intorsional subphases are slightly faster than their extorsional counterparts (* indicates that intorsional subphases are faster at the 95% level, $p<0.05$ t-test). For the first subphase (#) the relation is the opposite, extorsional subphases are faster. The data used are the pooled data of the spontaneous saccades of 10 chickens, 100-300 saccades per chicken.

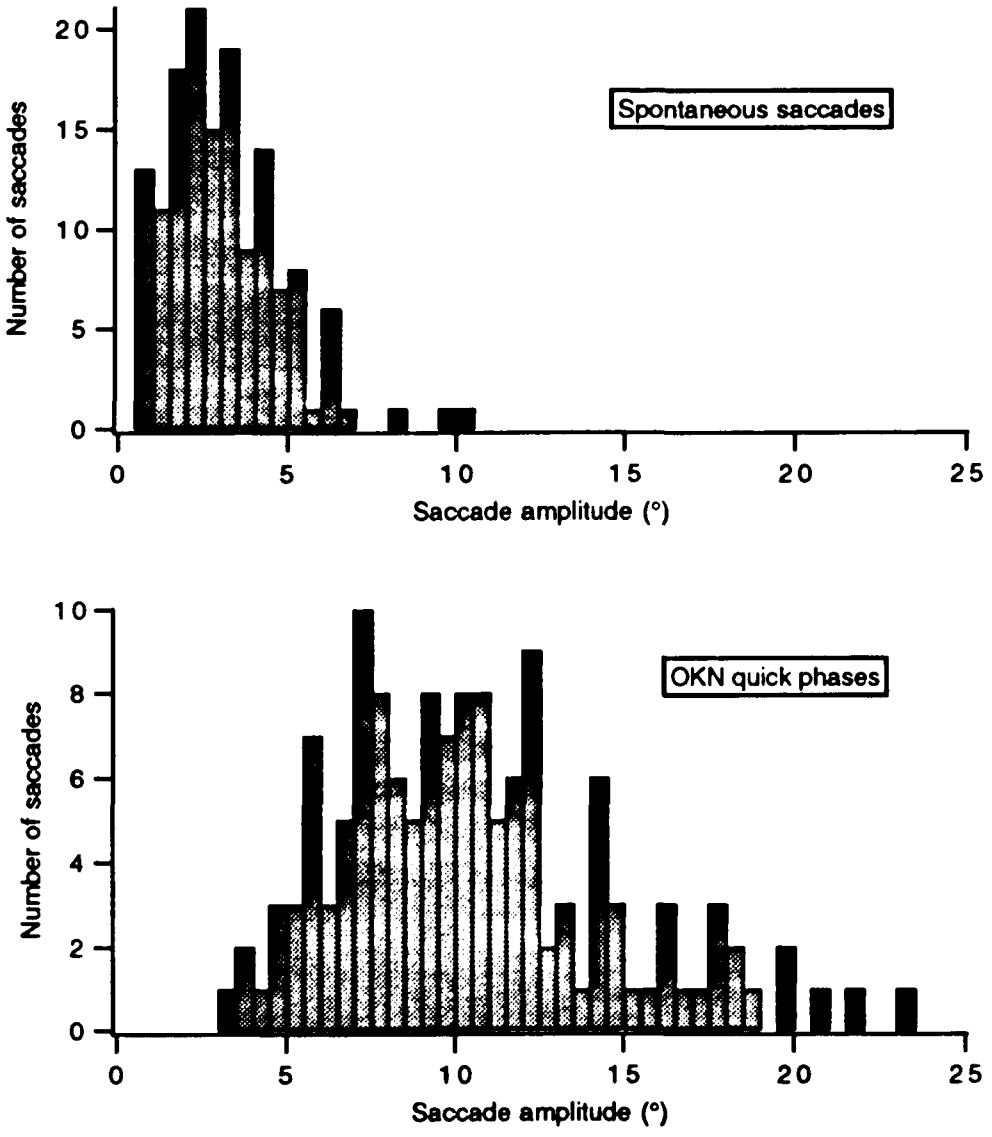

Figure 2.29
Amplitude of OKN quick phases. Distributions of amplitude for spontaneous saccades (top) and for OKN quick phases (bottom). During OKN the average amplitude of a saccade (quick phase) is 10.7 ° compared with 3.1° for spontaneous saccades (data from chicken-13).

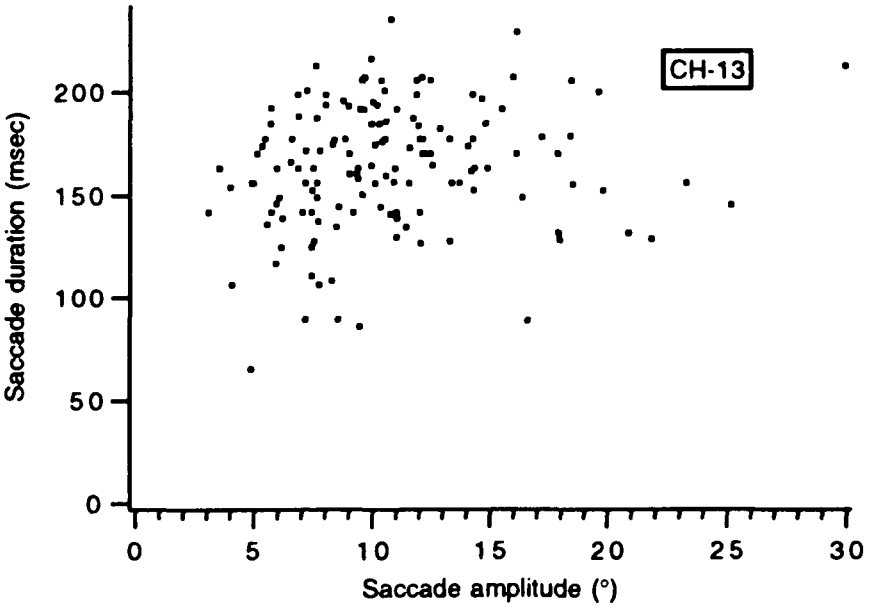

Figure 2.30
Independence between amplitude and duration for quick phases. As for spontaneous saccades (fig 2.17) no apparent relation exists between the duration and the amplitude of quick phases.

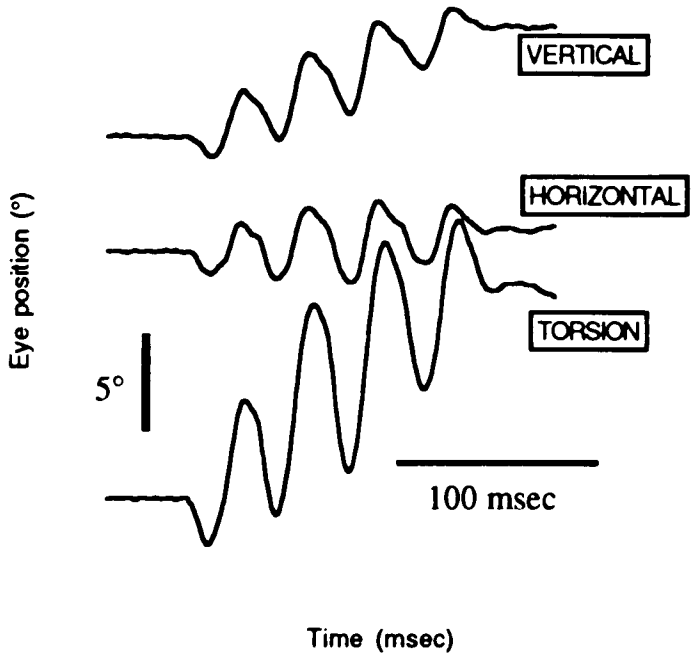

Figure 2.31
Example of intorsional quick phase. Intorsional quick phase showing the same oscillatory pattern found in spontaneous saccades (same frequency and same peak to peak amplitude). Because the OKN was triggered by an extorsionally moving pattern the change in the cyclotrorsional eye position is substantial. This large amplitude movement is a characteristic of quick phases.

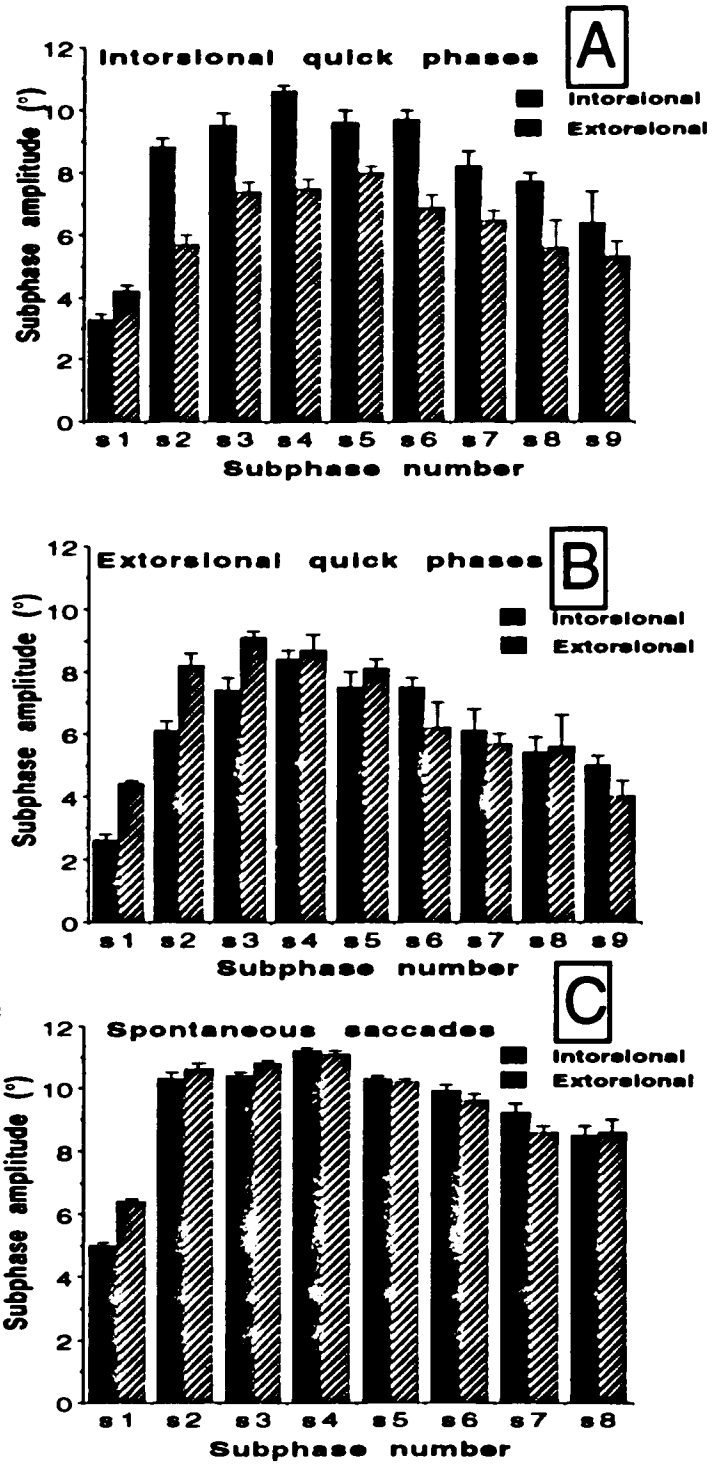

Figure 2.32
Amplitude of subphases sorted by type. The amplitude of subphases 1-9 was plotted in three conditions; Intorsional (A) and Extorsional (B) quick phases and for spontaneous saccades (C). Because the subphases were sorted according to their type sometimes the subphase moves in the same direction than the overall eye displacement (intorsional subphases in A, extorsional subphases in B). While during spontaneous saccades intorsionally and extorsionally going subphases have the same amplitude they differ during OKN quick phases.

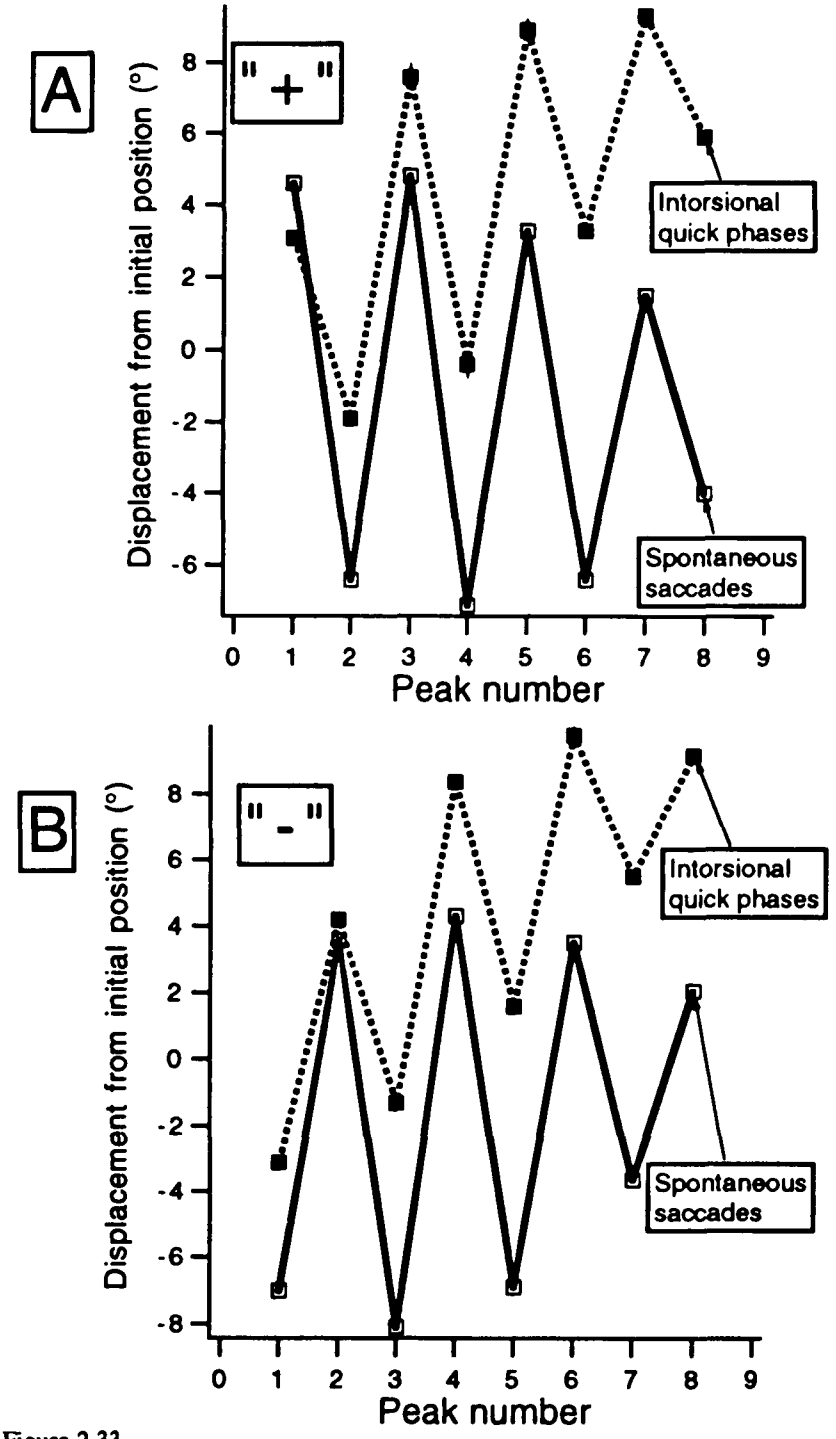

Figure 2.33
Average peak displacement in OKN quick phases and spontaneous saccades. The average displacement of peaks 1-8, with respect to initial position, is given for intorsional quick phases sorted by type (A=plus, B=minus). For comparison the same data for spontaneous saccades is given. In the case of quick phases, the peaks are gradually displaced from the initial position, instead of shifthing abruptly.

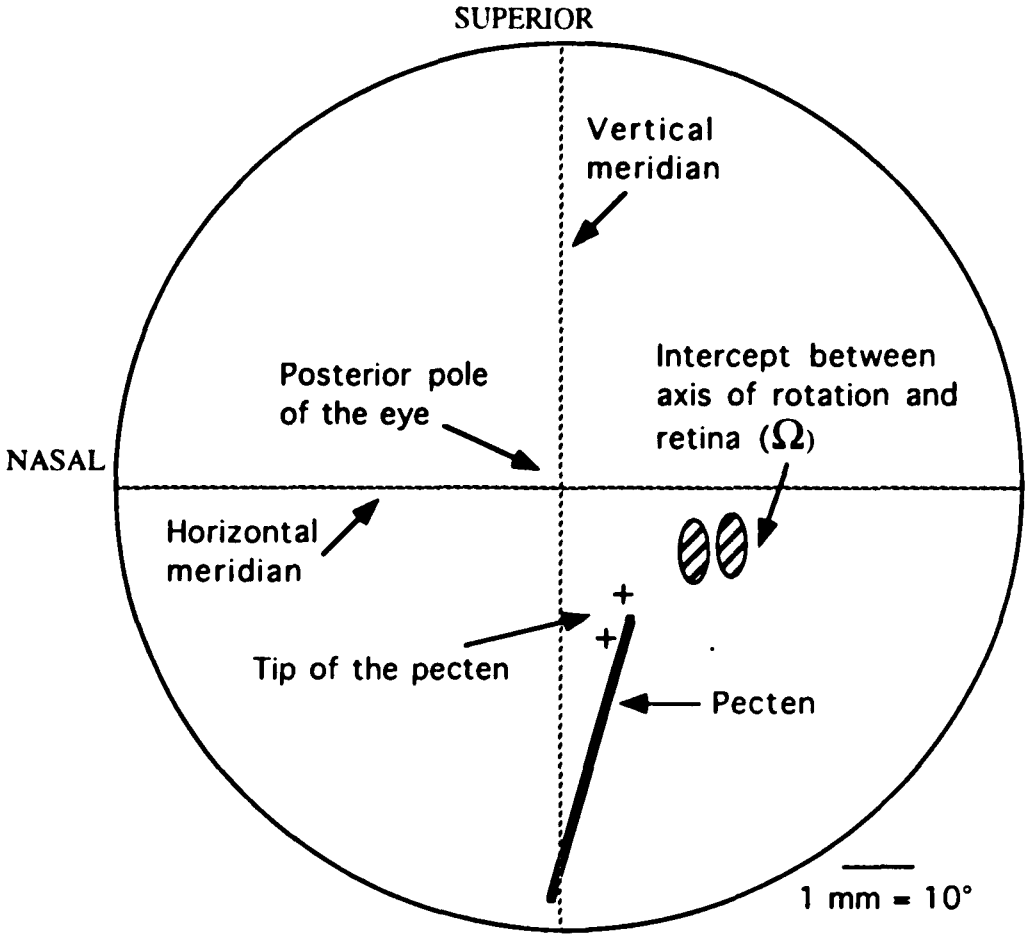

Figure 2.34
Relative position of the intercept of the instantaneous axis of rotation and the back of the left eye. Diagram representing the positions of the posterior pole, the tip of the pecten, the Ω region and the pecten orientation for the left eye. The diagram represents a frontal view of the back of the left eye. The Ω regions, determined in two chickens, are located at 1.5 mm approximately from the tip of the pecten (crosses). The determination of the Ω regions and the tip of the pecten were done in different chickens. Each hatched region represents the 95% confidence region for the intersection of the axis of rotation and the back of the eye. The conversion factor between retinal distance and angular distance was calculated based on the eye shape data found in Gottlieb, Fugate-Wentzek and Wallman (1987). The optic axis intercepts the posterior pole of the eye, the line representing the pecten is given only for orientation purposes only, it does not represent factual data obtained in this thesis but it was obtained from Bodnarenko (1989).

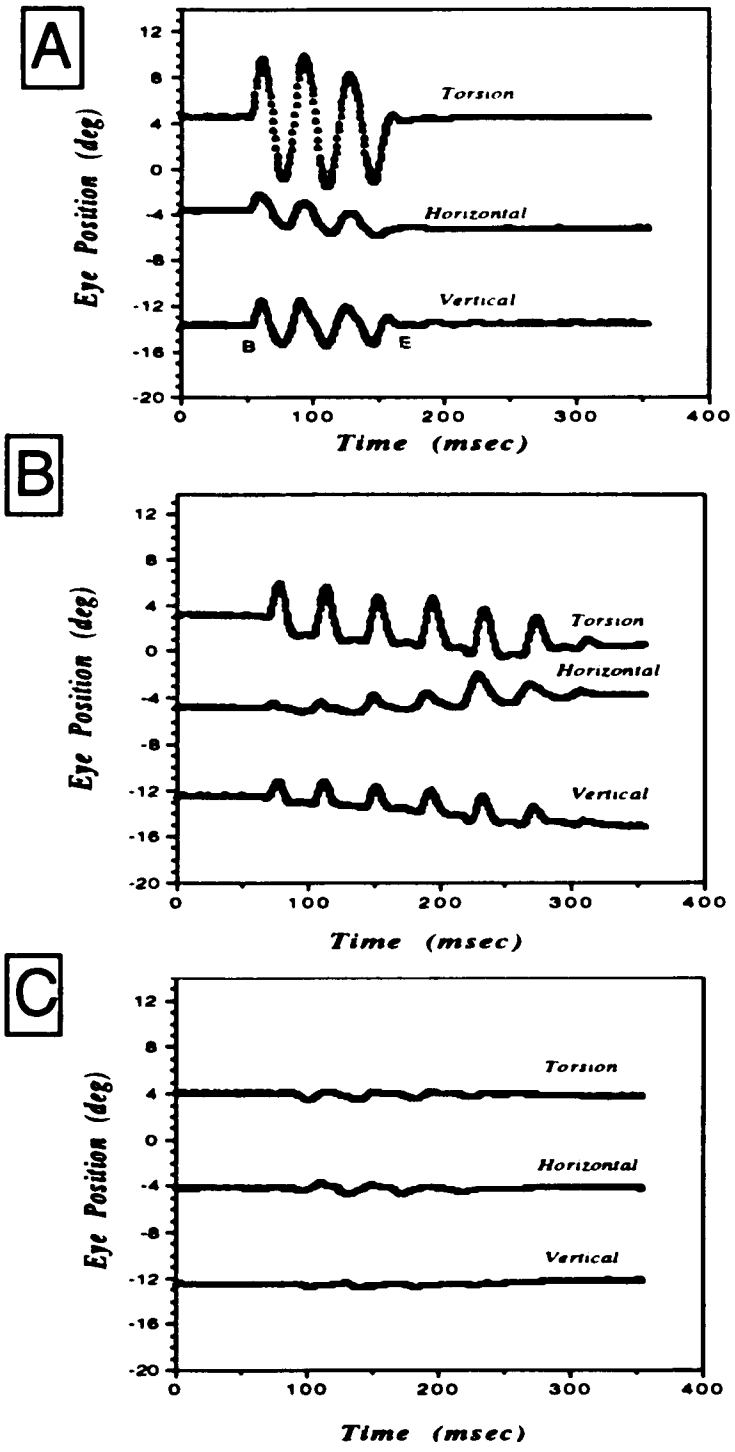

Figure 2.35
Effect upon oscillations of disabling the obliques. (A) Normal saccade,both obliques are intact. (B) Inferior oblique cut next to its insertion, saccadic oscillations are clipped of their extorsional part. (C) Both obliques disabled, the oscillations disappear almost completely, leaving only an oscillations with a 5% amplitude of the original.

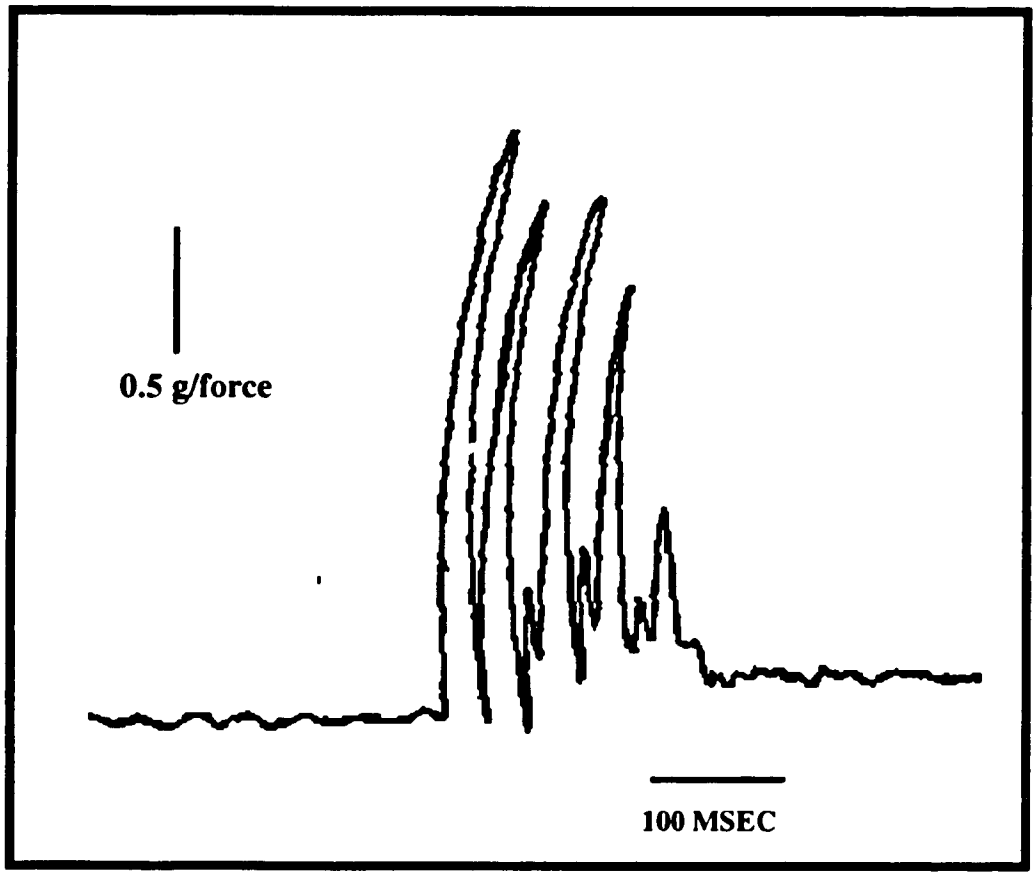

Figure 2.36
Tension generated by the superior oblique during a saccade. Digitized image of a polygraph record of the force produced by the superior oblique in an anesthetized chicken. The muscle insertion was detached from the dorsal aspect of the eyeball and attached to the force transducer. The pattern of force is obviously cyclical and the interpeak time is 40 msec approximately. When the nerve supply to this muscle was cut the oscillations disappeared immediately.

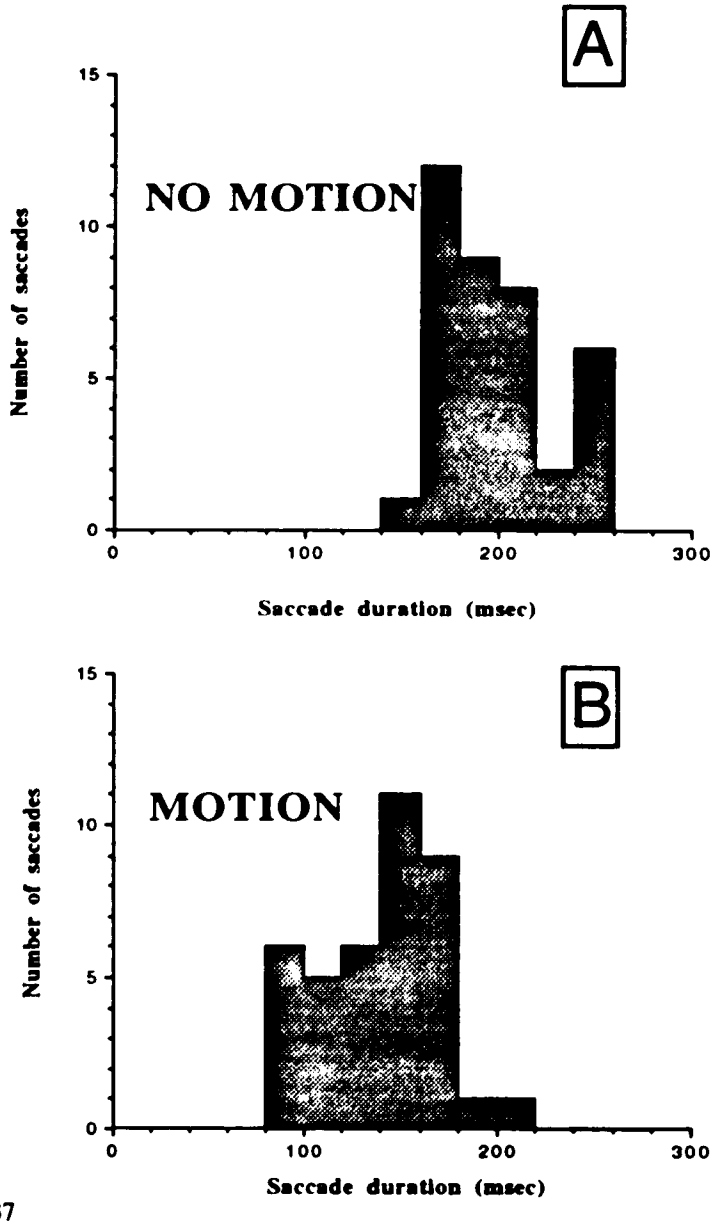

Figure 2.37
Saccade shortening by visual field motion. Example of the arrest of chicken saccades by motion of the visual field during saccades.
The two distributions of saccade durations are different at $p<0.001$, t test.
The motion of the visual surroundings (B) shortens saccades by 40 msec with respect to "un-stimulated" saccades (A). A similar result is obtained if a sound is given during the saccade.

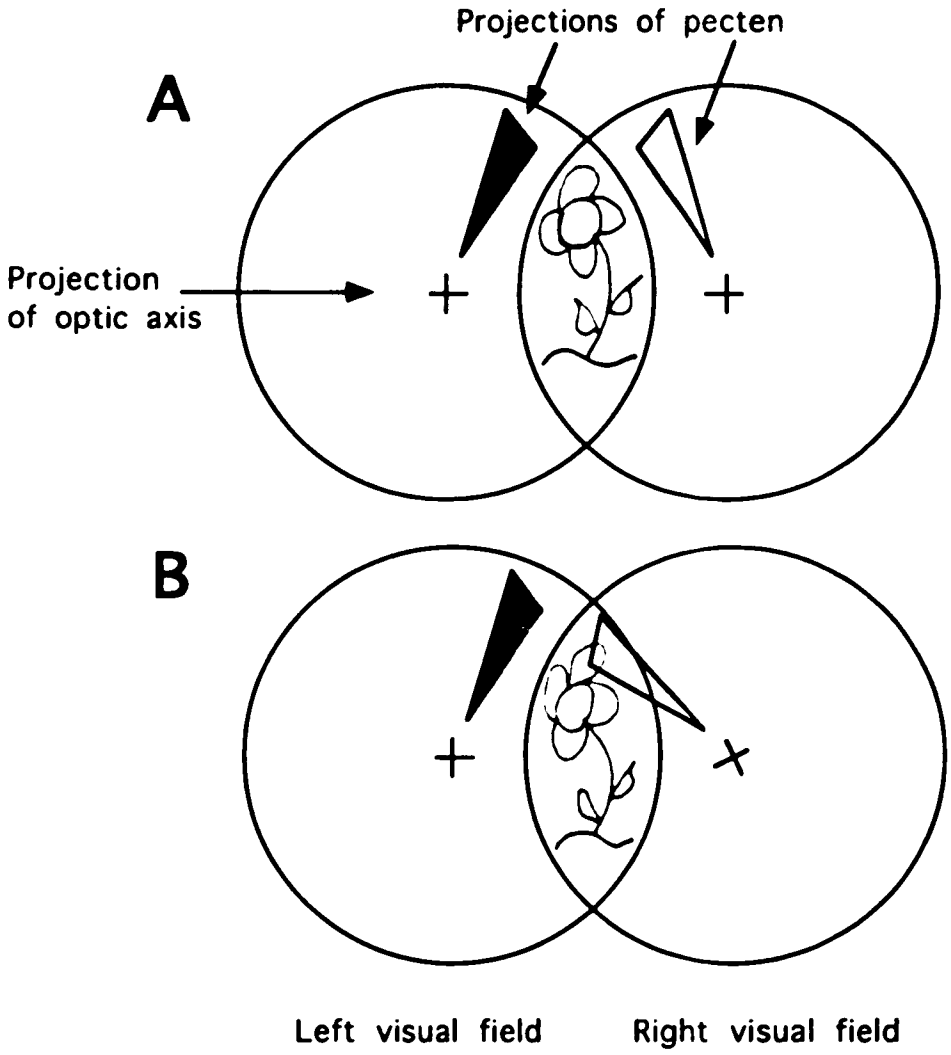

Figure 2.38
Schematic representation of the variations of the binocular field. A and B represents two configurations of the binocular field. In both cases the size of the binocular field is the same (B is obtained by a 20° rotation of the right visual field), but the locations of the right and left retinal images of the flower are different.

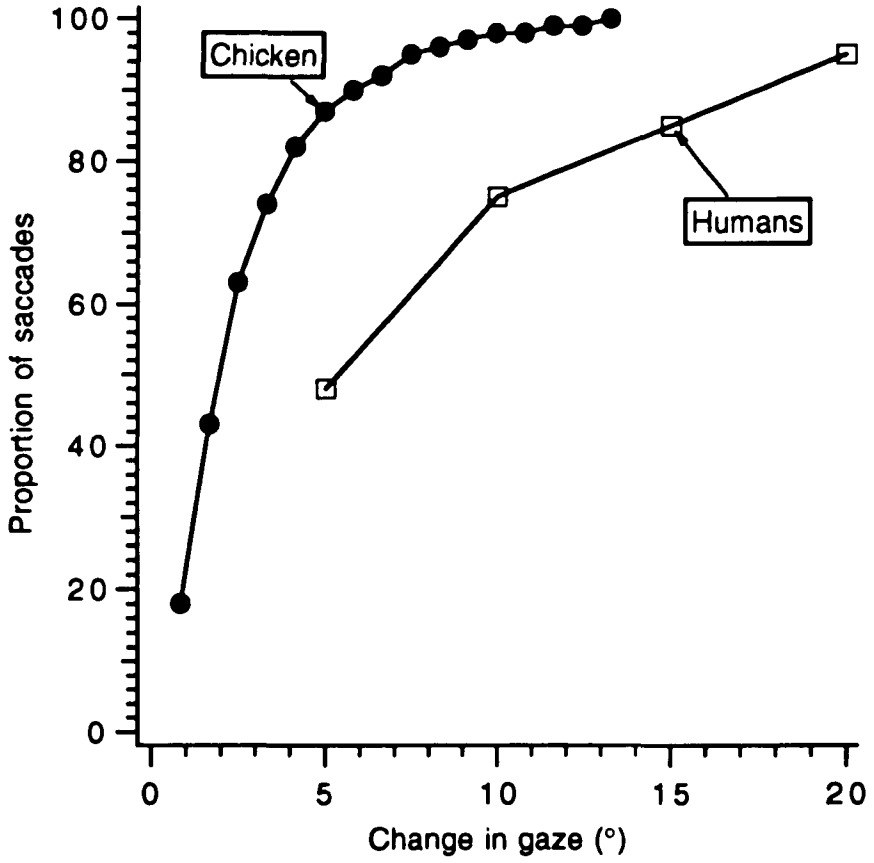

Figure 2.39
Distribution of changes of gaze direction in Humans and Chicks. This graph shows the proportion of saccades that move the direction of gaze less than a given amplitude. Thus 75% of chicken saccades move gaze less than 3.5°, while 75% of mammalian saccades move gaze 10° or less. This graph shows in a vivid form that most of chicken saccades leave the direction of gaze relatively unchanged.

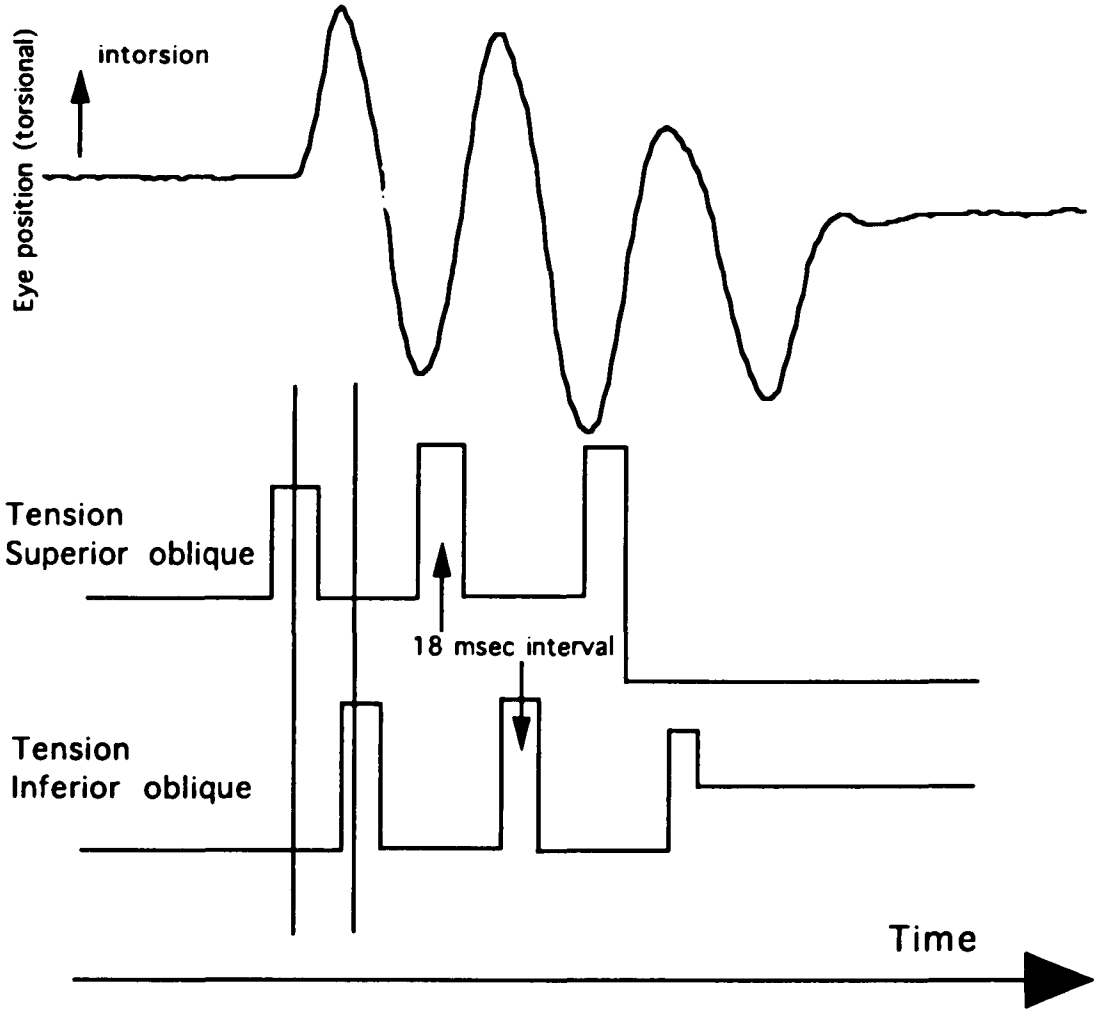

Figure 2.40
Postulated contractions of the obliques during saccades. Saccadic oscillations are produced by the succession of contractions of the superior and inferior obliques 18 msec apart. The superior oblique produces the intorsional subphases, the extorsional parts are produced by the inferior oblique.

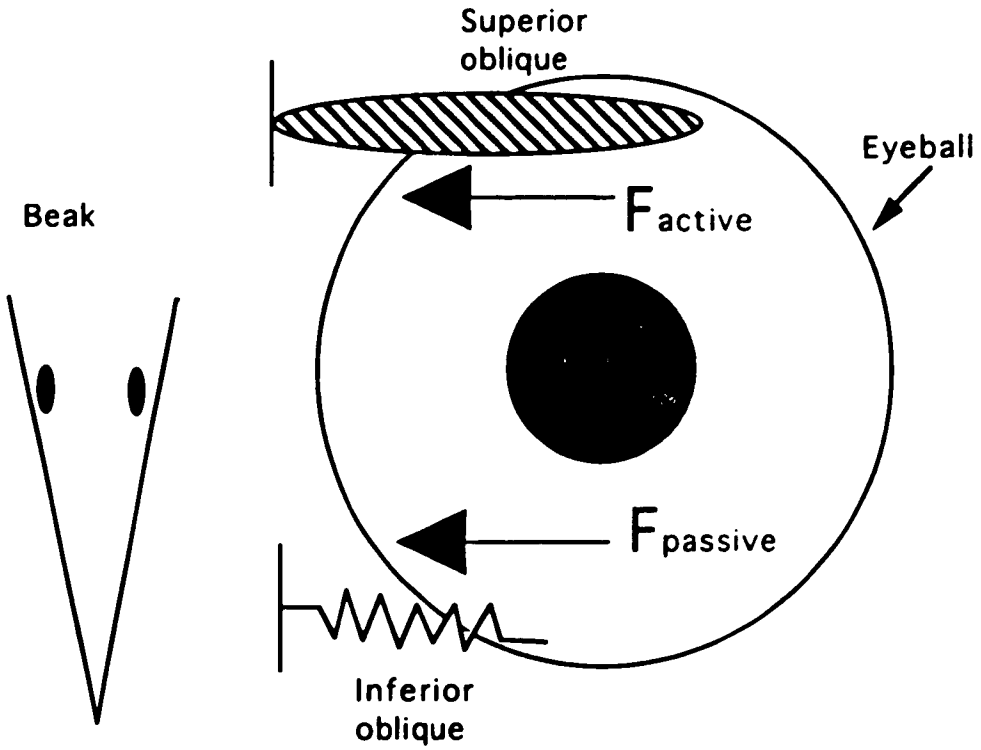

Figure 2.41
Representation of the forces applied to the eyeball during oscillations. This diagram represents the two main forces applied to the eyeball during **intorsional subphases** of oscillations for the left eye. The superior oblique provides an intorting force due to its active contraction. Ideally the 18 msec interval between the contractions of the two obliques is such that the force developed by the superior oblique (F-active) only has to oppose the viscoelastic properties of the inferior oblique. (F-passive). During **extorsional subphases** the roles of both obliques are reversed.

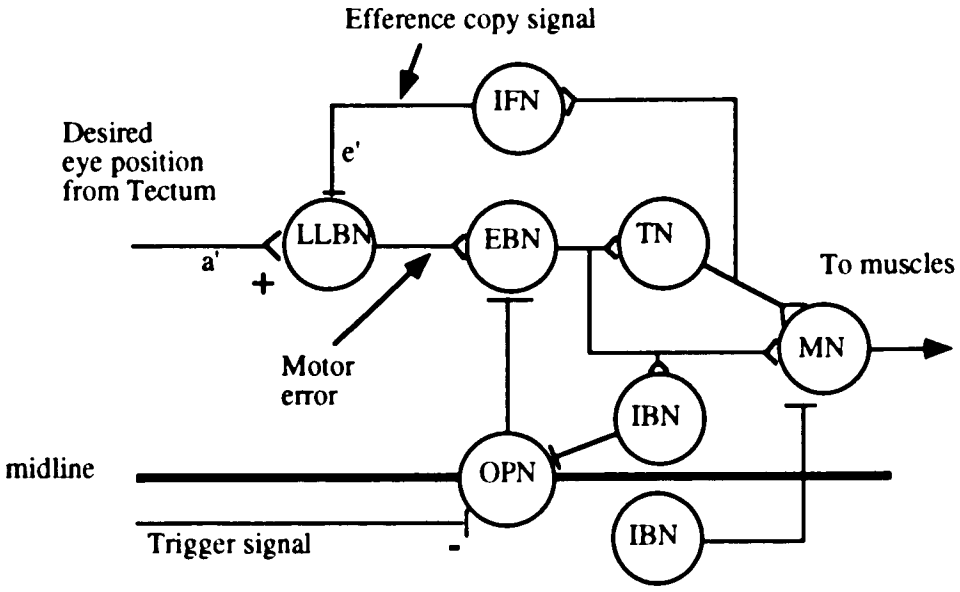

Figure 3.1
Simplified diagram of the "bang-bang" model.
This diagram illustrates the model of the saccadic machinery based on a feedback mechanism dependent upon motor error. EBN neurons are driven, indirectly, by two signals emanating from the optic tectum (*desired eye position* and *trigger*). Long Lead burst neurons (LLBN) produce the motor error signal by computing a'-e'. Inhibitory feedback neurons (IFN) use the output of tonic neurons (TN) to inhibit LLBN. During the periods of fixation, intersaccadic intervals, EBN are inhibited by Omnipause neurons (OPN). During saccades OPN are inhibited by inhibitory burst neurons (IBN) which are under the control of EBN. Motoneurons (MN) receive an inhibitory input from contralateral IBN.

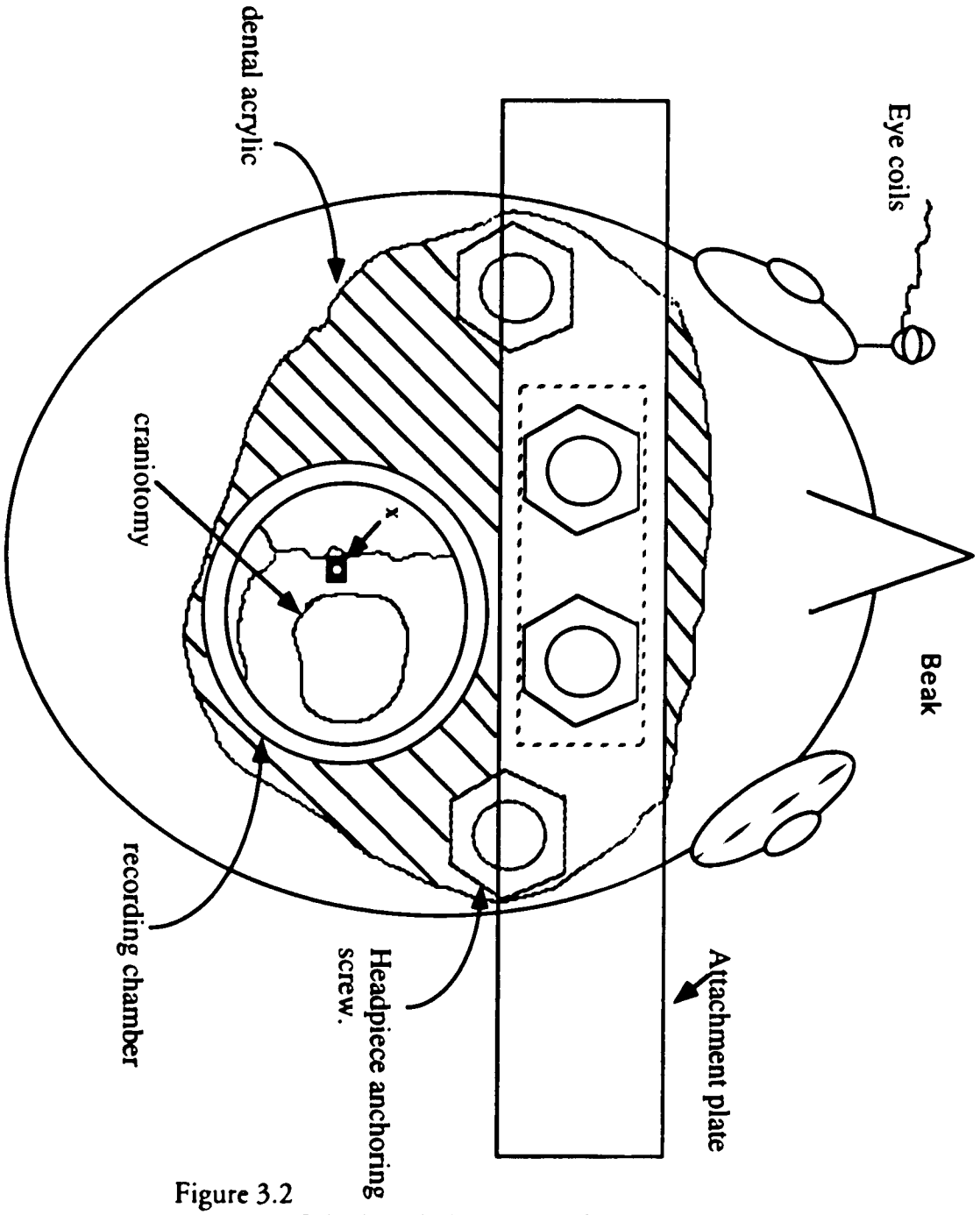

Figure 3.2
Diagram of chicken skull prepared for neuronal recording (top view). **x** marks the reference mark. The craniotomy was always unilateral, on the right side of the skull.

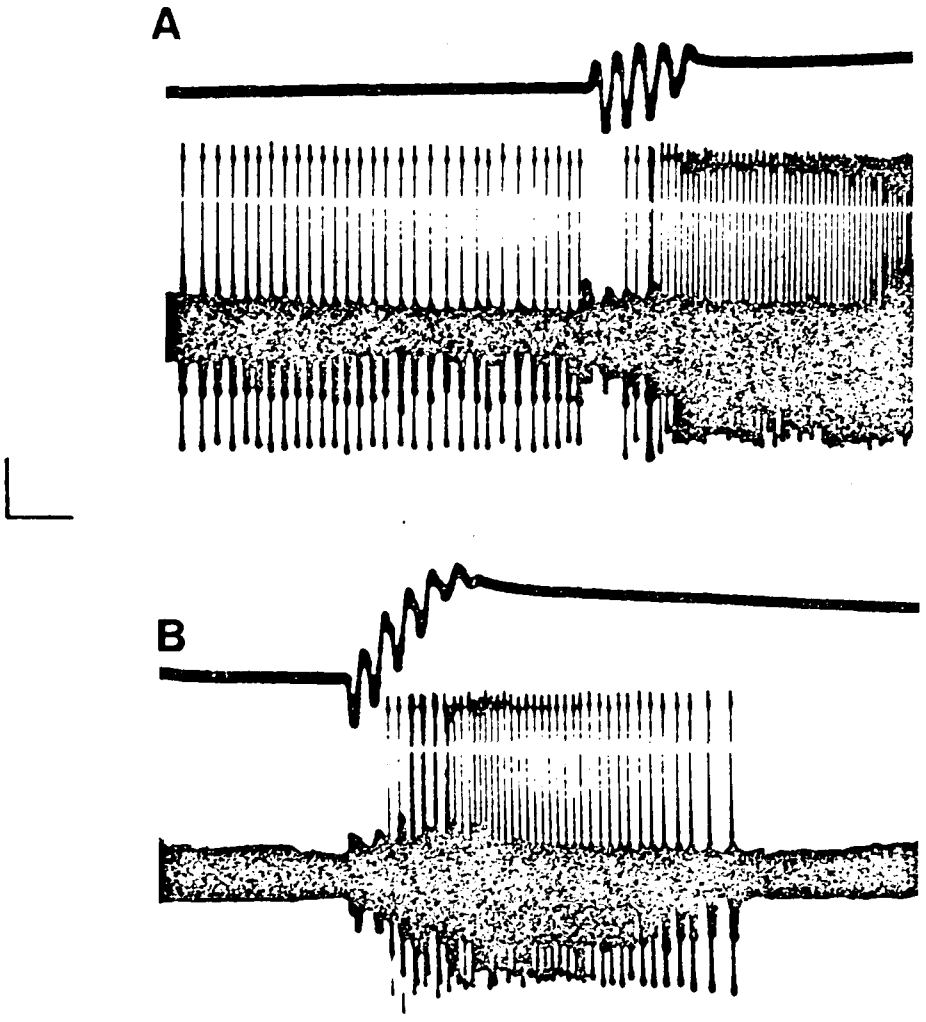

Figure 3.3
Discharge pattern of Tonic Motoneuron in the chicken trochlear. In each panel the lower trace is the activity of a trochlear motoneuron and the upper trace is the torsional component of eye position (upward=intorsion). Time calibration mark= 100 msec, position calibration mark= 5 degrees. A Typical example of tonic motoneuron activity during a spontaneous saccade. the cell stops firing for part of the saccade, even though the net eye movement goes toward a more intorsional eye position (the "on" direction). No pulse component is visible. By the end of the saccade, the motoneurons fires with the frequency required to hold the nex eye position. B Activity of a Tonic motoneurons during an intorsional 12° quick phase of OKN. The motoneuron begins to fire 50 msec after the beginning of the quick phase, with the highest frequency reached at the end of the saccade, when the eye is in an extreme intorsional eye position. During the subsequent extorsional slow phase, when the eye goes below the threshold position, the motoneuron stops firing.

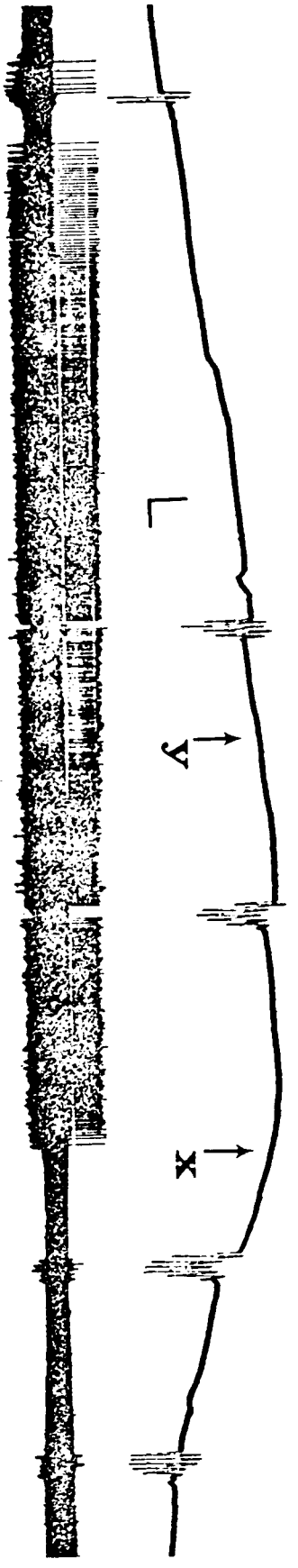

C Figure 3.3C *cont.*
Sensitivity to eye velocity. At point **x** the motoneuron ceases to fire even though the eye is in the "on" region of the motoneuron (compare with **y**). The difference in firing rate between **x** and **y** reflects that the discharge frequency is not only a function of eye position but of eye speed as well. Note how the motoneuron stops for all saccades in the record.

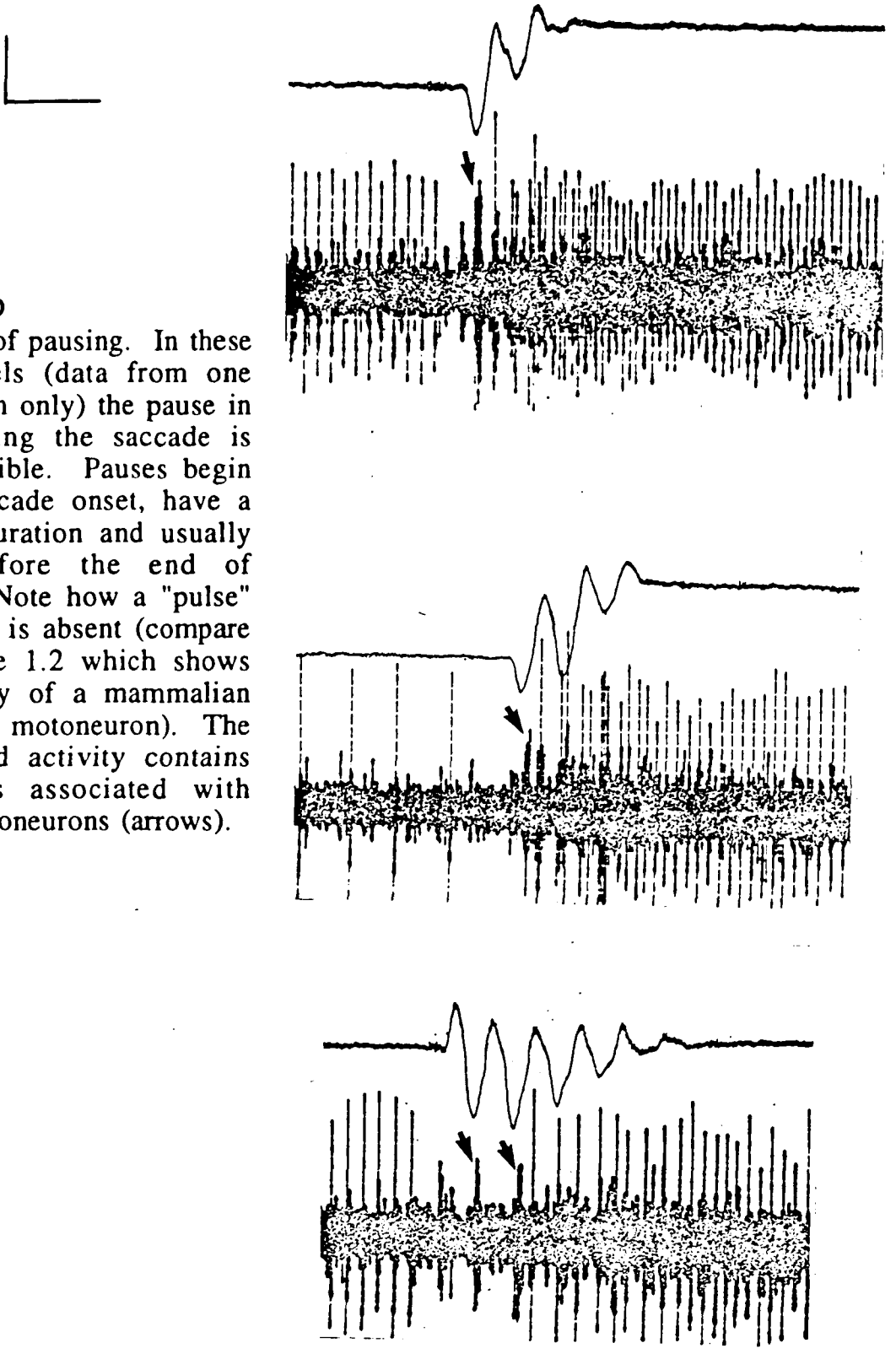

Figure 3.3D
Examples of pausing. In these three panels (data from one motoneuron only) the pause in firing during the saccade is clearly visible. Pauses begin before saccade onset, have a variable duration and usually finish before the end of saccade. Note how a "pulse" component is absent (compare with figure 1.2 which shows the activity of a mammalian extraocular motoneuron). The background activity contains the bursts associated with Phasic motoneurons (arrows).

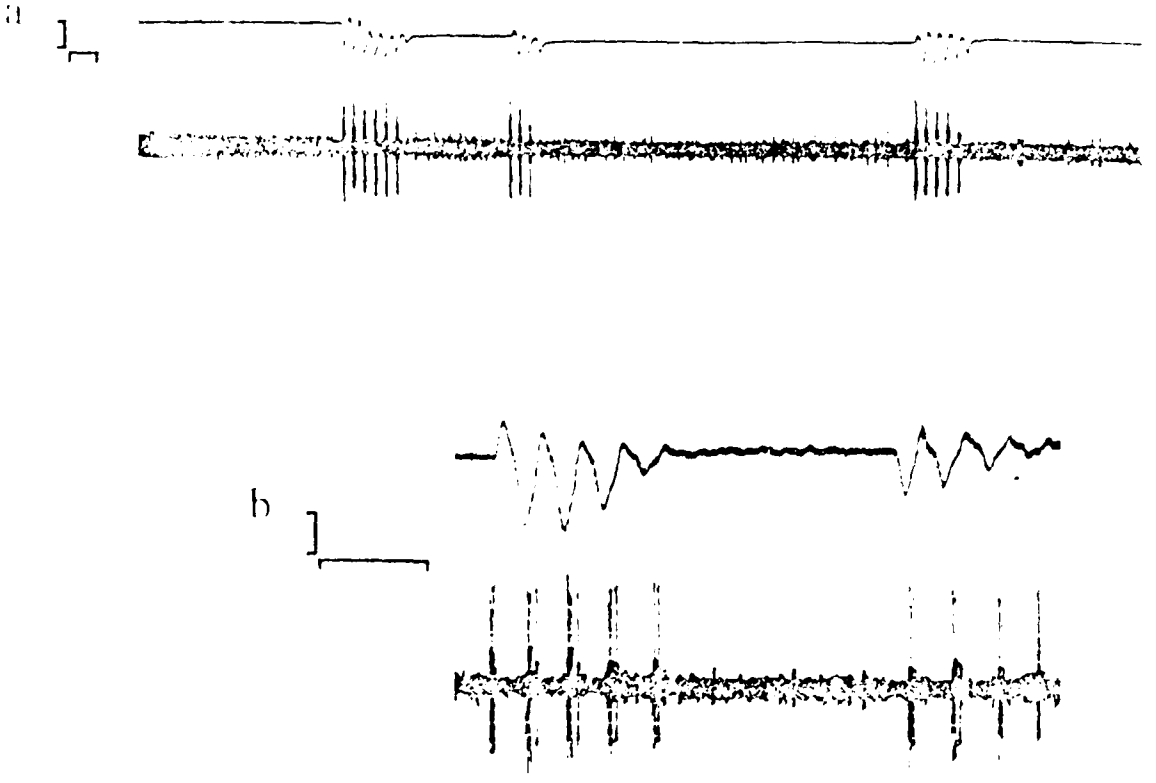

Figure 3.4
Discharge pattern of Phasic motoneuron in the chicken trochlear. (calibration as in figure 3.3).
a Typical discharge pattern of Phasic motoneuron. The cell is totally silent during fixations and active only during saccades. b Relation of Phasic response to the starting phase of saccades. During saccades beginning with an intorsional subphase (left) the first burst precedes the eye movement; during saccades beginning with an extorsional phase (right) the eye movement precedes the response.

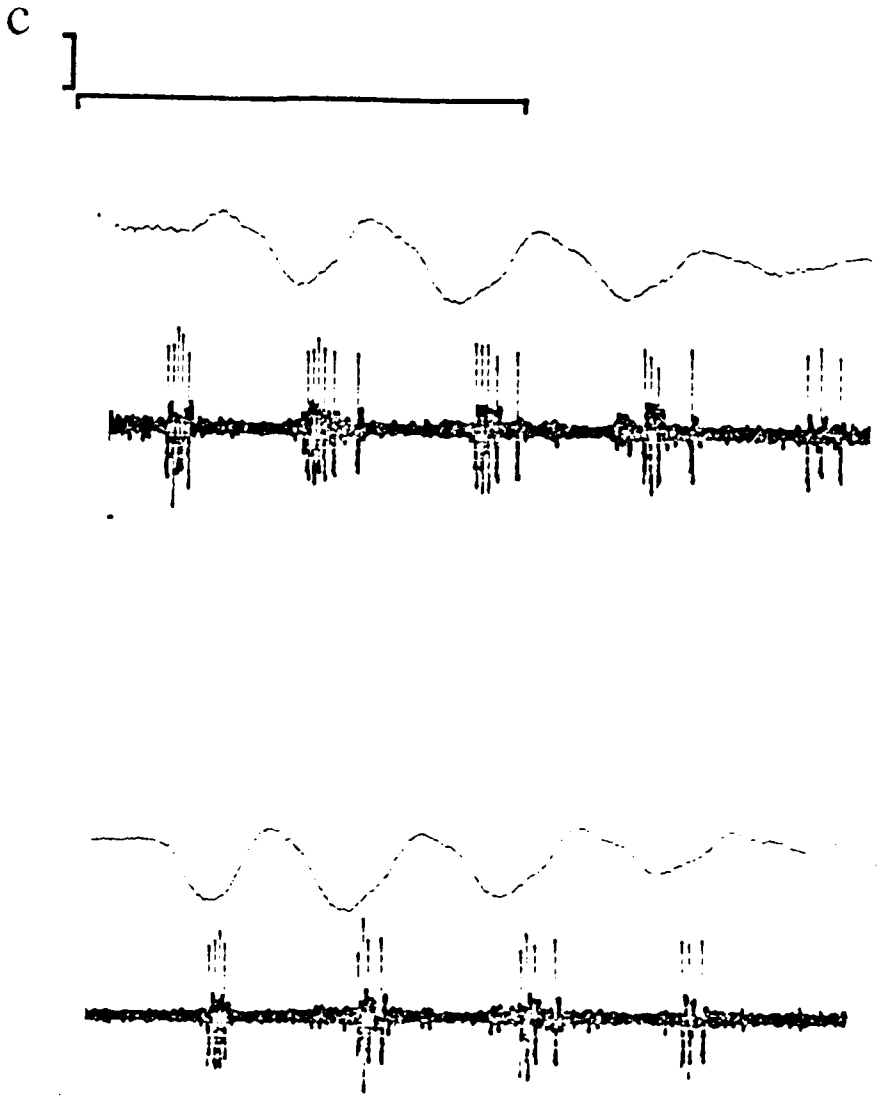

Figure 3.4 *cont.*
c Same saccades as in **b** but at a higher time magnification. Each burst of a phasic motoneuron is composed of 2-6 spikes. The maximal frequency reached by Phasic units is 800 spikes/sec. Note how, with the exception of the first burst of the upper panel, every burst begins after the beginning of the intorsional subphase.

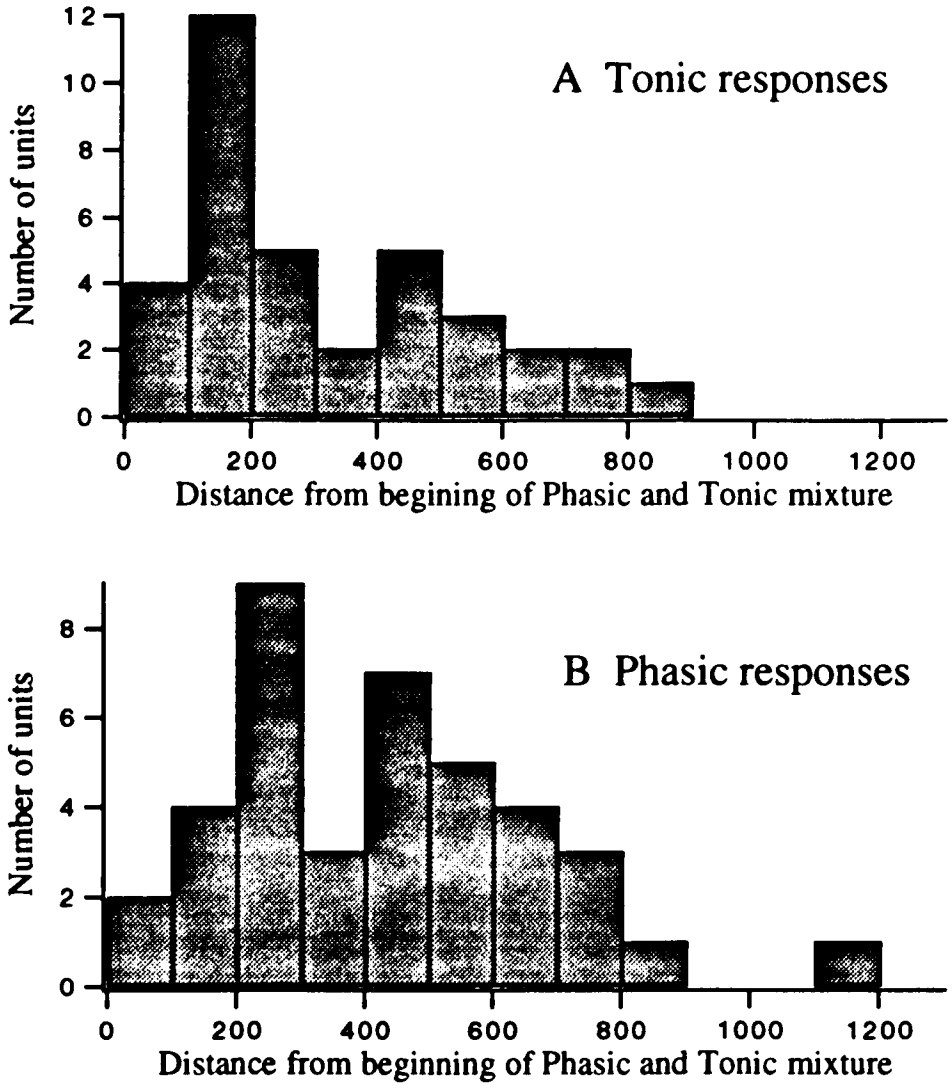

Figure 3.5 Distribution of Tonic (A) and Phasic (B) responses as a function of depth. Because this data was based on physiological data the beginning of trochlear nucleus was taken as the beginning of the tonic/phasic background activity. While both distributions are not identical, it is clear that Phasic and Tonic responses are not segregated along a dorso-ventral axis.

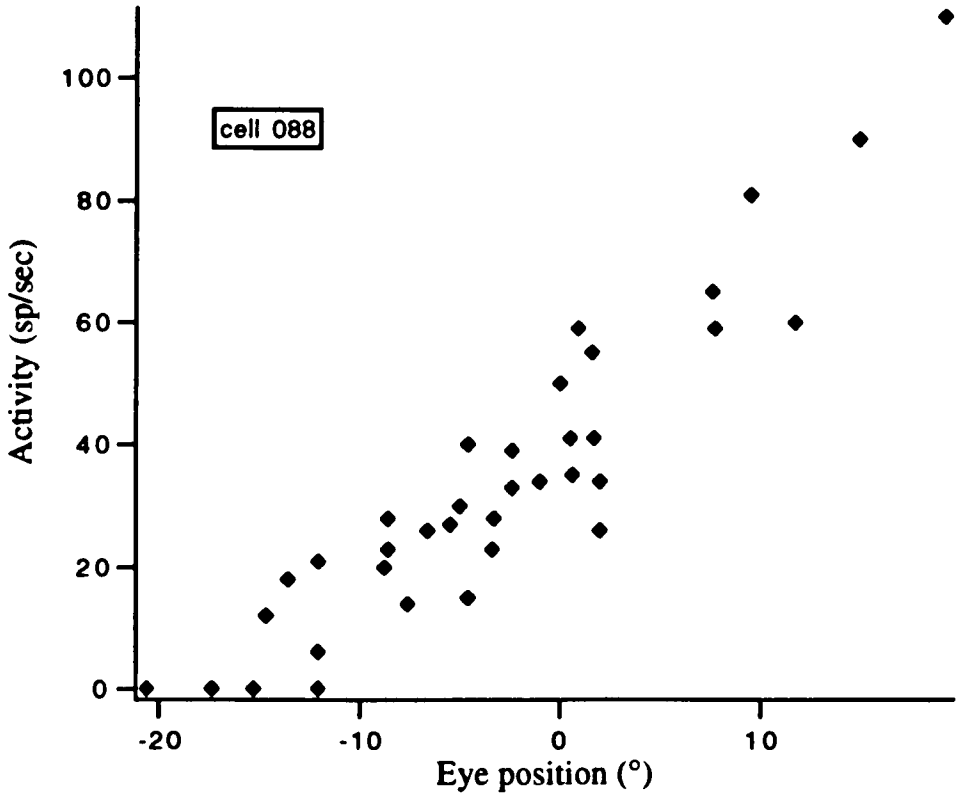

Figure 3.6
Position sensitivity for Tonic motoneuron. This unit increases its firing rate as the eye takes more intorsional positions. The activity is almost linearly related to eye position. The threshold for this unit is at -15°.

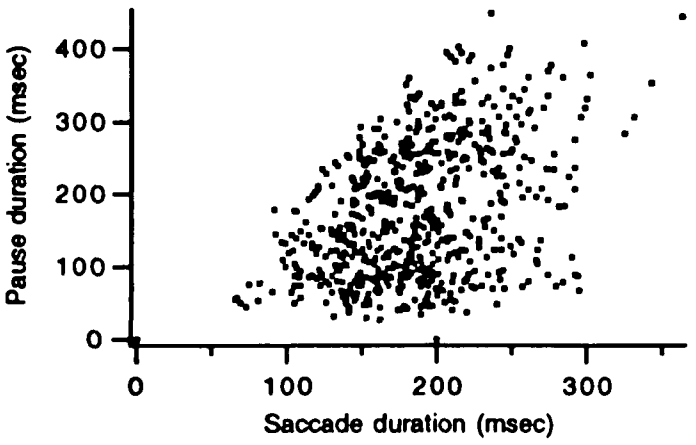

Figure 3.7
Plot of pause duration vs saccade duration (data from 5 tonic motoneurons). Pause duration is variable, but always greater than 35 msec, also its duration increases with saccade duration.

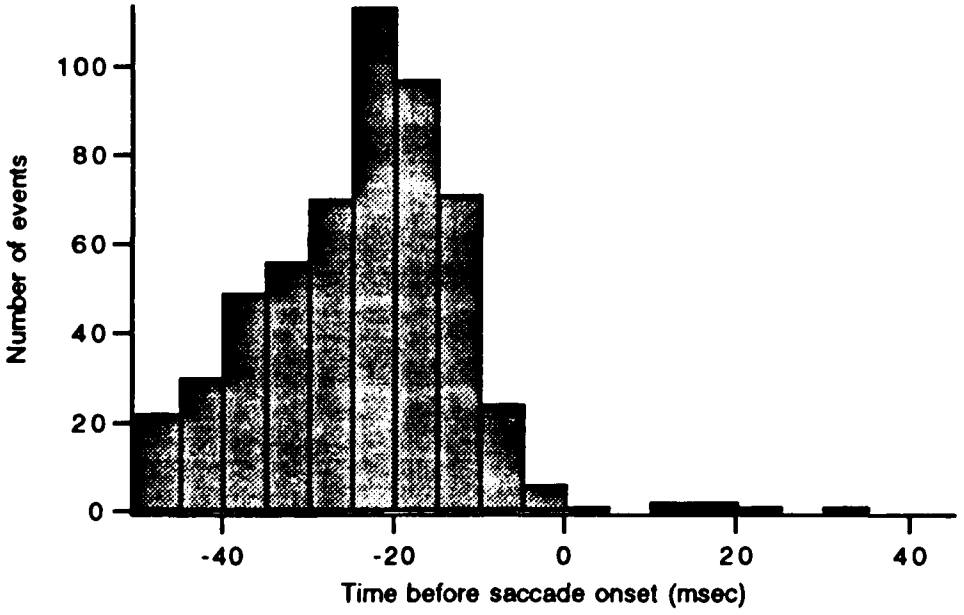

Figure 3.8
Histogram of the time interval between the onset of the pause and the beginning of saccade (pooled data from 30 Tonic motoneurons). In almost every ocasion the pause begins before the saccade (median=27 msec).

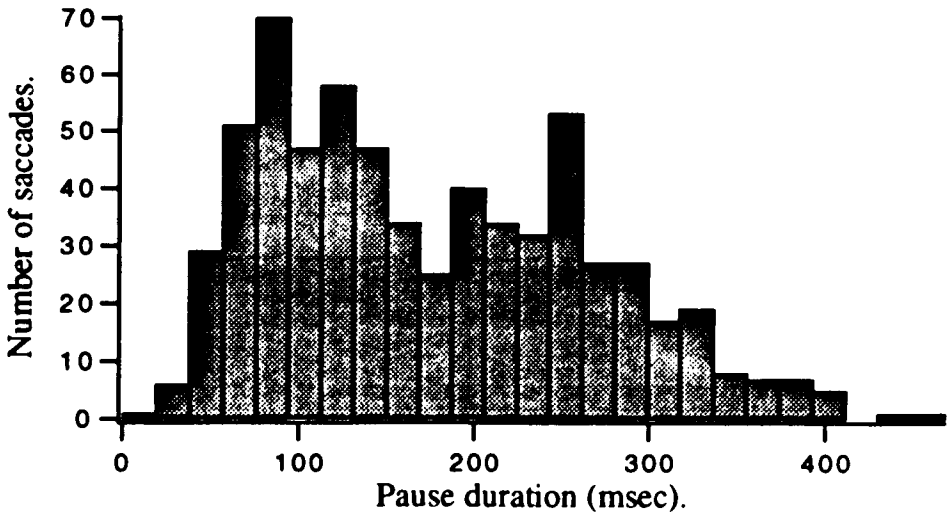

Figure 3.9
Histogram of pause duration. Data collected from saccades with torsional amplitudes of less than 5°, pooled data from 5 tonic motoneurons. Pauses always lasted at least 35-50 msec.

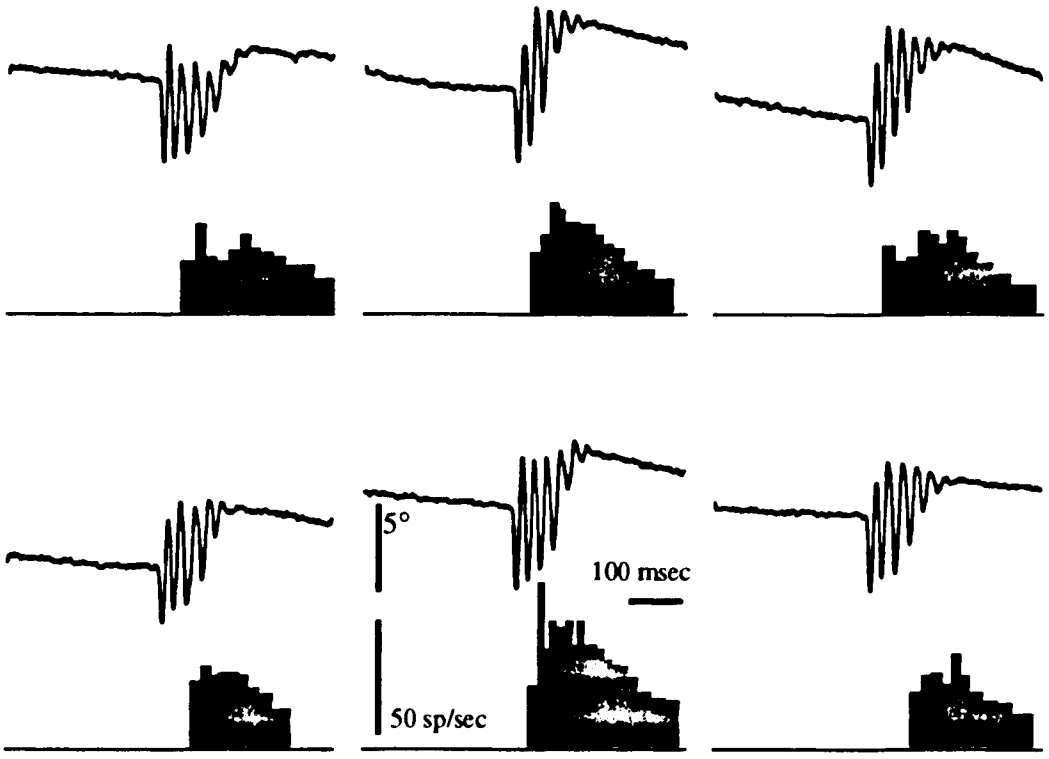

Figure 3.10
Activity of a Tonic motoneuron during OKN quick phases. This figure demonstrates how the net eye displacement is produced during saccades (upper trace= torsional eye position, lower trace= instantaneous firing frequency). Before saccade onset the cell is silent as the eye is in the motoneuron's "off" region and the eye moves extorsionally. A variable time interval after the beginning of the saccade the unit begins to fire. The high activity reached during the saccade moves the eye towards a more intorsional position. After the saccade ends, the unit diminishes its activity as the eye moves extorsionally towards the "off" region. The six panels are examples taken from one Tonic motoneuron.
Calibration marks apply to all panels.

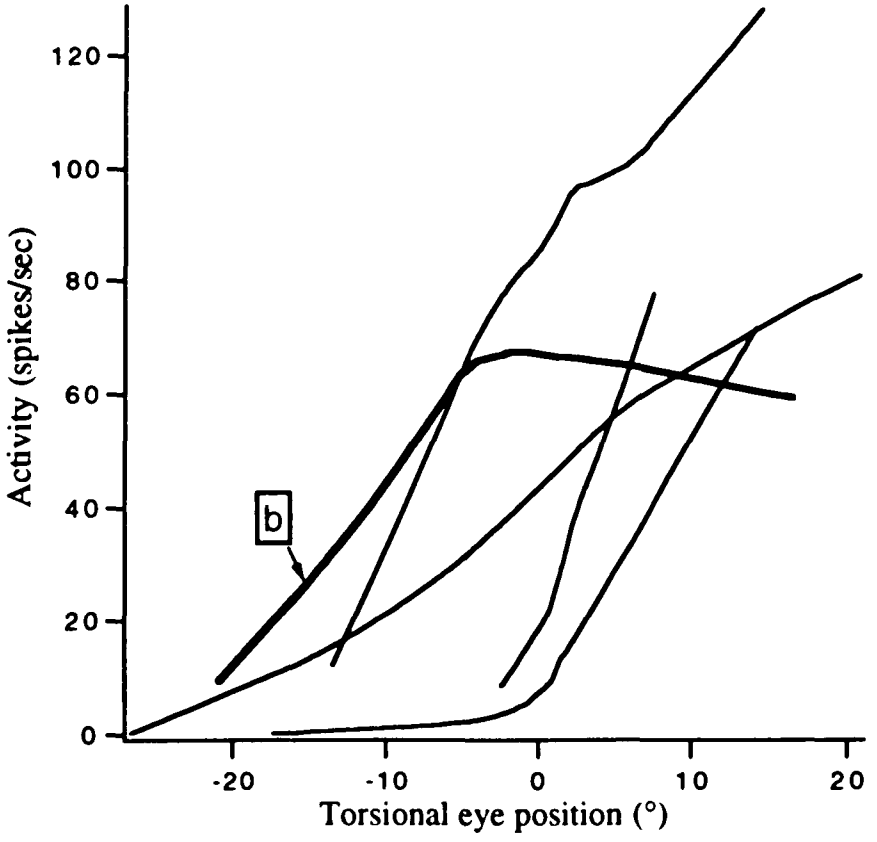

Figure 3.11
Relation between torsional eye position and firing frequency for 5 Tonic motoneurons. The curves are weighted regressions between eye position and activity. This procedure was used instead of a simple linear regression as simple linear models did not correctly fit some motoneuronal data. For example, curve **b** is linear in the lower and upper halves of the eye position range but it has two different slopes. The behavior of curve **b** was exhibited by 5 motoneurons (5/24). The eye position threshold was behaviorally measured in some units while in other is was extrapolated using regression curves as shown in this figure.

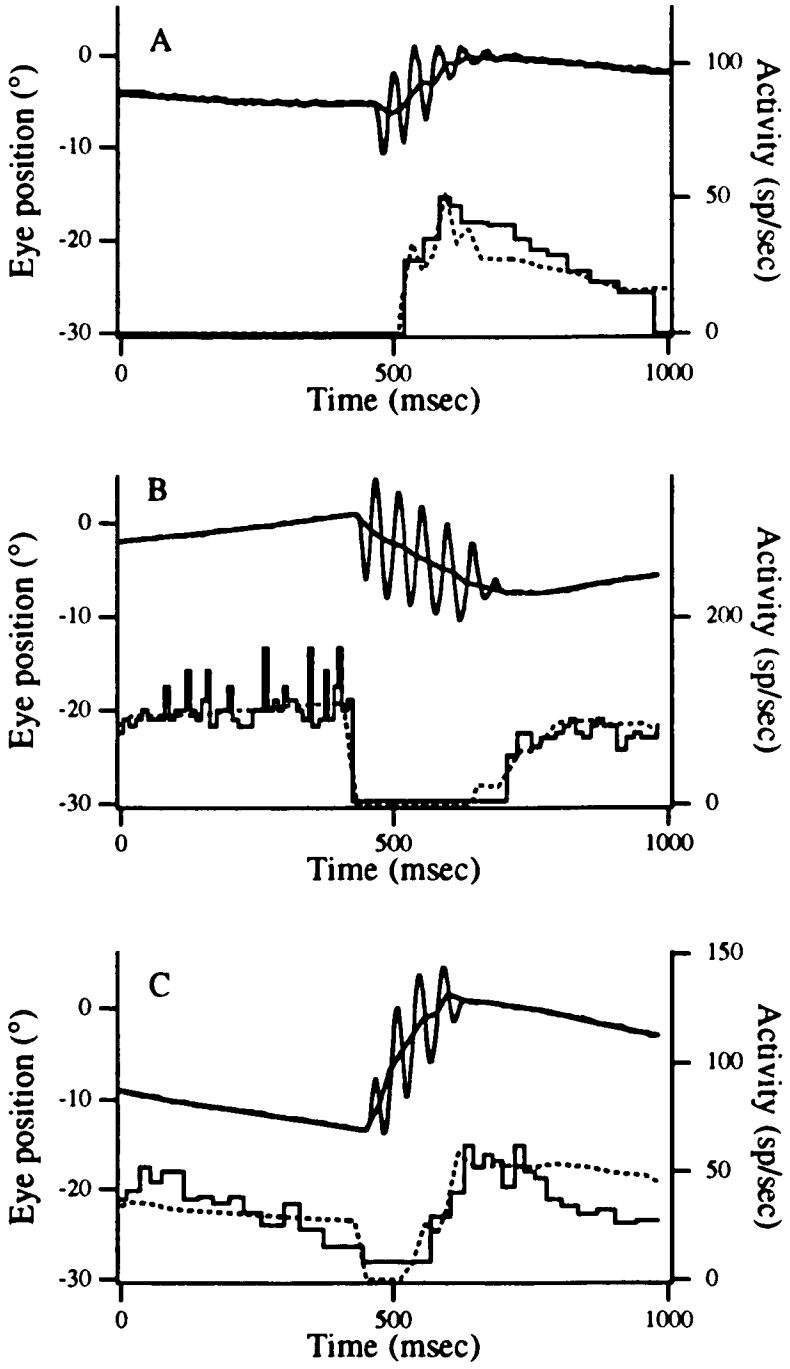

Figure 3.12
In the three panels A,B and C the two upper traces represent the real eye position and the interpolated "slow" component. During fixations these two traces are identical. The lower two traces represent the actual firing frequency of a Tonic Motoneuron (solid line) or the predicted frequency (broken line). Panel A (data from cell 190) shows the fit obtained with k=7.6 and r= 0.46. Panel B (data from cell 291) shows the fit obtained with k=2.0 and r= 0.2. Panel C (data from cell 291)shows the limits of the linear model. The "on" directed saccade starts and ends inside the "on" region of cell 291. The pause can only be accomodated by a negative value of r, in this case -0.4. This value while mathematically correct must be rejected as it is incompatible with the underlying physiology.

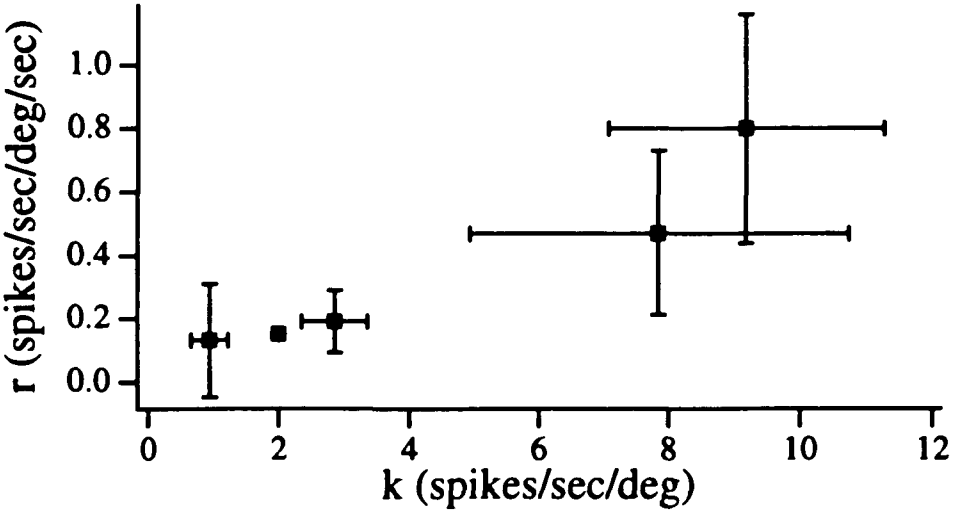

Figure 3.12D
Relation between k and r values. For five Tonic motoneurons the k and r values were determined according to a curve fitting procedure. For each cell, 10 saccades were used (bars are the standard deviation, determined in only 4 cells). K and r covary, a similar result has been reported in monkeys, cats and goldfish.

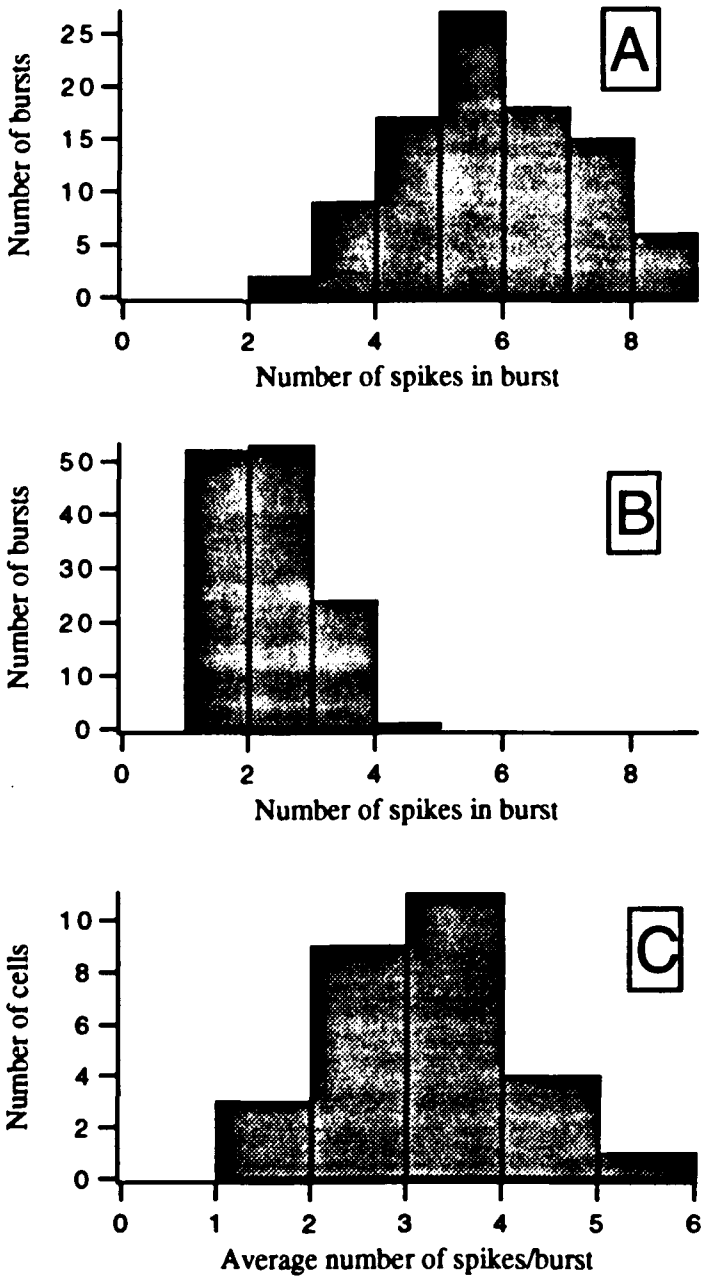

Figure 3.13
(A and B) Histograms of the number of spikes in bursts for two different cells. The Phasic motoneuron in A fires on average 5 spikes per burst, while the cell in B fires 2 spikes/burst. Histogram C shows the average number of spikes/burst for all 28 Phasic motoneurons. Thus, some phasic motoneurons fire, on average, 1.5 spikes/burst while others fire 5 spikes/burst.

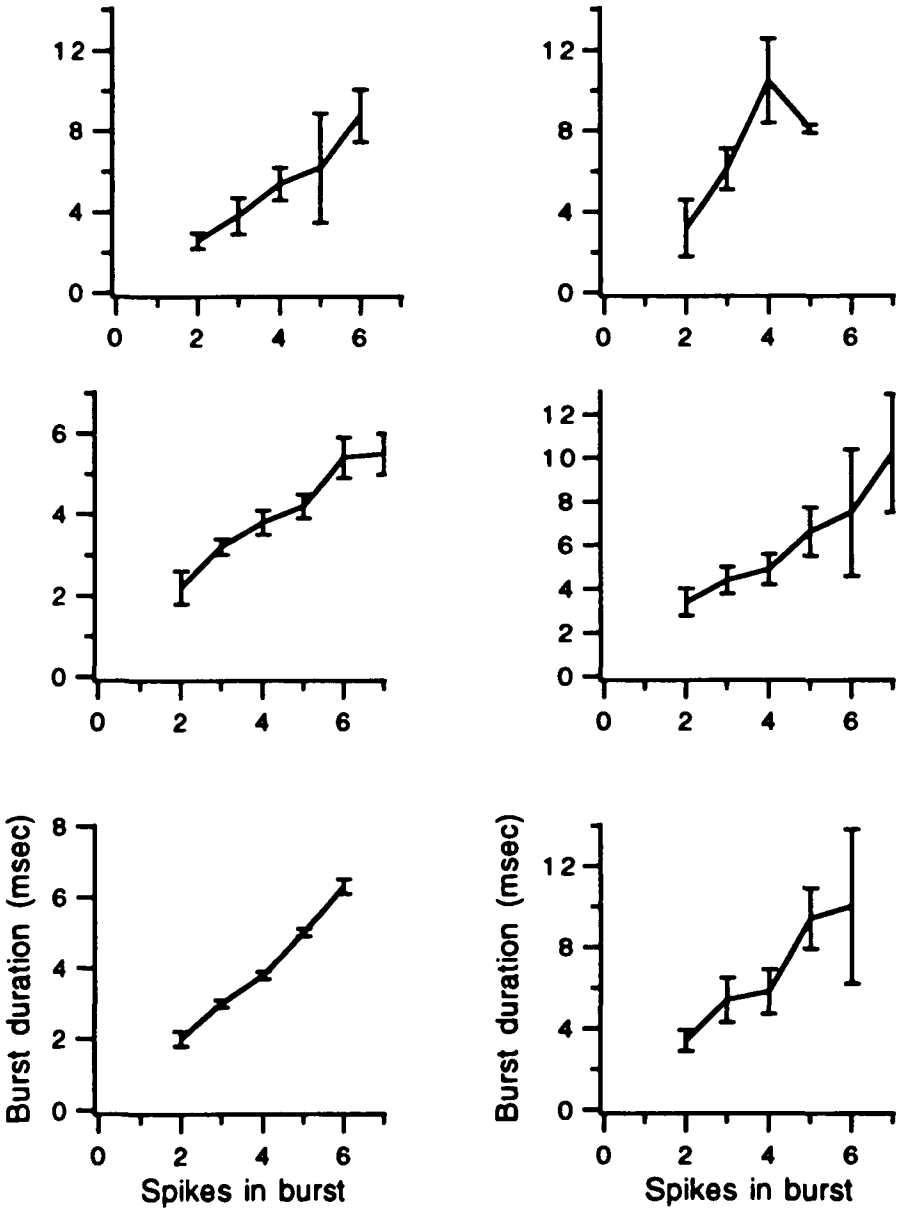

Figure 3.14
Relation between number of spikes in burst and median burst duration. Examples for 6 Phasic motoneurons. The number of spikes in a burst is highly correlated with its duration, longer bursts have more spikes. (error bars = 95% confidence interval for the median).

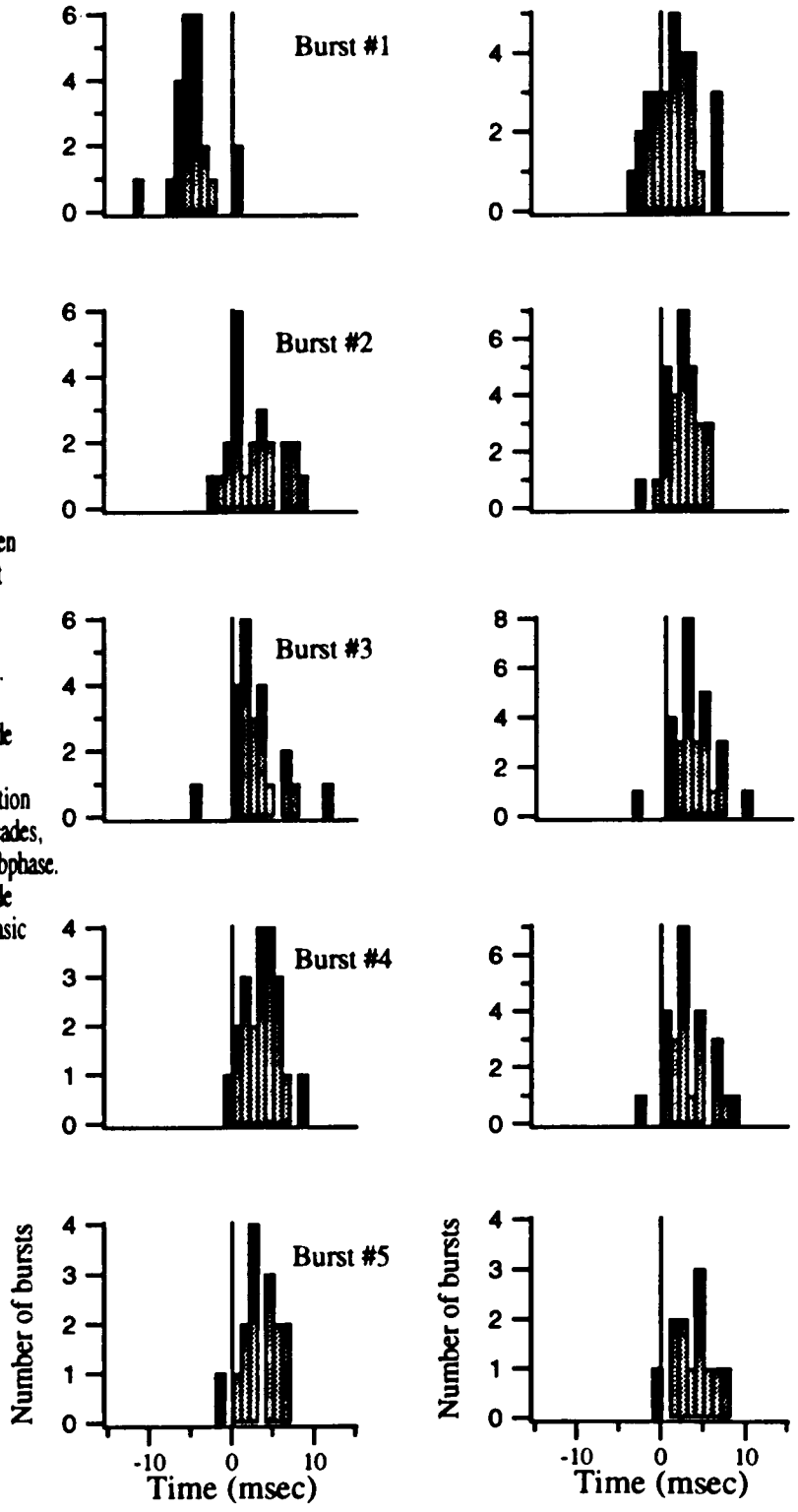

Figure 3.15
Histograms of the delay between burst onset and subphase onset for subphases 1,2,3,4 &5. (left side= "plus" saccades, right side = "minus" saccades). The vertical line at t=0 denotes either the beginning of a saccade (for Burst #1) or the initiation of a subphase. With the exception of the first burst of "plus" saccades, burst tend to begin after the subphase. The delays grows as the saccade progresses (data from one Phasic motoneuron).

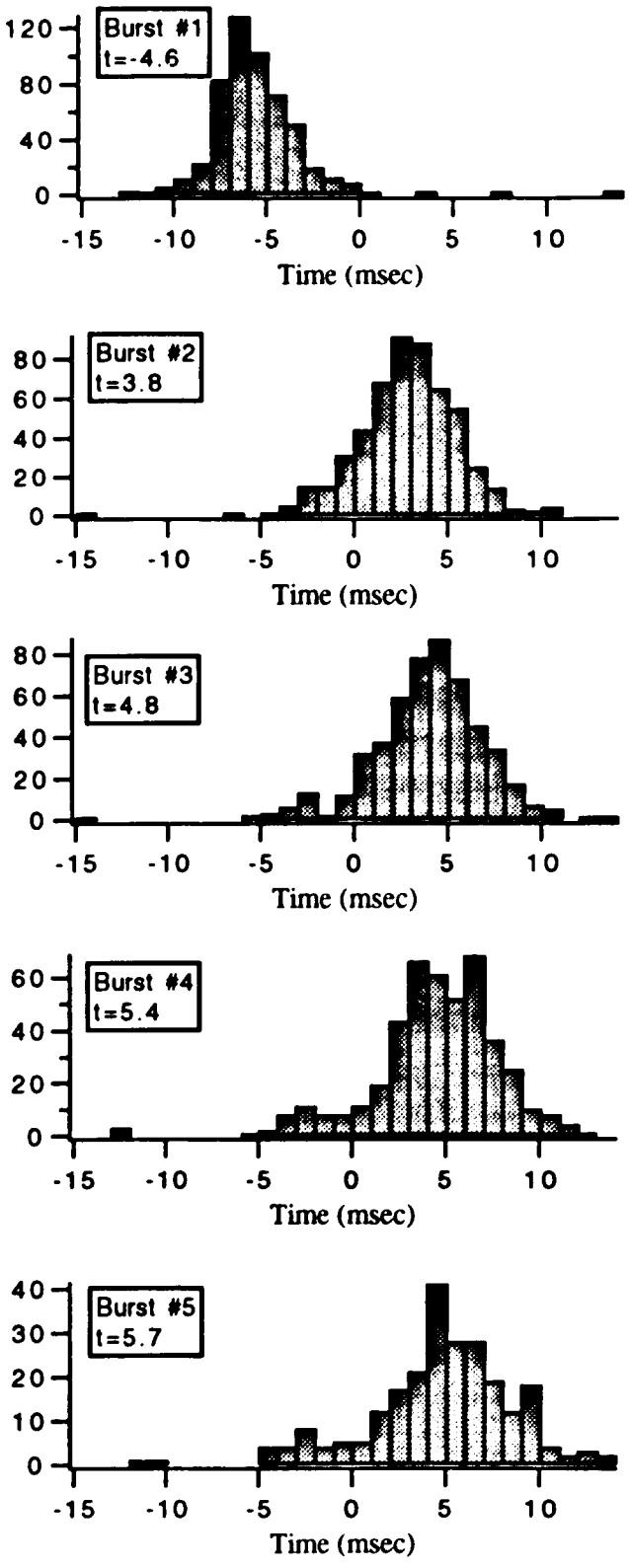

Figure 3.16
Histograms of burst's delay for the first five subphases of "plus" saccades. Cumulative data (28 phasic motoneurons) showing the distribution of delays. A universal property of phasic motoneurons is that their bursts always follows the initiation of an intorsional subphase. The first burst is an exception that shows that phasic responses are not proprioceptive but motor.

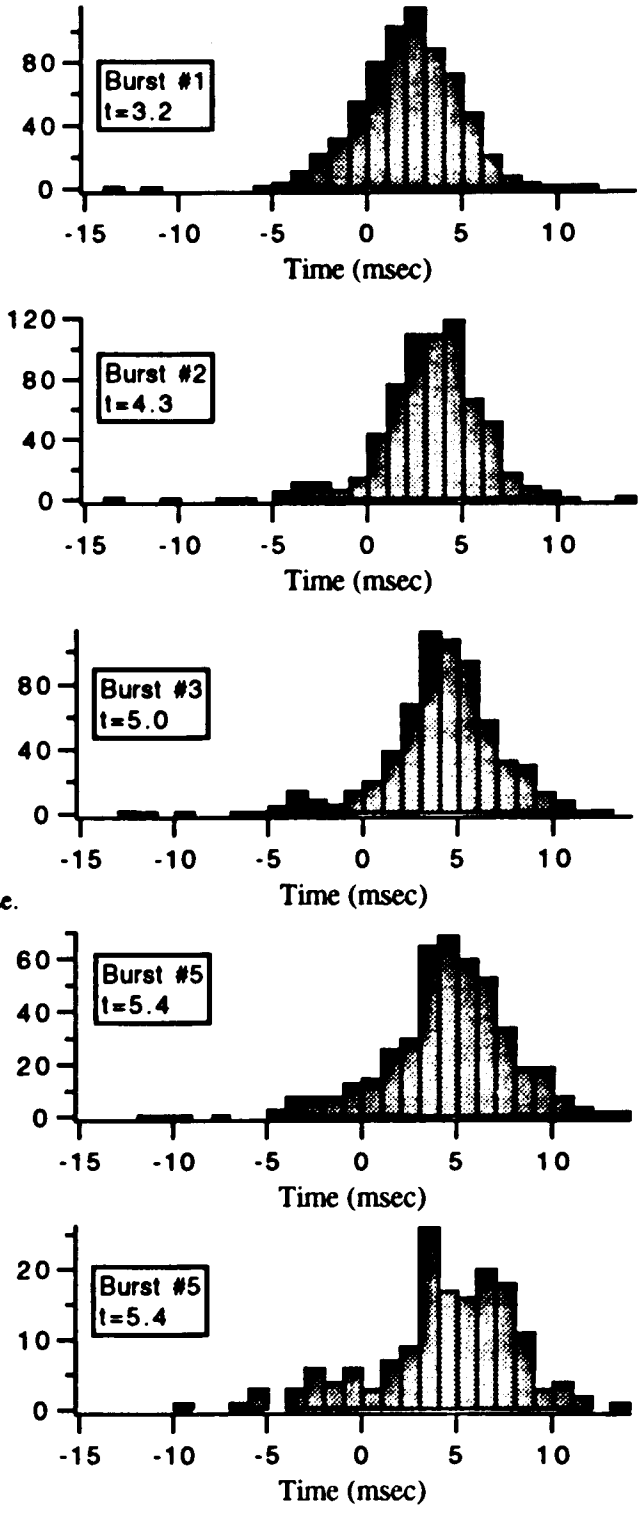

Figure 3.17
Histograms of burst's delay for the firsts five subphases of "minus" saccades. Data from 28 Phasic motoneurons. Note every burst is delayed 4-5 msec from the initiation of the subphase.

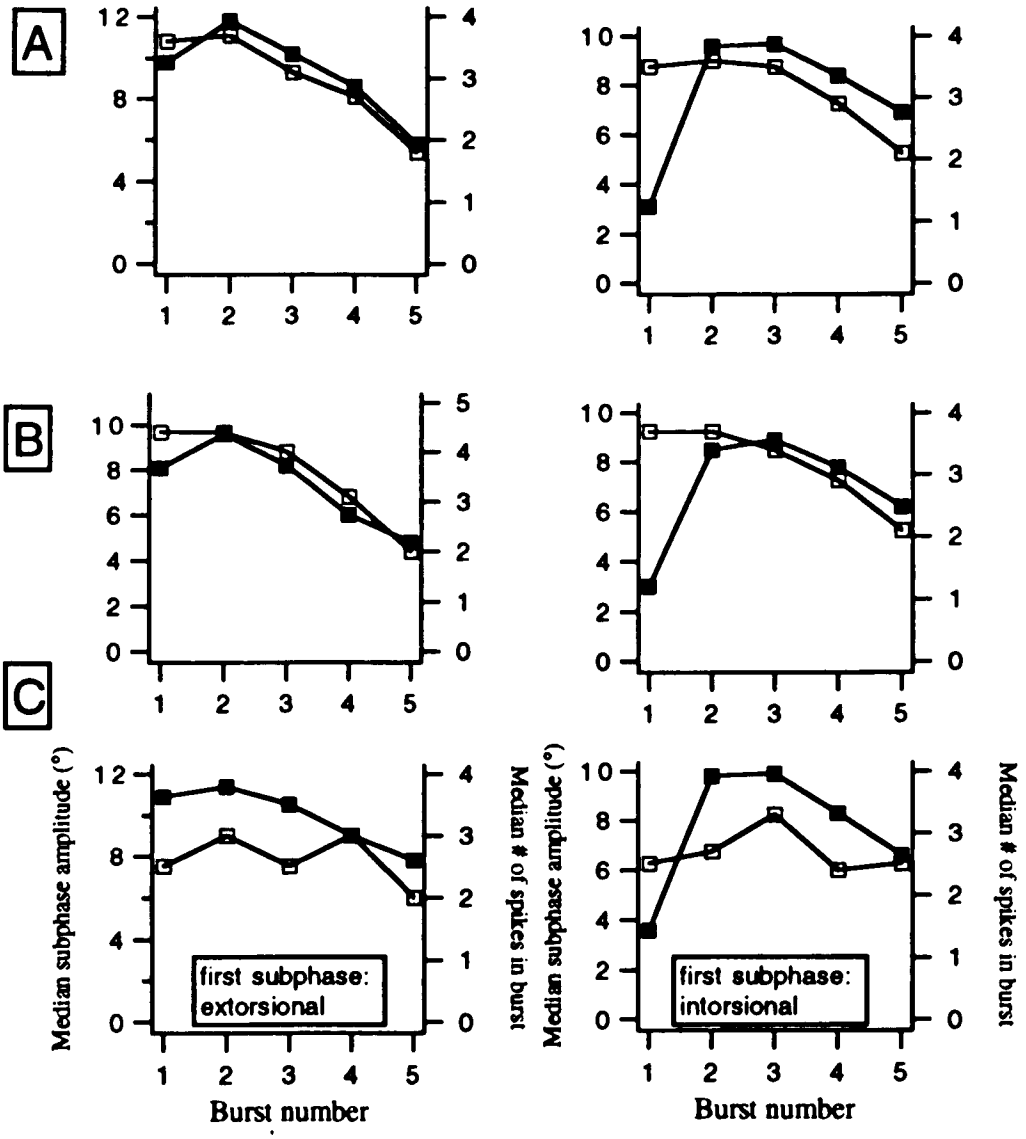

Figure 3.18
Variation of the median amplitude of subphases and of the median number of spikes in the corresponding bursts. In A and B the amplitude and the number of spikes covary together. (■ = median subphase amplitude, □ = median number of spikes in burst). The relationship is less clear for cell C. The median number of spikes of the first burst of "+" saccades is as high as for the second burst, but the amplitude of the first subphase is half of the other subphases (A and B, right side).

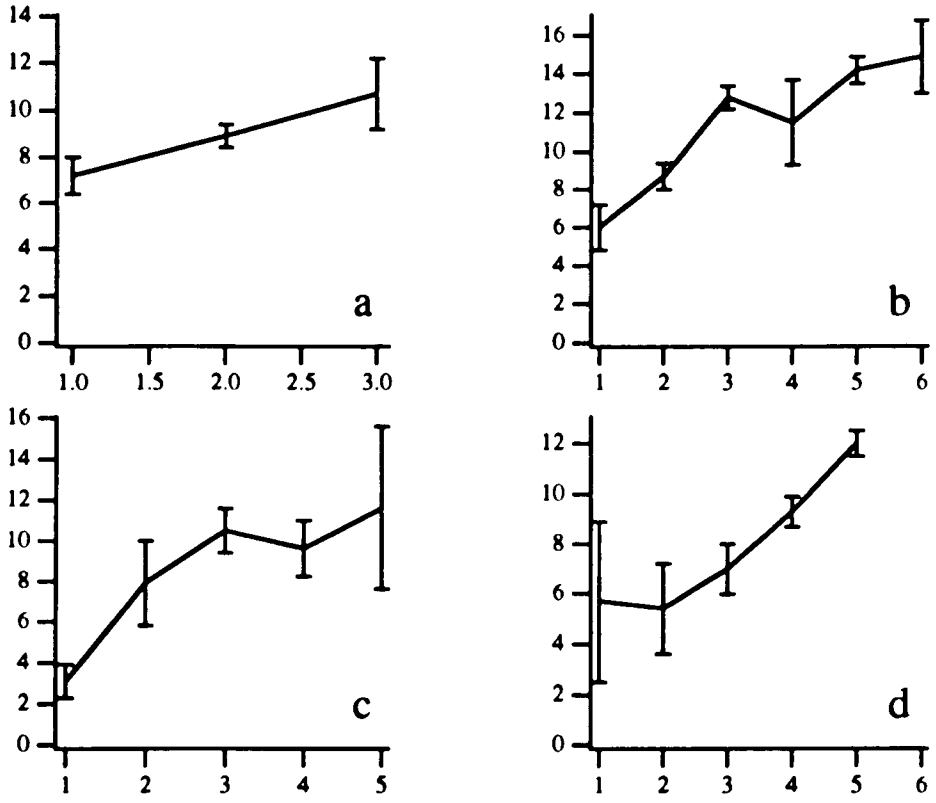

Figure 3.19
Relationship between number of spikes in burst and median amplitude of corresponding subphase for 5 Phasic motoneurons. The number of spikes in a burst increases with the amplitude of the subphase. Error bars are 95% confidence interval for the median. A clear monotonic relation appears in **a, b, c and d,** but is not present in **e** (error bars=95% confidence interval for the median, between40-100 saccades were used in each graph).

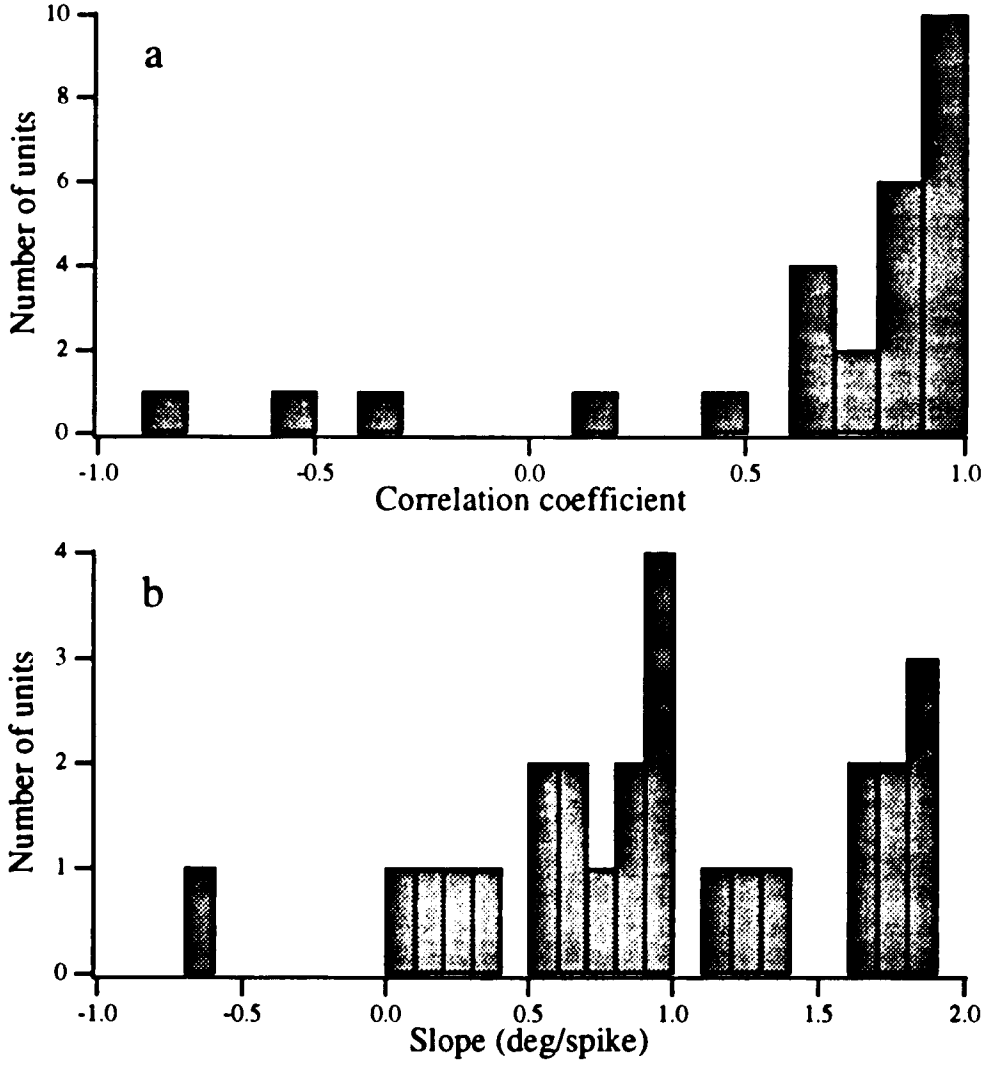

Figure 3.20
Histograms of the correlation coeficients (a) and slopes(b) of the plots between subphase amplitude and number of spikes for 27 Phasic motoneurons. These two histograms capture the correlation coefficent and the slope of graphs as in figure 3.19. Eighty percent% phasic motoneurons (22/27) show a correlation coefficient greater than 0.6 between median number of spikes per burst and subphase amplitude.

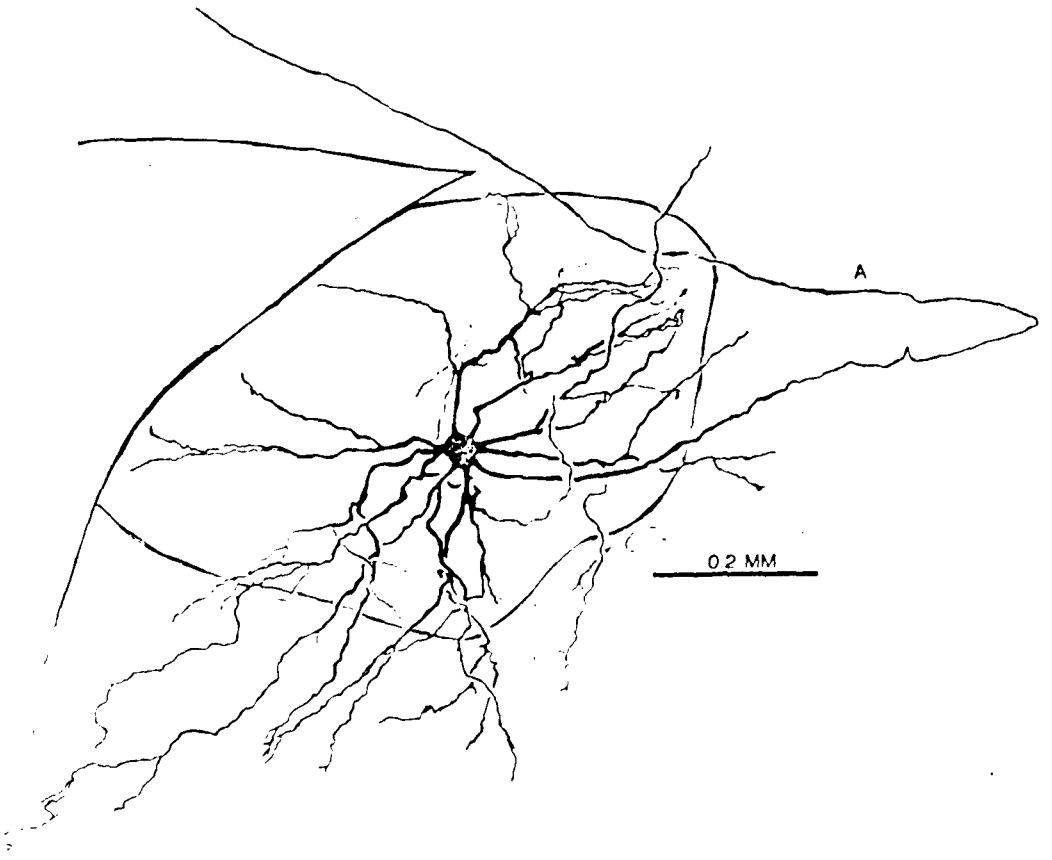

Figure 3.21
HRP filled Phasic motoneuron from the trochlear nucleus. This motoneuron was physiologically identified before injecting HRP. It has a soma size of 40 μm and its dendritic field extends beyond the boundaries of the nucleus into the medial longitudinal fasciculus (mlf). The axon (A) makes a detour, enters the fourth nerve and crosses towards the contralateral side.

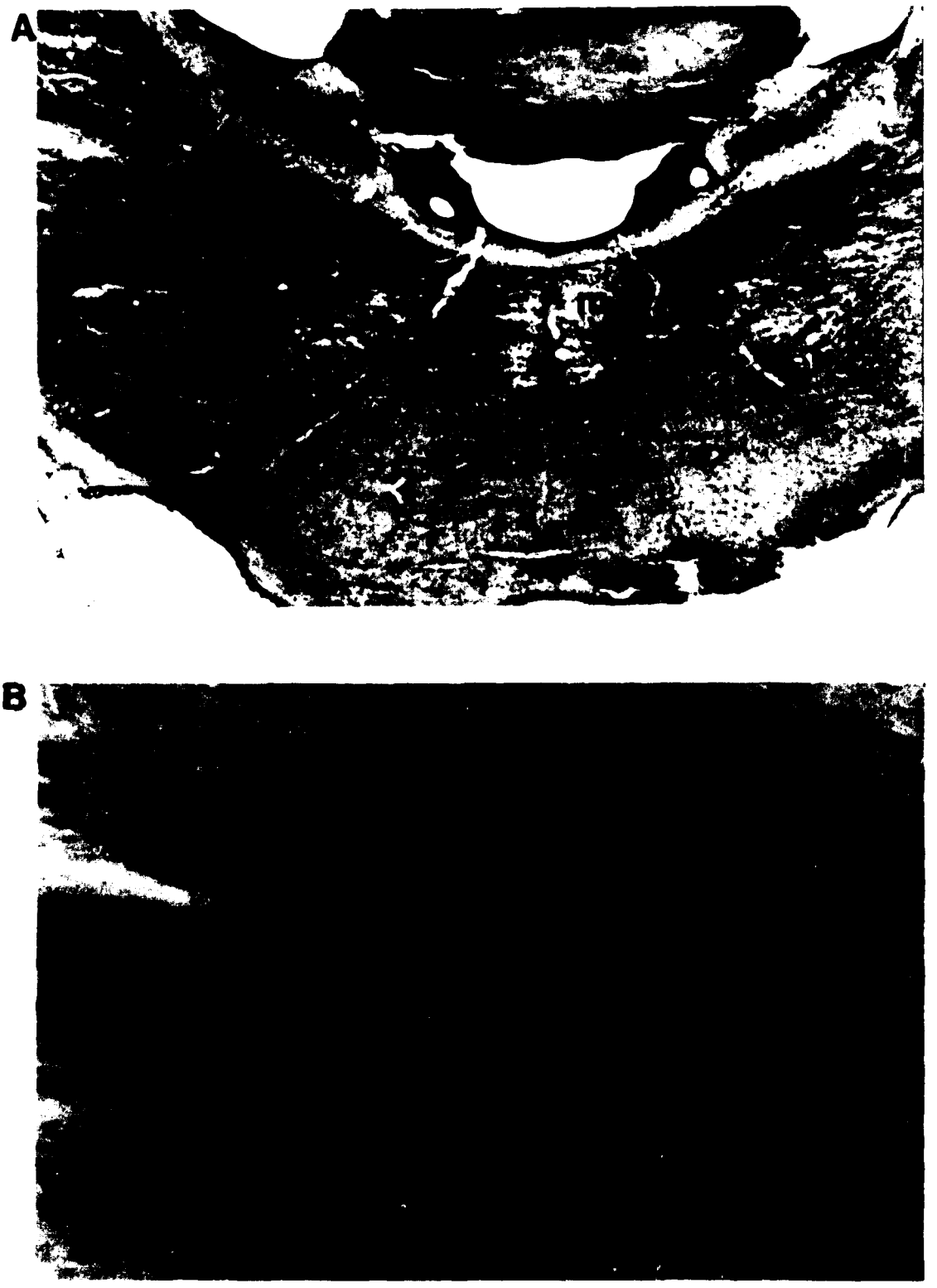

Figure 3.22
Transverse section through the brainstem of the chicken showing HRP labelled cells. **A** (low magnification) HRP labelled cells (big arrow) in the tangentialis after HRP deposition in the ipsilateral trochlear nucleus. Labelled fibers (small arrows) can be seen going into the pontine reticular formation and, after crossing the midline, towards the contralateral vestibular complex (m=medial longitudinal fasciculus). **B** High magnification micrograph of the labelled cells found in the tangentialis region.

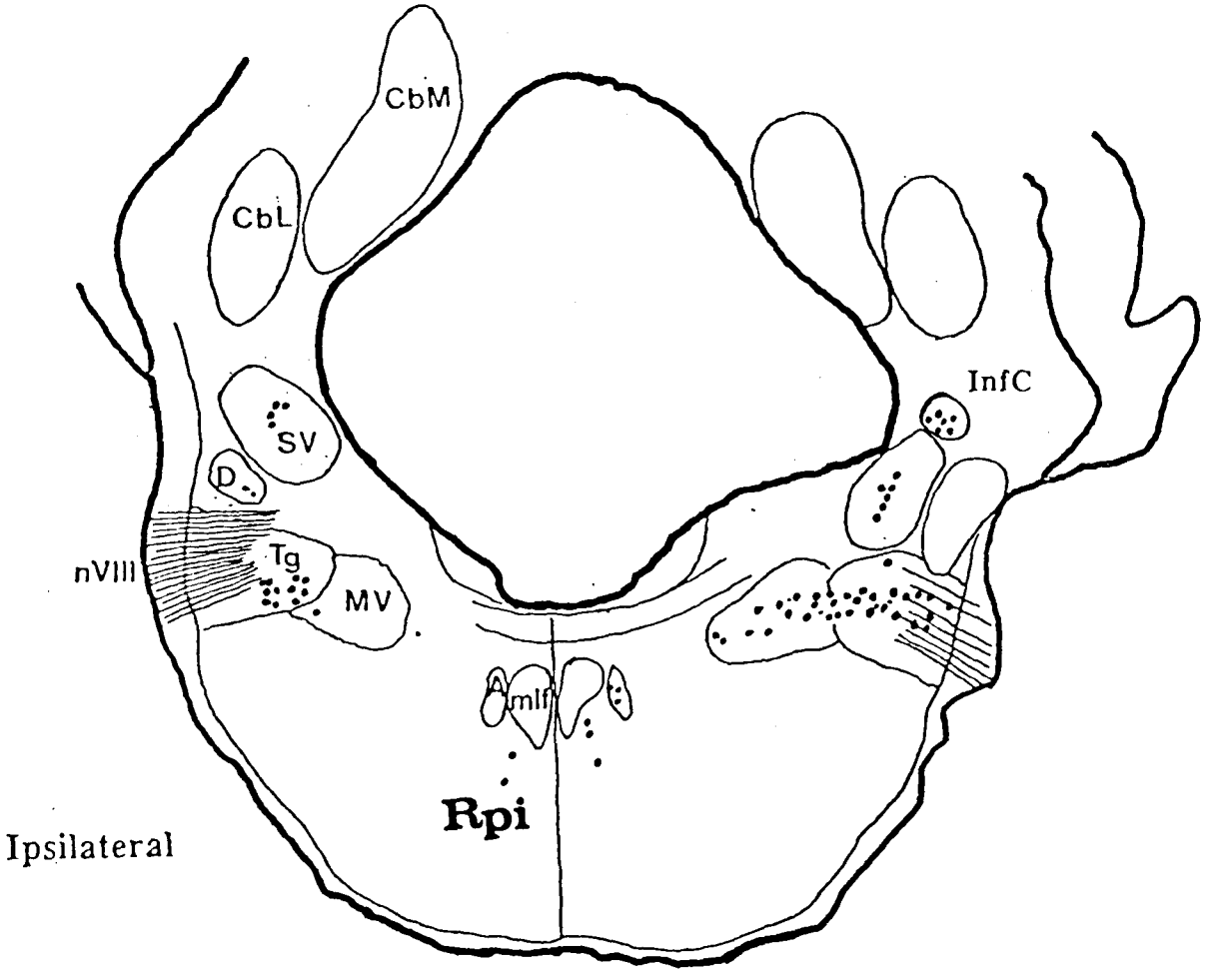

Figure 3.23
Summary of HRP labelled cells in chicken 1215. This diagram shows the location of labelled cells after a small iontophoretic injection of the tracer in the trochlear nucleus. Labelled cells were found in: ipsilateral side Reticular pontine formation (Rpi), Tangentialis (Tg), Superior vestibularis (Sv). contralateral side. Reticular pontine formation, Abducens (A), Tangentialis, Superior and Medial vestibularis (Mv) and the Infracerebellaris nucleus (InfC). [D= Deiters superioris, CbL and CbM cerebellaris nucleus pars lateral and medialis].

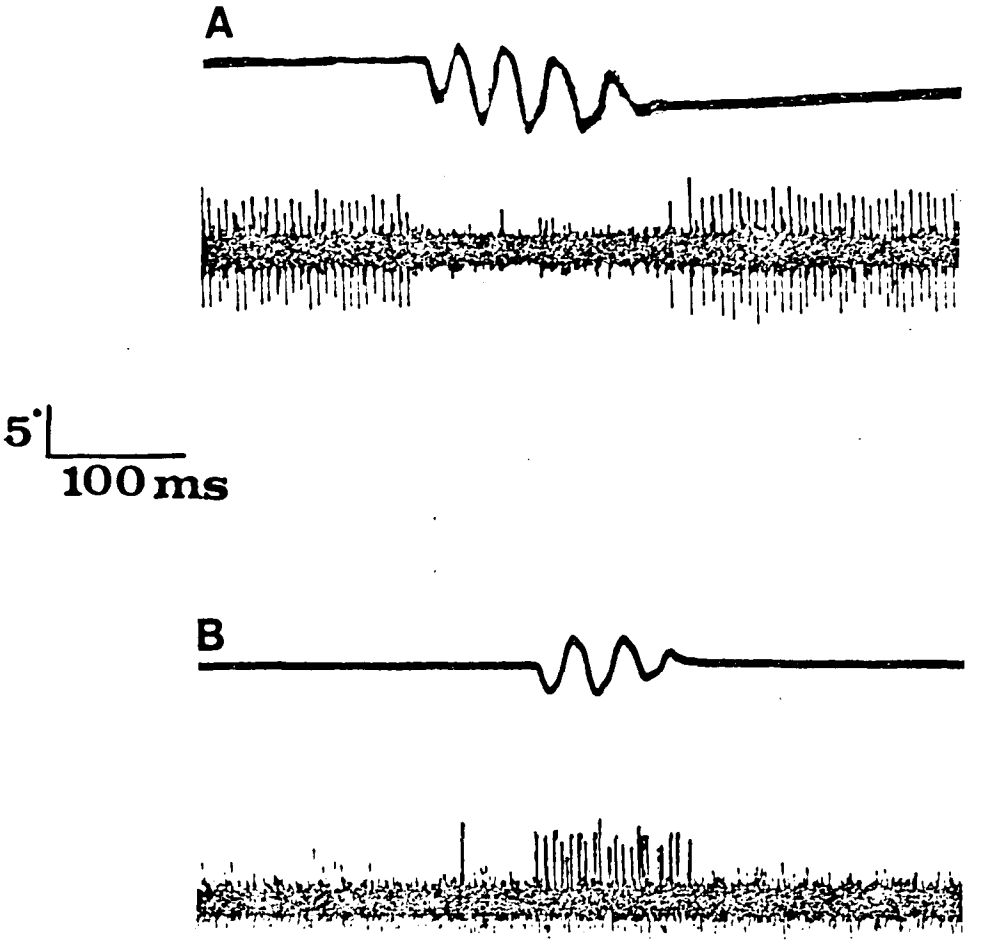

Figure 3.24
Saccade related responses found in the tangentialis medial vestibular border. A and B show the most common responses related to saccades found in the vestibular complex. Both responses were isolated in the border between the tangentialis and the vestibular medialis. The tonic response (A) always stopped before the saccade and had a frequency of 100 sp/sec. The burst of spikes (B) appeared for all saccades, independently of amplitude or direction. Note the different temporal structure of this burst and the bursts produced by Phasic motoneurons.

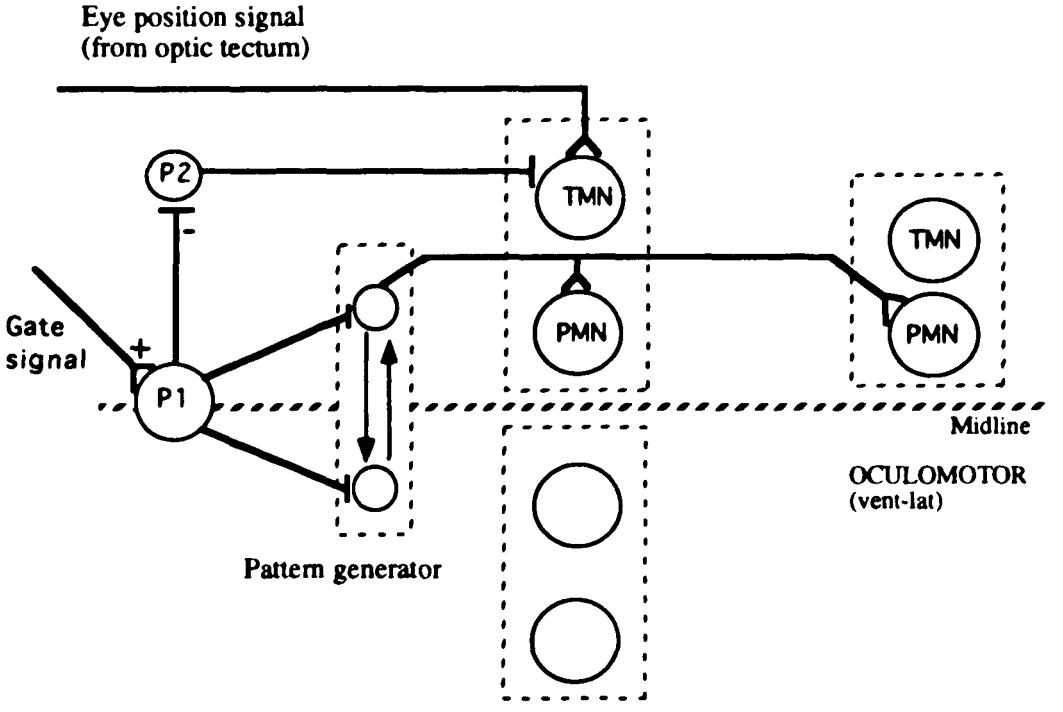

Figure 3.25
Model of saccadic circuit in the chick. This diagram represents the presumed connections between Phasic MN (PMN), Tonic MNs (TMN) with their pre-motor areas. During periods of fixations the pattern generator is totally silent as it is inhibited by the pause cell P1. A gate signal is continously "on" during fixations thus maintaining, via P1, the pattern generator off. TMN are active and their level of activity is defined by a tectal signal. In general right and left TMN receive different eye position signals during fixations. A saccade begins by a sudden turning off of the gate signal. As a result the cell P2 fires inhibiting, not totally, TMN. The disapperance of the gate signal also turns "on" the pattern generator which, by its internal characteristics, produces the two periodic, and exactly 180° out of phase, burst signals received by the PMN. For clarity only half of the circuit was drawn in this diagram.

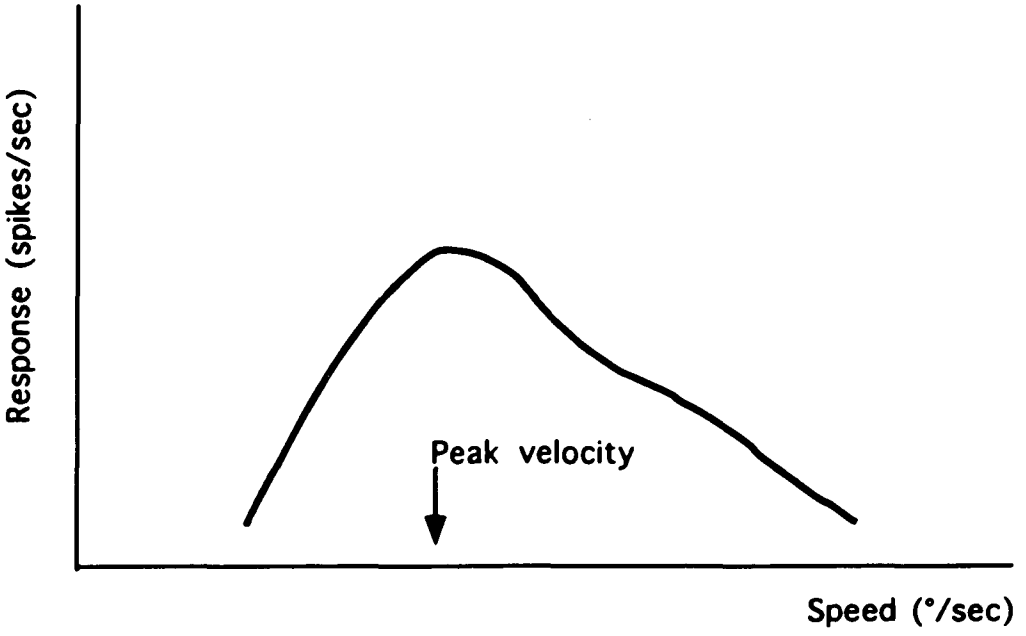

Figure 3.26
Speed sensitivity of tectal cell. Idealized example of the velocity tuning of a tectal cell in bird. This diagram does not correspond to any particular set of data but it captures the main elements of tectal cells. Tectal cells are mostly movement sensitive, they have a threshold velocity of about 0.1-2.0 °/sec, a peak (or optimal) velocity 20-70 °/sec and they can respond to very high stimulus velocity (400°/sec). Unfortunately the amount of data concerning the properties of tectal cells in the avian visual system is scarce.

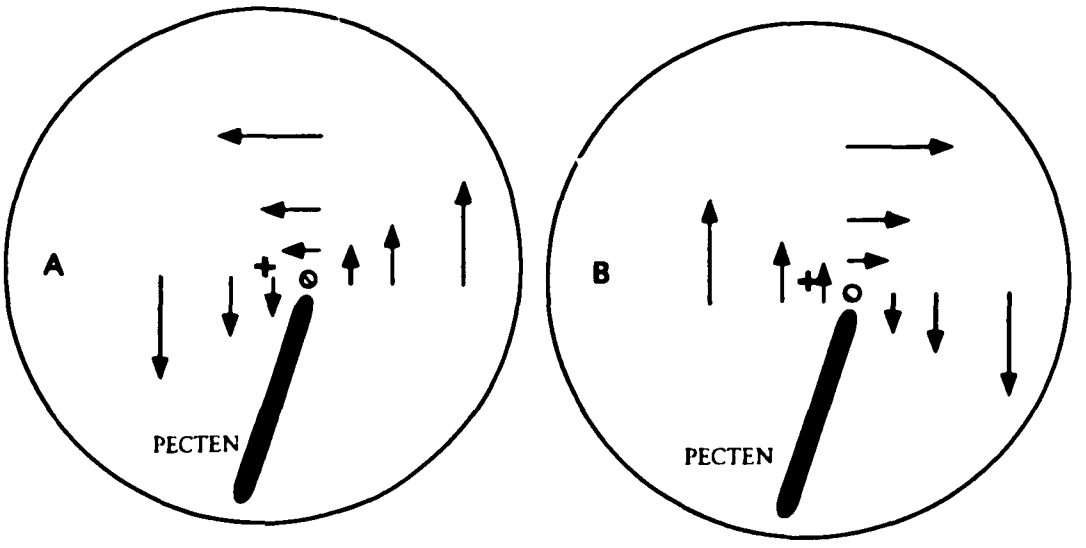

Figure 3.27
Schema representing the optic flow during the middle of an intorsional subphase (A) and the middle of an extorsional subphase (B). The tangential speed induced by oscillations increases towards the periphery (+=optic axis, o=axis of rotation). The position of the point o is located inside the Ω region (see figure 2.34). This peculiar alternating pattern is a direct consequence of the fact that oscillations are mostly produced by the alternate contractions of the two obliques.

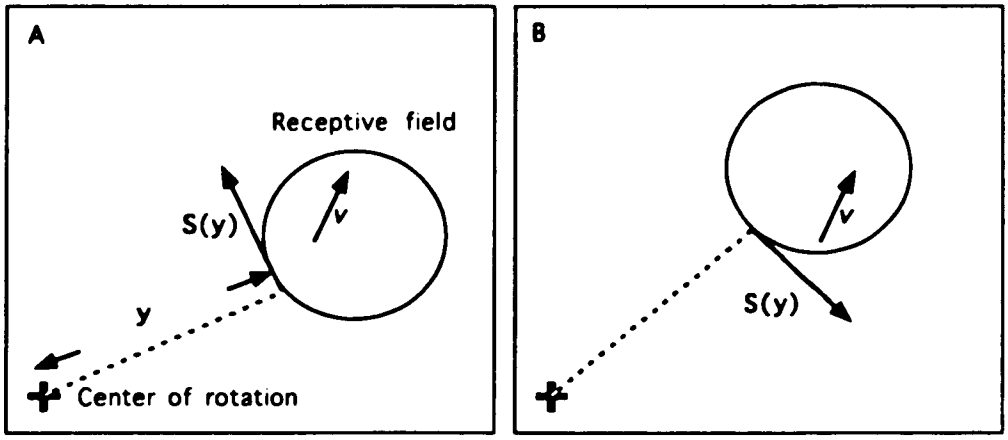

Figure 3.28A
Relative speeds between object and receptive field at two different moments of oscillations. The speed of a moving object relative to any receptive field changes during oscillations. Thus the response triggered by the object also changes. The basic idea is that the, during saccadic oscillations, each receptive field, located at eccentricity **y** moves with a sinusoidal speed **S(y)**, which is a function of the eccentricity of the receptive field. Thus the relative motion of any object moving at speed ***v*** changes

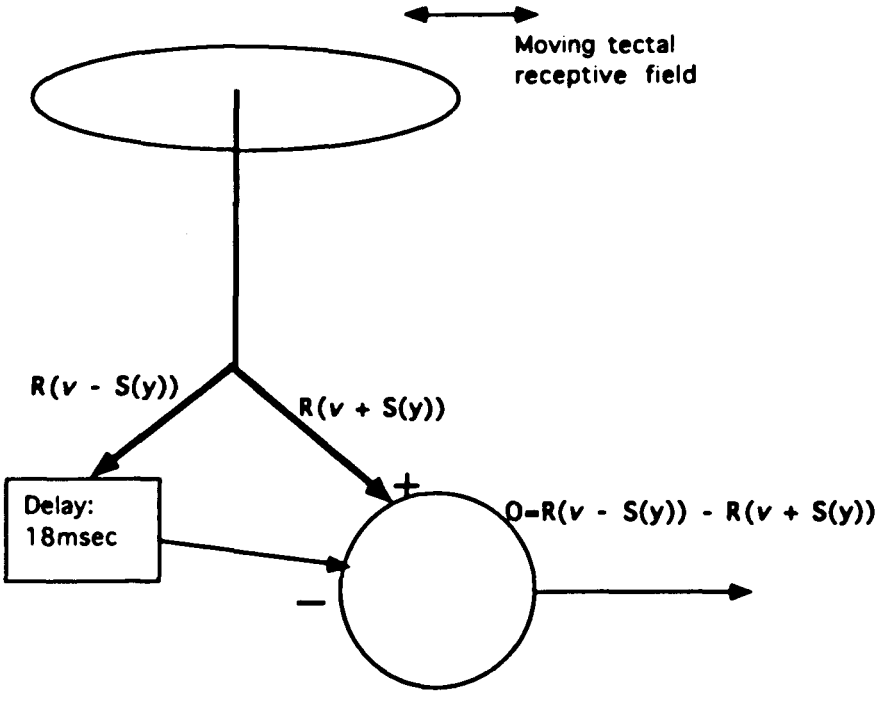

Figure 3.28B
Block operation of the proposed mechanism for enhancing movement detection using saccadic oscillations. A moving border will generate two responses in tectal cells depending on the relation between its speed and the eye rotation. These two responses will be different [**R(*v* - S(y))** vs **R(*v* + S(y))**]. Somehow one of these two responses would be stored in some neural circuit and compared to the other during the next cycle of the oscillation.

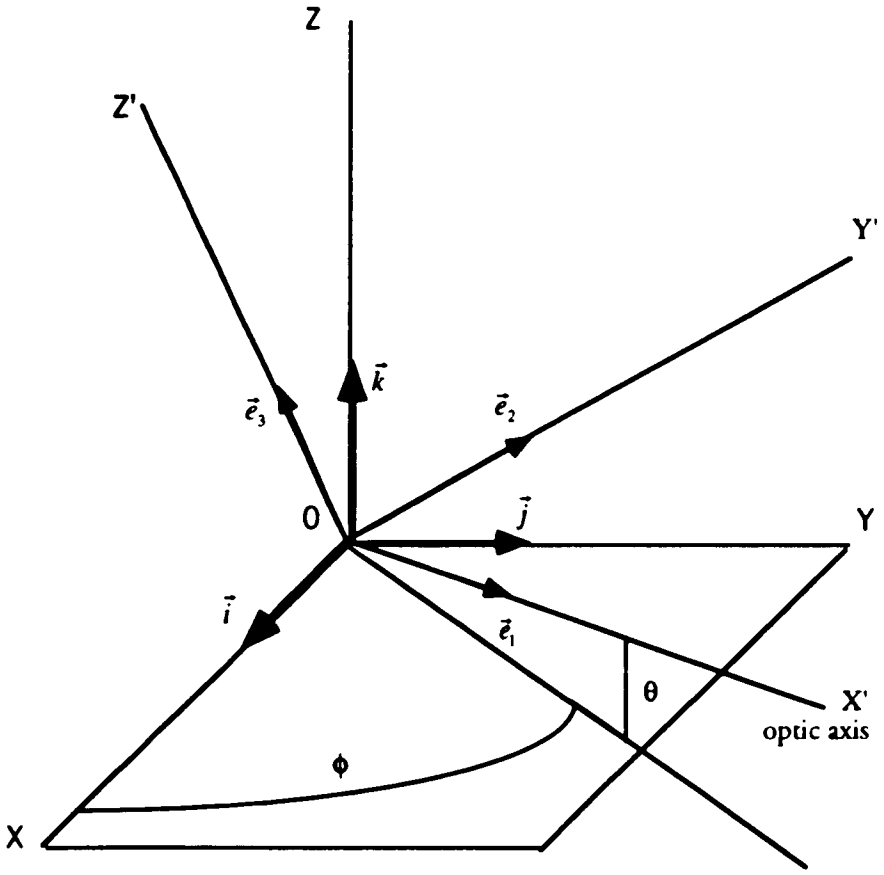

Figure A.1
Diagram showing the relation between reference frames. In this context the frame X'Y'Z' moves with the eye while the frame XYZ is static and centered in the eye orbit. This diagram is valid for the left eye. The Fick's angles θ and ϕ are given.

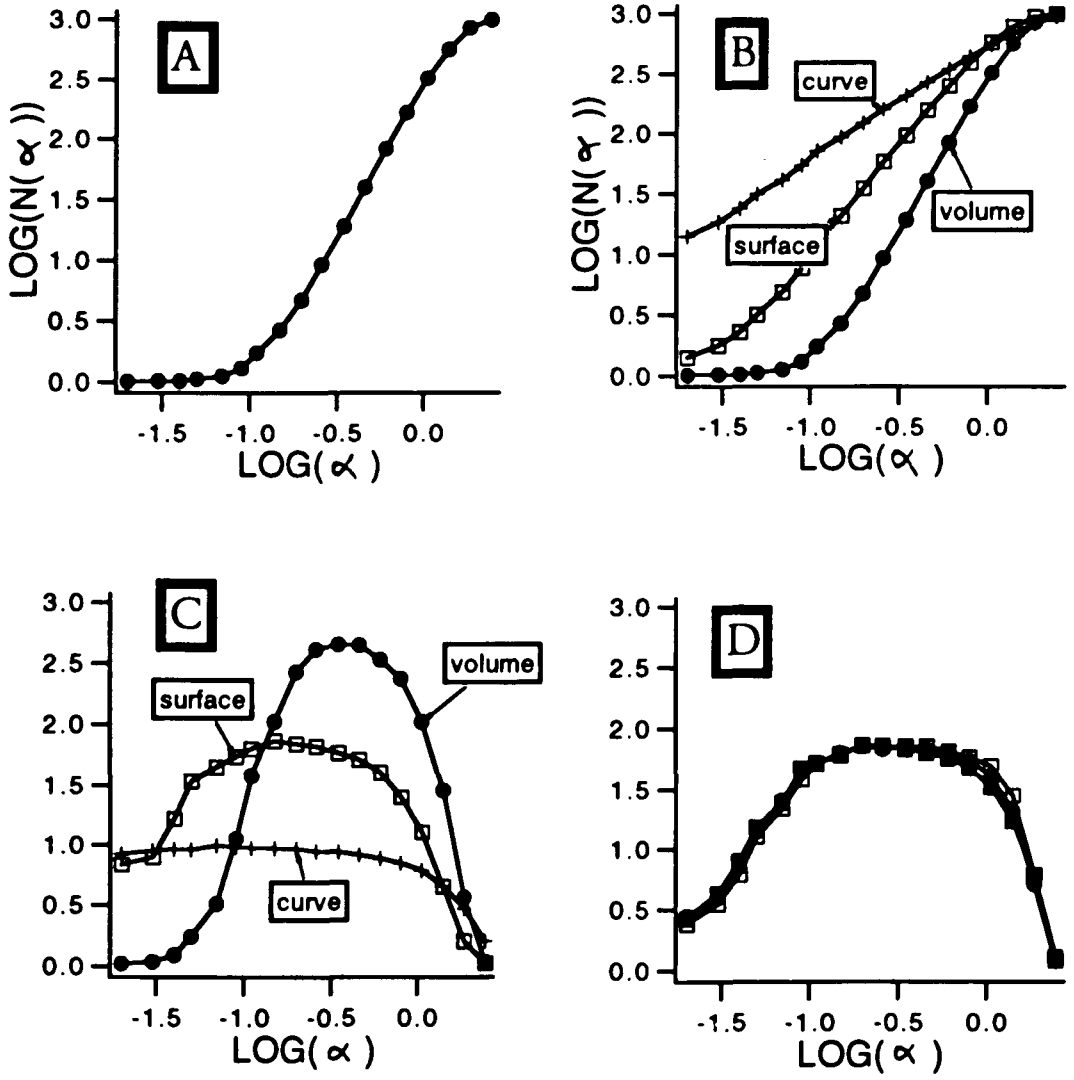

Figure B.1, B2, B3, and B4
(A) Plot LOG(N(∝)) vs LOG(∝) for a set of 1000 points extracted at random from the unitary cube. Ideally the slope should be 3. (B) Same plot for three different sets of points taken from a curve, a surface and a volume. The slopes reflect the "dimensionality" of the sample. Note that the slopes are not invariant for each curve. For small and large values of $\propto_i$ the slope tends to 0. The justification of this behavior is discussed in the text. (C) Plots of an approximation of the derivative of LOG(N(∝)), these curves give directly the value of the slopes at different scales. It is obvious that at mid range of the method gives the most correct result.
(D) same plot as in (C) but the 1000 data points were taken from three surfaces: a plane, a sphere and a "mexican-hat", note how the intermediate value of the slope (1.87) is similar for all three data sets.

BIBLIOGRAPHY

Abrahams, V.C., Rose, P.K. and Richmond, F.J.R. (1990). Properties and control of the neck musculature. In: M. D. Binder and L. M. Mendell (Eds.), The Segmental Motor System. Oxford, New York, pp. 59-71.

Aschoff, J.C., Becker, W. and Weinert, D. (1975). Computer analysis of eye movements: evaluation of the state of alertness and vigilance after Sulpiride medication. *J. Pharmacol. Clin.* **2**: 93-97.

Bahill, A.T., Adler, D. and Stark, L. (1975). Most naturally occurring saccades have amplitudes of 15° or less. *Invest. Ophthalmol.* **14**: 468-469.

Bahill, A.T., Brockenbrough, A. and Troost, B.T. (1981). Variability and development of a normative data base for saccadic eye movements. *Invest. Ophthalmo. Vis. Sci.* **21**: 116-125.

Bak, A.F. and Schmidt, E.M. (1977). An analog delay circuit for on-line visual confirmation of discriminated neuroelectric signals. *IEEE Trans. Biomed. Eng.* **24**: 69-71.

Barnes, G.R. (1979). Vestibulo-ocular function during co-ordinated head and eye movements to acquire visual targets. *J. Physiol. (Lond.)* **287**: 127-147.

Becker, W. (1989). Metrics. In: R. H. Wurtz and M. E. Goldberg (Eds.), The Neurobiology of Saccadic Eye Movements. Elsevier, Amsterdam, pp. 13-67.

Becker, W. and Jürgens, R. (1979). An analysis of the saccadic system by means of double step stimuli. *Vision Res.* **19**: 967-983.

Bodnarenko, S.R. (1989). A Neuroanatomical Study of the Connectivity of the Pretectal Lentiform Nucleus of the Mesencephalon (LM) in Chicken. Ph.D. Thesis in Psychology. City University of New York.

Boghen, D., Troost, B.T., Daroff, R.B., Dell'Osso, L.F. and Birkett, J.E. (1974). Velocity characteristics of normal human saccades. *Invest. Ophthalmol. Vis. Sci.* **13**: 619-623.

Brooks, B. and Holden, A.L. (1973). Suppression of visual signals by rapid image displacement in the pigeon retina: a possible mechanism for "saccadic" suppression. *Vision Res.* **13**: 1387-1390.

Burke, R.E. (1981). Motor units: Anatomy, physiology and functional organization. In: V. B. Brooks (Eds.), Handbook of Physiology: The Nervous System. American Physiological Society, Bethesda, Md., pp. 345-422.

Burke, R.E. (1990). Motor unit types: Some history and unsettled issues. In: M. D. Binder and L. M. Mendel (Eds.), The Segmental Motor System. Oxford, New York, pp. 207-221.

Cannon, S.C. and Robinson, D.A. (1985). An improved neural-network model for the neural integrator of the oculomotor system: more realistic neuron behavior. *Biol. Cyber.* **53**: 93-108.

Chard, R.D. and Gundlach, R.H. (1938). The structure of the eye of the homing pigeon. *J. Comp. Psychol.* **25**: 242-272.

Cleveland, W.S. (1979). Robust locally weighted regression and smoothing scatterplots. *J. Amer. Stat. Ass.* **74**(368): 829-836.

Collewijn, H. (1977). Eye and head movements in freely moving rabbits. *J. Physiol. (Lond.)* **266**: 471-498.

Collewijn, H., Ferman, L. and Van Den Berg, A.V. (1988). The behavior of human gaze in three dimensions. *Ann. New York Acad. Sci.* **545**: 105-127.

Crossland, W.J. and Hughes, C.P. (1978). Observations on the afferent and efferent connections on the avian isthmo-optic nucleus. *Brain Res.* **145**: 239-256.

Daunicht, W.J. (1988). A biophysical approach to the spatial function of eye movements, extraocular propioception and the vestibulo-ocular reflex. *Biol. Cybern.* **58**: 225-233.

Delgado-Garcia, J.M., Del Pozo, F. and Baker, R. (1986). Behavior of neurons in the abducens nucleus of the alert cat-I. Motoneurons. *Neurosci.* **17**(4): 929-952.

DeLuca, C. (1985). Control properties of motor units. *J. Exp. Biol.* **115**: 125-136.

Denny-Brown, D. (1949). Interpretation of the electromyogram. *Arch. Neurol. Psychiatry* **61**: 99-128.

Denny-Brown, D. and Pennybacker, J.B. (1938). Fibrillation and fasciculation in voluntary muscle. *Brain* **61**: 311-344.

Desmedt, J.E. and Godaux, E. (1981). Spinal motoneuron recruitment in man: Rank deordering with direction but not with speed of voluntary movement. *Science* **214**: 933-936.

Deubel, H. and Elsner, T. (1986). Threshold perception and saccadic eye movements. *Biol. Cybern.* **54**: 351-358.

Deubel, H., Wolf, W. and Hauske, G. (1984). The evaluation of the oculomotor error signal. In: A. G. Gale and F. Johnson (Eds.), Theoretical and applied aspects of eye movement research. Elsevier, pp. 55-62.

Dieringer, N. and Precht, W. (1986). Functional organization of eye velocity and eye position signals in abducens motoneurons of the frog. *J. Comp. Physiol.* **158**: 179-194.

Ehrlich, D. (1981). Regional specialization of the chick retina as revealed by the size and density of neurons in the ganglion cell layer. *J. Comp. Neurol.* **195**: 643-657.

Enoch, J.M. (1959). Effect of the size of a complex display upon visual search. *J. Opt. Soc. Am.* **49**: 280-286.

Evinger, C., Kaneko, C.R.S. and Fuchs, A.F. (1982). Activity of omnipause neurons in alert cats during saccadic eye movements and visual stimuli. *J. Neurophysiol.* **47**(5): 827-844.

Ferman, L., Collewjin, H. and Van Den Berg, A.V. (1987). A direct test of Listing's law: I Human ocular torsion measured in static tertiary positions. *Vision Res.* **27**: 929-938.

Fernand, V.S.V. and Hess, A. (1969). The occurence, structure and innervation of slow and twitch muscle fibres in the tensor tympani and stapedius of the cat. *J. Physiol. (Lond.)* **200**: 547-554.

Findlay, J.M. (1982). Global visual processing for saccadic eye movements. *Vision Res.* **22**: 1033-1045.

Frost, B.J. and DiFranco, D.E. (1976). Motion specific units in the pigeon optic tectum. *Vision Res.* **16**: 1229-1234.

Fry, G.A. and Hill, W.W. (1962). The center of rotation of the eye. *Am. Jour. Opto.* **39**: 581-595.

Fuchs, A.F. and Luschei, E.S. (1970). Firing patterns of abducens neurons of alert monkey in relation to horizontal eye movements. *J. Neurophysiol.* **33**: 382-392.

Fuchs, A.F., Scudder, C.A. and Kaneko, C.R.S. (1988). Discharge patterns and recruitment order of identified motoneurons and internuclear neurons in the monkey abducens nucleus. *J. Neurophysiol.* **60**(6): 1874-1895.

Gestrin, P. and Sterling, P. (1977). Anatomy and physiology of goldfish oculomotor system. II Firing pattern of neurons in abducens nucleus and surrounding medulla and their relation to eye movements. *J. Neurophysiol.* **40**(3): 573-588.

Gioanni, H., Rey, J., Villalobos, J., Richard, D. and Dalbera, A. (1983). Optokinetic nystagmus in the pigeon (*Columba livia*). *Exp. Brain Res.* **50**: 237-247.

Goldstein, H. (1965). Classical mechanics. Addison-Wesley Publishing Co., Reading.

Goldstein, H.P. and Robinson, D.A. (1986). Hysteresis and slow drift in abducens unit activity. *J. Neurophysiol.* **55**(5): 1044-1056.

Gottlieb, M.D., Fugate-Wentzek, L.A. and Wallman, J. (1987). Different visual deprivations produce different ametropias and different eye shapes. *Invest. Ophthalmol. Vis. Sci.* **28**(8): 1225-1235.

Granit, R. and Phillips, C.G. (1957). Differentiation of tonic from phasic alpha ventral horn cells by stretch, pinna and crossed extensor reflexes. *J. Neurophysiol.* **20**: 470-481.

Grillner, S. (1991). Recombination of motor pattern generators. *Current Biol.* **1**(4): 231-233.

Gutsu, I.P. (1970). The relationship between the reactions of neurons of the opticum of the pigeon's midbrain and the velocity of motion of visual stimuli. *Vestn. Mosk. Univ. (Biol.)* **25**: 108-110.

Hallet, P.E. and Lightstone, A.D. (1976). Saccadic eye movements to flashed targets. *Vision Res.* **16**: 107-114.

Hamada, T. (1984). A method for calibrating the gain of the electro-oculogram (EOG) using the optical properties of the eye. *J. Neurosci. Meth.* **10**: 259-265.

Harris, C.M. (1989). The ethology of saccades: a non-cognitive model. *Biol. Cybern.* **60**: 401-410.

Haustein, W. (1989). Considerations on Listing's law and the primary position by means of a matrix description of eye position control. *Biol. Cybern.* **60**: 411-420.

Haustein, W. and Mittelstaedt, H. (1990). Evaluation of retinal orientation and gaze direction in the perception of the vertical. *Vision Res.* **30**: 255-262.

Henn, V. (1988). Representation of three-dimensional space in the vestibular, oculomotor and visual systems. *Ann. New York Acad. Sci.* **545**: 1-9.

Henn, V. and Cohen, B. (1975). Activity in eye muscle motoneurons and brainstem units during eye movements. In: G. Lennerstrand and P. Bach-y-Rita (Eds.), Basic Mechanisms of Ocular Motility and their Clinical Implications. Pergamon Press, Oxford and New York, pp. 303-324.

Henneman, E. (1985). The size-principle:a deterministic output emerges from a set of probabilistic connections. *J. Exp. Biol.* **115**: 105-112.

Henneman, E. (1990). Comments on the logical basis of muscle control. In: M. D. Binder and L. M. Mendell (Eds.), The Segmental Motor System. Oxford University Press, New York, pp. vii-x.

Henneman, E., Clamann, H.P., Gillies, J.D. and Skinner, R.D. (1974). Rank order of motoneurones within a pool: law of combinations. *J. Neurophysiol.* **37**: 1338-1349.

Henneman, E. and Mendell, L.M. (1981). Functional organization of motoneuron pool and its inputs. In: V. B. Brooks (Eds.), Handbook of Physiology: The Nervous System. American Physiological Society, Bethesda, Md., pp. 423-507.

Henneman, E., Somjen, G. and Carpenter, D.O. (1965). Functional significance of cell size in spinal motoneurons. *J. Neurophysiol.* **28**: 560-580.

Hess, A. and Pilar, G. (1963). Slow muscle fibers in the extraocular muscles of the cat. *J. Physiol. (Lond.)* **169**: 780-798.

Hoffer, J.A., Loeb, G.E., Sugano, N., Marks, W.B., O'donovan, M.J. and Pratt, C.A. (1987). Cat hindlimb motoneurons during locomotion. III functional segregation in sartorius. *J. Neurophysiol.* **57**(2): 554-562.

Hughes, C.P. and Pearlman, A.L. (1974). Single unit receptive fields and the cellular layers of the pigeon optic tectum. *Brain Res.* **80**: 365-377.

Jampel, R. (1967). Multiple motor systems in the extraocular muscles of man. *Invest. Ophthalmol.* **6**: 288-293.

Jassik-Gerschenfeld, D. and Guichard, J.R. (1972). Visual receptive fields of single cells in the pigeon's optic tectum. *Brain Res.* **40**: 303-317.

Jurgens, R., Becker, W., Rieger, P. and Widderich, A. (1981). Interaction between goal-directed saccades and the vestibulo-ocular reflex (VOR) is different from interaction between quick phases and the VOR. In: A. F. Fuch and W. Becker (Eds.), Progress in oculomotor research. Elsevier/North-Holland, New York, pp. 11-18.

Kaneko, C., Evinger, C. and Fuchs, A. (1981). Role of cat pontine burst neurons in generation of saccadic eye movements. *J. Neurophysiol.* **46**(3): 387-408.

Karten, H.J. and Hodos, W. (1967). A stereotaxic atlas of the brain of pigeon (*Columba livia*). Johns Hopkins Press, Baltimore.

Keller, E.L. (1973). Accomodative vergence in the alert monkey: motor unit analysis. *Vision. Res.* **13**: 1565-1575.

Keller, E.L. and Robinson, D.A. (1971). Absence of a stretch reflex in extraocular muscle of the monkey. *J. Neurophysiol.* **34**: 908-919.

Kernell, D. and Sjoholm, H. (1975). Recruitment and firing rate modulation of motor unit tension in a small muscle of the cat's foot. *Brain Res.* **98**: 57-72.

King, W.M., Lisberger, S.G. and Fuchs, A.F. (1986). Oblique saccadic eye movements in primates. *J. Neurophysiol.* **56**: 769-784.

Koshland, G.F. and Smith, J.L. (1989). Mutable and inmutable features of paw-shake responses after hindlimb deafferentation in the cat. *J. Neurophysiol.* **62**(1): 162-173.

Labandeira-Garcia, J.L., Guerra-Seijas, M.J., Labandeira-Garcia, J.A. and Jorge-Barreiro, F.J. (1989). Afferent connections of the oculomotor nucleus in the chick. *J. Comp. Neurol.* **282**: 523-534.

Letelier, J.C., Evinger, C. and Wallman, J. (1987). The soma-dendritic organization of physiologically characterized avian extraocular motoneurons. *Soc. Neurosci. Abstr.* **13**(1): 172.

Levy-Schoen, A. and Blanc-Garin, J. (1974). On oculomotor programming and perception. *Brain Res.* **71**: 443-450.

Mandel, J. (1964). The statistical analysis of experimental data. Dover Publications, Mineola.

Marin, G., Letelier, J.C. and Wallman, J. (1990). Saccade-related responses of centrifugal neurons projecting to the chicken retina. *Exp. Brain Res.* **82**: 263-270.

Martin, G.R. (1986a). The eye of a passeriform bird, the European starling (Sturnus vulgaris): eye movement amplitude, visual fields and schematic optics. *J. Comp. Physiol. A* **159**: 545-557.

Martin, G.R. (1986b). Total panoramic vision in the mallard duck, Anas platyrhynchos. *Vision Res.* **26**: 1303-1305.

Martinoya, C., Rey, J. and Bloch, S. (1981). Limits of the pigeon's binocular field and direction for best binocular viewing. *Vision res.* **21**: 1193-1200.

McCue, M.P. and Guinan, J.J. (1988). Anatomical and functional segregation in the stapedius motoneuron pool of the cat. *J. Neurophysiol.* **60**: 1160-1180.

McVean, A. and Stelling, J. (1986). The mechanics of pigeon eye movements-are they like other vertebrates? *Behav. Brain Res.* **19**: 117-121.

Mendell, L.M., Collins, W.F. and Koerber, R.H. (1990). How are Ia synapses distributed on spinal motoneurons to permit orderly recruitment? In: M. D. Binder and L. M. Mendell (Eds.), The segmental motor system. Oxford University Press, New York, pp. 309-327.

Merrill, E.G. and Ainsworth, A. (1972). Glass-coated platinum-plated tungsten microelectrodes. *Med. Biol. Eng.* **10**: 662-672.

Mesulam, M.M. (1978). Tetramethyl benzidine for horseradish peroxidase neurohistochemistry. A non-carcinogenic blue reaction product with superior sensitivity for visualizing neural afferents and efferents. *J. Histochem. Cytochem.* **26**: 106-117.

Nakayama, K. (1975). Coordination of extraocular muscles. In: G. Lennerstrand and P. Bach-y-Rita (Eds.), Basic mechanisms of ocular motility and their clinical implications. Pergamon Press, Oxford, pp. 193-207.

Nelson, J.S., Goldberg, S.J. and McClung, J.R. (1986). Motoneuron electrophysiological and muscle contractile properties of superior oblique motor units in cat. *J. Neurophysiol.* **55**(4): 715-725.

Nemeth, P.M. (1990). Metabolic fiber types and influences on their transformations. In: M. D. Binder and L. M. Mendell (Eds.), The segmental Motor System. Oxford, New York, pp. 258-277.

Nye, P.W. (1969). The monocular eye movements of the pigeon. *Vision Res.* **9**: 133-144.

Optican, L.M., Frank, D.E., Smith, B.M. and Colburn, T.R. (1982). An amplitude and phase regulating magnetic field generator for an eye movement monitor. *Trans. Biomed. Eng. IEEE* **BME-29**(3): 206-209.

Ottes, F.P., Van Gisbergen, J.A.M. and Eggermont, J.J. (1984). Metrics of saccade responses to visual double stimuli: two different modes. *Vision Res.* **24**: 1169-1179.

Pachter, B. (1983). Rat extraocular muscle. I. Three dimensional cytoarchitecture, component fibre properties and innervation. *J. Anat.* **137**: 143-159.

Pastor, L.M. and Delgado-Garcia, J.M. (1992). Discharge patterns of abducens motoneurons in the goldfish. *J. Neurophysiol. (in press)*

Perry, H.V. and Cowey, A. (1985). The ganglion cell and cone distributions in the monkey's retina: implications for central magnification factors. *Vision Res.* **25**: 1795-1810.

Pettigrew, J.D., Wallman, J. and Wildsoet, C.F. (1990). Saccadic oscillations facilitate ocular perfusion from the avian pecten. *Nature* **343**(6256): 362-363.

Pratt, D.W. (1982). Saccadic eye movements are coordinated with head movements in walking chickens. *J. Exp. Biol.* **97**: 217-223.

Puesner, K.D. and Morest, D.K. (1977). The neuronal architecture and topography of the nucleus vestibularis tangentialis in the late chick embryo. *Neuroscience* **2**: 189-207.

Reichardt, W. (1987). Evaluation of optical motion information by movement detectors. *J. Comp. Physiol. (A)* **161**: 533-547.

Robinson, D.A. (1963). A method of measuring eye movements using a search coil in a magnetic field. *IEEE Trans. Biomed. Eng.* **10**: 137-145.

Robinson, D.A. (1964). The mechanics of human saccadic eye movements. *J. Physiol. (Lond.)* **174**: 245-264.

Robinson, D.A. (1968). The oculomotor control system: a review. *Proc. IEEE* **56**: 1032-1049.

Robinson, D.A. (1970). Oculomotor unit behavior in the monkey. *J. Neurophysiol.* **33**: 393-404.

Robinson, D.A. (1975). Oculomotor control signals. In: G. Lennestrand and P. Bach-y-Rita (Eds.), Basic Mechanisms of Ocular Motility and their Clinical Implications. Pergamon Press, Oxford, pp. 337-378.

Robinson, D.A. (1981). Control of eye movements. In: V. B. Brooks (Eds.), Handbook of Physiology: The Nervous System. American Physiological Society, Baltimore, Md., pp. 1275-1320.

Schiller, P.H. (1970). The discharge characteristics of single units in the oculomotor and abducens nuclei of the unanaesthetized monkey. *Exp. Brain Res.* **10**: 347-362.

Schmidt, D., Abel, L.A., Dell'Osso, L.F. and Daroff, R.B. (1979). Saccadic velocity characteristics: intrinsic variability and fatigue. *Aviat. Space Environ. Med.* **50**: 393-395.

Scudder, C. (1988). A new local feedback model of the saccadic burst generator. *J. Neurophysiol.* **59**: 1455-1475.

Shults, W.T., Stark, L., Hoyt, W.F. and Ochs, A.L. (1977). Normal saccadic structure of voluntary nystagmus. *Arch. Ophthalmol.* **95**: 1399-1404.

Skavensky, A. (1972). Inflow as a source of extraretinal eye position information. *Vision Res.* **12**: 221-229.

Sohal, G.S. and Holt, R.K. (1978). Identification of the trochlear motoneurons by retrograde transport of horseradish peroxidase. *Exp. Neurol.* **59**: 509-514.

Sohal, G.S., Knox, T.S., Allen, J.C., Arumugam, T., Campbell, L.R. and Yamashita, T. (1985). Development of the trochlear nucleus in the quail and comparative study of the trochlear nucleus, nerve and innervation of the superior oblique muscle in quail, chick and duck. *J. Comp. Neurol.* **239**: 227-236.

Sparks, D.L., Mays, L.E. and Porter, J.D. (1987). Eye movement induced by pontine stimulation: interaction with visually triggered saccades. *J. Neurophysiol.* **58**: 300-318.

Spencer, R.F. and Porter, J.D. (1988). Structural organization of the extraocular muscles. In: J. A. Buttner-Ennever (Eds.), Neuroanatomy of the Oculomotor System. Elsevier, Amsterdam, pp. 33-80.

Steinbach, M.J., Angus, R.G. and Money, K.E. (1974). Torsional eye movements of the Owl. *Vision Res.* **14**: 745-746.

Steinbach, M.J. and Money, K.E. (1973). Eye movements of the Owl. *Vision Res.* **13**: 889-891.

Turkel, J. and Wallman, J. (1977). Oscillating eye movements with possible visual function in birds. *Soc. Neuro. Sci. Abs.* **3**: 158.

Tweed, D. and Vilis, T. (1987). Implications of rotational kinematics for the oculomotor system in three dimensions. *J. Neurophysiol.* **58**: 832-849.

van Gisbergen, J.A., Robinson, D.A. and Gielen, S. (1981). A quantitative analysis of the generation of saccadic eye movements by burst neurons. *J. Neurophysiol.* **45**: 417-442.

Volkmann, F.C. (1986). Human visual suppression. *Vision Res.* **26**: 1401-1416.

Wallman, J. and Pettigrew, J.D. (1985). Conjugate and disconjunctive saccades in two avian species with contrasting oculomotor strategies. *J. Neurosci.* **5**: 1418-1428.

Wallman, J., Velez, J., Weinstein, B. and Green, A.E. (1982). Avian vestibulo-ocular reflex: adaptive plasticity and developmental changes. *J. Neurophysiol.* **48**: 952-967.

Wässle, H., Levick, W.R. and Cleland, B.G. (1975). The distribution of the alpha type of ganglion cells in the cat's retina. *J. Comp. Neurol.* **159**: 419-438.

Westheimer, G. (1954). Mechanism of saccadic eye movements. *Arch. Ophthal.* **52**: 710-724.

Wold, J.E. (1976). The vestibular nuclei in the domestic hen (Gallus domesticus). I. Normal anatomy. *Anat. Embryol.* **149**: 29-46.

Wold, J.E. (1978). The vestibular nuclei in the domestic hen (Gallus domesticus). III. Ascending projections to the mesencephalic eye motor nuclei. *J. Comp. Neurol.* **179**: 393-406.

Young, L.R. and Stark, L. (1963). Variable feedback experiments testing a sampled data model for eye tracking movements. *IEEE Trans. Hum. Factors Eng.* **1**: 38-50.